# UNIVERSIDAD NACIONAL AUTÓNOMA DE MÉXICO

## Doctorado en Ciencias Bioquímicas

MECANISMO MOLECULAR DE LA ACTIVIDAD ANTINFLAMATORIA DE LA JACAREUBINA Y EVALUACIÓN DE OTROS PRODUCTOS NATURALES SOBRE EL SISTEMA DE TRANSDUCCIÓN DE SEÑALES DEL RECEPTOR FcεRI EN CÉLULAS CEBADAS

TESIS

QUE PARA OPTAR POR EL GRADO DE:

Doctor en Ciencias

PRESENTA:
M. EN. C. JORGE IVAN CASTILLO ARELLANO

TUTOR PRINCIPAL
DRA. CLAUDIA GONZÁLEZ ESPINOSA
CINVESTAV SUR

MIEMBROS DEL COMITÉ TUTOR
DR. RICARDO REYES CHILPA INSTITUTO DE QUÍMICA
DR. JOSÉ PEDRAZA CHAVERRI DOCTORADO EN CIENCIAS BIOQUÍMICAS)

Ciudad Universitaria, enero, 2019

Este proyecto fue apoyado por el Consejo Nacional de Ciencia y Tecnología (Conacyt), Proyectos ANR-Conacyt 188565 y FC 1122 para Claudia González Espinosa, y DGAPA-PAPIIT-UNAM No. IG200418 para Ricardo Reyes Chilpa. También se contó con una beca de doctorado Conacyt No. 404373 para Jorge Ivan Castillo Arellano (JICA) y apoyo del Programa de Apoyo a los Estudios del Posgrado (PAEP) para la asistencia de JICA a los congresos de células cebadas y de inmunología en 2017 y 2018 en el Programa de Doctorado en Ciencias Bioquímicas de la UNAM. De la investigación contenida en esta tesis, la parte de purificación y caracterización química de los compuestos se llevó a cabo en el laboratorio 2-4A del Departamento de Productos Naturales del Instituto de Química de la Universidad Nacional Autónoma de México (UNAM), mientras que todas las pruebas biológicas *in vitro* e *in vivo* se llevaron a cabo en el laboratorio no. 11 del Departamento de Farmacobiología del Centro de Investigación y de Estudios Avanzados del Instituto Politécnico Nacional (Cinvestav-IPN), Unidad Sede Sur.

## Agradecimientos

A mi comité tutoral, formado por la Dra. Claudia González Espinosa del Cinvestav, por su apoyo, por todos sus consejos y enseñanzas durante los últimos 7 años. Al Dr. Ricardo Reyes Chilpa del Instituto de Química, por su amistad, sus consejos y por todo el apoyo en la parte química. Al Dr. José Pedraza Chaverri de la Facultad de Química, por su apoyo en la revisión de los tutorales y en los experimentos finales.

Un agradecimiento especial a la Dra. Isabel Arrieta Cruz del Instituto Nacional de Geriatría y a su alumna Ana Lilia López Alcantara, por su apoyo en la obtención del matarique de Chihuahua, la purificación de los cacalólidos y la publicación del artículo.

A los profesores que me evaluaron en el examen de candidatura y los que fungieron como sinodales del examen de titulación, la Dra. Marina Macías Silva, el Dr. Enrique Ortega Soto, la Dra. Silvia Laura Guzmán Gutiérrez, el Dr. José Guillermo Ávila Acevedo, la Dra. María Eugenia Gonsebatt Bonaparte y la Dra. Paula Licona Limón.

Del Cinvestav al M. en C. Alfredo Ibarra Sánchez y al técnico Rodolfo Pérez Lagunes del laboratorio 11 de la Sede Sur, al Dr. Jorge Fernández, a Ricardo Glaxiola Centeno, a Víctor Manuel García Gómez, a Benjamín E. Chávez Álvarez, a María Antonieta López López y a Ramón Gómez Martínez del Bioterio UPEAL.

Del Instituto de Química a los investigadores que operan los equipos de resonancia magnética nuclear Dra. Beatriz Quiroz García y de espectrometría de masas Dr. Javier Pérez Flores. A los técnicos M. en C. Antonio Nieto Camacho del laboratorio de pruebas biológicas, al M. en C. Simón Hernández Ortega del laboratorio de cristalografía de rayos X y a la M. en C. Lucía del Carmen Márquez Alonso del laboratorio de cromatografía.

## Dedicatoria

A mi familia.

A mis compañeros de laboratorio 11 de Farmacobiología del Cinvestav Sur Marian, Itzel, Karla, Abraham, Pablo, Eduardo, Nancy, Frida, Zyanya, Deysi, Marbella y Dulce.

A mis compañeros del laboratorio 2-4A del Instituto de Química Diane, Ana Lilia, Rocío, Juan Carlos, Félix, Edgar, Itzel, Dulce, Miriam, Griselda, Ignacio, Alfredo, Lucía, Paola, Karina, Karla, Laura, Mishel, Alma y Heidi.

## Lista de abreviaturas

**$(CD_3)_2CO$.** Acetona deuterada.
**$[Ca^{2+}]i$.** Concentración intracelular de calcio.
**$^{13}$C-RMN.** Resonancia magnética nuclear de carbono.
**$^{1}$H-RMN.** Resonancia magnética nuclear de protón.
**DNA.** Ácido Desoxirribonucleico.
**PCA.** Anafilaxia pasiva cutánea.
**RNA.** Ácido Ribonucleico.
**BMMCs.** Células cebadas derivadas de médula ósea.
**BSA.** Albúmina sérica bovina.
**CC** y **MCs.** Células cebadas.
**CCF.** Cromatografía de capa fina.
**CCL2.** C-C motif chemokine 2.
**$CDCl_3$.** Cloroformo deuterado.
**CG-EM** y **GC-MS.** Cromatografía de gases acoplada a una espectrometría de masas.
**COX-2.** Enzima cicloxigenasa 2.
**DAG.** Diacilglicerol.
**DCF-DA.** Diacetato de diclorofluoresceína.
**DHE.** Dihidroetidio.
**DMSO.** Dimetilsulfóxido.
**DNP-HSA.** Dinitrofenol acoplado a albúmina sérica humana.
**DPI.** Cloruro de difenileneiodonio.
**DPPH.** 2,2-difenil-1-picrilhidrazilo.
**eNOS o NOS3.** Sintasa de óxido nítrico 3-endotelial.
**ROS.** Especies reactivas de oxígeno.
**Eth.** Etidio.
**FcεRI.** Receptor de alta afinidad de la inmunoglobulina IgE.
**$FeSO_4$.** Sulfato de hierro.
**FURA-2AM.** Éster Fura-2-acetoximetílico.
**GM-CSF.** Factor estimulante de colonias de macrófagos y granulocitos.
**$H_2O_2$.** Peróxido de hidrógeno.
**HPLC.** Cromatografía de líquidos de alta resolución.
**IgE/Ag.** Complejo de inmunoglobulina tipo E y su antígeno.
**IL-13.** Interleucina 13.
**IL-1β.** Interleucina 1-beta.
**IL-3.** Interleucina 3.
**IL-4.** Interleucina 4.
**IL-6.** Interleucina 6.
**IL-8.** Interleucina 8.
**i.p.** Vía intraperitoneal.
**LDH.** Enzima lactato deshidrogenasa.
**$LTC_4$.** Leucotrieno C4.
**LTCC.** Canales de calcio tipo L.
**MPO.** Enzima mieloperoxidasa.
**NADPH.** Nicotinamida adenin nucleótido.
**nNOS o NOS1.** Sintasa de óxido nítrico 1-neuronal.
**NOX.** Enzima NADPH oxidasa.
**$O_2^{\cdot -}$.** Anión superóxido.
**$O_2^1$.** Oxígeno singulete.
**$O_3$.** Ozono.
**$OH^{\cdot}$.** Radical hidroxilo.
**$ONOO^-$.** Radical peroxinitrito.
**PI3K.** Fosfatidil inositol 3 cinasa.
**$PIP_3$.** Fosfatidil-inositol 3,4,5 trifosfato.
**PLCγ.** Fosfolipasa C.
**RE.** Retículo endoplásmico.
**ROCE.** Receptor Operated Calcium Entry.
**RT-PCR.** Transcriptasa reversa acoplada a Reacción en cadena de la polimerasa.
**SERCA.** ATPasa del retículo endoplásmico/sarcoplásmico.
**SOCE.** Store Operated Calcium Entry.
**STIM1.** Stromal interaction molecule 1.
**Thap.** Lactona sesquiterpénica Tapsigargina.
**TNF.** Factor de necrosis tumoral.
**TPA.** 12-O-tetradecanoilforbol-13-acetato ó Forbol Miristato Acetato (PMA).
**XO.** Enzima xantina oxidasa.

## CONTENIDO

## Indice de figuras

## 1.1. Abstract

**Background:** Mast cells (MCs) are important effectors in allergic reactions since they produce a number of pre-formed and de *novo* synthesized pro-inflammatory mediators in response to the high affinity IgE receptor (FcεRI) crosslinking. IgE/Antigen-dependent degranulation and cytokine synthesis in MCs have been recognized as relevant pharmacological targets for the control of deleterious inflammatory reactions. Despite the relevance of allergic diseases worldwide, efficient pharmacological control of mast cell degranulation has been elusive. Natural products can be a rich source of news molecules with anti-inflamatory activity.

**Aim:** In this work, the natural compounds jacareubin, cacalol, cacalone, cacalol acetate, maturin acetate and isoquercitrin were isolated from four medicinal plants, and their effect on main molecular activation parameters on bone marrow-derived mast cells (BMMCs) were evaluated.

**Material and methods:** Jacareubin was isolated from heartwood of tropical tree *Calophyllum brasiliense*. Cacalol and cacalone were isolated from roots of *Psacalium decompositum*, cacalol and maturin were produced by cacalol acetylation. Maturin acetate was isolated from roots of *P. peltatum*. Isoquercitrin was obtained from SIGMA. The identity and purity of the compounds was determined by $^{1}H$, and $^{13}C$ NMR, as well as GC-MS and HPLC-MS. β-hexosaminidase enzyme release from BMMCs treated with different concentrations of the compounds or vehicles, was determined using a colorimetric method. ROS production in BMMCs pretreated with jacareubin or cacalol was determined by fluorometric oxidation of DCF. Fluorometry (using FURA-2AM) in BMMCs pre-treated with jacareubin or cacalol allowed the determination of the mobilization of $Ca^{2+}$, which is essential for the degranulation process. Finally, two models were used to evaluate the anti-inflammatory activity of jacareubin *in vivo*: passive cutaneous anaphylaxis and ear edema induced by TPA in mouse.

**Results:** Among the six compounds evaluated, jacareubin and cacalol were the most efficient inhibitors of degranulation induced by IgE/Ag. These molecules blocked β-hexosaminidase release in a dose-response manner. Both blocked extracellular calcium influx triggered by IgE/Ag complexes. In addition, jacareubin also inhibited calcium influx triggered by the SERCA ATPase inhibitor thapsigargin (Thap). The inhibition of calcium entry correlated with a blockage on the reactive oxygen species (ROS) accumulation in MC. Anti-oxidant activity of jacareubin was determined by oxidation of DPPH, and was higher than that showed by α-tocopherol and caffeic acid, but similar to trolox. Jacareubin also showed inhibitory activity on xanthine oxidase (XO), but not on NADPH oxidase (NOX). Jacareubin inhibited passive anaphylactic reactions and TPA-induced edema in mice.

**Conclusion:** Our data demonstrate that jacareubin and cacalol are potent natural compounds, able to inhibit anaphylactic degranulation in mast cells by blunting FcεRI-induced calcium flux needed for secretion of granule content. Inhibition of calcium flux with both compounds is associated with blockage of ROS production in MC. Additionally jacareubin inhibit MC-dependent inflammation *in vivo*. Therefore, these compounds could be efficient anti-oxidant, anti-allergic, and anti-inflammatory molecules.

## 1.2. Resumen

**Antecedentes:** Las células cebadas (CC) son importantes efectores en las reacciones alérgicas, debido a que producen diversos mediadores pro-inflamatorios en respuesta a la activación del receptor de alta afinidad para la IgE (FcεRI) por complejos formados por la inmunoglobulina tipo E (IgE) y antígenos específicos (Ag). El proceso de exocitosis de mediadores pre-formados (desgranulación) ha sido propuesto como un blanco farmacológico relevante para el control de las alergias y otras reacciones inflamatorias controladas por las CC. A pesar de la gran prevalencia de los padecimientos alérgicos en el mundo, no se ha desarrollado aún ninguna estrategia farmacológica eficiente para controlar la desgranulación de las CC. Los productos naturales representan una fuente importante de moléculas con potencial efecto anti-inflamatorio.

**Objetivo:** Evaluar el efecto de los productos naturales: jacareubina, cacalol, cacalona, acetato de cacalol, acetato de maturina e isoquercitrina, sobre los principales parámetros de activación de CC derivadas de médula ósea de ratón (BMMCs), describiendo su mecanismo de acción a nivel molecular.

**Materiales y métodos:** La jacareubina fue aislada del duramen de la madera del árbol *Calophyllum brasiliense*. El cacalol y la cacalona fueron aislados de las raíces de *Psacalium decompositum*, el acetato de cacalol fue producido por modificación química a partir del cacalol. El acetato de maturina fue aislado de la raíz de *P. peltatum.* La isoquercitrina fue comprada a SIGMA. Se determinó la liberación de la enzima β-hexosaminidasa de BMMCs tratadas con los vehículos o diferentes concentraciones de los compuestos utilizando un método colorimétrico. La producción de ROS en BMMCs pretratadas con jacareubina o cacalol se determinó mediante la oxidación fluorométrica de DCF. Se determinó la actividad anti-oxidante de la jacareubina por oxidación de DPPH y la actividad enzimática de la xantina oxidasa. Mediante fluorometría (usando FURA-2AM) se determinó la movilización de $Ca^{2+}$, indispensable para el proceso de desgranulación, en BMMCs pre-tratadas con jacareubina o cacalol. Finalmente, se utilizaron dos modelos murinos para evaluar la actividad anti-inflamatoria de la jacareubina *in vivo*: el modelo de anafilaxia pasiva cutánea y el modelo de edema en el pabellón auricular, inducido por TPA.

**Resultados:** De los seis compuestos evaluados, la jacareubina y el cacalol fueron los inhibidores más eficientes de la desgranulación inducida por IgE/Ag. Ambos compuestos también fueron capaces de bloquear la movilización de $Ca^{2+}$ intracelular inducido por el IgE/Ag y, en el caso de la jacareubina, también por un inhibidor de la ATPasa del retículo endoplásmico (tapsigargina). La inhibición de la entrada de $Ca^{2+}$ observada con los dos compuestos estuvo asociada con el bloqueo de la acumulación de especies reactivas de oxígeno (ROS) en CC. La jacareubina tuvo una mayor capacidad antioxidante que los utilizados como referencia: el α-tocoferol, el trolox, el ácido cafeico y el cacalol. La jacareubina también mostró actividad inhibidora sobre la xantina oxidasa, pero no sobre la actividad de la NADPH oxidasa (NOX). *In vivo,* la jacareubina fue capaz de inhibir de una forma dependiente de la dosis la reacción inflamatoria en el modelo de anafilaxia pasiva cutánea y en el modelo de edema del pabellón auricular inducido por TPA.

**Conclusión:** La jacareubina y el cacalol son compuestos naturales capaces de inhibir de manera potente la desgranulación anafiláctica en células cebadas mediante el bloqueo de la movilización de $Ca^{2+}$ necesaria para la secreción del contenido granular. La inhibición está asociada al bloqueo en la producción de ROS que, en estas células, precede a la movilización de calcio. La jacareubina es, además, un compuesto que previene la inflamación dependiente de las CC *in vivo*, lo que sugiere que estos dos compuestos pueden ser eficientes moléculas anti-oxidantes, anti-alérgicas y anti-inflamatorias.

## 2. Introducción

### 2.1. Inflamación y alergia

Las alergias constituyen un importante problema de salud pública en el mundo. Cerca de 40% de personas padecen algún tipo de alergia, que puede manifestarse como rinitis alérgica (10-30 % en adultos), alergia a los alimentos (8 % en niños), alergia a los animales (15 % a los gatos y 10 % a los perros) [1,2]. Hasta la fecha no existe un tratamiento efectivo para curar este tipo de condiciones [3], y los que existen actualmente están dirigidos a calmar de manera paliativa los síntomas causados por el estado inflamatorio que ocurre en el desarrollo del episodio alérgico [4]. Las evidencias experimentales sugieren que las alergias están asociadas con el desarrollo de múltiples enfermedades crónico degenerativas, como la atopia [5], la enfermedad pulmonar obstructiva crónica (COPD) [6], el asma crónica y algunos tipos de cáncer [7–9].

### 2.2. Células cebadas

Las células cebadas (CC) son el principal tipo celular responsable de la reacción inflamatoria en las reacciones de hipersensibilidad tipo I [10]. Los alérgenos (antígenos) presentes en el ambiente son reconocidos por anticuerpos IgE, los cuales se unen al receptor de alta afinidad de IgE (FcεRI) que está presente en la membrana de las CC [11,12]. Esto lleva a la activación de una compleja cascada de señalización que induce la rápida exocitosis de compuestos pre-formados por un proceso llamado desgranulación anafiláctica. Además, ocasiona la síntesis de

mediadores pro-inflamatorios derivados del ácido araquidónico y la producción de citocinas proinflamatorias [13].

Las células cebadas (CC) se derivan de las células progenitoras hematopoyéticas mieloides $CD13^+$, $CD34^+$, $CD117^+$ de la médula ósea (Figura 1), que migran aún en un estado inmaduro a prácticamente todos los tejidos vascularizados y completan su maduración bajo la influencia de mediadores producidos localmente [14].

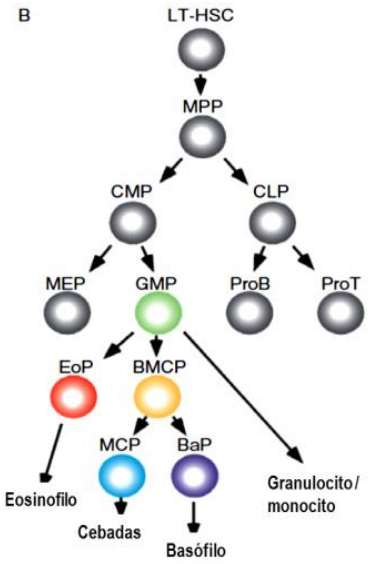


**Figura 1. Linaje y proceso de maduración de células cebadas a partir de una célula pluripotente de médula ósea (LT-HSC).**

Pero no solo el entrecruzamiento del receptor de la IgE con su antígeno induce la desgranulación anafiláctica en CC. También existen anafilotoxinas (fracción C5a del complemento y el compuesto 48/80 del veneno de abeja), neuropéptidos (sustancia P) y compuestos de bajo peso molecular como la tapsigargina y el ionóforo de calcio A23187 que la inducen [13].

Las CC tienen un papel esencial en la hipersensibilidad por contacto a través de una compleja interacción con diferentes tipos de células inmunes, que incluyen: células presentadoras de antígeno, linfocitos T y B, células NK, queratinocitos, células del endotelio y plaquetas [13].

## 2.3. Vía canónica de activación del FcεRI

Después de la unión del antígeno a la IgE en el receptor FcεRI, inmediatamente las cinasas de tirosinas Lyn y Fyn se activan y permiten la fosforilación de la cadena β del receptor. Esto establece sitios de unión para la proteína cinasa Syk, que se asocia a la cadena β y es activada por autofosforilación y por fosforilación dependiente de Lyn. Syk fosforila algunas proteínas adaptadoras como GAB2 y LAT. GAB2 media la activación de la fosfatidil inositol 3 cinasa (PI3K), que promueve la acumulación membranal del fosfatidil-inositol 3,4,5 trifosfato ($PIP_3$) y el re-arreglo del citoesqueleto para la secreción de gránulos. Por otro lado, la fosforilación de LAT lleva a la activación de la fosfolipasa C (PLCγ) que cataliza la producción de diacilglicerol (DAG) y fosfatidilinositol-3-fosfato ($IP_3$), para la liberación de calcio ($Ca^{2+}$) desde el retículo endoplásmico (RE). El vaciamiento de $Ca^{2+}$ del retículo endoplásmico lleva a la agregación del sensor de $Ca^{2+}$ llamado STIM1 en la membrana del RE, y su asociación con canales de $Ca^{2+}$ membranales como Orai y TRPC, permitiendo el rellenado de los almacenes intracelulares de $Ca^{2+}$ en un proceso conocido como “Store Operated Calcium Entry” (SOCE) [15–18]. La activación del FcεRI también provoca un rápido incremento de la concentración de especies reactivas de oxígeno (ROS) producidas por la NADPH oxidasa, la xantina oxidasa y la cadena respiratoria en la mitocondria [19–21]. Finalmente, los ROS activan (por un mecanismo que aún no ha sido bien definido) canales de calcio membranales activados por el receptor, iniciando una entrada de calcio denominada “Receptor Operated Calcium Entry” (ROCE), como los canales de calcio tipo L (LTCC como CaV1.2, CaV1.3 y CaV1.4) [22–24]. Es importante mencionar que la SOCE puede ser activada de manera independiente de la ROCE inhibiendo la enzima ATPasa del

RE con una lactona sesquiterpénica aislada de la planta *Thapsia garganica* (Apiaceae), llamada Tapsigargina (Thap). Esta molécula ocasiona el vaciamiento del RE y activa la entrada de $Ca^{2+}$ a través de Orai, sin activar a la ROCE (Figura 2). La movilización de $Ca^{2+}$ intracelular favorece la reorganización de actina y tubulina del citoesqueleto, lo que lleva a la fusión y liberación del contenido molecular pro-inflamatorio de las vesículas, en un evento conocido como desgranulación anafiláctica [25] y la síntesis de *novo* de citocinas pro-inflamatorias, prostaglandinas y leucotrienos, que llevan al reclutamiento de otras células del sistema inmune y a un estado alérgico agudo [26].

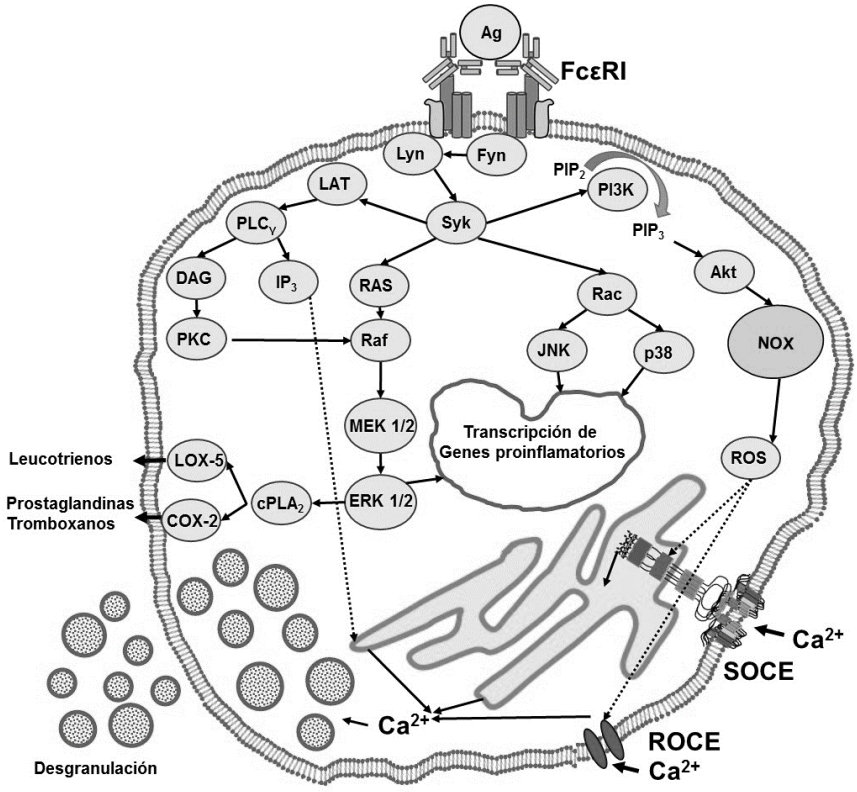


**Figura 2. Esquema general de la vía de señalización canónica del receptor FcεRI en células cebadas** [27,28].

## 2.4. Producción de especies reactivas de oxígeno (ROS).

Históricamente las especies reactivas de oxígeno (ROS) fueron vistas como sustancias tóxicas causantes del daño a biomoléculas, sin embargo, ahora se reconoce que las células utilizan los ROS para una variedad de mecanismos, tanto así, que los ROS sirven como importantes moléculas de señalización tanto en condiciones fisiológicas normales, como en condiciones de estrés [29].

Los ROS celulares pueden originarse como una consecuencia de exposición a factores ambientales, como los oxidantes químicos o la radiación de alta energía, pero también pueden ser producidas a propósito por enzimas endógenas como la NADPH oxidasa (NOX) y las oxidasas duales (DUOX). Alternativamente, las ROS pueden generarse como bioproductos o a través de reacciones no deseadas [29].

Importantes fuentes de ROS incluyen a enzimas del metabolismo del ácido araquidónico como las ciclooxigenasas, lipoxigenasas y el citocromo P450; enzimas catabólicas como la xantina oxidasa, citocromos de la cadena transportadora de electrones y oxidoreductasas del retículo endoplásmico (RE) que permiten el plegamiento de proteínas como las familias de proteínas ER oxidasa (Ero) y la quiescinsulfidrilo oxidasa (QSOX) [29].

Mientras que las ROS pueden producirse de forma compartamentalizada, algunas especies como el $H_2O_2$ puede cruzar las membranas celulares y facilitar su transporte a través de ciertos tipos de acuaporinas, extendiendo así su rango de difusión. En adición, células inmunes como los neutrófilos, poseen proteínas NOX sobre la membrana plasmática que puede generar grandes cantidades de superóxido extracelular. Así las fuentes endógenas de ROS pueden por lo tanto

actuar de una manera parácrina y potencialmente causar un daño oxidativo a otras células. En efecto los fagocitos expresan altos niveles de NOX2, y son capaces de producir a nivel milimolar de superóxido cuando fagocitan partículas como parte del mecanismo de defensa antimicrobiana, representando a la enzima NOX como la fuente más potente de ROS en este tipo celular. En todas las células, los complejos mitocondriales I y III de la cadena respiratoria producen ROS como un efecto secundario no deseado del transporte de electrones durante la fosforilación oxidativa [29].

Se estima que, bajo condiciones normales, la concentración de superóxido mitocondrial es 5-10 veces más alta que en el citosol y el núcleo, y ésta puede incrementarse bajo ciertas condiciones de estrés. Se ha postulado que los ROS mitocondriales contribuyen de manera significativa al daño de lípidos y proteínas que ocurre de manera natural en el envejecimiento y en varias patologías mitocondriales, como algunas cardiomiopatías.

En años recientes, las enzimas involucradas en el plegamiento de proteínas en el retículo endoplásmico se han ido reconociendo como otro sitio importante de producción de ROS. Las proteínas disulfuro isomerasas son las enzimas responsables para la formación del puente disulfuro, pero éste requiere electrones, que al final provienen del oxígeno molecular vía las oxidoreductasas de la familia Ero1 del RE o QSOX, que producen $H_2O_2$ como bioproducto. Cuando las mutaciones incrementan la actividad de Ero1 o cuando la actividad de las oxidoreductasas como Prx4, GPx7 y GPx8 que consume $H_2O_2$ del RE son comprometidas, el RE puede ser peroxidado [29].

## 2.5. Metabolitos secundarios de plantas con actividad anti-inflamatoria y anti-alérgica

La complejidad del sistema de señalización del receptor FcεRI y la falta de conocimiento detallado sobre el mecanismo que induce la producción selectiva de mediadores en CC, han complicado el desarrollo de terapias efectivas para las enfermedades alérgicas y para reacciones inflamatorias que dependen de las CC. Sin embargo, algunos polifenoles derivados de productos naturales han surgido como un importante grupo de agentes químicos con la capacidad de inhibición de las CC [30–34].

Entre los polifenoles aislados de plantas con actividad anti-alérgica recientemente estudiados están: 1) los flavonoides, como la luteolina y sus análogos [35–38], la quercetina [35,39], el resveratrol [40] la epigalocatequina 3-O-galato [41]; 2) Las cumarinas como la escoparona, los tunberginoles A y B, y el artekeiskeanol A [42–44]; 3) Los terpenos y derivados de sesquiterpenos como el timol, la deacetileupaserrina, la dehidroleucodina, la xantantina y el partenolido [27,45–47]; 4) las xantonas, encontradas en los frutos del mango y el mangostán, como la nujiangexantona A, las α-, γ-, y β-mangostinas y la mangiferina [48,49].

## 2.6. Mecanismos moleculares de inhibición de la inflamación por metabolitos secundarios conocidos.

Los metabolitos secundarios se clasifican de forma general en tres grupos de acuerdo a su origen biosintético en A) derivados del ácido shikímico, B) derivados del ácido mevalónico y C) derivados del ácido malónico. Aunque existen compuestos que se generan por la modificación y fusión de compuestos de los tres grupos mencionados.

Dentro de los compuestos derivados de la vías del ácido shikímico, están los compuestos nitrogenados (Figura 3), como los alcaloides, que han mostrado tener cierto grado de inhibición (5 – 60%) de la desgranulación anafiláctica inducida por IgE/Ag o compuesto 48/80 en células cebadas, reduciendo la fosforilación de proteínas como Syk, p38, Gab2, Akt y NFκB, así como de reducir la síntesis y secreción de citocinas pro-inflamatorias como TNF, IL-1β, IL-4, IL-6, IL-8 y leucotrieno $LTC_4$ [50–52].

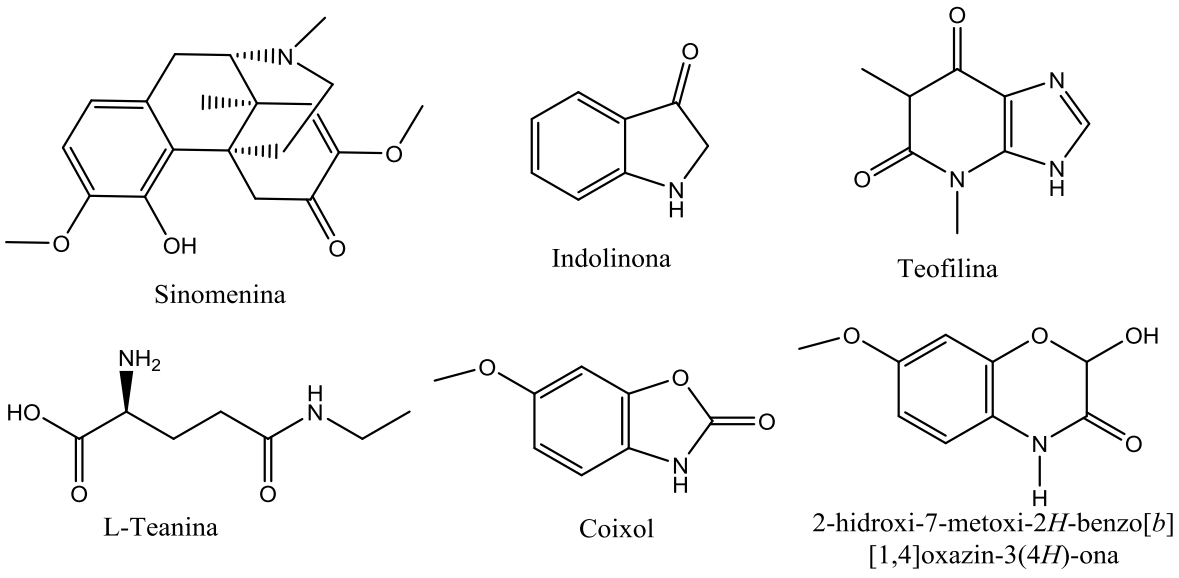


**Figura 3. Ejemplos de compuestos nitrogenados derivados de productos naturales que inhiben la desgranulación de las células cebadas.**

En el grupo de las cumarinas existen varios compuestos (Figura 4) con actividad inhibitoria (80 – 96%) de la desgranulación como es el caso de los tunberginoles A, B y F [50,53,54], el psoraleno [55], la escoparona [56] y el artekeiskeanol A[44], mostraron disminuir la fosforilación de proteínas como c-Jun, p38, IκB, AKt, JNK y p44/32, además de disminuir importantemente la movilización de $[Ca^{2+}]i$ y evitar la translocación de NFκB. También son capaces de reducir de forma moderada la secreción de citocinas pro-inflamatorias como TNF, IL-4, IL-6, IL-13, prostaglandinas y el leucotrieno LTC4.

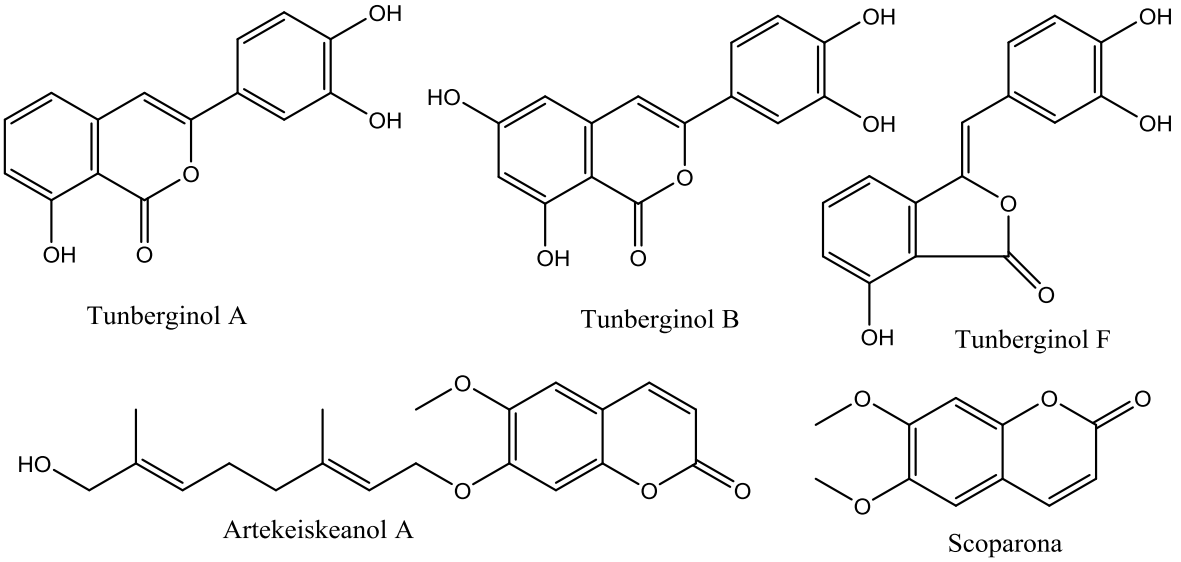


**Figura 4. Ejemplos de cumarinas derivadas de productos naturales que inhiben la desgranulación de las células cebadas.**

Los estilbenos como el piceatanol [57] y el resveratrol [40] (Figura 5) han mostrado tener actividad inhibitoria (78 – 100%) de la desgranulación anafiláctica, mediante la disminución de la fosforilación de Syk, ERK1/2 y NFκB, además de reducir la movilización de $[Ca^{2+}]i$ y la activación de COX-2. También mostraron capacidad para

reducir la expresión y secreción de citocinas pro-inflamatorias tales como TNF, IL-6 e IL-8 [40,57,58].

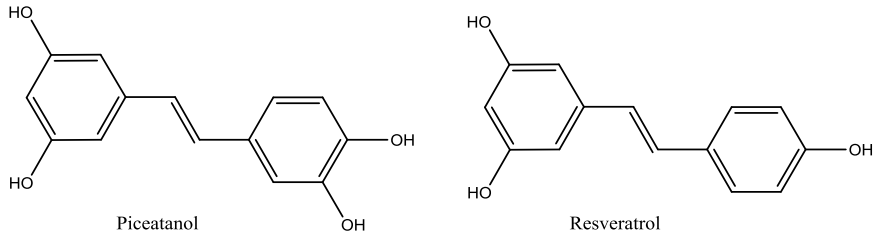


**Figura 5. Ejemplos de estilbenos derivados de productos naturales que inhiben la desgranulación de las células cebadas.**

El grupo de los flavonoides es el que más se ha estudiado y es donde se han encontrado más compuestos (Figura 6) con actividad inhibidora (40 – 95%) de la desgranulación anafiláctica inducida por IgE/Ag, el compuesto 48/80 o la combinación de TPA/A23187, siendo los más conocidos la luteolina [35,36,47,59–61] y su derivado 3´4´5´7-tetrametoxi-luteolina [38], baicaleina [35,62], quercetina[21,35,47,61–64], morina[65] y silibinina[56], entre muchos otros. Los principales mecanismos de bloqueo es mediante la inhibición de la fosforilación de las proteínas Fyn, Syk, LAT, PLCγ, PKC, ERK1/2, JNK y p38, además evitan la translocación nuclear de NFκB, reducen la movilización de $[Ca^{2+}]i$. Adicionalmente reducen la transcripción, biosíntesis y secreción de citocinas pro-inflamatorias como TNF, IL-1β , IL-4, IL-6, quimiocinas como IL-8 y CCL2, factores de crecimiento como GM-CSF. También reducen la transcripción y expresión de COX-2, del receptor FcεRI y la síntesis del leucotrieno $LTC_4$.

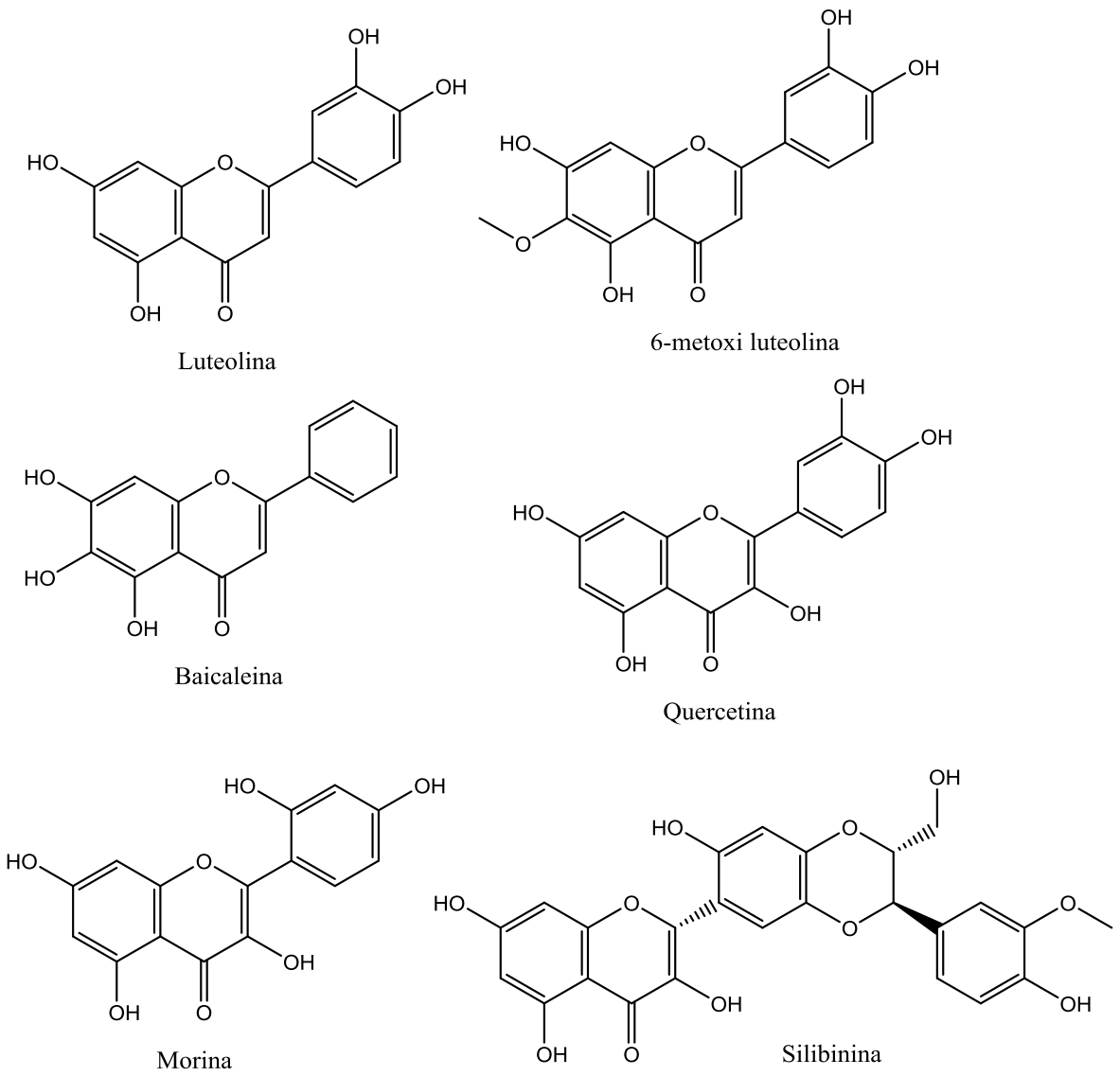


**Figura 6. Ejemplos de flavonoides derivados de productos naturales que inhiben la desgranulación de las células cebadas.**

En el caso de las catequinas la epigalocatequina-3-O-galato[41,66,67] y su derivado metilado[67], poseen actividad inhibidora (85 – 98%) de la desgranulación inducida por el compuesto 48/80, mediante la reducción de la actividad de la NADPH oxidasa y de la movilización de $[Ca^{2+}]i$, además de que estos compuestos reducen la expresión de la sub-unidad β del receptor FcεRI.

Los compuestos derivados de la vía del ácido mevalónico también presentan una gran diversidad con compuestos anti-inflamatorios, en parte debido a su similitud con la estructura del cortisol y los glucocorticosteroides que tienen una actividad anti-inflamatoria. Siendo los terpenos partenolido[45] y cucurbitacina E[68], así como los sesquiterpenos deacetileupaserrina, (3S,6R,7R,8R)-3-hidroxi-8-acetoxisarraceniloxigermacra-1(10),4,11(13)-trien-6,12-olido, (3S,6R,7R,8R)-3-hidroxi-8-(2'-metilbutiroiloxi)-14-oxomelampa-1(10),4-dien-6,12-olido y la eupaformosanina[27] (Figura 7), tienen una actividad inhibidora (60 – 85%) de la desgranulación inducida por IgE/Ag, mediante un mecanismo de inhibición de la fosforilación de p38, Akt y NFκB, reduce parcialmente la movilización de $Ca^{2+}$ intracelular, así como de la formación de microtúbulos dependiente de Fyn.

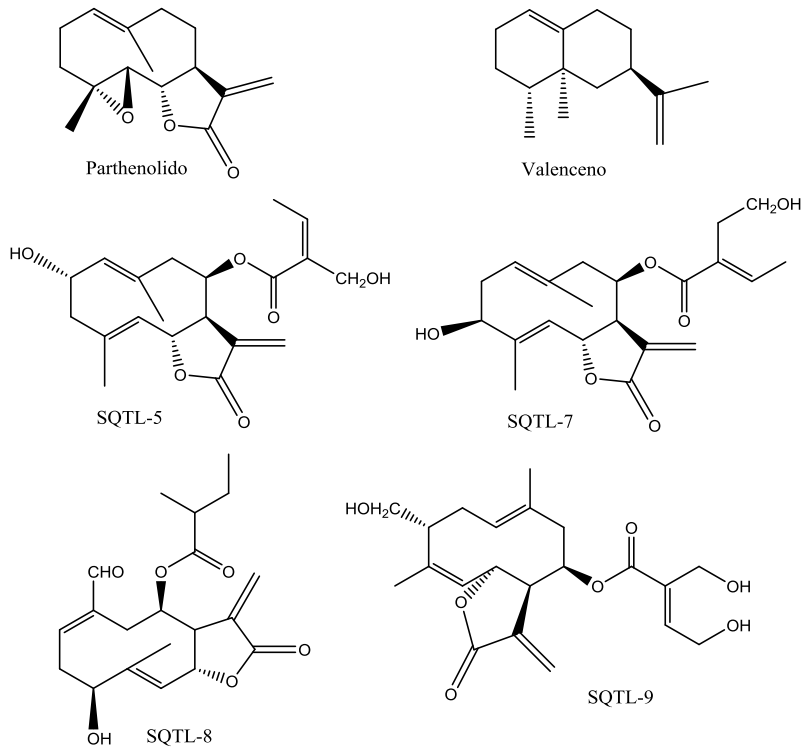


**Figura 7. Ejemplos de terpenos y sesquiterpenos derivados de productos naturales que inhiben la desgranulación de las células cebadas. SQTL-5: deacetileupaserrina. SQTL-7: (3S,6R,7R,8R)-3-hidroxi-8-acetoxisarraceniloxigermacra-1(10),4,11(13)-trien-6,12-olido. SQTL-8: (3S,6R,7R,8R)-3-hidroxi-8-(2'-metilbutiroiloxi)-14-oxomelampa-1(10),4-dien-6,12-olido. SQTL-9: eupaformosanina.**

Finalmente los compuestos derivados de la vía del ácido malónico entre los cuales se encuentran los policétidos como las xantonas, de las cuales hablaremos en este trabajo y se mencionaran con detalle más adelante.

Si bien se han caracterizado los efectos inhibidores de los compuestos derivados de productos naturales, no se conoce con detalle su mecanismo de acción y muchos de ellos no han sido llevados a la clínica por su baja solubilidad o por la presencia de isómeros inactivos difíciles de separar en la purificación, además de la falta de protección mediante algún sistema de propiedad intelectual y el alto costo de desarrollar medicamentos innovadores. Por estas razones, es importante el estudio y caracterización de otros compuestos naturales que pudieran tener (por su potencia, su eficacia y pocos efectos secundarios) un uso en el tratamiento de las alergias.

## 2.7. Xantona Jacareubina (Policétido)

La jacareubina y otras xantonas se encuentran en el duramen de la madera del árbol tropical *Calophyllum brasiliense* (Clusiaceae) donde este ha sido aislado en grandes cantidades. La jacareubina posee actividad fungistática y bacteriostática [69,70], así como una buena actividad citotóxica *in vitro* contra líneas celulares de HeLa y KB [71] (sublínea de células HeLa formadoras de células tumorales queratinizadas) y moderada actividad inhibidora de la $H^+$, $K^+$ ATPasa [72].

La jacareubina (Figura 8) fue descrita por primera vez en 1953 en la madera del árbol *Calophyllum brasiliense* [73,74] y ha sido propuesto como un marcador

quimotaxonómico para identificar la madera del duramen de múltiples especies del género *Calophyllum* [75–77]. Se ha demostrado previamente el papel antioxidante de la jacareubina y la xantona V, puesto que se ha evaluado su capacidad para atrapar iones oxidantes como $O_2^{\cdot -}$, $OH^{\cdot}$ y $ONOO^-$, de una forma dependiente de la concentración en el rango micromolar evitando la oxidación de proteínas, DNA o lípidos. Sin embargo estas moléculas son incapaces de atrapar el $H_2O_2$ [78].

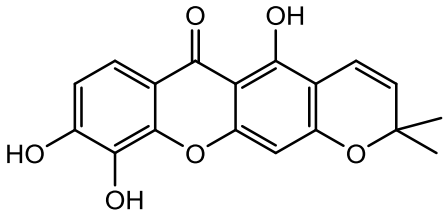


**Figura 8. Jacareubina**

## 2.8. Cacalólidos o eremofilanos (Sesquiterpenos)

Los cacalólidos son sesquiterpenos que han sido encontrados de forma abundante en plantas del género *Psacalium* (Asteraceae), siendo *P. decompositum* el más estudiado, debido a que ha sido usado como remedio en la medicina tradicional por campesinos y comunidades de la etnia Rarámuri en el estado de Chihuahua México, donde se consume la infusión de la raíz y el rizoma para tratar condiciones tales como enfermedades reumáticas, dolor, enfermedades renales y hepáticas, neuralgia, úlceras y resfriado. Estos órganos contienen cacalólidos sesquiterpenoides como cacalol, cacalona, epicacalona, maturina, 3-hidroxi-cacalolido, epi-3-hidroxi-cacalólido [79–81]. Los compuestos cacalol y cacalona (Figura 9) han mostrado ser los compuestos más activos al inhibir la inflamación producida en los modelos de edema inducido por carragenina en pata de rata, así como en el

edema inducido por TPA en la oreja de ratón [82]. En el mercado Sonora de plantas medicinales de la ciudad de México la raíz de *P. decompositum* es comúnmente sustituido por raíz de *P. peltatum* que crece en los bosques de pino cercanos a la ciudad, ambos se utilizan como remedio antidiabético debido a sus propiedades como hipoglucemiante [80], ambas especies son conocidas como “matarique” y las raíces y el rizoma del segundo también contienen cacalólidos, como maturina, acetato de maturina y maturinina, pero no presentan cacalol y cacalona [83].

El sesquiterpeno cacalol ha mostrado tener propiedades antioxidantes dirigidas específicamente contra el oxígeno singulete ($O_2^1$) y el ozono ($O_3$), pero no mostró actividad con el $H_2O_2$, ni tampoco con el superóxido ($O_2^{\cdot -}$) [84].

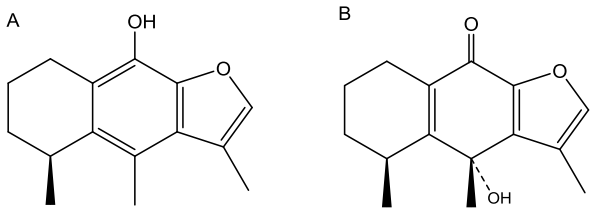


**Figura 9. A) cacalol y B) cacalona.**

## 2.9. Isoquercitrina o glucósido de quercetina (Flavonoide).

Otra planta utilizada en la medicina tradicional mexicana para tratar problemas inflamatorios asociados a CC es *Argemone platyceras* (Papaveraceae), también conocida como “Chicalote”, es una planta herbácea anual de amplia distribución en México y donde la infusión de los botones florales ha sido utilizado por grupos étnicos mazahuas y otomíes del estado de México como remedio para la tos, bronquitis y neumonía, está planta posee dos compuestos con propiedades anti-inflamatorias: la rutina y la isoquercitrina [85] (Figura 10).

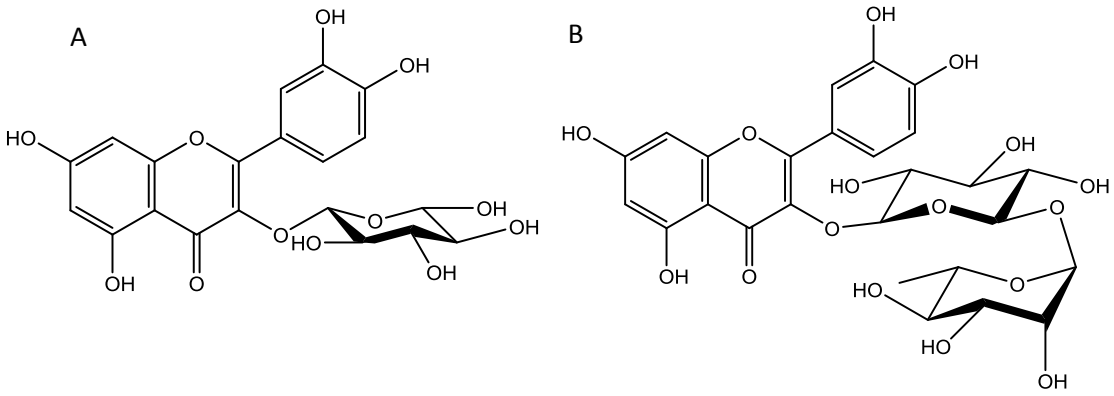


**Figura 10. A) Isoquercitrina y B) rutina.**

## 3. Planteamiento del problema

Hasta la fecha se carece de herramientas farmacológicas efectivas para el control de la desgranulación producida por el sistema de señalización del receptor FcεRI de las CC, debido a diversos factores, entre los que se encuentran la falta de conocimiento sobre el mecanismo de acción de los compuestos con actividad anti-inflamatoria. Por otro lado, la caracterización de nuevas moléculas capaces de inhibir la desgranulación, así como el conocimiento de los mecanismos de inhibición de esos principios activos, permitirá generar conocimiento de cómo la activación de un receptor membranal ocasiona la exocitosis de diversos compuestos celulares, permitiendo generar estrategias terapéuticas más eficientes para los padecimientos inflamatorios agudos y crónicos donde participan las CC.

## 4. Justificación

La secreción de citocinas y otros mediadores inflamatorios inducida por la activación del receptor FcεRI en las CC contribuye al desarrollo y mantenimiento de reacciones inflamatorias agudas y crónicas que pueden ser deletéreas. En este proyecto de investigación se pretende utilizar algunos compuestos naturales para caracterizar detalles importantes del acoplamiento del receptor FcεRI con la producción de mediadores inflamatorios en ese tipo celular. De manera particular, se utilizarán seis compuestos de origen natural cuya estructura química permite hipotetizar que pueden presentar actividad anti-inflamatoria (Figura 11).

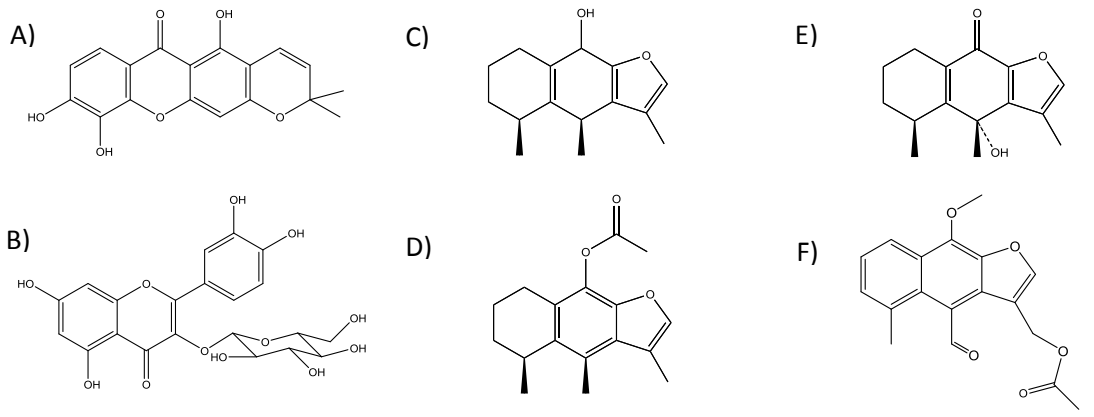


**Figura 11. Compuestos derivados de productos naturales que se utilizaron en este trabajo de investigación. A) Jacareubina (*Calophyllum brasiliense*); B) Isoquercitrina (*Argemone platyceras*); C) Cacalol; D) Acetato de cacalol; E) Cacalona; F) Acetato de maturina (*Psacalium decompositum* y *P. peltatum*).**

## 5. Hipótesis

1. Los compuestos jacareubina, cacalol, cacalona, acetato de cacalol, acetato de maturina e isoquercitrina tendrán efectos inhibidores sobre la secreción de mediadores pro-inflamatorios en las células cebadas estimuladas a través del receptor FcεRI.
2. Los compuestos ejercerán la inhibición a través de bloquear los sistemas de producción de radicales libres requeridos para la activación de las CC.

## 6. Objetivo general

Analizar la posible actividad inhibidora de los compuestos jacareubina, cacalol, cacalona, acetato de cacalol, acetato de maturina e isoquercitrina, sobre la liberación de mediadores inflamatorios estimulada por el receptor FcεRI en las CC, utilizando modelos *in vitro* e *in vivo*.

### 6.1. Objetivos particulares

1. Purificar e identificar, por métodos espectroscópicos, de los compuestos jacareubina, cacalol, cacalona, acetato de cacalol, acetato de maturina e isoquercitrina de sus fuentes naturales.
2. Determinar la capacidad de inhibición de la desgranulación de los compuestos jacareubina, cacalol, cacalona, acetato de cacalol, acetato de maturina e isoquercitrina.
3. Evaluar si el efecto anti-inflamatorio de los compuestos probados más activos incluye la modulación de la movilización de $Ca^{2+}$ a través de los sistemas ROCE y SOCE activados por el receptor FcεRI en las CC.
4. Determinar el efecto anti-inflamatorio de los compuestos más activos probados en la modulación de la producción de especies reactivas de oxígeno inducidas por el receptor FcεRI en CC.
5. Probar *in vivo* el compuesto natural más activo entre la jacareubina, cacalol, cacalona e isoquercitrina en un modelo murino de anafilaxia pasiva cutánea desencadenada por las CC y en un modelo *in vivo* de inflamación independiente.

## 7. Materiales y métodos

### 7.1. Reactivos

El anticuerpo monoclonal tipo E anti-dinitrofenol (IgE), diacetato de 2´7´-diclorofluoresceína (DCF-DA), dinitrofenol-albumina sérica humana (DNP-HSA), colorante azul de Evans, peróxido de hidrógeno ($H_2O_2$), 12-O-tetradecanoilforbol-13-acetato (TPA), hexadecil-trimetil-amonio bromuro (HTAB), N,N-dimetilformamida (DMF), Igepal, buffer de sales de fosfato (PBS), α-tocoferol, ácido cafeico, 3,3´,5,5´,tetrametil-benzidina (TMB), dihidroetidio (DHE), trizma base, HCl, tritón X-100, EDTA, NaF, EGTA, fenilmetano-sulfonil fluoruro, cadena simple de ácido deoxiribonucléico de salmón, nicotinamida adenin nucleótido (NADPH), HEPES, cloruro de difenileneiodonio (DPI), azul de nitrotetrazolio (NBT), $Na_2CO_3$, quercetina, isoquercetina e indometacina fueron comprados a Sigma-Aldrich (St. Louis, MO, USA), el antioxidante trolox de Calbiochem (San Diego, CA, USA), FURA-2AM de Thermo Fisher Scientific (Waltham, MA, USA), ketamine y xilazine de PISA agropecuaria (Hgo, México), todos los solventes orgánicos fueron comprados de J. T. Baker (Center Valley, PA, USA), el acetato de maturina fue proporcionado por el Dr. Manuel Jiménez Estrada, como se describe en [83], el acetato de cacalol fue proporcionado por el Dr. Ricardo Reyes Chilpa, el método de modificación química por acetilación a partir de cacalol se describen de acuerdo a [86], la jacareubina, el cacalol y la cacalona fueron purificados para este trabajo como se describe a continuación.

## 7.2. Colecta de material vegetal

Un árbol completo de *Calophyllum brasiliense* Cambess (Clusiaceae) fue colectado por J.I. Calzada de la selva Lacandona, Chiapas, México [87]. La identificación fue hecha por el colector, un ejemplar de herbario (JIC-3116) y una muestra de madera (00011-XALw) fueron depositados en el Herbario y Xilarium "Dr. Faustino Miranda", del Instituto de Ecología, A.C. en Xalapa, Veracruz, Méx.

Raíces de *Psacalium decompositum* fueron colectadas de acuerdo a lo descrito previamente [88].

## 7.3. Métodos espectroscópicos y espectrométricos

### 7.3.1. Purificación de la jacareubina

Tablones de madera de *C. brasiliense* fueron almacenados a temperatura de habitación, donde una parte fue convertida en virutas de madera (711.5 g), las cuales fueron extraídas con metanol exhaustivamente hasta agotamiento, el solvente del extracto fue destilado utilizando un rotaevaporador con vacío. El extracto seco (74 g) fue fraccionado por cromatografía en columna utilizando sílica gel 60, 1 Kg (Merck; Darmstadt, Germany) eluyendo con una fase móvil de hexano-acetato de etilo (7:3). El análisis de las fracciones se llevó a cabo por cromatografía de capa fina (CCF) en placas de sílica G/UV 254, 0.20 mm (Macherey-Nagel; Düren, Germany), las placas fueron observadas en luz ultravioleta 254 nm, 366 nm y finalmente se añadió una solución de sulfato cérico 1% en ácido sulfúrico 2N.

Las fracciones 138-227 formaron una mezcla de tres xantonas, incluída la jacareubina (9.85 g) (Rodríguez-Cabo, 2004), una muestra de 6 g fueron separados por cromatografía en columna, utilizando 120 g de sílica gel 70/230 (Macherey-Nagel; Düren, Germany) para purificar la jacareubina con una fase móvil inicial de hexano e incrementado gradualmente la polaridad con acetato de etilo. Las fracciones eluídas con la mezcla de hexano-acetato de etilo 87:13 correspondieron con la jacareubina la cual cristalizó con acetona, mediante una evaporación lenta.

Los cristales de jacareubina se obtuvieron como prismas rectangulares o cúbicos de 1-5 mm de longitud (figura 12), su punto de fusión fue de 260-270 °C, utilizando un aparato Fisher Johns (Scorpion Scientific; Illinois, USA).

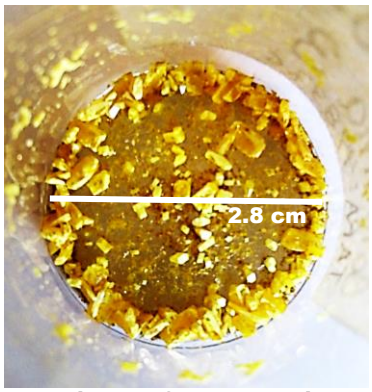


**Figura 12. Cristales de jacareubina obtenidos por cromatografía en columna fase normal.**

Los espectros de Resonancia Magnética Nuclear de la jacareubina fueron registrados con un equipo Bruker AVANCE III HD 700 MHz (Cambridge Isotope Laboratories, MA, USA) por comparación con la literatura [89,90]. $^{1}$H-RMN (700 MHz, $(CD_3)_2CO$). δ 13.55 (1H, s, 1″-OH), 8.94 (2H, s, 5″ y 6″-OH), 7,62 (1H, d, 8-H), 6.99 (1H, d, 1′-H), 6.68 (1H, d, 7-H), 6.33 (1H, s, 4-H), 5.73 (1H, d, 2′-H), 1.47 (6H, s, 4′-CH3, 5′-CH3) y $^{13}$C-RMN (175 MHz, $(CD_3)_2CO$) δ 181.30 (C-9), 161.08 (C-1), 158.67 (C-3), 157.85 (C-4a), 152.25 (C-6), 146.87 (C-5a), 133.23 (C-5), 128.65 (C-2′), 117.47 (C-8), 115.79 (C-7), 114.71 (C-8a), 113.83 (C-1′), 105.21 (C-2), 103.55 (C-9a), 95.52 (C-4), 78.96 (C-3′) y 28.48 (C-4′ y C-5′) (Espectros se encuentran en los

anexos, página 97). Se llevó a cabo una espectrometría de masas utilizando el método de Direct Analysis in Real Time (DART) m/z (%): 327$M^+$+1 (100); 326 (7) $M^+$, utilizando un equipo AccuTOF JMS-T100LC (Tokio, Japan).

La pureza de la jacareubina utilizada, fue determinada por cromatografía de líquidos de alta resolución (HPLC) acoplada a un detector UV–Vis Photo Diode Array y a un espectrómetro de masas Brucker Esquire 6000 (Bruker; Billerica, MA, USA). En los dos casos un pico con retención entre 15.6-16 min fueron observados. El análisis se llevó a cabo utilizando un equipo Agilent 1200 Series Binary SL (Agilent; Santa Clara, CA, USA), se utilizó una columna de sílica gel C-18 de 3.5 µm 100×2.1mm Eclipse Plus (Agilent; Santa Clara, CA, USA), con un detector Waters 2996 UV–Vis Photo Diode Array (Waters; Mildford, MA, USA) y un detector Mass Spectrometer Bruker Esquire 6000 (Bruker; Billerica, MA, USA), con una fase móvil de acetonitrilo-agua (7:3) con ácido acético 0.1%, con un flujo de 0.2 mL/min y temperatura de secado 300 °C.

### 7.3.2. Identificación de la estructura tridimensional de la jacareubina por difracción de rayos X

Este procedimiento se realizó en el laboratorio de rayos X por el técnico académico Simón Hernández ortega. Un prisma amarillo de jacareubina fue seleccionado y montado sobre fibra de vidrio y entonces fue colocado sobre un difractometro Brucker D8 venture (Bruker, Billerica, MA, USA) con una fuente de rayos X con microenfoque en un blanco de cobre (l=1.54178 Å), el detector fue colocado a 50 mm del cristal. Los marcos se recogieron con un ancho de escaneo

de 0.3° en el escaneo w y el tiempo de exposición de 10 s/marco a 150 K. Los marcos fueron integrados utilizando el Bruker SAINT software package (Bruker; Billerica, MA, USA) utilizando un algoritmo de integración marco-cercano. Ausencias sistemáticas e intensidad estadística fueron utilizadas en un grupo de espacio monocíclico. La estructura fue resuelta utilizando el método Patterson con el programa SHELXS-2014/7 [91]. Los átomos restantes se localizaron a través de unos pocos ciclos de refinamientos de mínimos cuadrados y diferencias de mapas de Fourier. Los átomos de hidrógeno se ingresaron en las posiciones calculadas, y se les permitió moverse en los átomos a los que están conectados. Los parámetros térmicos fueron refinados por átomos de hidrógeno sobre los grupos fenilo utilizando un Ueq = 1.2 Å y un Ueq = 1.5 Å para los grupos metilo al átomo precedente en todos los casos. Para todos los complejos, el ciclo final de refinamiento se llevó a cabo en todos los datos distintos de cero utilizando SHELXL-2014/7 [91]. La corrección de la absorción se aplicó usando el programa SADABS. Datos suplementarios para la jacareubina han sido depositados en el Centro de Datos Cristalográficos de Cambridge. Copia de esta información está disponible sin cargo a pedido del Director, CCDC, 12 Union Road, Cambridge CB2 1EZ, UK (fax: +44 1223 336033, email: deposit@ccdc.ac.uk o página de internet http://www.ccd.cam.ac.uk) citando el número de depósito CCDC 1845875.

### 7.3.3. Purificación del cacalol y la cacalona

Raíces y rizomas de *P. decompositum* fueron lavadas con agua y secadas, cortadas en pequeños fragmentos y fueron extraídos con n-Hexano en oscuridad a

temperatura de cuarto hasta agotamiento. Se tomaron 200 mg de extracto y se separaron en una placa preparativa fase normal utilizando una fase móvil de hexano-acetato de etilo (7:3).

Se aislaron 32 mg de cacalol y 15 mg de la cacalona de raíces de *Psacalium decompositum* de acuerdo a lo reportado [88]. El acetato de cacalol fue obtenido por acetilación de cacalol de acuerdo a como lo describe [86]. El acetato de maturina fue purificado como se describió previamente [83]. Los datos de identidad fueron corroborados por $^{1}$H-RMN y/o $^{13}$C-RMN en un equipo Bruker Avance III 300 MHz (Cambridge Isotope Laboratories, MA, USA), o utilizando HPLC Agilent 1200 Series Binary SL (Agilent; Santa Clara, CA, USA) utilizando una columna C-18 de sílica gel 3.5 µm 100 x 2.1 mm Eclipse Plus (Agilent; Santa Clara, CA, USA), con un detector: Waters 2996 UV-Vis Photo Diode Array (Waters; Mildford, Massachusetts, USA), o utilizando un cromatografía de gases acoplados a espectrometría de masas (GC-MS) JEOL GCmate (Peabody, Massachusetts, USA) los datos obtenidos fueron comparados con los reportados en la literatura para los cuatro cacalólidos.

**Cacalol:** $^{1}$H-RMN (300 MHz, $CDCl_3$, δ ppm) 7.24-7.22 (m, 1H), 4.78 (s, 1H), 3.24-3.01 (m, 1H), 2.98 (dd, J = 17.3, 4.9 Hz, 1H), 2.60 (m, 1H), 2.53 (s, 3H), 2.38 (d, 3H), 1.95-1.72 (m, 4H), 1.20-1.19 (d, J = 7.0 Hz, 3H) (Anexos, páginas 98); La CG-EM mostró un pico con una pureza de 93% a 23.9 minutos, este pico correspondió de acuerdo a la EM con el peso molecular del cacalol EI+ MS *m/z* 230 ($M^+$, 58), 215 (100) (Anexos, página 99 y 103), coincidiendo con lo previamente reportado [92].

**Acetato de cacalol:** $^{1}$H-RMN (300 MHz, $CDCl_3$, δ ppm) 7.24-7.23 (d, 1H), 3.29-3.22 (m, 1H), 2.87-2.78 (m, 1H), 2.57 (s, 3H), 2.39 (s, 3H), 2.38-2.37 (d, 3H), 1.94-1.76

(m, 4H), 1.21-1.18 (d, 3H); y $^{13}$C-RMN (75 MHz, ($CDCl_3$, δ ppm) 168.65, 145.18, 141.42, 135.43, 131.42, 127.09, 126.86, 124.93, 116.74, 29.97, 28.92, 23.43, 21.38, 20.49, 16.59, 14.26, 11.27 (Anexos, página 101).

**Mezcla de cacalona y epicacalona:** $^{1}$H-RMN (300 MHz, $CDCl_3$) 7.25 (d, 1H), 3.10-3.06 (m, 1H), 2.87-2.84 (m, OH), 2.49-2.44 (m, 1H), 2.19-2.18 (d, 3H), 1.73-167 (m, 5H), 1.58 (s, 3H), 1.29-1.27 (d, 3H) (Anexos, página 102); La CG-EM mostró dos picos con un área bajo la curva del 78.8% a 26.3 y 27 minutos, estos picos corresponden de acuerdo a la EM con el peso molecular de la cacalona y su isómero la epicacalona. EI+ MS *m/z* 246 ($M^+$, 45 y 60), 231 (70 y 90), 204 (20 y 40), 191 (100) coincidiendo con lo previamente reportado [93,94]. Los otros picos menores se reportan como cacalol y radulifonina B de acuerdo a la fragmentación de la EM (Anexos, páginas 103 y 104) [95].

**Acetato de maturina:** $^{1}$H-RMN (300 MHz, $CDCl_3$, δ ppm) 11.01 (s, 1H), 8.32-8.29 (dd, 1H), 7.84 (s, 1H), 7.43-7.41 (d, 2H), 5.34 (s, 2H), 4.45 (s, 3H), 2.80 (s, 3H), 2.09 (s, 3H) (Anexos, página 105). El HPLC mostró un pico con una pureza de 99% a 29.2 minutos, este pico corresponde de acuerdo a la EM con el peso molecular del acetato de maturina. EI+ MS *m/z* 312 ($M^+$, 100), 254 (90) de acuerdo a Rojano [83].

## 7.4. Animales de experimentación

Se utilizaron ratones C57BL/6J machos (25-30 g de peso), lote no. 000664, que fueron comprados a The Jackson Laboratories (Bar Harbor, ME, USA). Los ratones fueron criados en condiciones de esterilidad (ciclos de luz/oscuridad de 12 horas)

con acceso libre de agua y alimentos en la Unidad de Producción y Experimentación de Animales de Laboratorio (UPEAL) del Centro de Investigación y Estudios Avanzados del Instituto Politécnico nacional (Cinvestav) en la Ciudad de México. Todos los procedimientos con animales fueron aprobados por el Comité Institucional de Ética (CICUAL) del Cinvestav (Protocolo 074-13).

### 7.5. Cultivo y aislamiento de células cebadas derivadas de médula ósea.

Las BMMCs fueron diferenciadas a partir de la médula ósea de tibias y femurs de ratones de la cepa C57BL/6J como ha sido descrito previamente [96]. La médula ósea obtenida fue cultivada en medio RPMI 1640 (Sigma-Aldrich, St. Louis, MO, USA) suplementado con interleucina 3 (IL-3, 10 ng/mL; PeproTech, Rocky Hill, NJ, USA) y 10% de suero fetal bovino (FBS), 100 UI/mL de penicilina, 100 mg/mL de estreptomicina, 50 mM 2-ME y 13 aminoácidos no esenciales (Invitrogen, Carlsbad, CA, USA). Los cultivos fueron mantenidos por 6 semanas hasta su uso y el medio fue cambiado cada 5-7 días. Subsecuentemente, la diferenciación de las BMMCs fue determinada por la detección de la expresión del receptor FcεRI en la membrana plasmática de las células mediante citometría de flujo y por la liberación de β-hexosaminidasa después de la estimulación con IgE/Ag [97]. Solamente los cultivos 98% positivos que expresaron el receptor FcεRI y que mostraron una liberación de β-hexosaminidasa dosis respuesta después de la adición de IgE/Ag fueron utilizados en este estudio. Para cada experimento, las BMMCs fueron sensibilizadas con 100 ng/mL del anticuerpo monoclonal tipo IgE anti-DNP (clona SPE-7; Sigma-Aldrich, St. Louis, MO, USA) por 24 h a 37 °C. De manera rutinaria, después de la

sensibilización, las células fueron colectadas y resuspendidas en medio de cultivo fresco o en buffer Tyrode´s BSA (135 mM NaCl, 5 mM KCl, 1 mM $MgCl_2$, 1.8 mM $CaCl_2$, 5.6 mM glucosa, 0.5 g/L BSA, and 20 mM HEPES pH 7.4) para citotoxicidad y experimentos de calcio. Para los experimentos de producción de ROS, células sensibilizadas fueron lavadas y resuspendidas en buffer Tyrode´s sin BSA.

### 7.6. Solubilización de compuestos para experimentos *in vitro*.

Para la evaluación de los efectos *in vitro* de los compuestos sobre las células cebadas, la jacareubina fue disuelta al 0.1% de etanol, los cacalólidos y la isoquercitrina fueron disueltos al 0.1% de DMSO que se utilizaron como vehículos en todos los experimentos.

### 7.7. Prueba de citotoxicidad en BMMC

Se utilizó un ensayo colorimétrico para la cuantificación de la muerte celular: Cell Lysis Cytotoxicity Detection Kit (LDH, Roche Cat. No. 11 644 793 001, Roche; Mannheim, Germany), siguiendo las instrucciones del proveedor. Se usó el sobrenadante del medio de cultivo libre de células (1 millón de BMMCs) pre-tratadas por 15 min con concentraciones de jacareubina en el rango de 300 pM a 30 µM.

### 7.8. Análisis de la expresión de transcritos de nNOS y eNOS en BMMCs

El RNA total fue aislado de un millón de células o de los órganos y tejidos completos extraídos de los animales (corazón, hígado, riñón, cerebro, bazo, arteria

aorta, arteria renal) siendo lavados previamente con solución salina para quitar la sangre y fueron triturados con tijeras en un tubo estéril. Se añadieron 500 µL de Reactivo Trizol por 5 min en el mismo tubo en el que se hizo el estímulo, sin agitar fuerte, utilizando la punta de la pipeta para resuspender de arriba a abajo y homogenizar el lisado. Posteriormente se transfirió el lisado a un nuevo tubo estéril y se añadió 100 µL de cloroformo, mezclando vigorosamente, permitiendo la separación de fases a temperatura de habitación por 15 min. Posteriormente se centrifugó a 12000 ×g por 15 min 4 °C.

Se recuperó la fase acuosa (líquido transparente) en un tubo estéril y se añadieron 3 µL de solución de glucógeno y se mezcló bien. Posteriormente se añadió 250 µL de isopropanol, se mezcló y se deja precipitar a temperatura de habitación por 10 min, luego se centrifugó a 12000 ×g por 10 min 4 °C. Se lavó el pellet con 500 µL de etanol/agua DEPC frío al 75% y se centrifugó a 12000 ×g por 10 min, a 4 °C. Se dejó secar el botón por 5-10 min y se disolvió en 7.5 µL de solución de RNASecure para incubarse a 60 °C por al menos 10 min. Se utilizó un equipo NanoDrop para determinar la calidad del RNA purificado, obteniendo entre 214 – 228 µg/mL de RNA total de las BMMCs aisladas y 4630 – 6530 µg/mL de RNA total de los órganos.

Se generó la primera cadena de DNA complementario (cDNA) añadiendo en un tubo nuevo 5 µg de RNA de cada muestra, más 1 µL de oligo dT, se aforó con agua DEPC hasta 12 µL y se centrifugó unos segundos para bajar el contenido. Se colocó en baño maría a 65 °C por 5 min, se añadió 8 µL de la Master Mix [4 µL 10X PCR buffer; 1 µL Ribolock RNAse inhibitor (20U/µL); 2 µL dNTP Mix (10 mM); 1 µL

RevertAid Transcriptase Reverse (200 U/µL], posteriormente se centrifugó brevemente y se puso a incubar en baño maría a 42 °C por 60 min. Posteriormente se pasaron los tubos a otro baño maría a 70 °C por 5-10 min para terminar la reacción de generación de la cadena de DNA complementario. Se colocaron los tubos en hielo por 5 min, añadiendo inmediatamente 1 µL de RNAsa H a cada muestra; luego se incubaron por 20 min a 37 °C y se añadió agua DEPC hasta completar 150 µL en el tubo, posteriormente los tubos fueron almacenados a -80 °C hasta que se utilizaron.

Para obtener la segunda cadena complemetaria de DNA, se preparó 40.5 µL de una segunda Master Mix [5 µL 10X PCR buffer; 1 µL dNTP mix (10 mM); 0.4 µL Taq polimerasa; 34.1 µL de agua DEPC] más 7.5 µL del templado de la primera cadena más 1µL de la sonda del oligo específico.

Las amplificaciones de PCR fueron realizadas entre 25 – 40 ciclos de 1 min a 95 °C para la desnaturalización, 1 min a 60 °C para el alineamiento y 2 min a 72 °C para la extensión, utilizando las sondas de oligos NOS1 [(nNOS) 5′-AGAGATGGTCAACTATTTCCTGTCC-3′ y 3′-GGCTGCCTTTCTCCAGTTGTTC-5′]; NOS3 [(eNOS) 5′-AAGATCCGCTTCAACAGCAT-3′ y 3′-ACTTGCTGCTTTGCAGGTTT-5′]; GAPDH, [5′-ACCACAGTCCATGCC ATCAC-3′ y 3′-TCCACCACCCTGTTGCTGTA-5′] (Sigma Aldrich).

7.9. Determinación de la desgranulación de β-hexosaminidasa de CC.

La desgranulación de células cebadas fue utilizada como una medida de la actividad de la β-hexosaminidasa en sobrenadantes celulares como ha sido descrita previamente [97]. Dos millones de células sensibilizadas con IgE fueron centrifugadas a 500 ×g durante 5 min y resuspendidas en 1 mL de buffer Tyrode´s/BSA. Grupos independientes de células fueron tratadas con vehículo, 0.003, 0.03, 0.3, 3 o 30 μM de jacareubina por 15 min y entonces estimulados con antígeno (1, 3, 9 o 27 ng/mL de DNP-HSA). En el caso de los cacalólidos se utilizaron 0.3, 3 o 30 μM de cacalol; 3, 30 o 300 μM de cacalona; 1, 10 o 100 μM de acetato de cacalol y acetato de maturina y 10, 100 o 1000 μM de isoquercitrina por 15 min y estimuladas con antígeno (27 ng/mL de DNP-HSA) durante 30 min a 37 °C. Después de este tratamiento, las células fueron colocadas en hielo por 2 min y centrifugadas a 12000 ×g por 10 min a 4 °C. Sesenta microlitros del sobrenadante (Botón celular fragmentado con detergente Tritón) fueron colocados en una placa de 96 pozos conteniendo 40 μL de 1 mM de p-nitrofenil-N-acetil-β-D-glucosamina (P-NAG, Sigma-Aldrich, St. Louis, MO, USA), e incubada por una hora a 37 °C antes de la adición de 120 μL de solución “stop” ($Na_2CO_3$ 0.1 M/$Na_2HCO_3$ 0.1 M). La liberación de β-hexosaminidasa fue cuantificada por espectrofotometría en un lector de microplaca (Tecan Sunrise; Männedorf, Switzerland) a 405 nm, como se ha descrito previamente [98].

7.10. Determinación de la concentración de calcio intracelular ($[Ca^{2+}]i$) en CC

La concentración de calcio intracelular $[Ca^{2+}]i$ fue determinada en BMMCs sensibilizadas con IgE con diferentes tratamientos de jacareubina o cacalol (0.3, 3 o 30 µM). Se utilizaron 10 millones de células en buffer Tyrode´s/BSA y fueron pre-tratadas con 5 µM de Fura 2-AM por 30 min a 37 °C. Posteriormente las células fueron suspendidas en 2 mL de buffer Tyrode´s/BSA y colocadas en una celda. La fluorescencia fue medida a 510 nm después de ser excitada a 340 nm en intervalos de 1.16 segundos usando un espectrofluorómetro (Fluoromax 3 Jobin Yvon, Horiba, Japan). La concentración de calcio fue calculada usando la ecuación y los parámetros descritos por Grynkiewicz [99]. En un experimento estándar, la fluorescencia basal fue registrada durante 100 segundos previos a la adición del antígeno DNP-HSA (27 ng/mL) o tapsigargina (1 µM). En algunos experimentos se utilizaron BMMCs suspendidas en buffer Tyrode´s/BSA sin $Ca^{2+}$, por lo que en estos casos se añadió 1.8 mM de $CaCl_2$ (concentración final) a 200 segundos para determinar la entrada de calcio extracelular.

7.11. Producción de ROS y actividad antioxidante

Dos millones de BMMCs sensibilizadas fueron colectadas y resuspendidas en 1 mL de buffer Tyrode´s sin BSA en 1.5 mL tubos eppendorf de tapa plana para cada condición. Las células fueron preincubadas con vehículo, jacareubina, cacalol y los controles antioxidantes quercetina o trolox [100,101] se llevó a cabo por 15 min a 37 °C y posteriormente se añadió la DCF-DA (10 µM) por 15 min, después las células fueron estimuladas con antígeno (27 ng/mL de DNP-HSA) por 0, 1, 5, 10, 15, 30 y

60 min. Se utilizó el cloruro de cobalto ($CoCl_2$, 100 nM) y el sulfato de fierro ($FeSO_4$, 1200 µM) como control para inducir ROS [78,102]. Una vez finalizada la reacción, los tubos fueron centrifugados a 750 ×g a 4 °C por 5 minutos, el sobrenadante fue descartado y se añadió 300 µL de Igepal 0.1% a 37 °C y se pipeteó vigorosamente hasta romper el botón celular. Los tubos fueron entonces centrifugados a 12000 ×g por 5 minutos a 4 °C y 200 µL del sobrenadante fueron colocados en una placa de 96 pozos. La fluorescencia fue determinada por excitación a 488 nm y detectada a 565 nm en un luminómetro de microplacas BioTek modelo FLx800 (BioTek; Winooski, VT, USA) por 1 hora, tomando lecturas cada 15 minutos, método modificado de Itoh [21], valores mostrados son el promedio de las cinco mediciones tomadas.

### 7.12. Actividad de la NADPH oxidasa

La actividad de la NADPH oxidasa fue valorada mediante la oxidación fluorogénica del dihidroetidio (DHE) a etidio (Eth) por efecto del superóxido producido [103]. Se utilizaron $1X10^6$ BMMCs que fueron resuspendidas en 40 µL de buffer de lisis helado (20 mM tris HCl pH 7.4, 1 % triton X-100, 150 mM NaCl, 1 mM EDTA, 50 mM NaF, 1 mM, EGTA y 1 mM fluoruro de fenilmetilsulfonilo), mediante pipeteo y sujeto a tres ciclos de congelamiento-descongelamiento utilizando nitrógeno líquido y hielo, respectivamente. Los lisados fueron incubados con DHE (0.02 mmol/L), DNA de salmón (0.5 mg/l) y NADPH (0.2 mmol/L) en buffer HEPES (25 mmol/L) y 1 mmol/L EDTA) en presencia o ausencia de 0.3, 3 y 30 µM de jacareubina. El inhibidor de la NADPH oxidasa, difenil-eneiodonio (DPI; 0.1 mmol/L),

fue usado para confirmar que la NADPH oxidasa fuera la fuente de superóxido. La fluorescencia de Eth-DNA fue medido a una longitud de onda de excitación de 480 nm y de emisión de 610 nm durante 2.5 h a 37 °C utilizando un lector de fluorescencia de micro placas (Synergy HT multi-mode reader, Biotek, Winooski, VT, USA).

### 7.13. Actividad de la xantina oxidasa

La oxidación de DHE por superóxido producido por la xantina oxidasa (0.1 mU) fue probado en una mezcla master mix que contenía xantina (0.122 mM), EDTA (0.122 mM), DNA de salmón (0.5 mg/mL), azul de nitrotetrazolio (NBT, 30.6 µM), $Na_2CO_3$ (49 mM) [104]. La fluorescencia de Eth-DNA fue medido a una longitud de onda de excitación de 480 nm y de emisión de 610 nm durante 2.5 h a 37 °C utilizando un lector de fluorescencia de micro placas (Synergy HT multi-mode reader, Biotek, Winooski, VT, USA). En los tratamientos, la jacareubina fue agregada antes de la adición de la enzima. El vehículo (etanol) *per se* no modificó la actividad de la enzima.

### 7.14. Modelo de anafilaxia pasiva cutánea (PCA)

Se utilizaron grupos de 5 – 10 ratones para cuatro dosis de jacareubina, uno de apocinina, el inhibidor de PLC (U73122) y el control basal y positivo. Cada ratón fue anestesiado con 17 µL de ketamina y 1.1. µL de xilazina disuelta en 160 µL de solución salina e inyectada vía intraperitoneal (i.p.). Para la sensibilización con IgE,

5 µL (100 ng de anticuerpo monoclonal anti-DNP IgE) se administró en la oreja izquierda y 5 µL de vehículo (solución salina) fueron inyectados en la oreja derecha (oreja control). Veinticuatro horas después de la sensibilización, los animales fueron retados con 100 µL (200 µg del antígeno DNP-HSA) con 1% de azul de evans disuelto, administrado a través de la vena de la cola [38,105]. Vehículo o diferentes dosis de jacareubina fueron administradas intraperitonealmente a cada ratón 2 horas antes del reto con antígeno. Una vez que el ratón fue expuesto al antígeno, el ratón fue puesto en descanso con libre acceso al alimento y agua por 30 minutos. Los ratones fueron sacrificados utilizando una cámara de $CO_2$, y porciones similares de la dos orejas de cada ratón fueron cortadas, pesadas e incubadas por 12 horas a 65 °C con 300 µL de N,N, Dimetilformamida para extraer el colorante azul de Evans del tejido de la oreja. Doscientos microlitros de cada muestra fueron tomados y colocados en una placa de 90 pozos para ser leída en un espectrofotómetro VersaMax ROM v.2.14 (Molecular Devices; San Jose, CA, USA) a 620 nm.

### 7.15. Modelo de edema inducido por TPA en oreja de ratón

El modelo de edema en oreja de ratón inducido por TPA se llevó a cabo utilizando ratones machos Swiss Webster (Charles River, Wilmington, MA, USA) de 4 semanas de edad de 20 – 30 g, de acuerdo al método descrito en la literatura [106] con algunas modificaciones. Una solución de TPA (2.5 µg) en etanol (10 µL) fue aplicado tópicamente en ambas caras de la oreja derecha del ratón. Después de 10 min, la jacareubina se disolvió en acetona-etanol 1:1 y se aplicó (10 µL en cada cara de la oreja). En la oreja izquierda se administró primero etanol (10 µL) y

posteriormente una mezcla de acetona-etanol (20 µL). Cuatro horas después los ratones fueron sacrificados en una cámara de $CO_2$ e inmediatamente después se realizó un corte circular de 7 mm de diámetro de cada oreja. La inflamación fue determinada como la diferencia en el peso entre la oreja izquierda y derecha. La inhibición de edema (EI %) fue calculado por la ecuación: $EI\% = 100 - \left( \frac{B \times 100}{A} \right)$ donde A es el edema inducido por el TPA solo y B es el edema inducido por el TPA más el efecto de la jacareubina. Se utilizó indometacina disuelta en acetona:metanol 1:1 como fármaco de referencia. Todos los procedimientos animales fueron aprobados por el Comité de Ética Institucional CICUAL-IQ (protocolo CICUAL-IQ-004-17).

7.16. Actividad de la mieloperoxidasa

Actividad de la mieloperoxidasa (MPO) en tejido fue determinada en biopsias tomadas de las orejas del experimento de edema inducido por TPA, 4h después de la administración utilizando el método de Bradley [107] y Suzuki [108] modificado. Una biopsia de las orejas de cada ratón fueron colocadas en un tubo cónico de 1.0 mL con PBS (80 mM, pH 5.4) que contienen 0.5% de bromuro de hexadeciltrimetilamonio. Cada muestra fue homogenizada por 30 s a 4 °C con una pequeña muestra en un equipo de laboratorio Tissue Tearor Homogenizer model 125 (OMNI International; Kennesaw, GA, USA). El homogenado fue sujeto a tres ciclos de congelamiento-descongelamiento, sonicado por 20 s y centrifugado a 13,400 ×g por 15 min a 4 °C. El sobrenadante resultante (10 µL) fue colocado en

una placa de 96 pozos con 180 µL de PBS + HTAB fue agregado y la placa fue calentada a 37 °C. Después 20 µL de una solución de 0.017% de peróxido de hidrógeno fue agregado a cada pozo. Para el ensayo de MPO, 20 µL de 18.4 mM 3,3´,5,5´,tetrametilbenzidina en 50% de dimetilformamida líquida fue agregada a cada pozo para iniciar la reacción. Las placas fueron incubadas a 37 °C por 5 min. Finalmente la reacción se detuvo con 20 µL de $H_2SO_4$ 2 M. La actividad de la MPO fue determinada por colorimetría utilizando un lector de microplacas BioTek Microplate Reader (BioTek; Winooski, VT, USA) a una longitud de onda de 450 nm. La actividad de la MPO (medida por cuadruplicado en cada muestra) fue expresada como un porcentaje de inhibición con respecto al control.

### 7.17. Análisis estadístico

Todos los datos fueron representados como el promedio ± la desviación estándar del promedio (SD) utilizando el programa GraphPad Prism® software versión 6 (GraphPad Software; La Jolla, CA, USA). El análisis estadístico fue hecho mediante la prueba de análisis de varianza (ANOVA) de una vía seguido por un análisis de Dunett que se utilizó para comparar varios grupos con el control. De manera adicional se utilizó la prueba de t-Student y Kolmogorov-Smirnoff como comprobación. Se calculó el coeficiente de correlación de Pearson para las pruebas de edema inducido en oreja por TPA y MPO. Los valores de $p < 0.05$ se consideraron significativos.

## 8. Resultados

### 8.1. Estructura, purificación y estabilidad de la jacareubina

Los datos de RMN $^{1}H$ y $^{13}C$ de la jacareubina aislada de la madera de *C. brasiliense* correspondieron con los previamente reportados de la especie relacionada *Garcinia xantochymus* y del hongo *Amauroderma amoiensis* [89,90]. La jacareubina es un policétido tetracíclico, que presenta una estructura compuesta por un sistema C6-C3-C6, con una anillo extra derivado de la ciclización del sustituyente γ,γ-dimetilalil unido al C-2 y C-3 del anillo A. Esta es la primera vez que la estructura molecular de un cristal de jacareubina es reportado basada en su difracción de rayos X (Figura 13). El compuesto presenta una estructura plana y rígida con tres sustituyentes hidroxilo, el hidroxilo del C-1 forma un puente de hidrógeno intramolecular con el O-4 del grupo carbonilo. El átomo de hidrógeno en el O6 se ordena en dos posiciones, refinado como 57/43 % del factor de ocupación del sitio, mostrando un puente de hidrógeno intramolecular con los átomos O-2 y O-5 y puentes de hidrógeno intermoleculares con O-6. La celda cristalina planar muestra que el arreglo de las moléculas de jacareubina en un arreglo de cuña, el anillo B de una molécula se une con el anillo B de otra molécula a través de un puente de hidrógeno establecido por los hidroxilos en C-5 y C-6, otro puente de hidrógeno se forma entre el O-2 de una molécula y el hidroxilo en C-6 de otra molécula (Figura 14). El análisis con HPLC-MS mostró un pico mayor (99.39%) que eluye a 16 min y que coincidió con la masa molecular de la jacareubina *m/z* $M^{+}$-1 = 325 (Figura 15) indicando la pureza de la jacareubina utilizada.

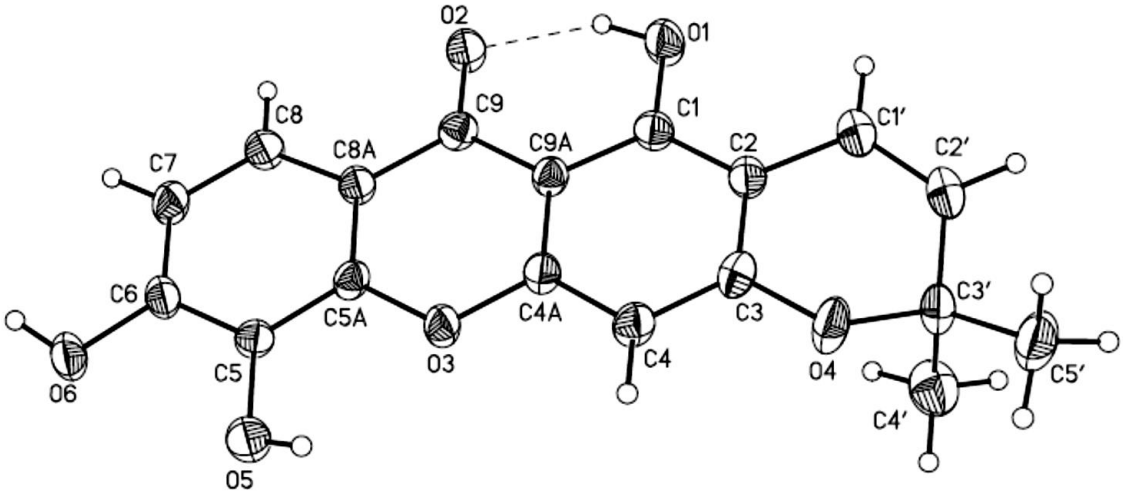


**Figura 13. Estructura tridimensional de la jacareubina obtenida por difracción de rayos X.**

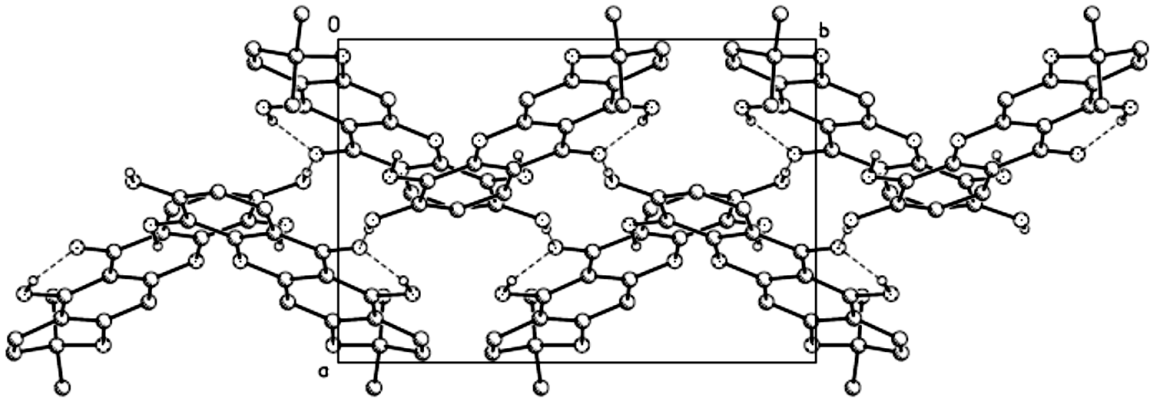


**Figura 14. Celda del cristal de jacareubina obtenida por difracción de rayos X.**

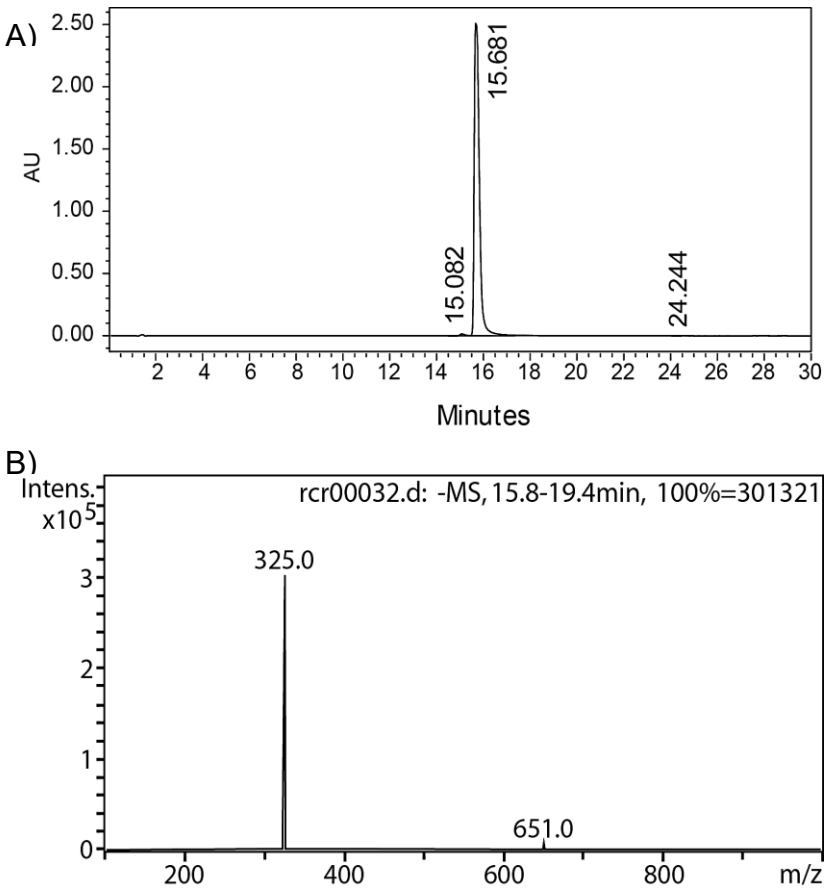


**Figura 15. Pureza de la jacareubina utilizada en este estudio determinada por A) HPLC-UV acoplado a B) espectrometría de masas ($M^+$-1).**

## 8.2. La jacareubina inhibe la desgranulación inducida por el receptor FcεRI

Se utilizó la liberación de la enzima lactato deshidrogenasa (LDH) como un marcador de muerte celular, la jacareubina no mostró actividad citotóxica sobre las BMMCs a concentraciones de 300 pM - 30 µM (Figura 16), no se observó una liberación significativa de la enzima LDH después de ser incubada con la Jacareubina durante 15 minutos, comparada con el $H_2O_2$, el cual fue citotóxico. Tampoco se observó la desgranulación espontánea a ninguna de las concentraciones de jacareubina utilizadas (Figura 17). Debido a estos resultados, este rango de concentraciones fue utilizado para los experimentos subsecuentes.

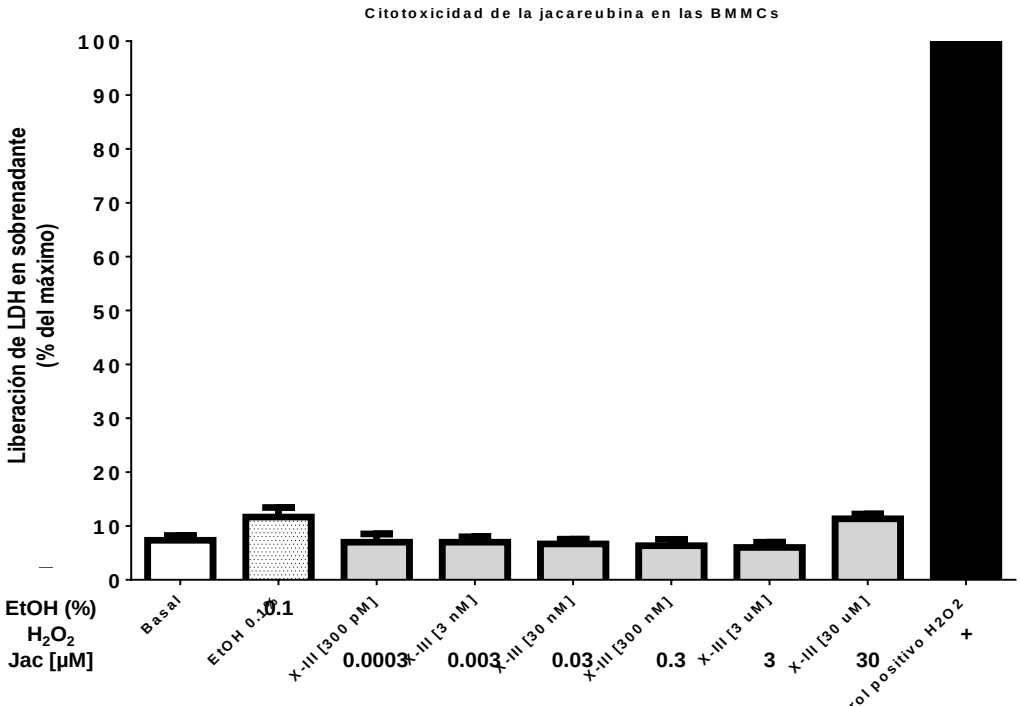


**Figura 16. Citotoxicidad determinada por la liberación de la enzima LDH en BMMCs con diferentes concentraciones de jacareubina, n = 3. ANOVA de una vía con comparación múltiple de Dunnet (*p < 0.05). EtOH = Vehículo de etanol al 0.1 %.**

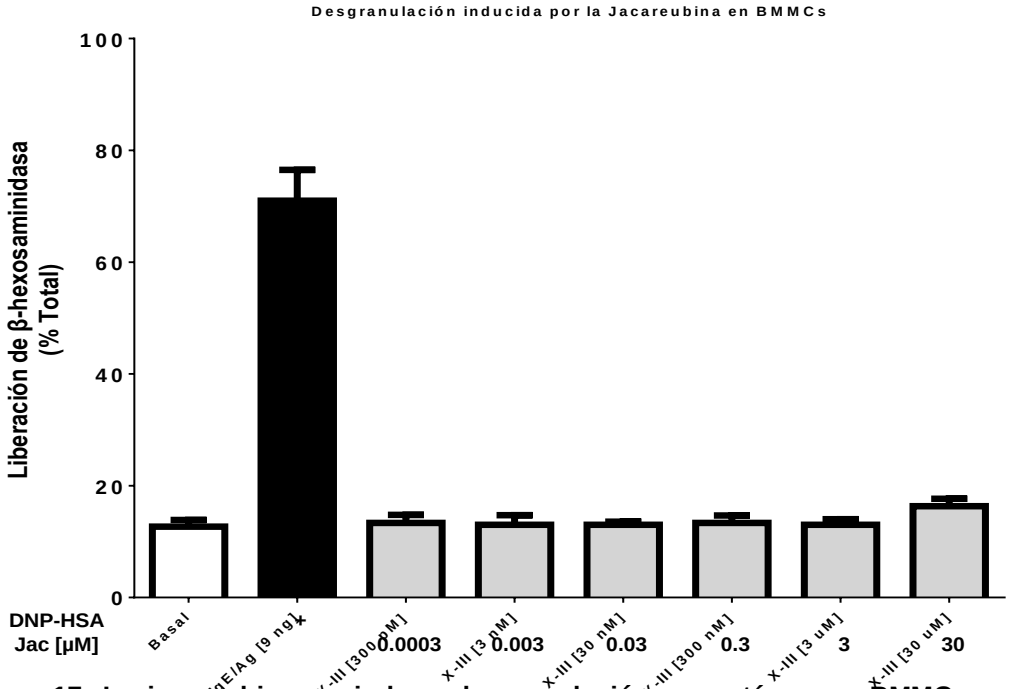


**Figura 17. La jacareubina no induce desgranulación espontánea en BMMCs a diferentes concentraciones, n = 3. ANOVA de una vía con comparación múltiple de Dunnet (*p < 0.05).**

Para evaluar las acciones de la Jacareubina sobre la activación de las CC, BMMCs fueron sensibilizadas 24 horas con 100 ng/mL del anticuerpo monoclonal tipo IgE anti-DNP. Después de esto, las células fueron incubadas en presencia de diferentes concentraciones de jacareubina a 37 °C. Después de 15 min, las células fueron estimuladas con diferentes concentraciones del antígeno (DNP-HSA) y se determinó la actividad de la β-hexosaminidasa en el sobrenadante. Como se observa en la figura 18-A, la jacareubina inhibió la desgranulación de una manera dependiente de la concentración ($IC_{50}$ = 0.046 μM). También, los efectos de la jacareubina fueron evaluados sobre la desgranulación inducida por la tapsigargina (Thap), un inhibidor de la ATPasa de $Ca^{2+}$ del retículo sarco/endoplásmico (SERCA), que activa la secreción mediante el incremento del contenido intracelular de calcio en CC [109], independientemente del entrecruzamiento y activación del receptor FcεRI. La jacareubina fue capaz de inhibir la desgranulación inducida por la Thap de una manera dependiente de la concentración (Figura 18-B). Finalmente, la desgranulación inducida mediante la combinación del activador de la $PKC_{\alpha/\beta}$ (TPA) y el ionóforo de calcio A23187 fue también sensible a la acción de la jacareubina (Figura 18-C).

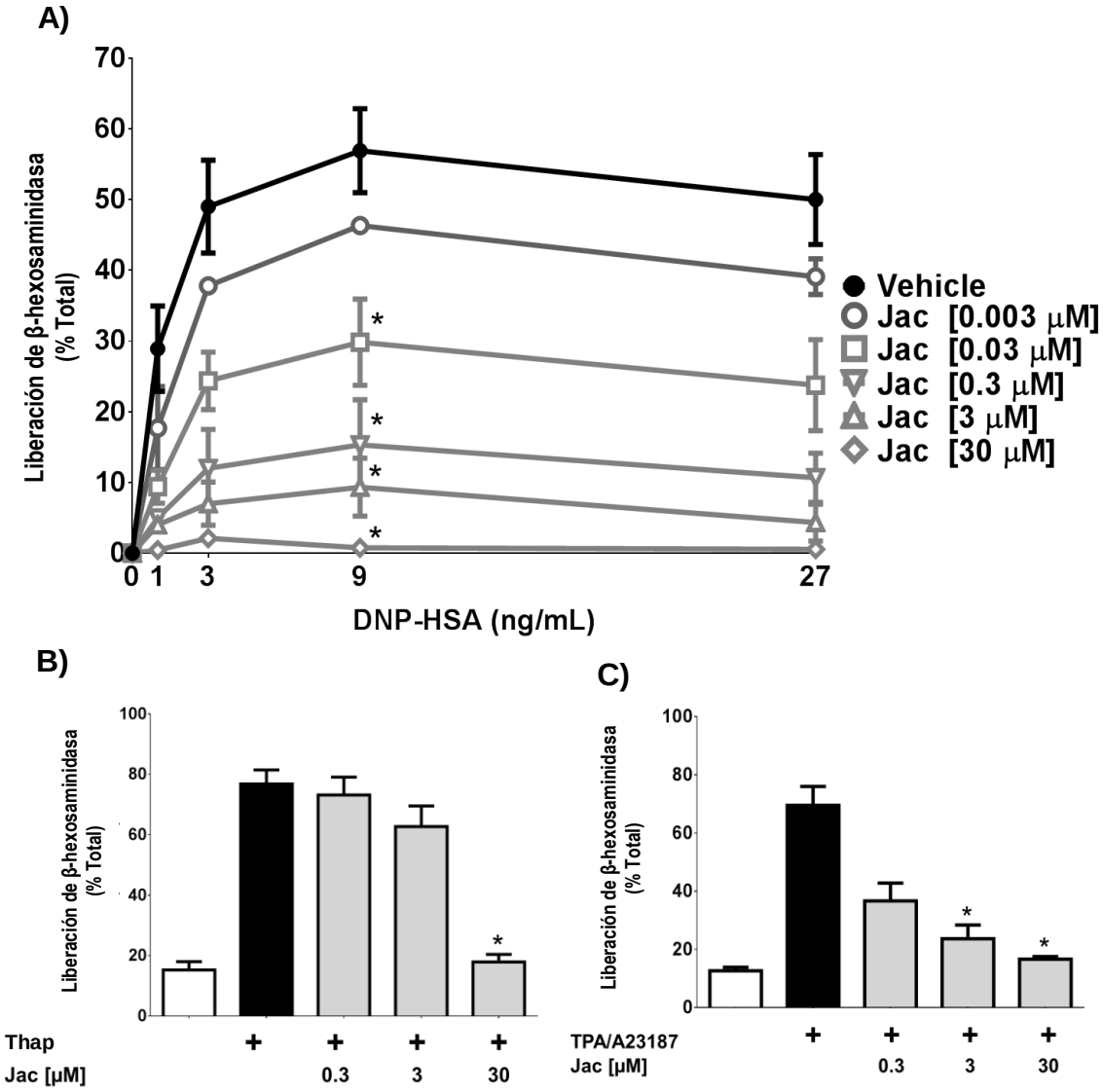


**Figura 18. La jacareubina inhibe la desgranulación inducida por diferentes activadores en células cebadas en una forma dependiente de la concentración. A) Curva concentración – respuesta de la desgranulación inducida por IgE/Ag en BMMCs pre-tratadas con diferentes concentraciones de jacareubina o con vehículo solamente, n = 3 - 6. B) Efecto del pre-tratamiento con jacareubina sobre la desgranulación inducida por Thap en BMMCs, n = 3. C) Efecto del pretratamiento con jacareubina sobre la desgranulación inducida por el TPA/A23187, n = 3. ANOVA de una vía con comparación múltiple de Dunnet (*p < 0.05).**

8.3. La jacareubina interfiere con la movilización del calcio intracelular inducido por el receptor FcεRI en BMMCs.

El efecto de la jacareubina sobre la movilización de calcio inducido por el receptor FcεRI en BMMCs, fue evaluado. Las células fueron pre-cargadas con el compuesto FURA 2AM, con el vehículo o con diferentes concentraciones de jacareubina 15 min antes de ser estimuladas con 27 ng/mL del antígeno DNP-HSA. Los cambios sobre la fluorescencia del FURA 2-AM fueron registrados como se describe en la sección de Materiales y Métodos. Como se observa en la figura 19-A, la adición del antígeno causó un rápido incremento en la concentración de calcio $[Ca^{2+}]i$, que produjo valores máximos alrededor de los 300 s después de la estimulación. La pre-incubación con jacareubina evitó la movilización de calcio de una manera dependiente de la concentración, produciendo una inhibición completa a la concentración de 30 µM (Figura 19). La cuantificación de la tasa de incremento de calcio y los niveles máximos obtenidos con cada tratamiento son mostrados en la tabla 1. La adición de la jacareubina no modificó la velocidad de aumento de calcio (la pendiente) cuando se utilizaron 0.3 o 3 µM, pero este parámetro fue bloqueado completamente solo con 30 µM. Sin embargo, el incremento máximo de $[Ca^{2+}]i$ fue afectado desde la concentración de 0.3 µM (Figura 19).

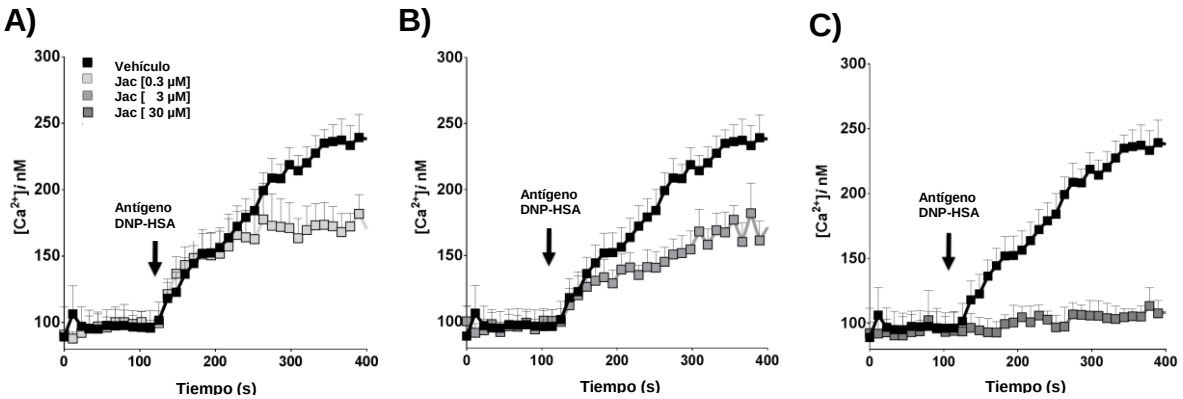


**Figura 19. La jacareubina inhibió la movilización de calcio inducida por la activación del receptor FcεRI en células cebadas dependiente de la concentración. A) – C) Trazos representativos del aumento de calcio intracelular inducido por la adición del antígeno DNP-HSA en BMMCs pre-tratadas con vehículo o con diferentes concentraciones de jacareubina, n = 3 – 6. ANOVA de una vía con comparación múltiple de Dunnet (*p < 0.05).**

Tabla 1. Efecto de la jacareubina en la $[Ca^{2+}]i$ inducida por el FcεRI en BMMCs.

| Tratamiento | Tasa de incremento $[Ca^{2+}]i$ | Máxima $[Ca^{2+}]i$ (nM) |
|---|---|---|
| Vehículo | 0.648 ± 0.09 | 239.3 ± 17.31 |
| Jac [0.3 µM] | 0.584 ± 0.193 | 181.8 ± 14.55 |
| Jac [3.0 µM] | 0.335 ± 0.029 | 182.1 ± 22.73 |
| Jac [ 30 µM] | 0.095 ± 0.07* | 113.4 ± 13.94* |

El aumento de calcio intracelular después de la activación del receptor FcεRI en células cebadas es controlado por el vaciamiento de los almacenes intracelulares y por la apertura de los canales de calcio membranales. Para poder determinar el punto de acción de la jacareubina, incubamos BMMCs con vehículo o diferentes concentraciones del compuesto en un buffer libre de calcio y estimulamos con antígeno a los 100 segundos. Como se esperaba, después de la adición de calcio a la celda a los 200 segundos (para alcanzar una concentración de 1.8 mM de $Ca^{2+}$ extracelular), un importante incremento de la concentración de calcio intracelular fue observado debido a la entrada de calcio a través de la apertura de canales membranales (Figura 20). La pre-incubación con jacareubina bloqueó la entrada de calcio extracelular inducida por la activación del receptor FcεRI de una manera

dependiente de la concentración. Cuando se utilizaron 0.3 µM de jacareubina, se observó solamente una ligera diferencia con respecto a las células sin tratar, pero la adición de 3 µM bloqueó la movilización de calcio máxima en 50% y a 30 µM inhibió por completo el flujo de calcio (Figuras 20 B y C). Un análisis detallado de los parámetros de entrada de calcio mostraron que la jacareubina disminuye tanto la tasa de incremento, como el máximo de $[Ca^{2+}]i$ (Tabla 2).

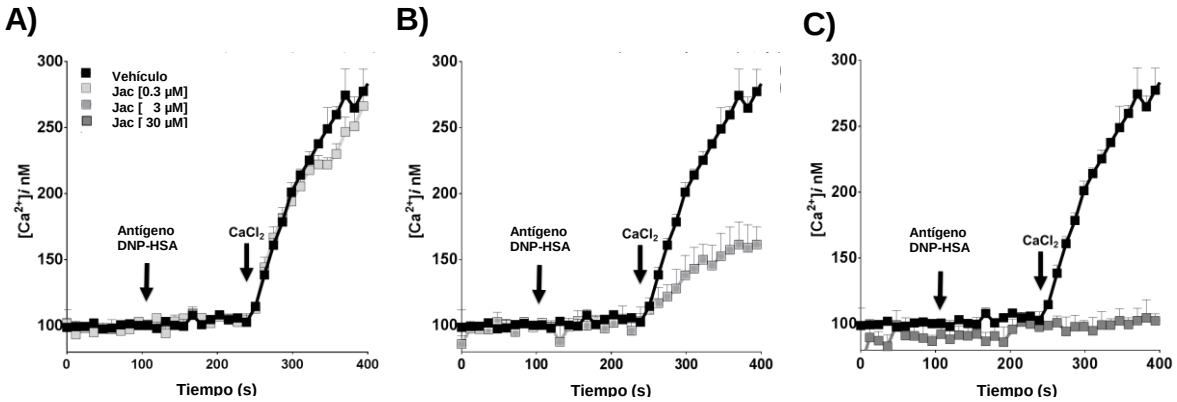


**Figura 20. La jacareubina inhibe el flujo de calcio extracelular inducido por la activación del receptor FcεRI en células cebadas. A) – C) BMMCs fueron resuspendidas en un buffer libre de calcio y con la adición del antígeno DNP-HSA. Después de 200 s, el calcio fue añadido a la celda hasta alcanzar 1.8 mM. A) – C). Trazos representativos del aumento de calcio intracelular en células pre-tratadas con vehículo o diferentes concentraciones de jacareubina, n = 3. ANOVA de una vía con comparación múltiple de Dunnet (*p < 0.05). $CaCl_2$ = Cloruro de calcio.**

Tabla 2. Efecto de la jacareubina sobre el flujo de $Ca^{2+}$ extracelular estimulado por el receptor FcεRI en BMMCs.

| Tratamiento | Tasa de incremento $[Ca^{2+}]i$ | Máximo $[Ca^{2+}]i$ (nM) |
|---|---|---|
| Vehículo | 1.407 ± 0.127 | 264.7 ± 8.459 |
| Jac [0.3 µM] | 1.216 ± 0.104 | 266.3 ± 11.99 |
| Jac [3.0 µM] | 0.368 ± 0.061* | 161.4 ± 17.23* |
| Jac [ 30 µM] | 0.080 ± 0.027* | 104.5 ± 13.71* |

El incremento en el $[Ca^{2+}]i$ después de la activación del receptor FcεRI que conlleva la activación de las dos principales vías: el Receptor Operated Calcium Entry (ROCE) y el Store Operated Calcium Entry (SOCE) [109–111]. La primera de ellas ocurre debido a la activación de los canales de calcio que requiere la participación

de proteínas y mensajeros que no inducen el vaciamiento de almacenes de calcio intracelulares [109,110]. La otra vía de SOCE, ocurre después de la activación del receptor de $IP_3$ en el retículo endoplásmico y es disparada cuando los almacenes intracelulares son movilizados y las células requieren el rellenado de los compartimentos de almacenamiento [17,18,112]. La SOCE puede ser activada farmacológicamente por Thap, una lactona sesquiterpénica que inhibe la ATPasa de $Ca^{2+}$ del retículo sarco/endoplásmico (SERCA). Para analizar si la jacareubina puede inhibir la SOCE, las células fueron tratadas con vehículo o con diferentes concentraciones de jacareubina por 15 min en buffer libre de $Ca^{2+}$. La $[Ca^{2+}]i$ basal fue medida por 100 s antes de la adición de Thap (Figura 21). Después de 200 s, se añadió el $Ca^{2+}$ a la celda para alcanzar 1.8 mM y los cambios sobre la $[Ca^{2+}]i$ fueron evaluados durante 200 s. Como se puede observar en la figura 21, la Thap indujo, como se esperaba, un discreto aumento en la concentración de $[Ca^{2+}]i$ que correspondió al vaciamiento de los almacenes de calcio intracelular del RE y después de la adición de $Ca^{2+}$ extracelular, la entrada de este ion a través del mecanismo mediado por STIM1/Orai repusieron el $Ca^{2+}$ en el retículo endoplásmico. El pre-tratamiento con jacareubina (0.3 μM) disminuyó el incremento máximo de $Ca^{2+}$ (Figura 21-A), mientras que a concentraciones mayores (3 y 30 μM) inhibió de manera evidente tanto la tasa de incremento, como el máximo de concentración de $Ca^{2+}$ (Figuras 21-B y tabla 21-C).

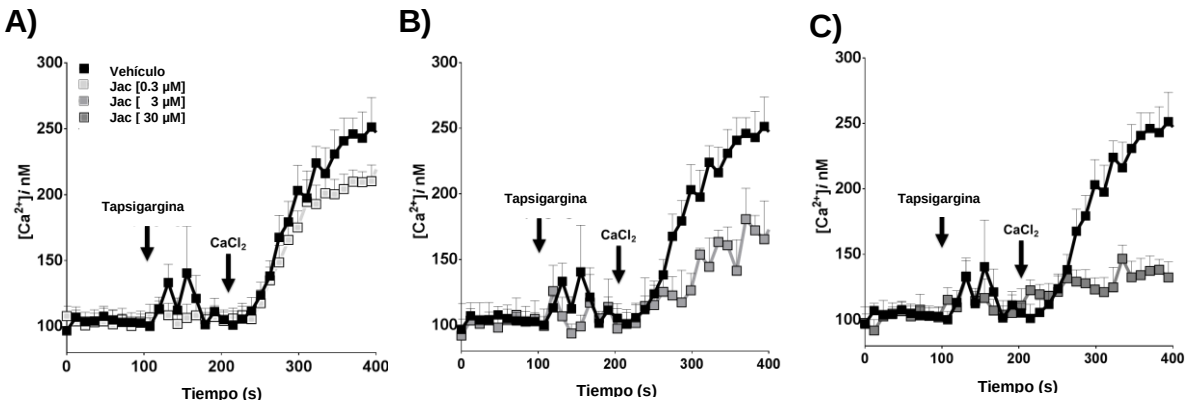


**Figura 21. La jacareubina inhibe el flujo de calcio inducido por la Thap en células cebadas de una manera dependiente de la concentración. A) – C) Trazos representativos del aumento de calcio intracelular inducidos por Thap (1 µM) en BMMCs pre-tratadas con vehículo o con diferentes concentraciones de jacareubina en buffer libre de $Ca^{2+}$, n=3-5. ANOVA de una vía con comparación múltiple de Dunnet (*p < 0.05). $CaCl_2$ = Cloruro de calcio.**

Tabla 3. Efecto de la jacareubina sobre el flujo de $Ca^{2+}$ extracelular inducido por Thap en BMMCs.

| Tratamiento | Tasa de incremento $[Ca^{2+}]i$ | Máximo $[Ca^{2+}]i$ |
|---|---|---|
| Vehículo | 1.212 ± 0.219 | 251.3 ± 22.34 |
| Jac [0.3 µM] | 0.931 ± 0.139 | 210.2 ± 12.34 |
| Jac [3.0 µM] | 0.423 ± 0.095* | 180.7 ± 23.49* |
| Jac [ 30 µM] | 0.092 ± 0.044* | 146.6 ± 10.4* |

## 8.4. La jacareubina evita la producción de ROS inducido por IgE/Ag en CC.

Una característica común entre ROCE y SOCE observado en distintas preparaciones de CC es su modulación por la producción de especies reactivas de oxígeno (ROS) [23,109,113]. Se sugiere que la jacareubina puede inhibir la producción de ROS disparado por el receptor FcεRI y esto puede causar efectos sobre el incremento de calcio intracelular en CC. Para someter a prueba esta hipótesis, se determinó la capacidad antioxidante de la jacareubina y la comparamos con otras moléculas con propiedades anti-oxidantes previamente reportadas, considerando la posible relación entre la capacidad anti-oxidante y la inhibición de la activación de las CC. La figura 22-A muestra que la jacareubina reduce el DPPH a menores

concentraciones que el α-tocoferol y el trolox, mientras que comparado con la quercetina mostró menor capacidad anti-oxidante. La capacidad anti-oxidante de la quercetina y el trolox fue relacionada con la capacidad de bloquear la desgranulación dependiente de IgE/Ag, debido a que se requirió de bajas concentraciones de quercetina para inhibir la liberación de β-hexosaminidasa (Figura 22-C). Sin embargo, cuando se compararon con la jacareubina, la xantona mostró una mayor capacidad de inhibición de la desgranulación y la movilización de $Ca^{2+}$ inducido por IgE/Ag que el trolox y la quercetina (Figura 22-D). Cuando a los compuestos antes mencionados se les evaluó su capacidad para bloquear la producción de especies reactivas de oxígeno dependientes de la activación del receptor FcεRI, la jacareubina inhibió la oxidación de DCF de una forma dependiente de la concentración (Figura 22-B). Cabe mencionar que la sensibilización con IgE monomérica por si sola es capaz de inducir un aumento permanente en los ROS intracelulares en BMMCs hasta un 40% con respecto a las BMMCs sensibilizadas (basal). Mientras que la suma de los ROS producidos por la IgE monomérica más la inducción de la producción de ROS por IgE/Ag supera en más de 100% con respecto a las BMMCs sin sensibilizar (Figura 23, t = 15 min).

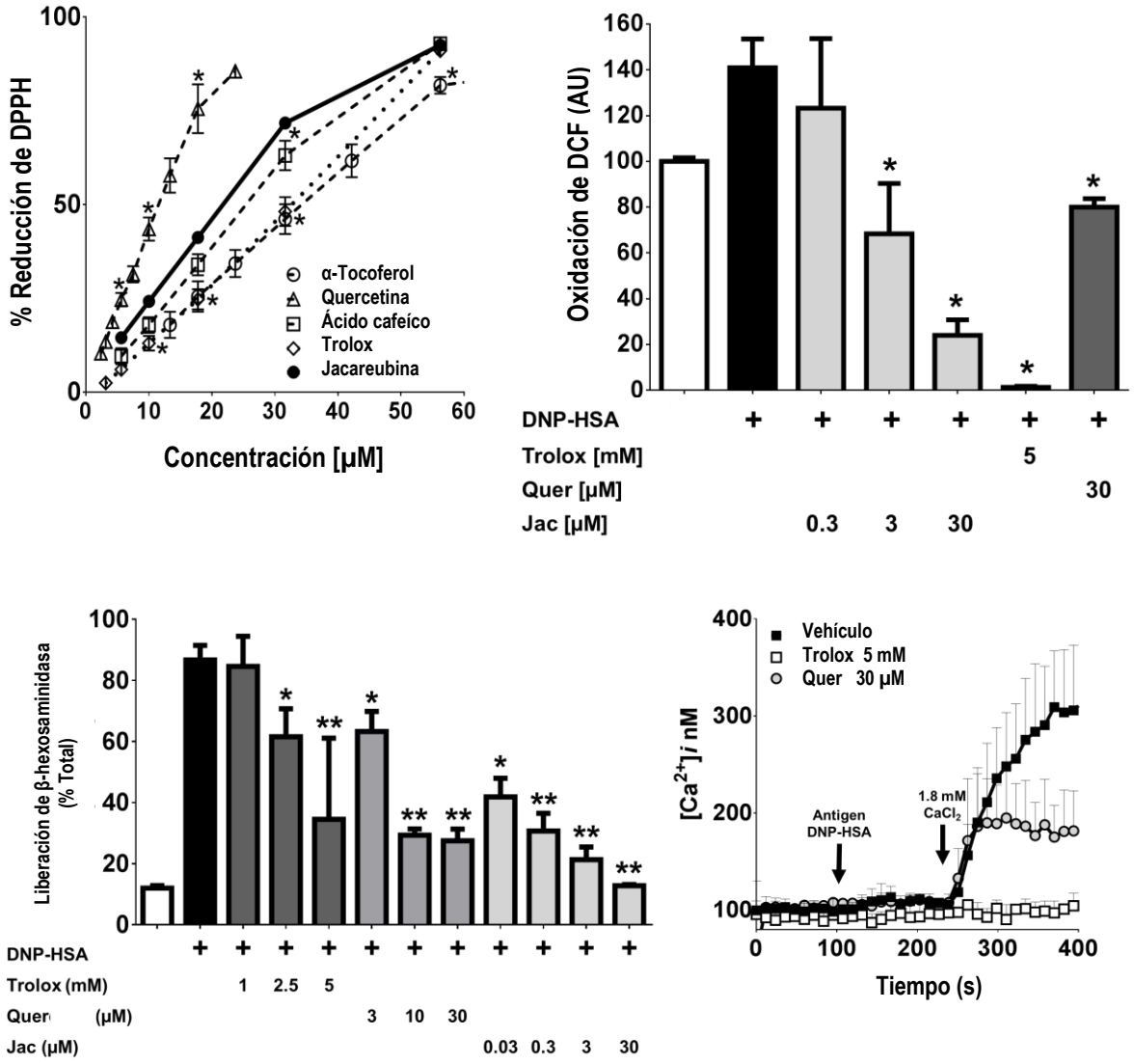


**Figura 22. La jacareubina mostró una importante actividad anti-oxidante en comparación con el trolox y la quercetina. A) Actividad anti-oxidante de la jacareubina comparada con otros anti-oxidantes, determinado por la reducción del DPPH, n = 3. B) Inhibición de la desgranulación inducida por la activación del receptor FcεRI por trolox, quercetina y jacareubina, n = 3. C) Inhibición de la movilización de calcio inducida por IgE/Ag por trolox y quercetina, n = 3. D). La oxidación de la DCF por la activación del receptor FcεRI en BMMCs pre-tratadas con diferentes concentraciones de jacareubina (valores obtenidos de las células pre-tratadas con trolox y quercetina fueron incluídos como controles), n = 3. ANOVA de una vía con comparación múltiple de Dunnet (*p < 0.05).**

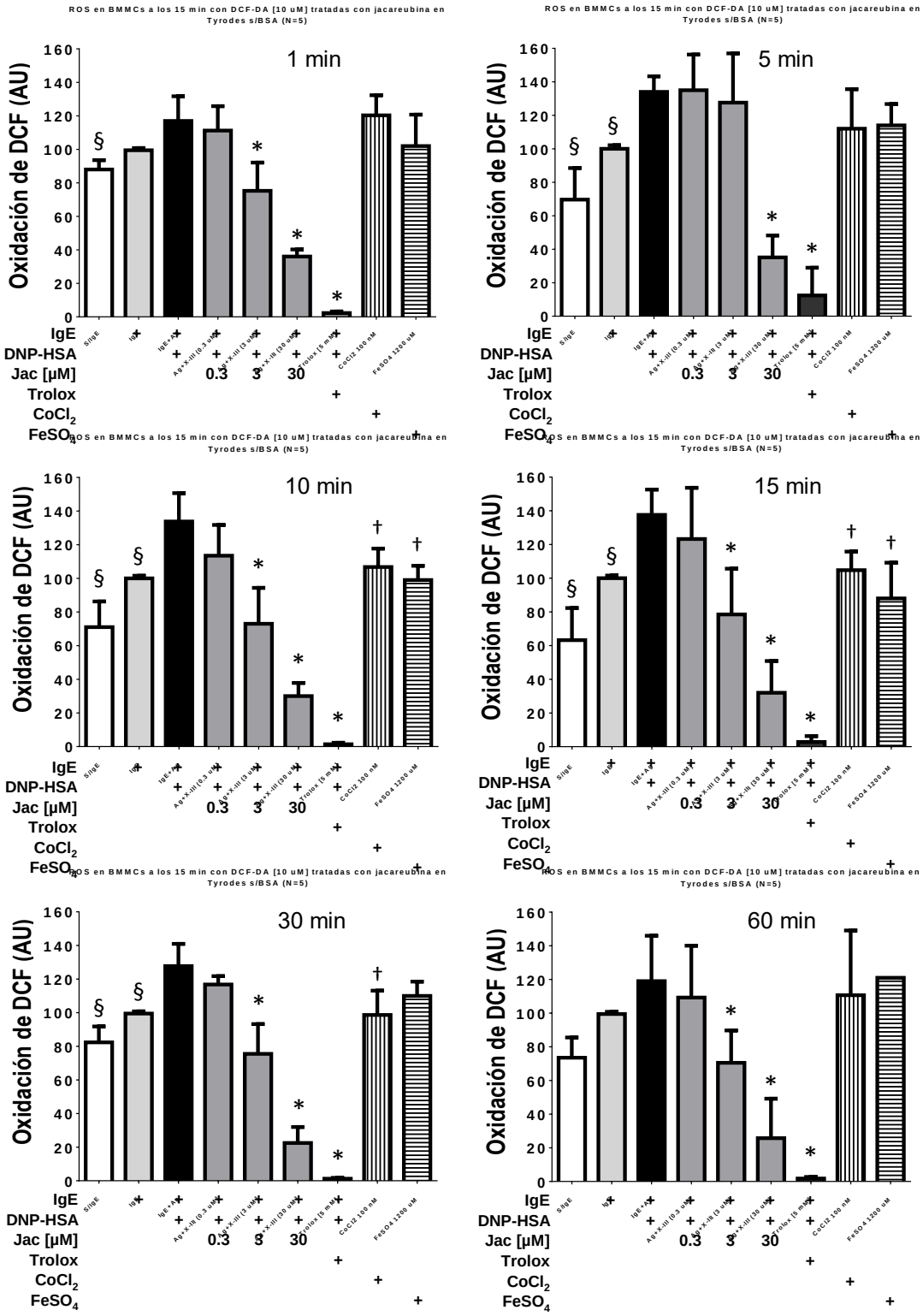


**Figura 23. Producción de ROS inducido por IgE/Ag en BMMCs a 1, 5, 10, 15, 30 y 60 min. § diferencias del antígeno DNP-HSA con respecto al basal y a las BMMCs sin sensibilizar. n = 3 – 6. ANOVA de una vía con comparación múltiple de Dunnet (*p < 0.05). † diferencias del antígeno DNP-HSA con respecto a los controles de inducción de ROS con $CoCl_2$ (100 nM) y $FeSO_4$ (1200 µM).**

Para establecer el mecanismo por el que la jacareubina puede inhibir la acumulación de ROS en BMMCs, las células fueron estimuladas con IgE/Ag en la presencia del buffer o de diferentes concentraciones de la jacareubina para determinar la actividad del complejo molecular de la NADPH oxidasa (NOX). Como se observa en la Figura 24-A, la jacareubina no fue capaz de bloquear la activación de NOX dependiente del receptor FcεRI en ninguna de las concentraciones probadas. El inhibidor de la NOX conocido como DPI fue usado como un control positivo y los efectos esperados de este compuesto fueron observados. Sin embargo, en un ensayo libre de células, se determinó que la actividad de la xantina oxidasa fue inhibida por la jacareubina dependiente de la concentración (Figura 24-B).

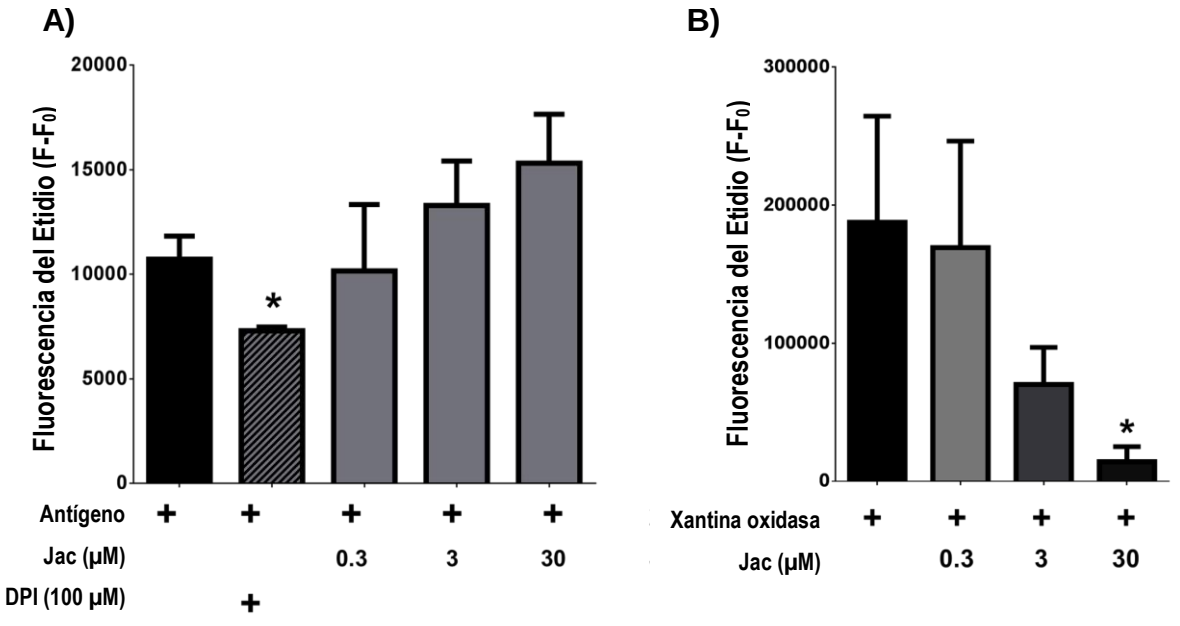


**Figura 24. La jacareubina no inhibe la activación de NOX dependiente del receptor FcεRI, pero es capaz de inhibir a la xantina oxidasa (XO) en un ensayo libre de células. A) La actividad de NOX inducida por IgE/Ag en células pre-tratadas con DPI o diferentes concentraciones de jacareubina, n = 3. B) La actividad de la xantina oxidasa se determinó en la presencia de distintas concentraciones de jacareubina, n = 3. ANOVA de una vía con comparación múltiple de Dunnet (*p < 0.05).**

8.5. Expresión de las isoformas constitutivas nNOS y eNOS en BMMCs

Con el fin de analizar la presencia de las isoformas constitutivas de la NOS en células cebadas, para descartar su posible participación en la producción de especies reactivas de oxígeno y nitrógeno, se realizó una RT-PCR a partir de RNAs purificados de distintos tejidos del ratón y de BMMCs. Las reacciones de RT-PCR se realizaron en presencia de oligonucleótidos específicos para la nNOS y la eNOS. Como puede observarse en la Figura 25, en estado basal no se encontró la expresión de la isoforma neuronal nNOS (carril 4). De igual manera no se encontró la expresión de la isoforma endotelial, eNOS (carriles 2 y 3), a pesar de que otros tejidos del ratón si las expresaban en abundancia (carriles 6, 7, 9, 10 y 12).

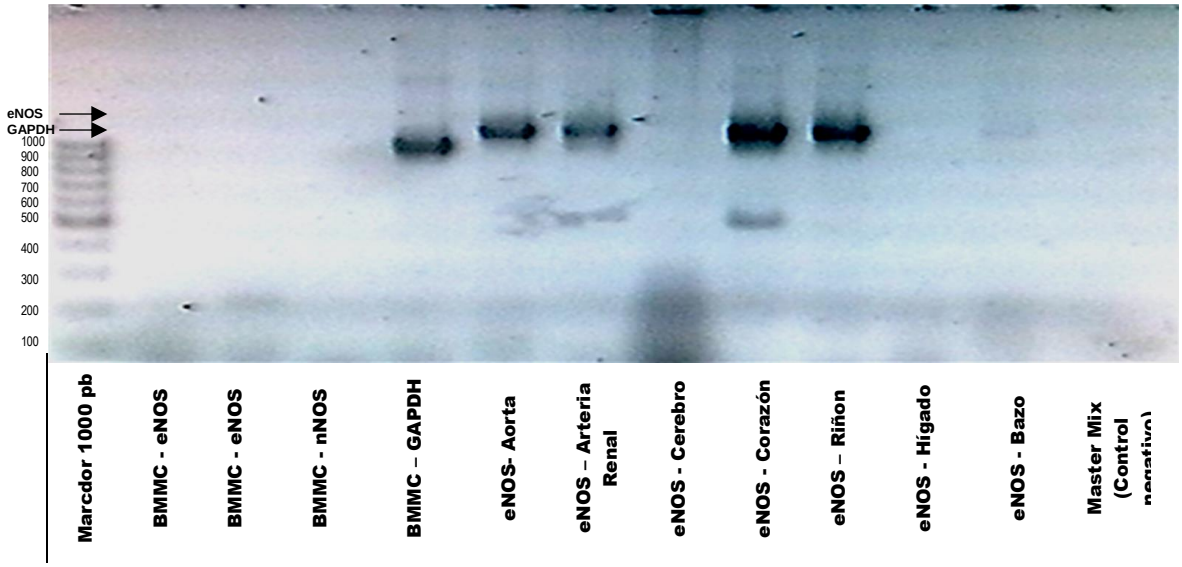


**Figura 25. Imagen representativa de la expresión del gen de eNOS en BMMCs y tejidos de ratón C57BL/6J por RT-PCR. Se observó la expresión de eNOS en los carriles: 6) Arteria aorta, 7) arteria renal, 9) corazón, 10) riñon y 12) bazo. Sin embargo no se observó la amplificación de la eNOS en BMMCs en los carriles 2 y 3 (n = 3).**

8.6. La jacareubina inhibe cambios en la permeabilidad vascular y reacciones inflamatorias *in vivo* dependiente de células cebadas.

Para evaluar el efecto de la jacareubina sobre la desgranulación de células cebadas *in vivo*, nosotros utilizamos el modelo de anafilaxia pasiva cutánea, donde los cambios inmediatos sobre la permeabilidad vascular dependen completamente de la activación de las células cebadas [38,105]. Como se observa en la figura 26-A, la jacareubina inhibió la inflamación dependiente del receptor FcεRI hasta en un 88% en dosis entre 1.0 y 33.3 mg/Kg vía intraperitoneal (i.p.), administradas 2 horas antes del reto con el antígeno DNP-HSA. Estas dosis fueron utilizadas, debido a que se ha reportado que a estas dosis no se produce ningún efecto toxico agudo o crónico sobre el ratón [114].

A continuación para evaluar la actividad anti-inflamatoria de la jacareubina en procesos inflamatorios que han sido asociados con otras células del sistema inmune (monocitos y neutrófilos), probamos el efecto del compuesto en el modelo de edema inducido en oreja de ratón por TPA, determinando el edema producido y la actividad de la mieloperoxidasa (MPO). Como se observa en la figura 26-B, la jacareubina inhibió el edema inducido por TPA en una forma dependiente de la dosis, de 7 a 68% y su bloqueo fue similar al observado con el anti-inflamatorio de referencia indometacina. En cuanto a la actividad de la MPO, la jacareubina inhibió de 13 % hasta 81% (Figura 26-C).

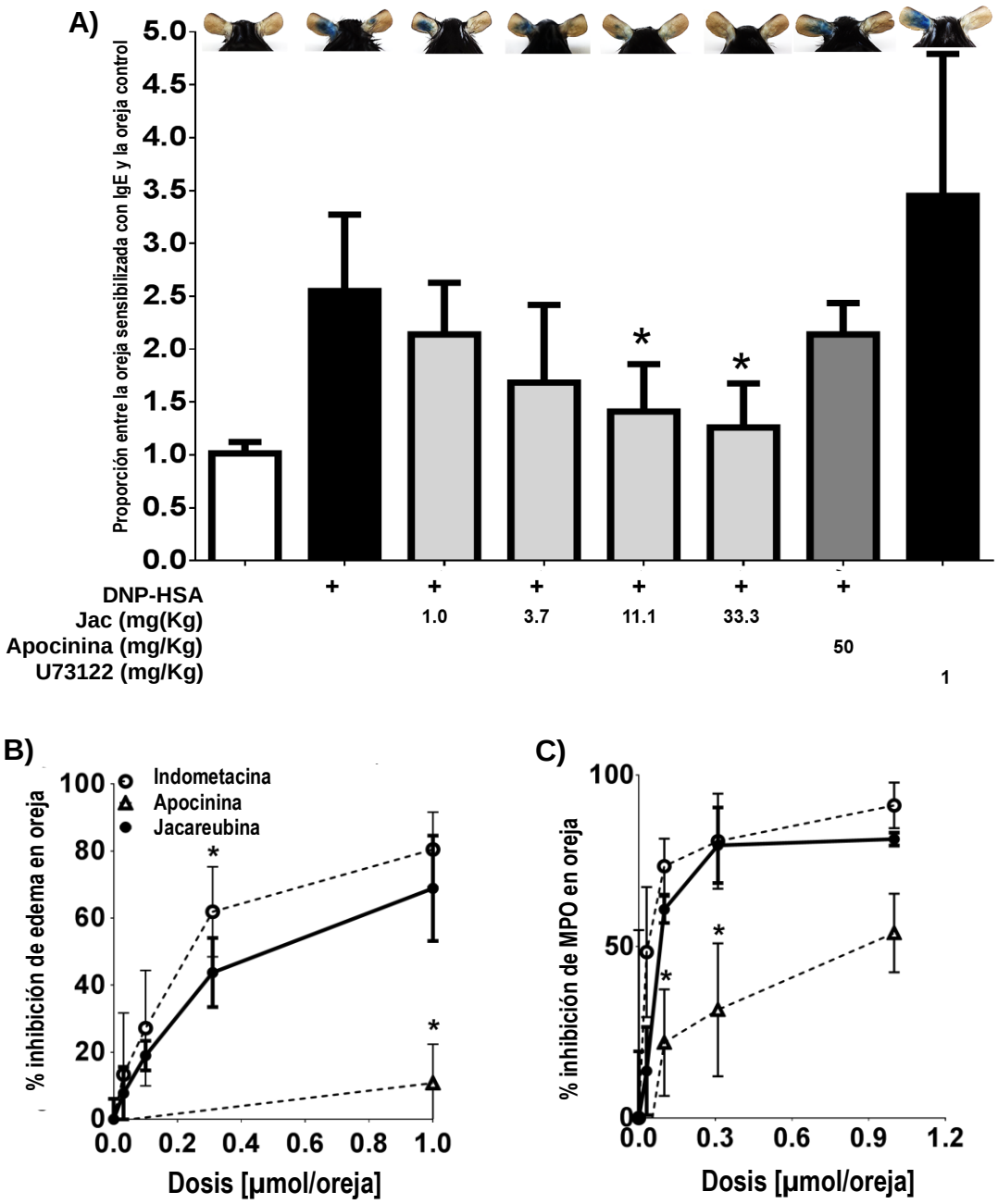


**Figura 26. La jacareubina redujo la inflamación *in vivo* dependiente de CC e independiente de CC. A) Anafilaxia pasiva fue observada en la oreja de los ratones tratados con distintas dosis de jacareubina, n = 5 – 10. El inhibidor de la NOX (apocinina) y el de PLCγ (U73122) fueron utilizados como referencia. B) Edema en oreja inducido por TPA en ratones pre-tratados con diferentes dosis de jacareubina administrada vía tópica en la oreja izquierda (los resultados se muestran como porcentaje de inhibición con respecto al control de TPA únicamente); la indometacina y el inhibidor de la NOX, apocinina, fueron utilizados como referencia. C) La actividad de la MPO en el tejido fue medida en biopsias tomadas de orejas 4h después de la administración de TPA, los resultados son expresados como porcentaje de la inhibición con respecto al control, la indometacina y el inhibidor de la NOX, apocinina, fueron utilizados como referencia. n = 5. ANOVA de una vía con comparación múltiple de Dunnet y coeficiente de correlación de Pearson (*p < 0.05).**

8.7. <u>El cacalol inhibe la desgranulación inducida por el receptor FcεRI en CC.</u>

Entre los cuatro cacalólidos evaluados, el cacalol mostró la actividad inhibidora más potente sobre la desgranulación inducida por IgE/Ag con 88 % (30 µM), seguido del acetato de maturina y de cacalol con una inhibición de 100 % y 85 % (100 µM) y finalmente la cacalona con un 100 % de inhibición (300 µM) (Figura 27).

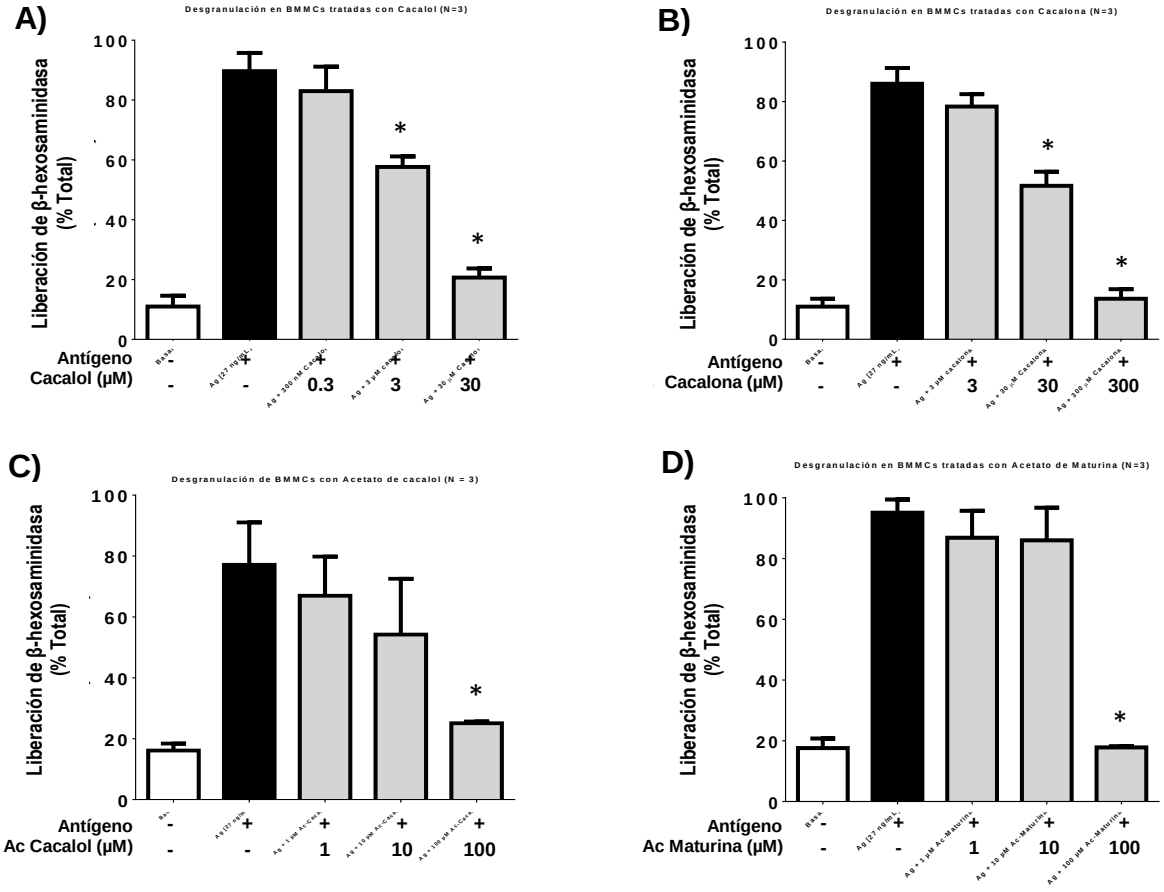


**Figura 27. Los calanólidos inhibieron la desgranulación inducida por IgE/Ag en BMMCs. A) Efecto del pre-tratamiento con cacalol sobre la desgranulación inducida por el antígeno DNP-HSA, n = 3. B) Efecto del pre-tratamiento con acetato de cacalol sobre la desgranulación inducida por el antígeno DNP-HSA, n = 3. C) Efecto del pre-tratamiento con cacalona sobre la desgranulación inducida por el antígeno DNP-HSA, n = 3. D) Efecto del pre-tratamiento con acetato de maturina sobre la desgranulación inducida por el antígeno DNP-HSA, n = 3. One way ANOVA with Dunnett´s multiple comparisons test (*p < 0.05).**

8.8. <u>El cacalol interfiere con la producción de ROS inducida por IgE/Ag en CC.</u>

El cacalol entre las concentraciones de 30 y 300 µM fue capaz de inhibir casi por completo la producción de ROS en células cebadas cuando fueron retadas con el antígeno DNP-HSA (Figura 28), cuando se comparó con el antioxidante de referencia trolox (5 mM).

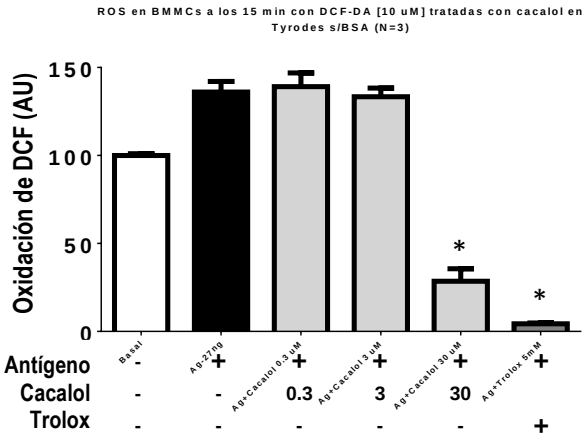


**Figura 28. El cacalol mostró una importante actividad anti-oxidante en comparación con el trolox. La oxidación de DCF inducida por la IgE/Ag en BMMCs pre-tratadas con diferentes concentraciones de cacalol (valores obtenidos de las células pre-tratadas con trolox fueron incluídos como control), n = 3. Prueba de ANOVA de una vía con comparaciones múltiples de Dunnett (*p < 0.05).**

8.9. <u>El cacalol interfiere con la movilización de $[Ca^{2+}]i$ inducida por IgE/Ag en CC.</u>

El cacalol mostró ser capaz de inhibir cerca de 40% del máximo de movilización de $[Ca^{2+}]i$ requerido para inducir la desgranulación dependiente de IgE/Ag entre 0.3 y 3 µM, mientras que inhibió casi completamente la movilización de $[Ca^{2+}]i$ a 30 µM (Figura 29).

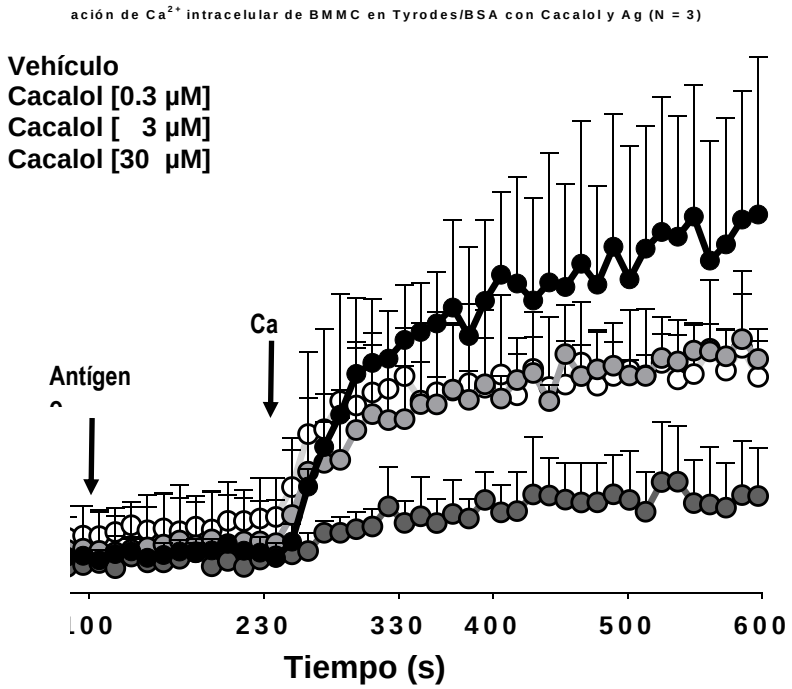


**Figura 29. El cacalol inhibe el flujo de calcio extracellular inducido por IgE/Ag en células cebadas. BMMC fueron resuspendidas en buffer libre de calcio y se añadió el antígeno DNP-HSA después de 100 segundos, el calcio fue añadido a la celda a una concentración de 1.8 mM. Trazo representativo del calcio intracelular que aumentó en células pre-tratadas con vehículo o con diferentes concentraciones de cacalol, n = 3. One way ANOVA with Dunnett´s multiple comparisons test (*p < 0.05).**

Tabla 4. Efecto del cacalol sobre el flujo de $Ca^{2+}$ extracelular estimulado por el receptor FcεRI en BMMCs.

| Tratamiento | Tasa de incremento $[Ca^{2+}]i$ | Máximo $[Ca^{2+}]i$ |
|---|---|---|
| Vehículo | 1.630 ± 0.016 | 334.2 ± 105.7 |
| Cacalol [0.3 µM] | 0.903 ± 0.350* | 225.3 ± 24.24 |
| Cacalol [3.0 µM] | 0.869 ± 0.202* | 237.4 ± 19.81 |
| Cacalol [ 30 µM] | 0.309 ± 0.245* | 144.0 ± 19.57* |

8.10. La isoquercetrina no inhibe la desgranulación inducida por IgE/Ag en CC

La isoquercitrina no mostró actividad para inhibir la desgranulación inducida por el receptor FcεRI en células cebadas en comparación con su precursor, la quercetina, que se sabe que tiene una buena actividad anti-inflamatoria *in vitro* e *in vivo* (Figura 30).

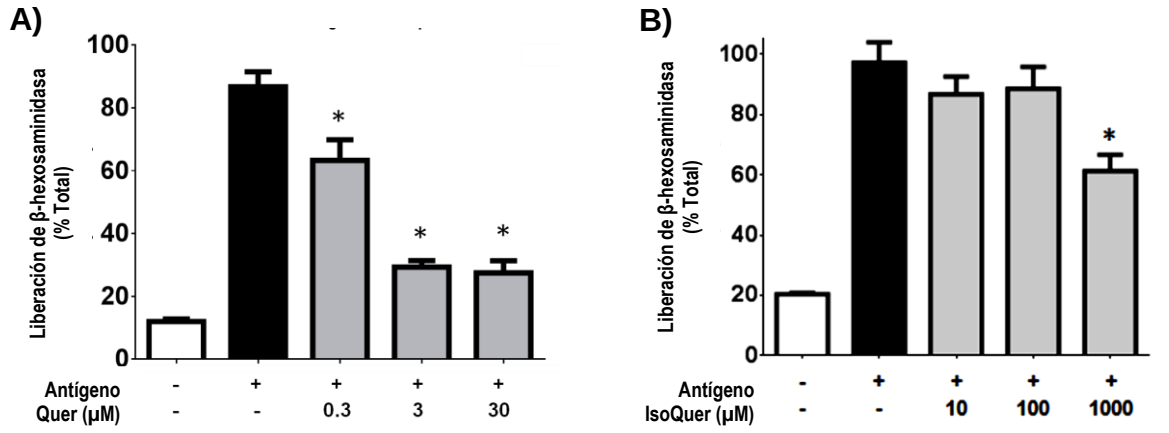


**Figura 30. Inhibición de la desgranulación inducido por IgE/Ag en células cebadas pre-tratadas con Quercetina e Isoquercitrina. n = 3. Prueba de ANOVA de una vía con comparaciones múltiples de Dunnett (*p < 0.05). Quer = Quercetina; IsoQue = Isoquercitrina.**

## 9. Discusión

Las plantas medicinales que han sido utilizadas por la humanidad desde sus orígenes constituyen una fuente potencial de compuestos naturales con propiedades anti-inflamatorias. Sin embargo, en la mayoría de los casos se desconocen las características moleculares de los compuestos activos, las concentraciones a las cuales son activos y, sobre todo, cuál es el mecanismo molecular mediante el cual inhiben estos compuestos sobre las células responsables de la inflamación.

En este estudio, se reporta por primera vez la estructura de la xantona jacareubina, la cual fue determinada por difracción de rayos X y sus efectos sobre la desgranulación de células cebadas fueron evaluados. La jacareubina mostró una alta actividad inhibidora sobre la desgranulación inducida por la activación del receptor FcεRI de las células cebadas mediante el bloqueo de la movilización del $Ca^{2+}$ extracelular activada por el complejo IgE/Ag, la tapsigargina o el TPA/A23187. La jacareubina también mostró una importante actividad anti-oxidante y a esto se le puede atribuir el efecto sobre la movilización de calcio, debido a la dependencia del fenómeno de generación de ROS. Mientras que la jacareubina no mostró actividad inhibidora significativa sobre la actividad de la NOX inducida por el FcεRI, esta inhibió la actividad de la xantina oxidasa en un ensayo libre de células. Finalmente, este compuesto ejerce acciones anti-inflamatorias *in vivo*, bloqueando reacciones inflamatorias que dependen de las células cebadas pero también de la activación de otras células del sistema inmune.

La estructura rígida y plana de la jacareubina fue claramente evidenciada por la difracción de rayos X y puede limitar la posibilidad de bloquear múltiples blancos moleculares inespecíficos. Las xantonas con un esqueleto de tres anillos han demostrado tener actividad anti-inflamatoria en células cebadas., como la nujiangexantona A, las mangostinas α, β y γ, la mangiferina y su aglicona el noratiriol (Figura 31) [49,115–118]. Nuestros resultados mostraron que la jacareubina, es la más potente xantona y la única con un anillo extra que se origina de la ciclización del sustituyente dimetil alil en el C-2, confiriéndole propiedades hidrofóbicas en esa región de la molécula. En el otro extremo de la molécula, sustituyentes hidroxilo en C-5 y C-6 permiten la interacción de la jacareubina debido a los puentes de hidrógeno con carbonilos de la membrana de fosfolípidos, de una manera similar a como se ha reportado para el colesterol [119]. De manera interesante, otras xantonas menos potentes como la nujiangexantona A y las mangostinas mantienen el sustituyente dimetil alil sin ciclizar, la mangiferina es el menos potente y el más hidrofílico debido a la presencia de cuatros sustituyentes hidroxilo y uno de glucosa. Otros compuestos con esqueletos similares como el Emodin, una antraquinona, posee un esqueleto similar a las xantonas, debido a la presencia de un sistema de tres anillos, pero con dos sustituyentes carbonilo, este es capaz de inhibir la liberación de β-hexosaminidasa inducida por IgE/Ag en BMMCs [120].

La actividad antioxidante de la jacareubina en la prueba de reducción de DPPH es similar a la previamente reportada [89,121]. La actividad antioxidante ha sido propuesta como el principal mecanismo responsable de la inhibición de la desgranulación en células cebadas que se asocia a muchos compuestos naturales [39,122]. Los grupos hidroxil fenólicos en xantonas ha sido importante para contribuir a

la actividad anti-oxidante de estos compuestos, pero este no siempre es el caso. Por ejemplo, la γ-mangostina y la garcinona A y B mostraron una mayor respuesta anti-oxidante que otras xantonas con un mayor número de sustituyentes hidroxilo en la prueba de reducción de DPPH [49,89]. La jacareubina mostró ser un mejor anti-oxidante que el α-tocoferol y el ácido cafeico, a pesar de que no posee un alto número de sustituyentes hidroxilo.

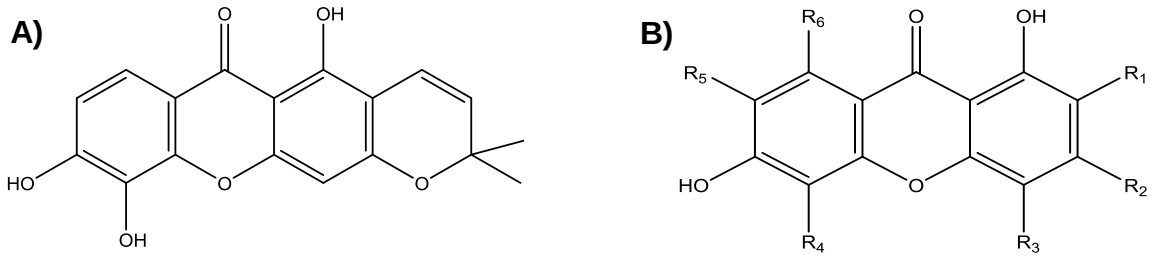


| | | | | |
|---|---|---|---|---|
| **Mangostina α** | **$R_1$, $R_6$ =** | **$R_2$ = OH** | **$R_3$, $R_4$ = H** | **$R_5$ = $OCH_3$** |
| **Mangostina β** | **$R_1$, $R_6$ =** | **$R_2$, $R_5$= $OCH_3$** | **$R_3$, $R_4$ = H** | |
| **Mangostina γ** | **$R_1$, $R_6$ =** | **$R_2$, $R_5$= OH** | **$R_3$, $R_4$ = H** | |
| **Nujiangexantona A** | **$R_1$ = OH** | **$R_2$ = $OCH_3$** | **$R_3$, $R_5$, $R_6$=** | **$R_4$ = OH** |
| **Mangiferina** | **$R_1$ = Glucosa** | **$R_2$, $R_5$ = OH** | **$R_3$, $R_4$, $R_6$ = H** | |
| **Noratiriol** | **$R_1$ = H** | **$R_2$, $R_5$ = OH** | **$R_3$, $R_4$, $R_6$ = H** | |

**Figura 31. La jacareubina presenta una estructura única entre las xantonas con actividad anti-inflamatoria. A) Jacareubina. B) Xantonas con actividad anti-inflamatoria en células cebadas previamente descritas (Se muestra en la parte de abajo los sustituyentes sobre la estructura general de las xantonas).**

La desgranulación de células cebadas después del entrecruzamiento del receptor FcεRI ha sido considerado el principal blanco en la investigación farmacológica para controlar la inflamación y alergia, debido a que la liberación de mediadores preformados ocurre muy rápido y la secreción de compuestos dispara inmediatas e intensas reacciones. La búsqueda de compuestos seguros capaces de inhibir la

desgranulación de células cebadas ha llevado a la identificación de varias moléculas con diferentes capacidades de inhibición y distintos mecanismos de acción. Nuestros datos muestran que la Jacareubina es una de las más potentes de las xantonas que se han probado en la desgranulación de células cebadas inducida por IgE/Ag. Cuando utilizamos 0.046 μM y 30 μM, este compuesto inhibe 50 y 97% la liberación de β-hexosaminidasa respectivamente, mientras la nujiangexantona A mostró una actividad máxima inhibidora a 50 μM (causando 95% de la inhibición en BMMCs) [48], pero su $IC_{50}$ se encontraba entre 1 y 10 μM, mientras que la mangostina α exhibió acciones inhibitorias con una $IC_{50}$ entre 10 y 20 μM, con un máximo de inhibición de la liberación de histamina en células RBL-2H3 de 80% a 20 μM [49]. Las xantonas son capaces de inhibir la desgranulación de células cebadas en un amplio rango de concentraciones, por ejemplo la mangiferina requiere 118 μM para inhibir el 50% de la desgranulación en células cebadas (Tabla 5), inducido por el compuesto 48/80 (un secretagogo comúnmente usado en células cebadas) [117]. Es importante hacer notar, que a ninguna de las concentraciones de jacareubina evaluadas, se provocó citotoxicidad en células cebadas. Este dato concuerda con lo observado con otras células del sistema inmune, como células mononucleares de sangre humana (PBMC) [114].

Además de las xantonas, otros productos naturales de tipo polifenólico han sido encontradas que son efectivas para inhibir la desgranulación de células cebadas en cerca del 70% y en los mismo rangos de concentración que la jacareubina, entre estos se encuentran flavonoides como la luteolina [35,37], la tetrametoxiluteolina [38], y la quercetina [35]. Sin embargo, debido a la polaridad de las xantonas, estas exhiben

una mejor solubilidad que los flavonoides mencionados y sus características pueden favorecer que alcancen una mayor concentración en los tejidos [13].

Aunque la evidencia muestra que algunas xantonas inhiben la movilización en células cebadas, el mecanismo específico por el que lleva a cabo su acción no ha sido determinado aún [49]. La descripción de los efectos de las xantonas sobre el sistema de señalización del receptor FcεRI incluyen, por ejemplo, el bloqueo de la fosforilación de Tyr en las proteínas de señalización iniciales, como la fosfolipasa A2, cinasas de la familia de Src y las MAPK [48]. Nuestros resultados muestran que la jacareubina es capaz de bloquear eficientemente la movilización de calcio en respuesta a la activación del receptor FcεRI en BMMCs y los datos indican el bloqueo de alguno de los canales de calcio membranales activados por el receptor FcεRI y la Thap.

En células cebadas, la activación del receptor FcεRI lleva a la activación de la PLC que produce diacilglicerol (DAG) e $IP_3$ que activa el canal de calcio $IP_3R$ causando el vaciamiento de los almacenes de calcio intracelular. Este evento lleva a la entrada de calcio desde el espacio extracelular por los canales de calcio membranales que constituyen al “Store Operated Calcium Entry” (SOCE), que puede ser activado por la Thap, el inhibidor de la ATPasa de SERCA. La SOCE opera principalmente a través de la familia de canales iónicos Orai, siendo Orai1 el más relevante en células del sistema inmune [113,123]. Después del vaciamiento de los almacenes de calcio intracelulares, la región Hand-EF del sensor de calcio STIM que está localizado en el lado de la membrana interna del retículo endoplásmico pierde el $Ca^{2+}$ que lo mantenían estabilizado, y provoca un cambio conformacional

que lleva a la oligomerización y extensión de STIM para formar con otros canales de membrana Orai el poro que facilita el rellenado de los almacenes de $Ca^{2+}$ en el retículo endoplásmico [29,124].

Diferentes estudios han sugerido que existe una muy cercana relación entre la producción de ROS y la entrada de calcio en células no excitables [109]. Por ejemplo, la producción de ROS promueve la glutationilación de las cisteínas C49 y C56 presentes en la región interna de STIM en el RE, que causa que la afinidad de $Ca^{2+}$ por parte de la región Hand-EF de STIM se reduzca, permitiendo la extensión de STIM y su oligomerización con Orai en la membrana plasmática [19,29,124]. En células cebadas, la activación del receptor FcεRI lleva a la activación de la NADPH oxidasa y la producción de ROS que promueve la activación del eje de señalización LAT-PLCγ [125]. Debido a que la jacareubina inhibe la producción de ROS dependiente de la activación del receptor FcεRI, es posible hipotetizar que este compuesto puede prevenir las modificaciones dependientes de reacciones redox de STIM y que son necesarias para la formación de la SOCE en células cebadas.

El bloqueo de la acumulación de ROS dependiente de la jacareubina puede también explicar la inhibición de la desgranulación promovida por la combinación del TPA/A23187, debido a que la Thap y el ionóforo de calcio A23187 también llevan a una rápida producción de ROS en células cebadas [126]. Interesantemente en este trabajo, aunque la actividad antioxidante de la jacareubina fue más alta que la mostrada por el trolox, pero más baja que la detectada para quercetina. La xantona fue la más potente en la inhibición de la desgranulación inducida por IgE/Ag. La

actividad anti-oxidante no mostró una correlación directa con la capacidad de los compuestos probados en bloquear la entrada de calcio de los tres compuestos.

El mecanismo por el que la jacareubina bloquea la desgranulación y movilización de calcio inducida por IgE/Ag en BMMCs ha mostrado que no incluye la inhibición de NOX. Por otra parte, la otra enzima productora de superóxido: la xantina oxidasa, fue inhibida por esta xantona. A pesar de que la xantona noratiriol que es estructuralmente relacionada a la jacareubina y que el noratiriol si mostró actividad inhibidora de la NOX y PLC en neutrófilos[115].

Nuestros datos indican que un mecanismo posible de acción de la jacareubina, además de su capacidad de atrapar ROS, es que puede también inhibir a la xantina oxidasa, ya que previamente ha sido descrito que la mangiferina puede inhibir a la xantina oxidasa ($IC_{50}$ = 21.7 μM), al igual que otros siete de sus derivados semi-sintéticos ($IC_{50}$ 4.6 – 20 μM), este modelo de inhibición fue simulado por docking molecular y se encontró que los compuestos se insertan en un túnel cercano hacia el complejo de Molibdeno (IV) en el sitio activo de la enzima[127]. Debido a la similitud estructural que tiene la mangiferina con la jacareubina, esto sugiere que la jacareubina posiblemente está bloqueando a la xantina oxidasa de manera similar, pero con una mayor potencia ($IC_{50}$ 0.3 – 3 μM), incluso que el alopurinol ($IC_{50}$ = 24.4 μM), el cual es el fármaco de referencia.

La actividad anti-oxidante de la jacareubina puede contribuir también a prevenir la activación de la PLCγ inducida por IgE/Ag, debido a que se ha demostrado que la producción de ROS es esencial para la fosforilación de la PLCγ en células cebadas [125], véase figura 32.

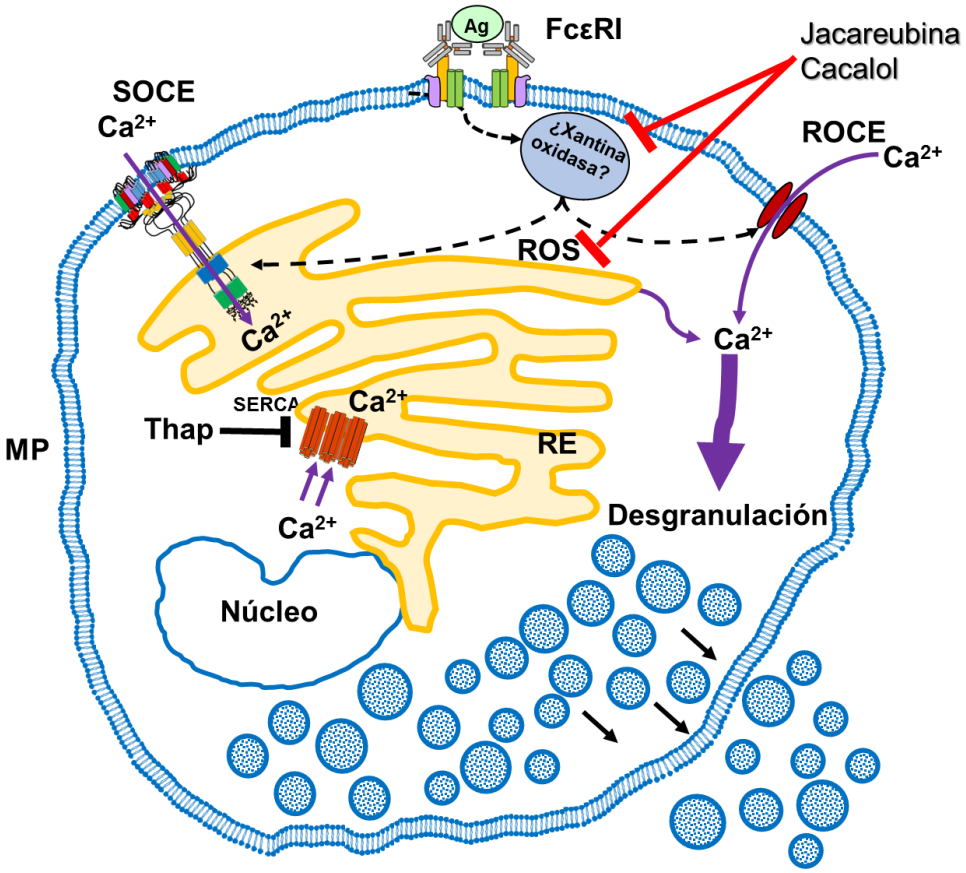


**Figura 32. Resumen de los puntos de control de la jacareubina y el cacalol en el sistema de señalización del receptor FcεRI en células cebadas. La jacareubina y el cacalol inhibieron la desgranulación y la movilización de calcio extracelular inducido por el IgE/Ag y la tapsigargina. Está inhibición correlaciona con el bloqueo de la generación de ROS en este tipo celular. MP = Membrana plasmática; RE = Retículo endoplásmico; ROS = Especies Reactivas de Oxígeno; SERCA = ATPasa del retículo endoplásmico/sarcoplásmico.**

La jacareubina puede ejercer sus acciones inhibitorias por mecanismos adicionales, hay evidencia con otros polifenoles los cuales son capaces de inhibir a la proteína cinasa Syk, como el piceatanol, la morina, la nujiangexantona A, las mangostinas α, β, γ y la emodina [48,49,65,120,128]. Por lo tanto es posible especular que

la jacareubina puede también inhibir a esta importante cinasa involucrada en el sistema de señalización del receptor FcεRI (veáse figura 2).

Tabla 5. Xantonas con actividad inhibidora de la desgranulación de CC.

| Fuente de origen y compuesto | Activador | % Inhibición de la desgranulación | Blancos moleculares inhibidos y actividad regulatoria |
|---|---|---|---|
| *Calophyllum brasiliense*<br>Jacareubina* [30 µM] | IgE/Ag | 97% β-Hexosaminidasa | ↓100% de ROS de activación<br>↓90% movilización of $Ca^{2+}$<br>Bloquea a la xantina oxidasa |
| [30 µM]<br>[30 µM] | TPA/A23187<br>Tapsigargina | 93% β- Hexosaminidasa<br>97% β- Hexosaminidasa[129] | ↓70% movilización of $Ca^{2+}$ |
| *Garcinia nujiangensis*<br>Nujiangexantona A* [50 µM] | IgE/Ag | 95% β- Hexosaminidasa[48] | ↓Fosforilación de Syk y Src<br>↓Producción de citocinas y eicosanoides tipo $PGD_2$ y $LTC_4$ |
| *Garcinia mangostana*<br>Mangostina α [20 µM]** | IgE/Ag | 80% Histamina[49] | ↓ >90% movilización de $Ca^{2+}$<br>↓ <10% de ROS<br>↓ Fosforilación de Syk.<br>↓Fosforilación de PLCγ1/2 y de ERK1/2. |
| [12 µM]* | TPA/A23187 | 50% Histamina[116] | ↓IL-6, $PGD_2$ y $LTC_4$.<br>Suprime la expresión de COX-2. |
| *G. mangostana*<br>Mangostina γ [20 µM]** | IgE/Ag | 50% Histamina[49] | ↓50% movilización de $Ca^{2+}$<br>↓50% de ROS<br>↓ Fosforilación de Syk.<br>↓Fosforilación de PLCγ1/2 y ERK1/2. |
| [12 µM]* | TPA/A23187 | 50% β- Hexosaminidasa[116] | |
| *G. mangostana*<br>Mangostina β [20 µM]** | IgE/Ag | 45% Histamina[49] | ↓20% movilización de $Ca^{2+}$<br>↓ <10% de ROS<br>↓ Fosforilación de Syk.<br>↓Fosforilación de PLCγ1/2 y ERK1/2. |
| *Mangifera indica L.*<br>Mangiferina [118 µM]*** | Compuesto 48/80 | 50% Histamina[118] | Bloquea a la xantina oxidasa[127] |

* Se utilizaron células cebadas derivadas de médula ósea (BMMCs).
** Se utilizaron células RBL-2H3.
*** Se utilizaron células cebadas de peritoneo de rata.

El efecto de la jacareubina en las reacciones anafilácticas dependientes de las células cebadas se observaron *in vivo*, debido a que este compuesto suprime la extravasación del colorante azul de Evans inducida por la IgE/Ag (un efecto mediado por la histamina secretada por las células cebadas) y el edema inducido por TPA en el ratón, una respuesta dependiente de la producción de prostaglandinas por otras células residentes del sistema inmune[130]. El bloqueo de la acumulación de ROS puede contar de manera importante para este efecto, debido a que la producción de ROS es esencial para la desgranulación de células cebadas inducida por el receptor FcεRI [125], así como para la producción de prostaglandinas en otras células [131]. El efecto de la jacareubina en inhibir la anafilaxia pasiva cutánea fue similar o más potente a lo observado con otros compuestos naturales como la morina (30 mg/Kg), teorinina (1 mg/Kg) y la teanina (1 mg/Kg), los cuales mostraron inhibición por 40, 42 y 44%, respectivamente [52,65,132,133]. Las xantonas similares a la jacareubina como las mangostinas no han demostrado tener efectos tóxicos en estudios pre-clínicos y clínicos [134,135]. La jacareubina se presenta aquí como un nuevo fármaco con potencial para el desarrollo de compuestos anti-inflamatorios derivados de productos naturales para tratar enfermedades relacionadas con células cebadas.

Con respecto a los cacalólidos, los resultados *in vitro* sugieren que el cacalol tiene la mayor actividad de inhibición de los cuatro compuestos probados en la desgranulación dependiente del receptor FcεRI en células cebadas, probablemente debido a su estructura química inestable, que puede llevar a una rápida descomposición hacia otros compuestos más estables mientras asimilan electrones derivados de los ROS [84] producidos por la activación del receptor FcεRI en CC, que son importantes para la activación de los canales de calcio dependientes de SOCE

y que a su vez estos son necesarios en la activación de receptores tipo Fc de múltiples células del sistema inmune [113,136].

Mientras el acetato de cacalol, que es un derivado del cacalol producido por acetilación que vuelve a la molécula más estable a las condiciones ambientales, este mostró una menor actividad de inhibición de la desgranulación de células cebadas. El acetato de maturina que se obtiene del "matarique" (*P. peltatum*), mostró ser estable bajo condiciones ambientales y los resultados de inhibición de la desgranulación fueron similares a los del acetato de cacalol. La baja actividad de ambos compuestos posiblemente se debe a los grupos sustituyentes acetilo que no les permite aceptar electrones no apareados de ROS [137,138].

Sobre la cacalona, aunque previamente se ha descrito que es un compuesto con una actividad anti-inflamatoria y anti-oxidante mayor que el cacalol en el modelo *in vivo* de edema en oreja de ratón inducido por TPA [82]. Este compuesto mostró una pobre actividad inhibitoria sobre la desgranulación inflamatoria inducida por IgE/Ag en células cebadas, probablemente debido a que los dos modelos evaluados de inflamación son producidos por diferentes células del sistema inmune, otra posibilidad puede ser que la cacalona purificada resultó ser una mezcla 1:1 con su isómero de epi-cacalona (Anexos, páginas 100 – 104), que probablemente sea inactiva [94].

Sin embargo, el cacalol no es el único sesquiterpeno con buena actividad para inhibir la desgranulación dependiente del receptor FcεRI. Otros sesquiterpenos reportados en la literatura son el partenólido que inhiben la desgranulación de células cebadas, así como de reducir la activación de NFκB y la formación de

microtúbulos dependientes de la cinasa Fyn [45]. Otros sesquiterpenos con actividad similar al cacalol son la deacetileupaserrina, (3S, 6R, 7R, 8R)-3-hidroxi-8-acetoxisarraceniloxigermacra-1, 4,11(13)-trien-6,12-olido, (3S, 6R, 7R, 8R)-3-hidroxi-8-(2'-metilbutiroiloxi)-14-oxomelampa-1(10), 4-dien-6,12-olido y la eupaformosanina, en el que su mecanismo está principalmente asociado con la inhibición de la fosforilación de las proteínas p38 y Akt. También como de una inhibición parcial de la movilización de calcio intracelular $[Ca^{2+}]i$ [27].

Inesperadamente, la isoquercitrina no tuvo un efecto importante sobre la desgranulación de la CC en el modelo *in vitro*. Esto puede deberse a que el compuesto como tal sea un profármaco que debe metabolizarse a quercetina para ejercer sus efectos [13,35]. En el medio utilizado para la estimulación de las BMMCs, las enzimas encargadas de la transformación de la isoquercitrina pueden no haber estado presentes.

La jacareubina fue el compuesto con la mejor respuesta anti-inflamatoria al evaluarse en el modelo *in vitro* de desgranulación e *in vivo* en el modelo de anafilaxia pasiva cutánea y de edema en oreja de ratón inducida por TPA, además de demostrar una estabilidad química muy alta y una baja toxicidad que fue corroborada también por otro grupo de investigación independiente [114]. El mecanismo propuesto de inhibición de la jacareubina está basado en los resultados de esta tesis, que muestran que es capaz de inhibir la acumulación de ROS. Se ha demostrado que los ROS son producidos por enzimas como la xantina oxidasa tras la activación del receptor FcεRI [15]. La ausencia de ROS que son necesarios para activar los canales de $Ca^{2+}$ membranales de ROCE y SOCE impiden la movilización de los gránulos que almacenan el contenido pro-inflamatorio [113,123], la falta de $Ca^{2+}$

intracelular impide la activación de otras proteínas necesarias para la desgranulación como la calcineurina, PLCγ y PKC [28]. El hallazgo de la actividad antioxidante y anti-inflamatoria de la jacareubina representa un avance significativo en la caracterización de los mecanismos de acción de moléculas naturales con propiedades anti-inflamatorias y abre la puerta a explorar con más detalle las consecuencias de la inhibición de la SOCE en la activación de otras células de la inmunidad innata y adaptativa, como macrófagos y linfocitos B y T, activados vía receptores Fcγ, TCR o BCR, los cuales señalizan también mediante la movilización de $Ca^{2+}$ intracelular[136].

Con respecto a la presencia de la nNOS y la eNOS en CC, no encontramos la expresión de los RNAm de la nNOS ni de la eNOS, pese a que los oligonucleótidos lograron amplificar un producto específico en otros tejidos. Este hallazgo sugiere que la cantidad basal de eNOS es muy pequeña en este tipo celular.

## 10. Conclusiones

Es necesario continuar con la búsqueda de inhibidores y estabilizadores de las células cebadas efectivos, ya que su papel en varias enfermedades mentales (autismo y meningioma), enfermedades metabólicas (diabetes, obesidad, ateroesclerosis y síndrome coronario agudo), y de hipersensibilidad (asma y alergias), ha quedado documentado en las última décadas.

En esta tesis doctoral encontramos un potente efecto inhibidor de la jacareubina y el cacalol sobre la desgranulación inducida por IgE/Ag en CC, mientras que los otros cuatro compuestos mostraron un efecto inhibidor más modesto. El efecto del cacalol y la jacareubina depende del bloqueo de la movilización de calcio intracelular indispensable para la desgranulación. Ambos compuestos también presentaron una potente actividad antioxidante que se asocia con el bloqueo sobre la movilización de calcio intracelular, debido a su dependencia de la presencia de ROS. La jacareubina, adicionalmente, bloquea la producción de ROS, inhibiendo principalmente a la xantina oxidasa, ya que la NADPH oxidasa no tiene una participación importante en este proceso. Finalmente, se demostró que la jacareubina posee actividad anti-inflamatoria *in vivo*, al bloquear reacciones inflamatorias dependientes de CC, pero también de la activación de otras células inmunes.

## 11. Literatura citada


1. Pawankar, R., Canonica, G. W., Holgate, S. T., Lockey, R. F. & Blaiss, M. S. *World Allergy Organization White Book on Allergy: Update 2013*. *WAO white book on allergy : update 2013* (2013). doi:10.1186/1939-4551-7-12

2. Gershwin, L. J. Comparative Immunology of Allergic Responses. *Annu. Rev. Anim. Biosci.* **3,** 327–346 (2015).

3. *Allergy Frontiers: Therapy and Prevention Volume 5*. (Springer, 2010). doi:10.1007/978-4-431-99362-9

4. Kristiansen, M. *et al.* Allergen immunotherapy for the prevention of allergy: A systematic review and meta-analysis. *Pediatr. Allergy Immunol.* **28,** 18–29 (2017).

5. El-Feky R. A. Mast cell and atopy. *Egypt J. Pediatry Allergy Immunol ogy* **9,** 55–62 (2011).

6. Roos, A. B. *et al.* Increased IL-17RA and lL-17RC in End-Stage COPD and the Contribution to Mast Cell Secretion of FGF-2 and VEGF. *Respiratory Research* **18,** (2017).

7. Jiménez-Andrade, G. Y., Ibarra-Sánchez, A., González, D., Lamas, M. & González-Espinosa, C. Immunoglobulin e induces VEGF production in mast cells and potentiates their pro-tumorigenic actions through a Fyn kinase-dependent mechanism. *J. Hematol. Oncol.* **6,** (2013).

8. Hwang, C. Y. *et al.* Prevalence of atopic dermatitis, allergic rhinitis and asthma in Taiwan: A national study 2000 to 2007. *Acta Derm. Venereol.* **90,** 589–594 (2010).

9. Varricchi, G. *et al.* Are mast cells MASTers in cancer? *Frontiers in Immunology* (2017). doi:10.3389/fimmu.2017.00424

10. Hurst, D. S. & Venge, P. Evidence of eosinophil, neutrophil, and mast-cell mediators in the effusion of OME patients with and without atopy. *Allergy Eur. J. Allergy Clin. Immunol.* **55,** 435–441 (2000).

11. Logsdon, S. L. & Oettgen, H. C. Anti-ige therapy: Clinical utility and mechanistic insights. *Curr. Top. Microbiol. Immunol.* **388,** 39–61 (2015).

12. Karhausen, J. & Abraham, S. N. How mast cells make decisions. *Journal of Clinical Investigation* **126,** 3735–3738 (2016).

13. Weng, Z. *et al.* Quercetin is more effective than cromolyn in blocking human mast cell cytokine release and inhibits contact dermatitis and photosensitivity in humans. *PLoS One* **7,** (2012).

14. Arinobu, Y., Iwasaki, H. & Akashi, K. Origin of Basophils and Mast Cells. *Allergol. Int.* **58,** 21–28 (2009).

15. Suzuki, Y., Yoshimaru, T., Inoue, T. & Ra, C. Discrete generations of

intracellular hydrogen peroxide and superoxide in antigen-stimulated mast cells: Reciprocal regulation of store-operated $Ca^{2+}$channel activity. *Mol. Immunol.* **46,** 2200–2209 (2009).

16. Fasolato, C., Hoth, M., Matthews, G. & Penner, R. $Ca^{2+}$ and $Mn^{2+}$ Influx through Receptor-Mediated Activation of Nonspecific Cation Channels in Mast-Cells. *Proc. Natl. Acad. Sci. U. S. A.* **90,** 3068–3072 (1993).

17. Parekh, A. B., Fleig, A. & Penner, R. The store-operated calcium current I(CRAC): nonlinear activation by InsP3 and dissociation from calcium release. *Cell* **89,** 973–980 (1997).

18. Artalejo, a R., Ellory, J. C. & Parekh, a B. $Ca^{2+}$-dependent capacitance increases in rat basophilic leukemia cells following activation of store-operated Ca2+ entry and dialysis with high-$Ca^{2+}$-containing intracellular solution. *Pflugers Arch.* **436,** 934–9 (1998).

19. Suzuki, Y., Yoshimaru, T., Inoue, T., Niide, O. & Ra, C. Role of oxidants in mast cell activation. *Chemical Immunology and Allergy* **87,** 32–42 (2005).

20. Inoue, T., Suzuki, Y., Yoshimaru, T., & Ra, C. Nitric oxide positively regulates Ag (I)-induced $Ca^{2+}$ influx and mast cell activation: role of a nitric oxide synthase-independent pathway. *J. Leukoc. Biol.* **86,** 1365–1375 (2009).

21. Itoh, T. *et al.* Inhibitory effects of whisky congeners on IgE-mediated degranulation in rat basophilic leukemia RBL-2H3 cells and passive cutaneous anaphylaxis reaction in mice. *J. Agric. Food Chem.* **58,** 7149–7157 (2010).

22. Yoshimaru, T., Suzuki, Y., Inoue, T. & Ra, C. L-type $Ca^{2+}$channels in mast cells: Activation by membrane depolarization and distinct roles in regulating mediator release from store-operated $Ca^{2+}$channels. *Mol. Immunol.* **46,** 1267–1277 (2009).

23. Suzuki, Y., Inoue, T. & Ra, C. L-type $Ca^{2+}$ channels: A new player in the regulation of $Ca^{2+}$ signaling, cell activation and cell survival in immune cells. *Molecular Immunology* **47,** 640–648 (2010).

24. Suzuki, Y., Inoue, T. & Ra, C. NSAIDs, mitochondria and calcium signaling: Special focus on aspirin/salicylates. *Pharmaceuticals* **3,** 1594–1613 (2010).

25. Blank, U. & Rivera, J. The ins and outs of IgE-dependent mast-cell exocytosis. *Trends in Immunology* (2004). doi:10.1016/j.it.2004.03.005

26. Krystel-Whittemore, M., Dileepan, K. N. & Wood, J. G. Mast cell: A multi-functional master cell. *Frontiers in Immunology* **6,** (2016).

27. Itoh, T., Oyama, M., Takimoto, N., Kato, C., Nozawa, Y., Akao, Y., & Iinuma, M. Inhibitory effects of sesquiterpene lactones isolated from Eupatorium chinense L. on IgE-mediated degranulation in rat basophilic leukemia RBL-2H3 cells and passive cutaneous anaphylaxis reaction in mice. *Bioorg. Med. Chem.* **17,** 3189–3197 (2009).

28. Manikandan, J., Kothandaraman, N., Hande, M. P. & Pushparaj, P. N. Deciphering the structure and function of FcεRI/mast cell axis in the regulation of allergy and anaphylaxis: A functional genomics paradigm. *Cellular and Molecular Life Sciences* **69,** 1917–1929 (2012).

29. Nunes, P. & Demaurex, N. Redox regulation of store-operated $Ca^{2+}$ entry. *Antioxid. Redox Signal.* **21,** 915–32 (2014).

30. Perez, R. M. Anti-inflammatory activity of compounds isolated from plants. *TheScientificWorldJournal [electronic Resour.* **1,** (2001).

31. Singh, A., Holvoet, S. & Mercenier, A. Dietary polyphenols in the prevention and treatment of allergic diseases. *Clinical and Experimental Allergy* **41,** 1346–1359 (2011).

32. Finn, D. F. & Walsh, J. J. Twenty-first century mast cell stabilizers. *British Journal of Pharmacology* **170,** 23–37 (2013).

33. Dong Kim, J. *et al. Morus bombycis* extract suppresses mast cell activation and IgE-mediated allergic reaction in mice. *J. Ethnopharmacol.* **146,** 287–293 (2013).

34. Kim, J. H. yun. *et al. Rhamnus davurica* leaf extract inhibits Fyn activation by antigen in mast cells for anti-allergic activity. *BMC Complement. Altern. Med.* **15,** 80 (2015).

35. Kimata, M. *et al.* Effects of luteolin, quercetin and baicalein on immunoglobulin E-mediated mediator release from human cultured mast cells. *Clin. Exp. Allergy* **30,** 501–508 (2000).

36. Jeon, I. H. *et al.* Anti-inflammatory and antipruritic effects of luteolin from perilla (*P. frutescens L*.) leaves. *Molecules* **19,** 6941–6951 (2014).

37. Sun-Yup, S., Park, J. R. & Byun, D. S. 6-Methoxyluteolin from *Chrysanthemum zawadskii var. latilobum* suppresses histamine release and calcium influx via down-regulation of FcεRI α chain expression. *J. Microbiol. Biotechnol.* **22,** 622–627 (2012).

38. Weng, Z., Patel, A. B., Panagiotidou, S. & Theoharides, T. C. The novel flavone tetramethoxyluteolin is a potent inhibitor of human mast cells. *J. Allergy Clin. Immunol.* **135,** 1044–1052.e5 (2015).

39. Ninomiya, M. *et al.* Phenolic constituents isolated from *Fragaria ananassa* Duch. inhibit antigen-stimulated degranulation through direct inhibition of spleen tyrosine kinase activation. *Bioorganic Med. Chem.* **18,** 5932–5937 (2010).

40. Morikawa, T., Xu, F., Matsuda, H., & Yoshikawa, M. Structures of Novel Norstilbene Dimer, Longusone A, and Three New Stilbene Dimers, Longusols A, B, and C, with Antiallergic and Radical Scavenging Activities from Egyptian Natural Medicine *Cyperus longus*. *Chem. Pharm. Bull.* **58,** 1379–1385 (2010).

41. Fujimura, Y., Umeda, D., Yamada, K. & Tachibana, H. The impact of the 67 kDa laminin receptor on both cell-surface binding and anti-allergic action of tea catechins. *Arch. Biochem. Biophys.* **476,** 133–138 (2008).

42. Wang, Q., Matsuda, H., Matsuhira, K., Nakamura, S., Yuan, D., & Yoshikawa, M. Inhibitory effects of thunberginols A, B, and F on degranulations and releases of TNF-α and IL-4 in RBL-2H3 cells. *Biol. Pharm. Bull.* **30,** 388—392 (2007).

43. Choi, Y. H., & Yan, G. H. Anti-allergic effects of scoparone on mast cell-mediated allergy model. *Phytomedicine* **16,** 1089–1094 (2009).

44. Hong, J. *et al.* Suppression of the antigen-stimulated RBL-2H3 mast cell activation by artekeiskeanol A. *Planta Med.* **75,** 1494–1498 (2009).

45. Miyata, N. *et al.* Inhibitory effects of parthenolide on antigen-induced microtubule formation and degranulation in mast cells. *Int. Immunopharmacol.* **8,** 874–880 (2008).

46. Penissi, A. B. *et al.* Novel anti-ulcer α,β-unsaturated lactones inhibit compound 48/80-induced mast cell degranulation. *Eur. J. Pharmacol.* **612,** 122–130 (2009).

47. Zhu, H., Tang, S. A., Qin, N., Duan, H. Q., & Jin, M. H. Anti-inflammatory constituents from *Inula japonica*. *China J. Chinese Mater. medica* **39,** 83–88 (2014).

48. Lu, Y. *et al.* The natural compound nujiangexanthone A suppresses mast cell activation and allergic asthma. *Biochem. Pharmacol.* **100,** 61–72 (2015).

49. Itoh, T., Ohguchi, K., Iinuma, M., Nozawa, Y. & Akao, Y. Inhibitory effect of xanthones isolated from the pericarp of *Garcinia mangostana L.* on rat basophilic leukemia RBL-2H3 cell degranulation. *Bioorganic Med. Chem.* **16,** 4500–4508 (2008).

50. Matsuda, H. *et al.* Inhibitory effects of thunberginols A and B isolated from Hydrangeae Dulcis Folium on mRNA expression of cytokines and on activation of activator protein-1 in RBL-2H3 cells. *Phytomedicine* **15,** 177–184 (2008).

51. Oh, J. *et al.* Syk/Src pathway-targeted inhibition of skin inflammatory responses by carnosic acid. *Mediators Inflamm.* (2012). doi:10.1155/2012/781375

52. Kim, N. H., Jeong, H. J. & Kim, H. M. Theanine is a candidate amino acid for pharmacological stabilization of mast cells. *Amino Acids* **42,** 1609–1618 (2012).

53. Wang, Q. *et al.* Inhibitory effects of thunberginols A, B, and F on degranulations and releases of TNF-alpha and IL-4 in RBL-2H3 cells. *Biol. Pharm. Bull.* **30,** 388–392 (2007).

54. Matsuda, H., Shimoda, H. & Yoshikawa, M. Structure-requirements of

isocoumarins, phthalides, and stilbenes from hydrangeae dulcis folium for inhibitory activity on histamine release from rat peritoneal mast cells. *Bioorganic Med. Chem.* **7,** 1445–1450 (1999).

55. Hua, J. M. *et al.* 5-Methoxy-8-(2-hydroxy-3-buthoxy-3-methylbutyloxy)-psoralen isolated from *Angelica dahurica* inhibits cyclooxygenase-2 and 5-lipoxygenase in mouse bone marrow-derived mast cells. *Arch. Pharm. Res.* **31,** 617–621 (2008).

56. Choi, Y. H. & Yan, G. H. Silibinin attenuates mast cell-mediated anaphylaxis-like reactions. *Biol. Pharm. Bull.* **32,** 868–75 (2009).

57. Shaik, G. M., Dráberová, L., Heneberg, P. & Dráber, P. Vacuolin-1-modulated exocytosis and cell resealing in mast cells. *Cell. Signal.* (2009). doi:10.1016/j.cellsig.2009.04.001

58. Kang, O. H. *et al.* Anti-inflammatory mechanisms of resveratrol in activated HMC-1 cells: Pivotal roles of NF-κB and MAPK. *Pharmacol. Res.* (2009). doi:10.1016/j.phrs.2009.01.009

59. Inoue, T., Sugimoto, Y., Masuda, H. & Kamei, C. Antiallergic Effect of Flavonoid Glycosides Obtained from *Mentha piperita L* . *Biol. Pharm. Bull.* (2002). doi:10.1248/bpb.25.256

60. Kang, O. H., Choi, J. G., Lee, J. H. & Kwon, D. Y. Luteolin isolated from the flowers of *Lonicera japonica* suppresses inflammatory mediator release by blocking NF-κB and MAPKs activation pathways in HMC-1 cells. *Molecules* (2010). doi:10.3390/molecules15010385

61. Bronner, C. & Landry, Y. Kinetics of the inhibitory effect of flavonoids on histamine secretion from mast cells. *Agents Actions* (1985). doi:10.1007/BF01983124

62. Morikawa, T., Xu, F., Matsuda, H. & Yoshikawa, M. Structures and radical scavenging activities of novel nor-stilbene dimer, longusone A, and new stilbene dimers, B, and C, from Egyptian herbal medicine *Cyperus longus*. *Heterocycles* (2002).

63. Passante, E., Ehrhardt, C., Sheridan, H. & Frankish, N. RBL-2H3 cells are an imprecise model for mast cell mediator release. *Inflamm. Res.* (2009). doi:10.1007/s00011-009-0028-4

64. Park, S. G. *et al.* Evaluation of anti-allergic properties of caffeic acid phenethyl ester in a murine model of systemic anaphylaxis. *Toxicol. Appl. Pharmacol.* (2008). doi:10.1016/j.taap.2007.08.003

65. Kim, J. W. *et al.* Morin inhibits Fyn kinase in mast cells and IgE-mediated type I hypersensitivity response *in vivo*. *Biochem. Pharmacol.* **77,** 1506–1512 (2009).

66. Li, G. Z., Chai, O. H. & Song, C. H. Inhibitory effects of epigallocatechin gallate on compound 48/80-induced mast cell activation and passive cutaneous

anaphylaxis. *Exp. Mol. Med.* (2005). doi:10.1038/emm.2005.39

67. Nishikawa, H., Wakano, K. & Kitani, S. Inhibition of NADPH oxidase subunits translocation by tea catechin EGCG in mast cell. *Biochem. Biophys. Res. Commun.* (2007). doi:10.1016/j.bbrc.2007.08.015

68. Yoshikawa, M., Nakamura, S., Kato, Y., Matsuhira, K. & Matsuda, H. Medicinal flowers. XIV. New acylated oleanane-type triterpene oligoglycosides with antiallergic activity from flower buds of chinese tea plant (*Camellia sinensis*). *Chem. Pharm. Bull. (Tokyo).* (2007). doi:10.1248/cpb.55.598

69. Reyes-Chilpa, R., Jimenez-Estrada, M. & Estrada-Muñiz, E. Antifungal Xanthones from *Calophyllum brasiliensis* Heartwood. *J. Chem. Ecol.* **23,** 1901–1911 (1997).

70. Yasunaka, K. *et al.* Antibacterial activity of crude extracts from Mexican medicinal plants and purified coumarins and xanthones. *J. Ethnopharmacol.* **97,** 293–299 (2005).

71. Kaennakam, S., Siripong, P. & Tip-Pyang, S. Kaennacowanols A-C, three new xanthones and their cytotoxicity from the roots of *Garcinia cowa*. *Fitoterapia* **102,** 171–176 (2015).

72. Reyes-Chilpa, R. *et al.* Inhibition of gastric $H^+$,$K^+$-ATPase activity by flavonoids, coumarins and xanthones isolated from Mexican medicinal plants. *J. Ethnopharmacol.* **105,** 167–172 (2006).

73. King, F. E., King, T. J., & Manning, L. C. 804. The chemistry of extractives from hardwoods. Part XIV. The constitution of jacareubin, a pyranoxanthone from *Calophyllum brasiliense*. *J. Chem. Soc.* 3932–3937 (1953).

74. Bhanu, S., Scheinmann, F., & Jefferson, A. Xanthones from the heartwood of *Calophyllum ramiflorum*. *Phytochemistry* **14,** 298–299 (1975).

75. Scheinmann, F. & Sripong, N. A. Xanthones from the heartwood of *Calophyllum neo-ebudicum*: comments, on the taxonomic value of jacareubin in *Calophyllum* species. *Phytochemistry* **10,** 1331–1333 (1971).

76. Kumar, V., Ramachandran, S. & Sultanbawa, M. U. S. Xanthones and triterpenoids from timber of *Calophyllum inophyllum*. *Phytochemistry* **15,** 2016–2017 (1976).

77. Bhanu, S., Scheinmann, F. & Jefferson, A. Xanthones from the heartwood of *Calophyllum ramiflorum*. *Phytochemistry* (1975). doi:10.1016/0031-9422(75)85068-0

78. Blanco-Ayala, T. *et al.* Antioxidant properties of xanthones from *Calophyllum brasiliense*: Prevention of oxidative damage induced by $FeSO_4$. *BMC Complement. Altern. Med.* **13,** (2013).

79. Alarcon-Aguilar, F. J. *et al.* Effects of three Mexican medicinal plants (Asteraceae) on blood glucose levels in healthy mice and rabbits. *J.*

*Ethnopharmacol.* **55,** 171–177 (1997).

80. Alarcon-Aguilar, F. J. *et al.* Hypoglycemic activity of root water decoction, sesquiterpenoids, and one polysaccharide fraction from *Psacalium decompositum* in mice. *J. Ethnopharmacol.* **69,** 207–215 (2000).

81. Romo de Vivar, A., Pérez-Castorena, A.-L., Arciniegas, A. & Villaseñor, J. L. Secondary Metabolites from Mexican Species\nof the Tribe Senecioneae (Asteraceae). *J. Mex. Chem.* **51,** 160–172 (2007).

82. Jimenez-Estrada, M. *et al.* Anti-inflammatory activity of cacalol and cacalone sesquiterpenes isolated from *Psacalium decompositum*. *J. Ethnopharmacol.* **105,** 34–38 (2006).

83. Rojano-Vilchis, N.; Jimenez-Estrada, M.; Nieto Camacho, A.; Torres Avilez, A.; Bye, R.; Chavez Avila, V.; Canales-Martinez, K.; Martinez-Elizalde, K. and Rodriguez-Monroy, M. Isolation and anti-inflammatory effects of maturin acetate from the roots of *Psacalium peltatum* (Asteraceae). *J. Med. Plants Res.* **7,** 1600–1607 (2013).

84. Jiménez-Estrada, M., Reyes-Chilpa, R., Navarro-Ocaña, A. & Arrieta-Baez, D. Reactivity of several reactive oxygen species (ROS) with the sesquiterpene cacalol. *Nat. Prod. Commun.* **3,** 479–482 (2008).

85. Fernandez, J. *et al.* Isoquercitrin from *Argemone platyceras* inhibits carbachol and leukotriene D4-induced contraction in guinea-pig airways. *Eur. J. Pharmacol.* **522,** 108–115 (2005).

86. Anaya, A. L., Hernández-Bautista, B. E., Torres-Barragán, A., León-Cantero, J. & Jiménez-Estrada, M. Phytotoxicity of cacalol and some derivatives obtained from the roots of *Psacalium decompositum* (A. Gray) H. Rob. & brettell (Asteraceae), matarique or maturin. *J. Chem. Ecol.* **22,** 393–403 (1996).

87. P.G.M., B. Caracterización tecnológica de veinte especies maderables de la Selva Lacandona. *Madera y Bosques* **1,** 9–38 (1995).

88. Campos, M. G., Oropeza, M., Torres-Sosa, C., Jiménez-Estrada, M. & Reyes-Chilpa, R. Sesquiterpenoids from antidiabetic *Psacalium decompositum* block ATP sensitive potassium channels. *J. Ethnopharmacol.* **123,** 489–493 (2009).

89. Zhong, F., Chen, Y., Wang, P., Feng, H. & Yang, G. Xanthones from the bark of *Garcinia xanthochymus* and their 1,1-diphenyl-2-picrylhydrazyl radical-scavenging activity. *Chinese J. Chem.* **27,** 74–80 (2009).

90. Zhang, S. S. *et al.* Chemical constituents from the fungus *Amauroderma amoiensis* and their in vitro acetylcholinesterase inhibitory activities. *Planta Med.* **79,** 87–91 (2013).

91. Sheldrick, G. M. SHELXT - Integrated space-group and crystal-structure determination. *Acta Crystallogr. Sect. A Found. Crystallogr.* **71,** 3–8 (2015).

92. Kedrowski, B. L. & Hoppe, R. W. A concise synthesis of (±)-cacalol. *J. Org. Chem.* **73,** 5177–5179 (2008).

93. Yuste, F., Díaz, E., Walls, F. & Jankowski, K. The Structure of Cacalone. *Journal of Organic Chemistry* **41,** 4103–4106 (1976).

94. Inman, W. D., Luo, J., Jolad, S. D., King, S. R. & Cooper, R. Antihyperglycemic sesquiterpenes from *Psacalium decompositum*. *J. Nat. Prod.* **62,** 1088–1092 (1999).

95. Garduño-Ramírez, M. L. *et al.* New modified eremophilanes from the roots of *Psacalium radulifolium*. *J. Nat. Prod.* **64,** 432–435 (2001).

96. Madera-Salcedo, I. K., Cruz, S. L. & Gonzalez-Espinosa, C. Morphine Prevents Lipopolysaccharide-Induced TNF Secretion in Mast Cells Blocking IκB Kinase Activation and SNAP-23 Phosphorylation: Correlation with the Formation of a β-Arrestin/TRAF6 Complex. *J. Immunol.* **191,** 3400–3409 (2013).

97. Manetz, T. S. *et al.* Vav1 Regulates Phospholipase C Activation and Calcium Responses in Mast Cells. *Mol. Cell. Biol.* **21,** 3763–3774 (2001).

98. Saitoh, S. *et al.* LAT Is Essential for FcεRI-Mediated Mast Cell Activation. *Immunity* **12,** 525–535 (2000).

99. Grynkiewicz, G., Poenie, M. & Tsien, R. Y. A new generation of $Ca^{2+}$ indicators with greatly improved fluorescence properties. *J. Biol. Chem.* **260,** 3440–3450 (1985).

100. Davies, M. J., Forni, L. G. & Willson, R. L. Vitamin E analogue Trolox C. E.s.r. and pulse-radiolysis studies of free-radical reactions. *Biochem. J.* **255,** 513–22 (1988).

101. Bentayeb, K., Rubio, C. & Nerín, C. Study of the antioxidant mechanisms of Trolox and eugenol with 2,2′-azobis(2-amidinepropane)dihydrochloride using ultra-high performance liquid chromatography coupled with tandem mass spectrometry. *Analyst* **137,** 459–470 (2012).

102. García-Román, J., Ibarra-Sánchez, A., Lamas, M. & González Espinosa, C. VEGF secretion during hypoxia depends on free radicals-induced Fyn kinase activity in mast cells. *Biochem. Biophys. Res. Commun.* **401,** 262–267 (2010).

103. Satoh, M. *et al.* NAD(P)H oxidase and uncoupled nitric oxide synthase are major sources of glomerular superoxide in rats with experimental diabetic nephropathy. *Am J Physiol Ren. Physiol* **288,** F1144-52 (2005).

104. Oberley, L. W. & Spitz, D. R. [61] Assay of Superoxide Dismutase Activity in Tumor Tissue. *Methods Enzymol.* **105,** 457–464 (1984).

105. Klemm, S. *et al.* The Bcl10-Malt1 complex segregates Fc epsilon RI-mediated nuclear factor kappa B activation and cytokine production from mast cell degranulation. *J. Exp. Med.* **203,** 337–347 (2006).

106. Carlson, R. P., Lynn, O. D., Chang, J. & Lewis, A. J. Modulation of mouse ear edema by cyclooxygenase and lipoxygenase inhibitors and other pharmacologic agents. *Agents Actions* **17,** 197–204 (1985).

107. Bradley, P. P., Priebat, D. A., Christensen, R. D. & Rothstein, G. Measurement of cutaneous inflammation: Estimation of neutrophil content with an enzyme marker. *J. Invest. Dermatol.* **78,** 206–209 (1982).

108. Suzuki, K., Ota, H., Sasagawa, S., Sakatani, T. & Fujikura, T. Assay method for myeloperoxidase in human polymorphonuclear leukocytes. *Anal. Biochem.* **132,** 345–352 (1983).

109. Yoshimaru, T., Suzuki, Y., Inoue, T. & Ra, C. L-type $Ca^{2+}$ channels in mast cells: Activation by membrane depolarization and distinct roles in regulating mediator release from store-operated Ca2+ channels. *Mol. Immunol.* **46,** 1267–1277 (2009).

110. Suzuki, Y., Inoue, T. & Ra, C. L-type $Ca^{2+}$ channels: A new player in the regulation of Ca2+ signaling, cell activation and cell survival in immune cells. *Molecular Immunology* **47,** 640–648 (2010).

111. Ashmole, I. & Bradding, P. Ion channels regulating mast cell biology. *Clin. Exp. Allergy* **43,** 491–502 (2013).

112. Suzuki, Y., Yoshimaru, T., Inoue, T. & Ra, C. Discrete generations of intracellular hydrogen peroxide and superoxide in antigen-stimulated mast cells: Reciprocal regulation of store-operated $Ca^{2+}$ channel activity. *Mol. Immunol.* **46,** 2200–2209 (2009).

113. Saul, S. *et al.* A calcium-redox feedback loop controls human monocyte immune responses: The role of ORAI $Ca^{2+}$channels. *Sci. Signal.* **9,** (2016).

114. García-Niño, W. R., Estrada-Muñiz, E., Valverde, M., Reyes-Chilpa, R. & Vega, L. Cytogenetic effects of Jacareubin from *Calophyllum brasiliense* on human peripheral blood mononucleated cells *in vitro* and on mouse polychromatic erythrocytes *in vivo*. *Toxicol. Appl. Pharmacol.* **335,** 6–15 (2017).

115. Hsu, M. F., Raung, S. L., Tsao, L. T., Lin, C. N. & Wang, J. P. Examination of the inhibitory effect of norathyriol in formylmethionyl- leucyl-phenylalanine-induced respiratory burst in rat neutrophils. *Free Radic. Biol. Med.* **23,** 1035–1045 (1997).

116. Chae, H. S., Oh, S. R., Lee, H. K., Joo, S. H. & Chin, Y. W. Mangosteen xanthones, α-and γ-mangostins, inhibit allergic mediators in bone marrow-derived mast cell. *Food Chem.* **134,** 397–400 (2012).

117. García, D., Escalante, M., Delgado, R., Ubeira, F. M. & Leiro, J. Anthelminthic and Antiallergic Activities of *Mangifera indica L*. Stem Bark Components Vimang and Mangiferin. *Phyther. Res.* **17,** 1203–1208 (2003).

118. Rivera, D. G. *et al.* Anti-allergic properties of *Mangifera indica L*. extract

(Vimang) and contribution of its glucosylxanthone mangiferin. *J. Pharm. Pharmacol.* **58,** 385–92 (2006).

119. Ikonen, E. Cellular cholesterol trafficking and compartmentalization. *Nature Reviews Molecular Cell Biology* **9,** 125–138 (2008).

120. Kim, D.-Y. *et al.* Emodin attenuates A23187-induced mast cell degranulation and tumor necrosis factor-α secretion through protein kinase C and IκB kinase 2 signaling. *Eur. J. Pharmacol.* **723,** 501–506 (2014).

121. Zhang, X., Jiao, W. U., Zhuang, Han., Wen-li, Mei., & Hao-Fu, D. Antioxidant and Cytotoxic Phenolic Compounds of Areca Nut(*Areca catechu*). *Chem. Res. Chinese Univ.* **26,** 161—164 (2010).

122. Zalawadia, R., Gandhi, C., Patel, V. & Balaraman, R. The protective effect of *Tinospora cordifolia* on various mast cell mediated allergic reactions. *Pharm. Biol.* **47,** (2009).

123. Wajdner, H. E. *et al.* Orai and TRPC channel characterization in FcεRI-mediated calcium signaling and mediator secretion in human mast cells. *Physiol. Rep.* **5,** (2017).

124. Hawkins, B. J. *et al.* S-glutathionylation activates STIM1 and alters mitochondrial homeostasis. *J. Cell Biol.* **190,** 391–405 (2010).

125. Suzuki, Y. *et al.* Fc epsilon RI signaling of mast cells activates intracellular production of hydrogen peroxide: role in the regulation of calcium signals. *J. Immunol.* **171,** 6119–6127 (2003).

126. Goldman, R., Moshonov, S. & Zor, U. Generation of reactive oxygen species in a human keratinocyte cell line: role of calcium. *Arch. Biochem. Biophys.* **350,** 10–8 (1998).

127. Hu, L. *et al.* Discovery of novel xanthone derivatives as xanthine oxidase inhibitors. *Bioorganic Med. Chem. Lett.* (2011). doi:10.1016/j.bmcl.2011.04.140

128. Ruzza, P., Biondi, B. & Calderan, A. Therapeutic prospect of Syk inhibitors. *Expert Opin. Ther. Pat.* **19,** 1361–1376 (2009).

129. Castillo-Arellano, J.; Guzmán-Gutiérrez, S.; Ibarra-Sáncheza, A.; Hernández-Ortega, S.; Nieto-Camacho, A.; Medina-Campos, O.; Pedraza-Chaverri, J.; Reyes-Chilpa, R.; González-Espinosa, C. Jacareubin inhibits FcεRI-induced extracellular calcium entry and production of reactive oxygen species required for anaphylactic degranulation of mast cells. *Biochem. Pharmacol.* **154,** 344–356 (2018).

130. Cosentino-Gomes, D., Rocco-Machado, N. & Meyer-Fernandes, J. R. Cell signaling through protein kinase C oxidation and activation. *International Journal of Molecular Sciences* **13,** 10697–10721 (2012).

131. Korbecki, J., Baranowska-Bosiacka, I., Gutowska, I. & Chlubek, D. The effect

of reactive oxygen species on the synthesis of prostanoids from arachidonic acid. *Journal of Physiology and Pharmacology* **64,** 409–421 (2013).

132. Han, S. J. *et al.* Magnolol and honokiol: inhibitors against mouse passive cutaneous anaphylaxis reaction and scratching behaviors. *Biol. Pharm. Bull.* **30,** 2201–3 (2007).

133. Glushkov, R. G. *et al.* A new group of 1-and 7-[ω-(benzhydryl-1-alkyl]-3methylxanthine derivatives with antihistamine activity. *Pharm. Chem. J.* **45,** 1–11 (2011).

134. Chitchumroonchokchai, C. *et al.* Xanthones in Mangosteen Juice Are Absorbed and Partially Conjugated by Healthy Adults. *J. Nutr.* **142,** 675–680 (2012).

135. Gutierrez-Orozco, F. & Failla, M. L. Biological activities and bioavailability of mangosteen xanthones: A critical review of the current evidence. *Nutrients* **5,** 3163–3183 (2013).

136. Feske, S., Wulff, H. & Skolnik, E. Y. Ion Channels in Innate and Adaptive Immunity. *Annu. Rev. Immunol.* **33,** 291–353 (2015).

137. Juárez-Vázquez, M. del C., Alonso-Castro, A. J., Rojano-Vilchis, N., Jiménez-Estrada, M. & García-Carrancá, A. Maturin acetate from *Psacalium peltatum* (Kunth) Cass. (Asteraceae) induces immunostimulatory effects in vitro and in vivo. *Toxicol. Vitr.* **27,** 1001–1006 (2013).

138. Gómez-Vidales, V., Granados-Oliveros, G., Nieto-Camacho, A., Reyes-Solís, M. & Jiménez-Estrada, M. Cacalol and cacalol acetate as photoproducers of singlet oxygen and as free radical scavengers, evaluated by EPR spectroscopy and TBARS. *RSC Adv.* **4,** 1371–1377 (2014).

# 12. Anexos

Espectro de $^{1}$H-RMN (700 MHz) de la Jacareubina

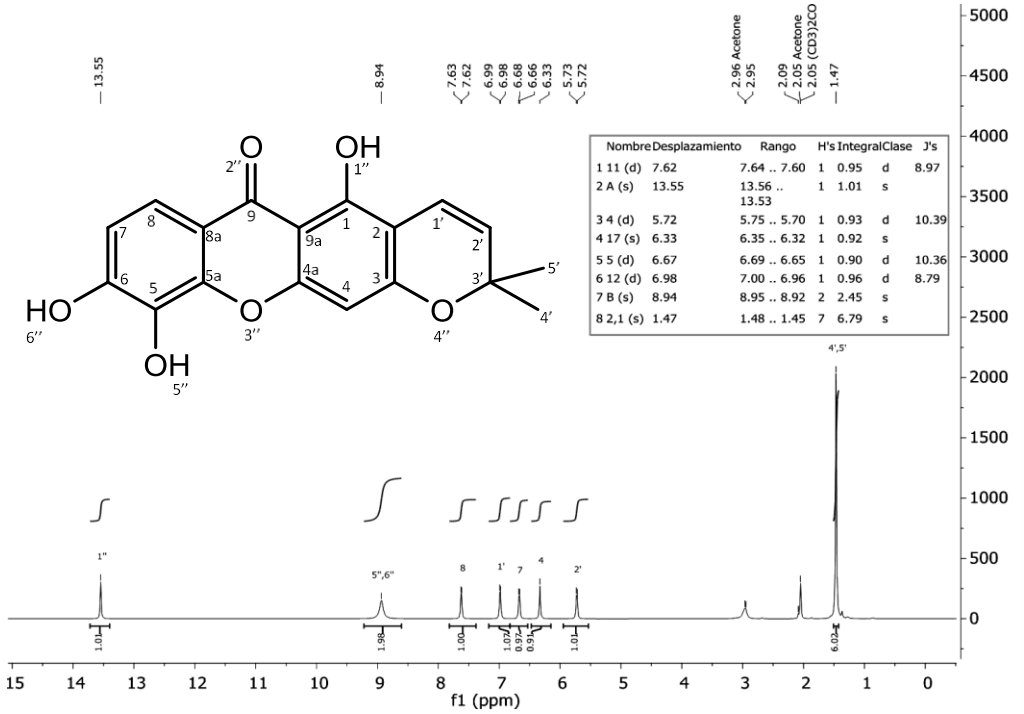


Espectro de $^{13}$C-RMN (175 MHz) de la Jacareubina

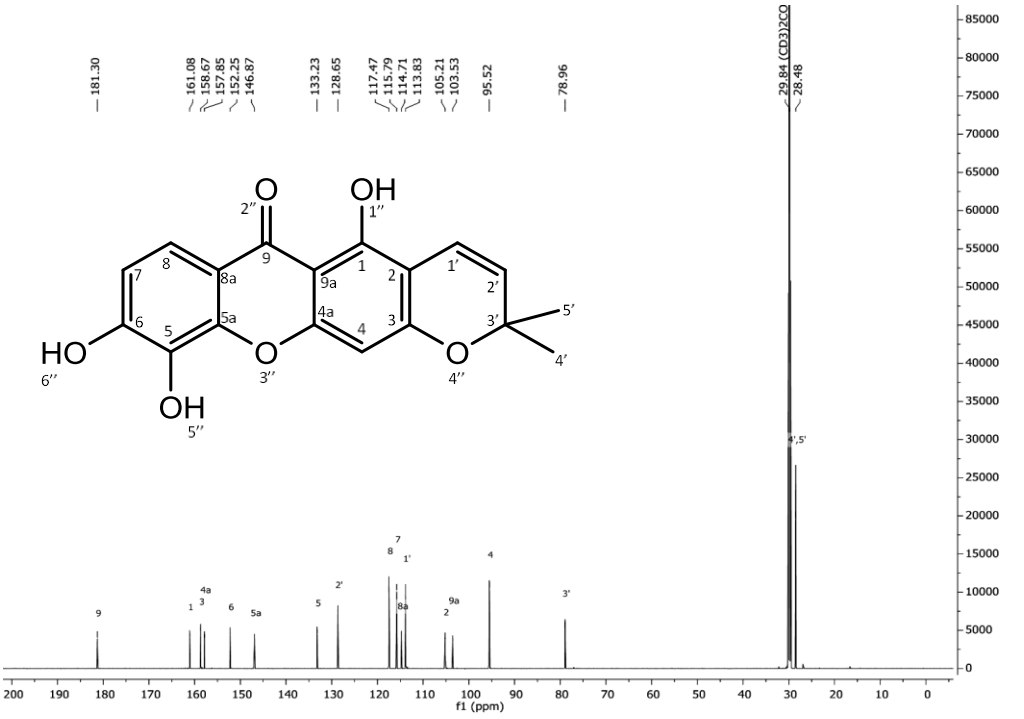

Espectro de $^{1}$H-RMN (300 MHz) del Cacalol.

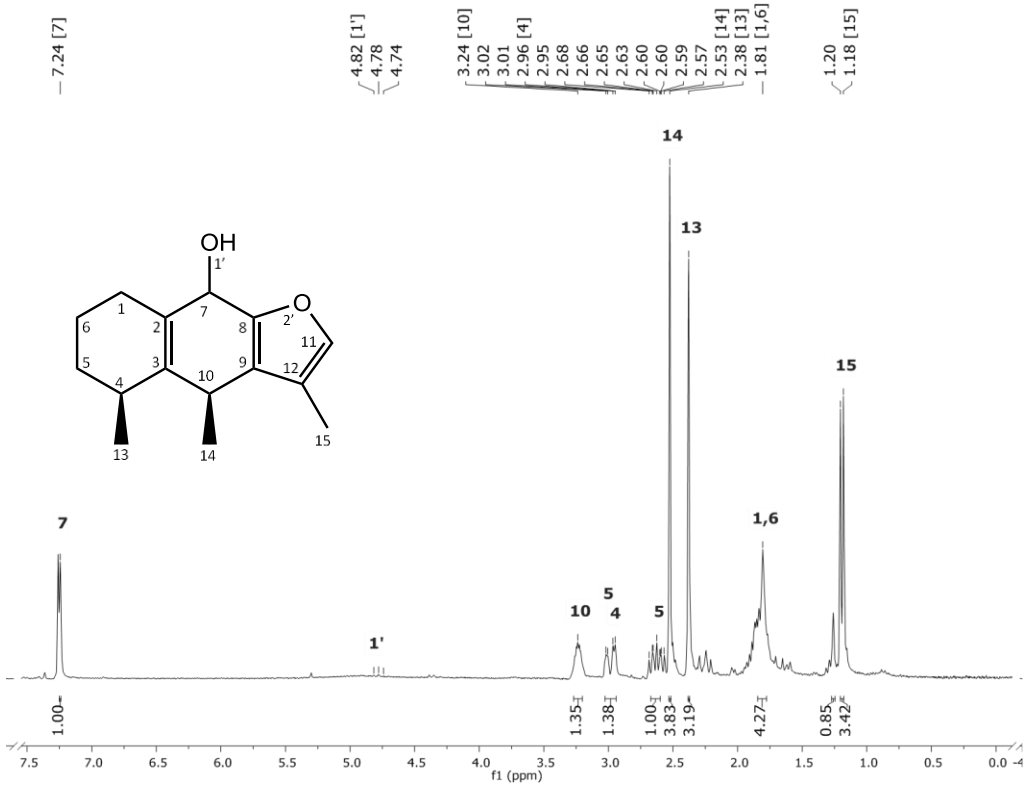


Cromatografía de gases acoplada a espectrometría de masas del cacalol

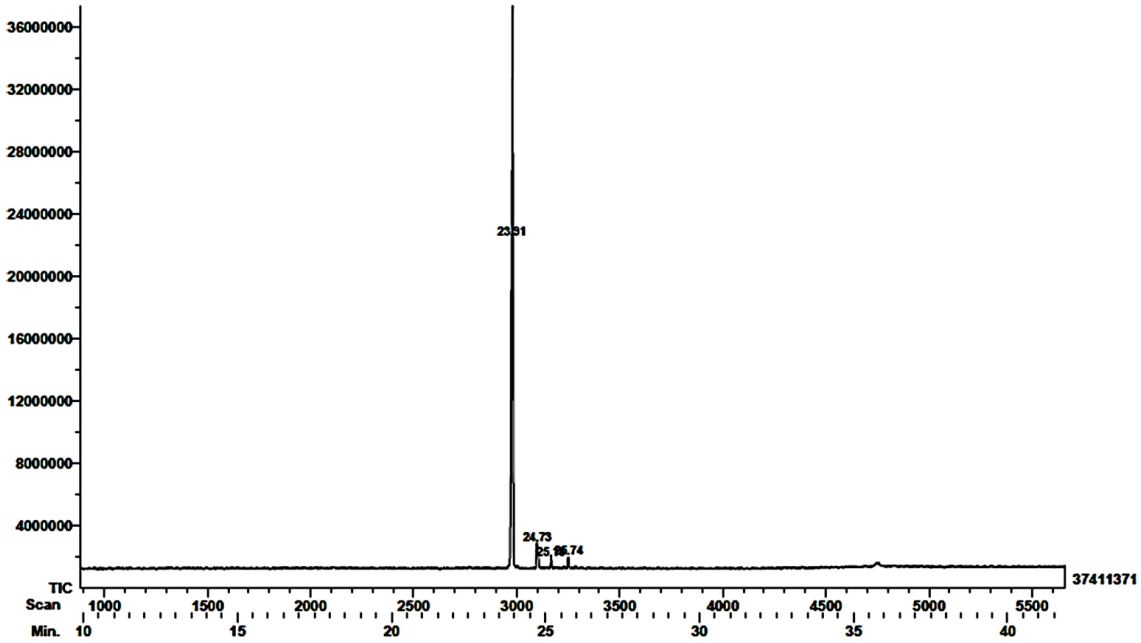

Patrón de fragmentación por impacto electrónico del pico con tiempo de retención 23.91 min correspondiente al cacalol en EM.

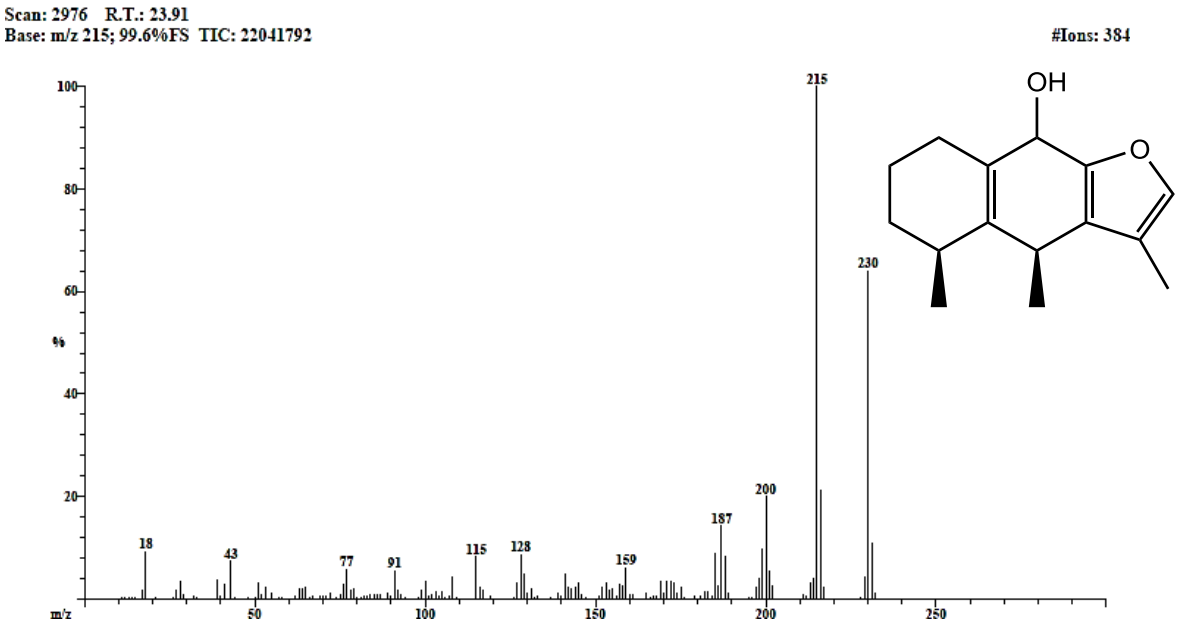


Patrón de fragmentación por impacto electrónico del pico con tiempo de retención 24.73 min correspondiente a la cacalona en EM.

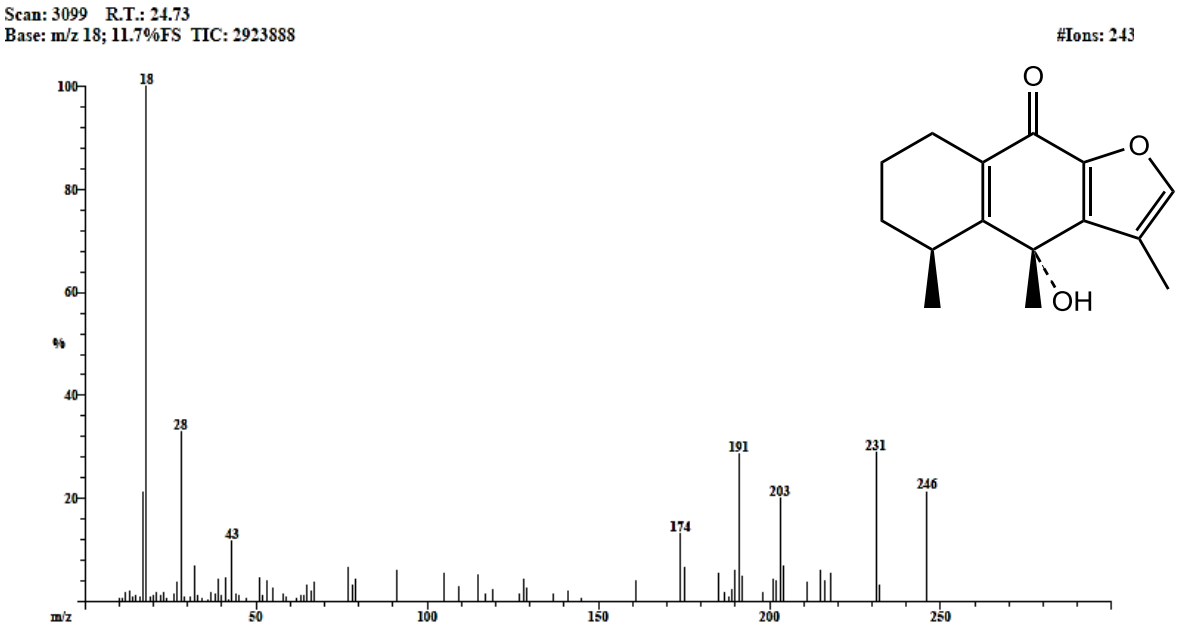

Patrón de fragmentación por impacto electrónico del pico con tiempo de retención 25.18 min correspondiente a la epi-cacalona en EM.

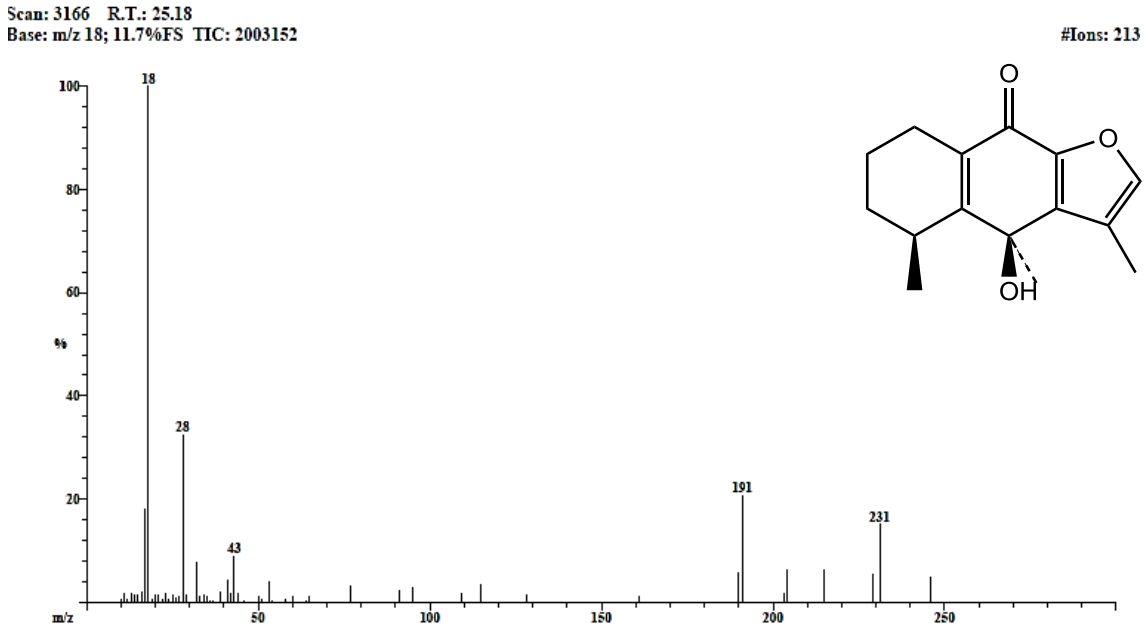


Patrón de fragmentación por impacto electrónico del pico con tiempo de retención 25.74 min correspondiente al No identificado.

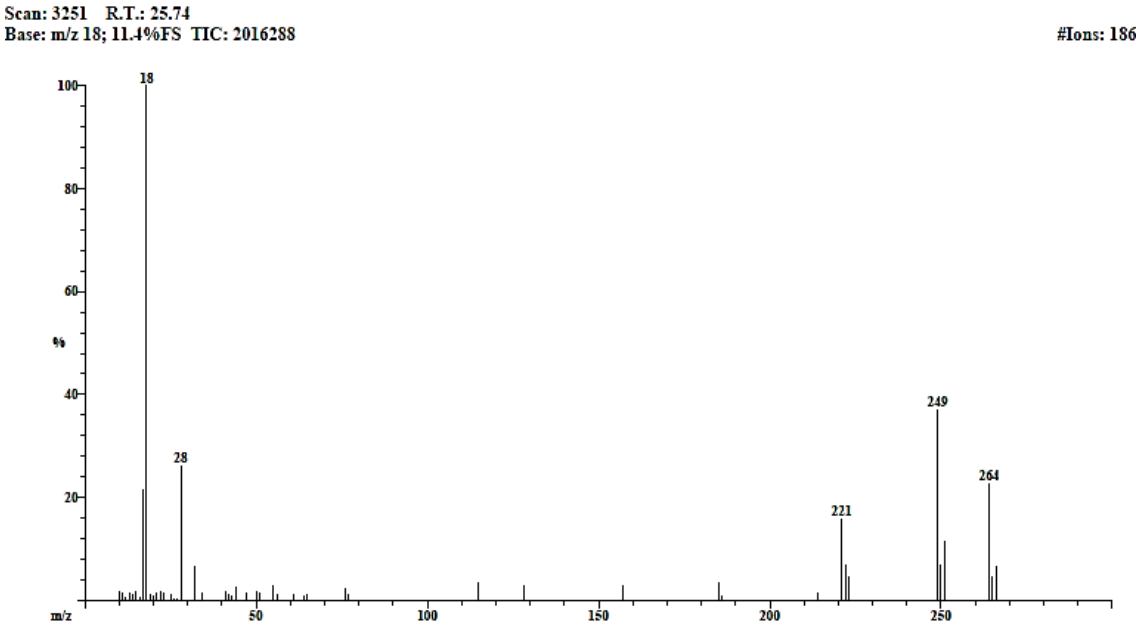

Espectro de $^{1}$H-RMN (300 MHz) del acetato de cacalol.

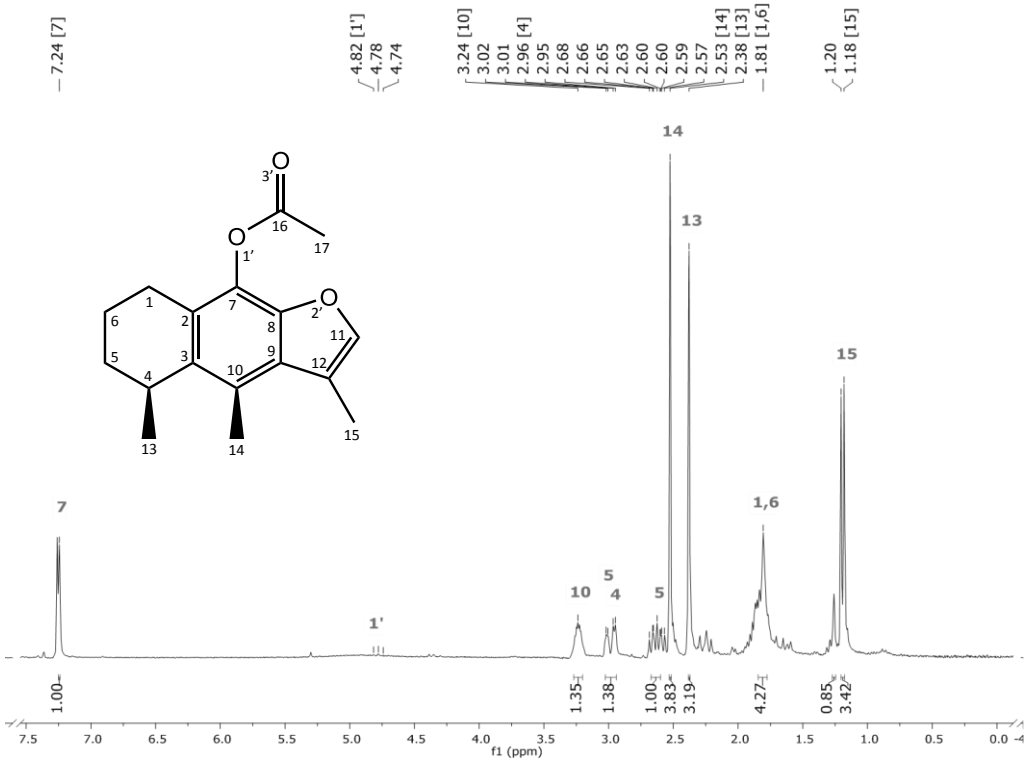


Espectro de $^{13}$C-RMN (75 MHz) del acetato de cacalol.

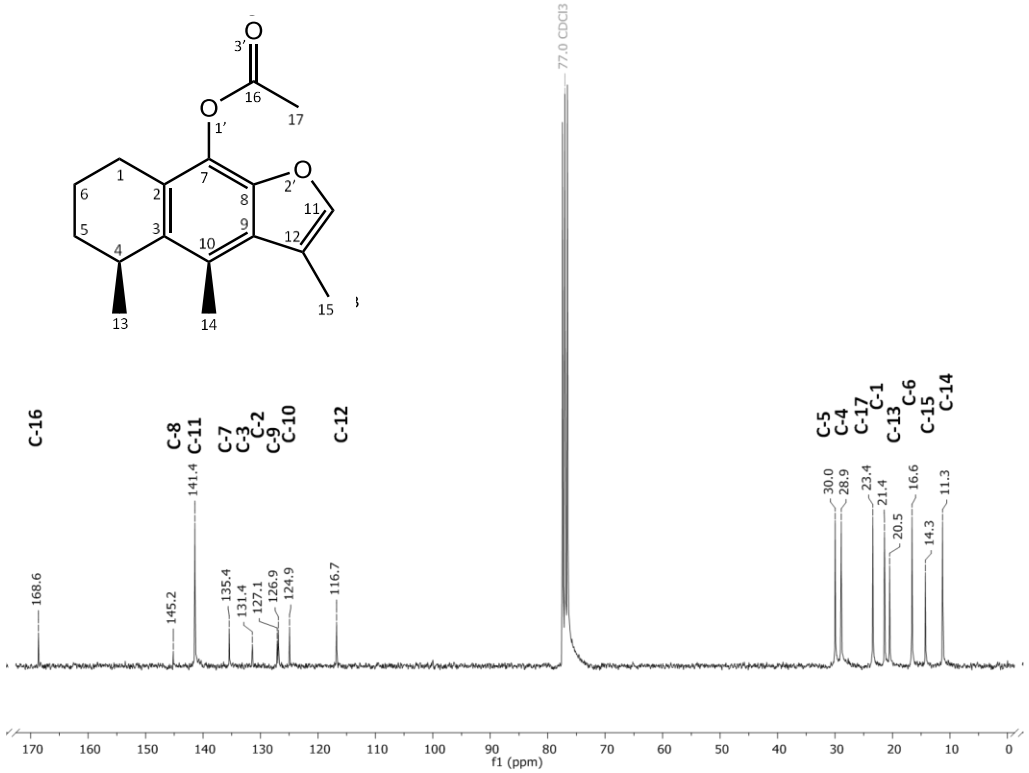

Espectro de $^{1}$H-RMN (300 MHz) de la cacalona.

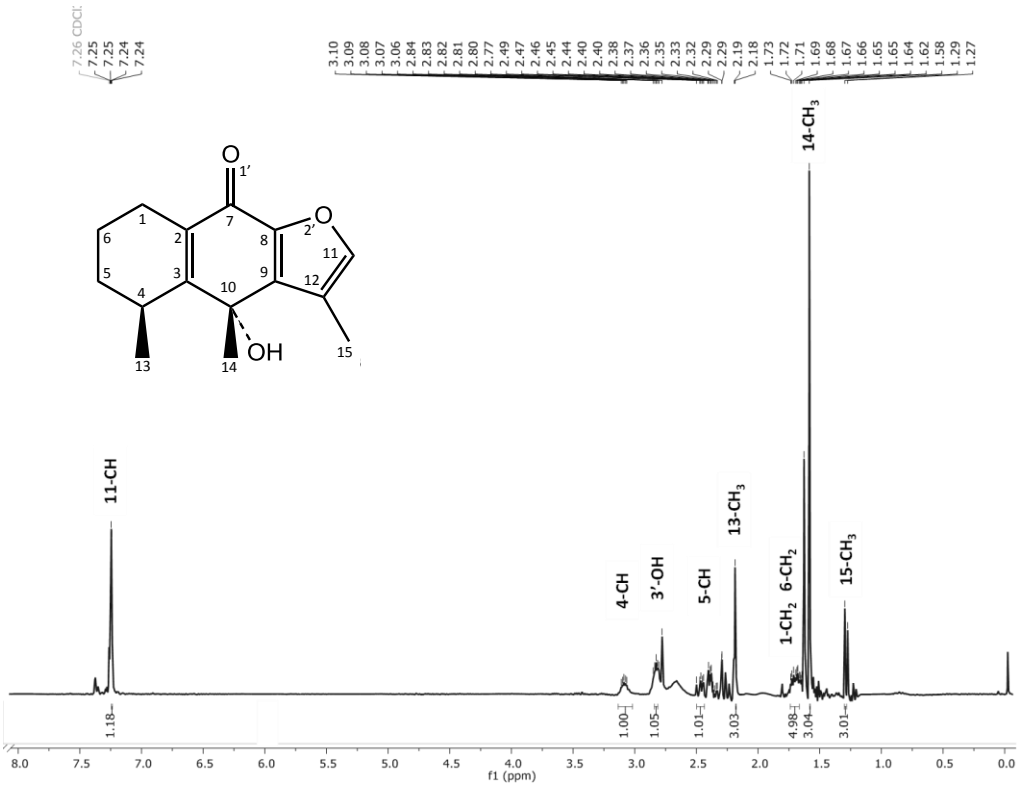


Cromatografía de gases acoplada a espectrometría de masas de la cacalona.

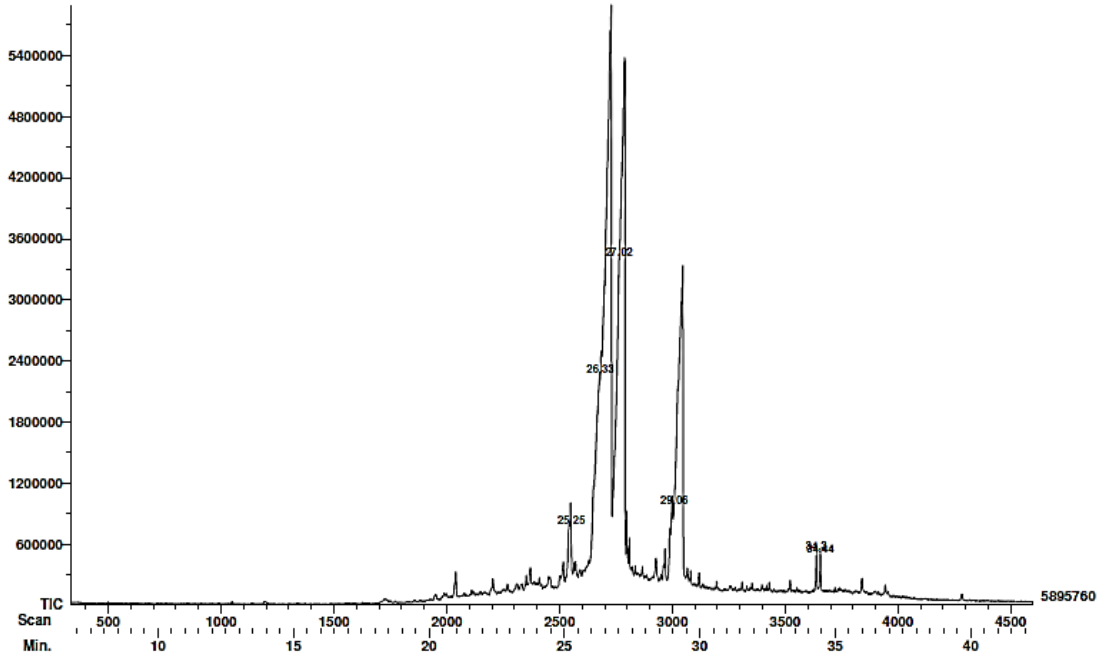

Patrón de fragmentación por impacto electrónico del pico con tiempo de retención 25.25 min correspondiente al cacalol en EM.

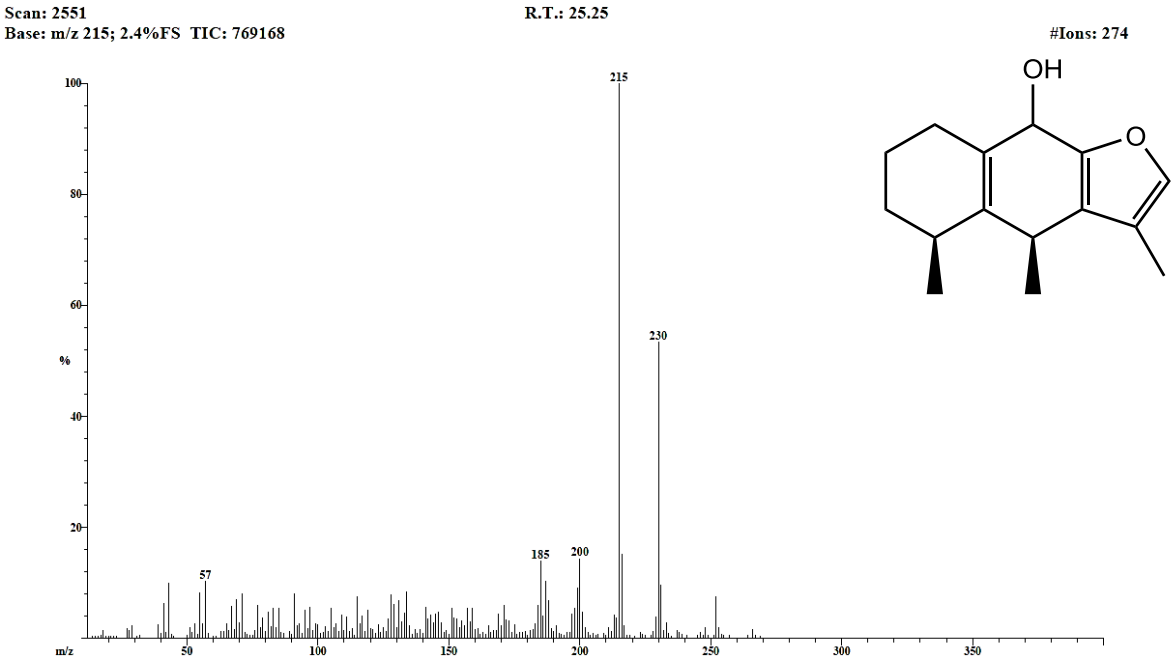


Patrón de fragmentación por impacto electrónico del pico con tiempo de retención 26.33 min correspondiente a la cacalona en EM.

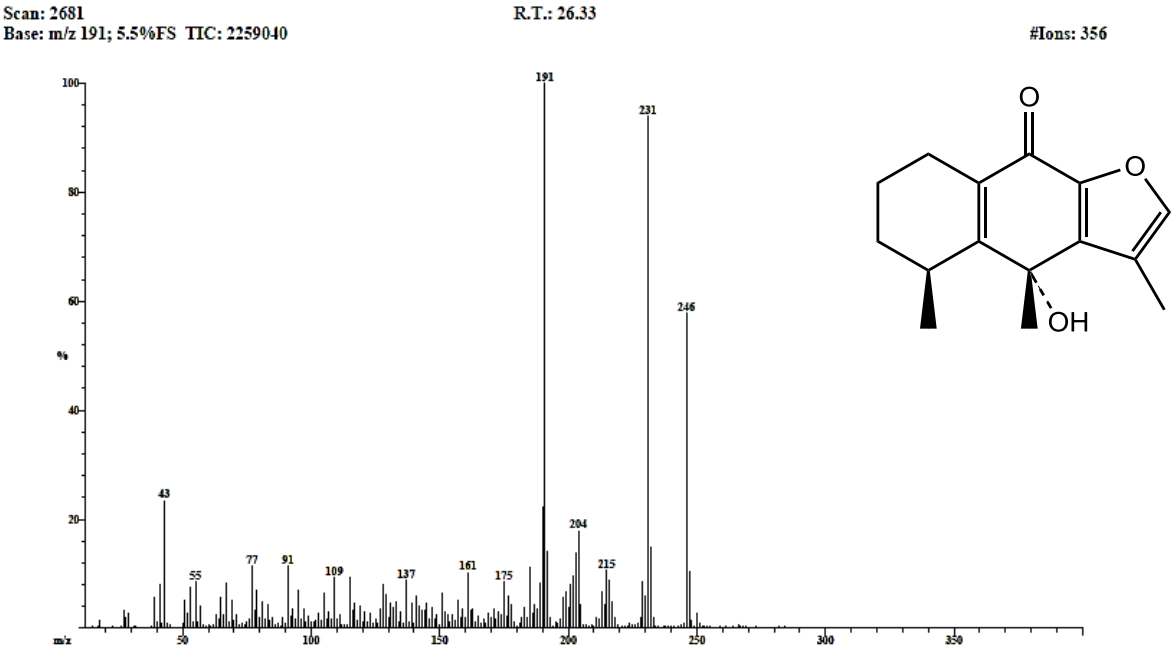

Patrón de fragmentación por impacto electrónico del pico con tiempo de retención 27.02 min correspondiente a la epi-cacalona en EM.

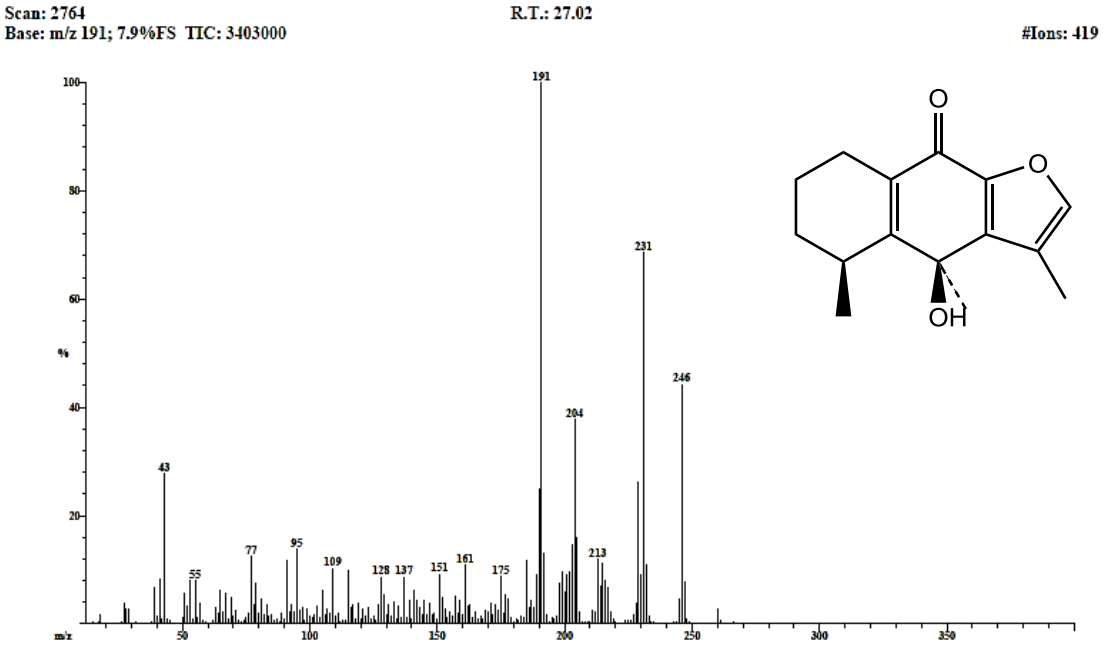


Patrón de fragmentación por impacto electrónico del pico con tiempo de retención 29.06 min correspondiente a la Radulifolina B en EM.

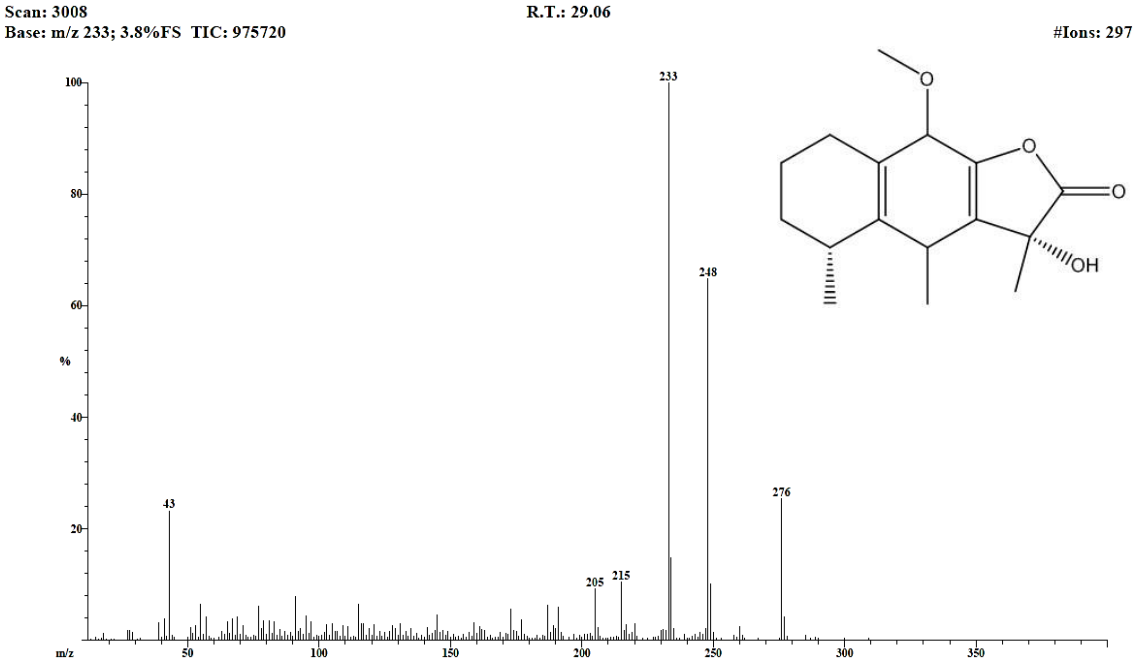

Espectro de $^{1}$H-RMN (300 MHz) del acetato de maturina.

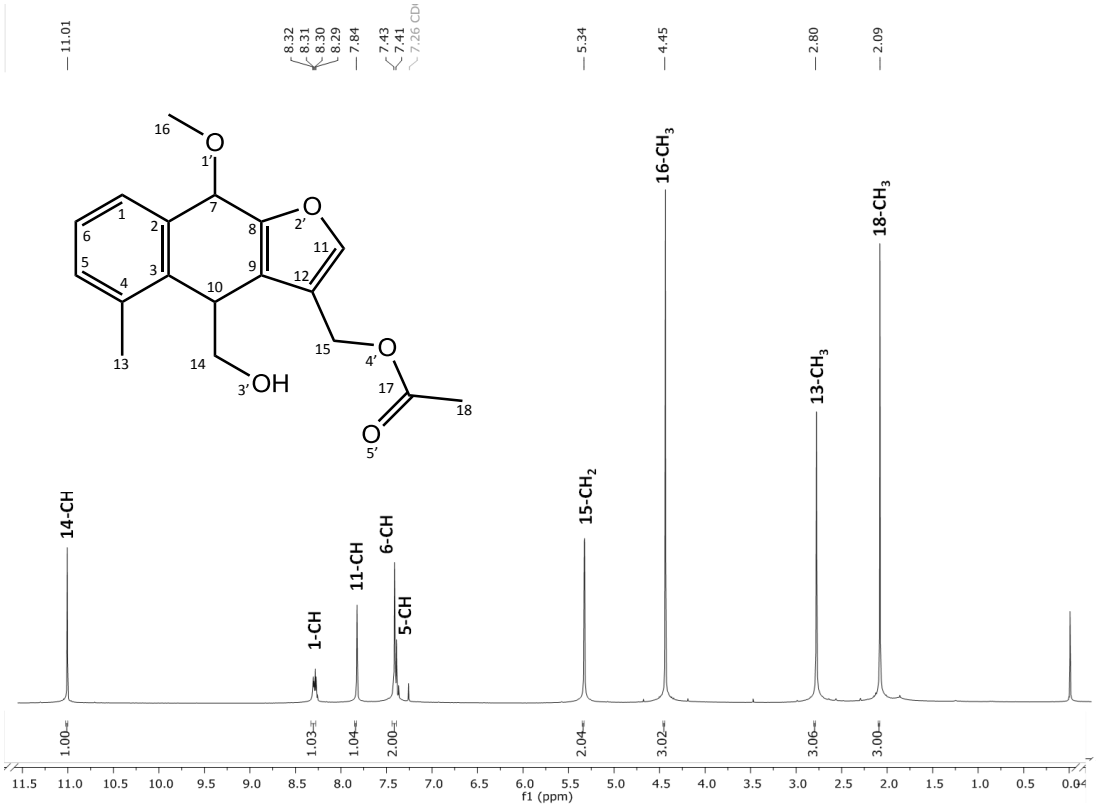

## 13. Artículos publicados

Biochemical Pharmacology 154 (2018) 344–356

Contents lists available at ScienceDirect

Biochemical Pharmacology

journal homepage: www.elsevier.com/locate/biochempharm

# Jacareubin inhibits FcεRI-induced extracellular calcium entry and production of reactive oxygen species required for anaphylactic degranulation of mast cells

J.I. Castillo-Arellano[a,c], S.L. Guzmán-Gutiérrez[b], A. Ibarra-Sánchez[a], S. Hernández-Ortega[c], A. Nieto-Camacho[c], O.N. Medina-Campos[d], J. Pedraza-Chaverri[d], R. Reyes-Chilpa[c,*], C. González-Espinosa[a,*]

[a] Departamento de Farmacobiología, Centro de Investigación y de Estudios Avanzados del IPN, Mexico
[b] Departamento de Inmunología, Catedrática CONACyT-Instituto de Investigaciones Biomédicas, Universidad Nacional Autónoma de México, Mexico
[c] Instituto de Química, Universidad Nacional Autónoma de México, Mexico
[d] Departamento de Bioquímica, Facultad de Química, Universidad Nacional Autónoma de México, Mexico

ARTICLE INFO

*Keywords:*
Mast cells
*Calophyllum brasiliense*
Xanthone jacareubin
Calcium channel regulation
Reactive oxygen species
Passive cutaneous anaphylaxis

ABSTRACT

Mast cells (MCs) are important effectors in allergic reactions since they produce a number of pre-formed and *de novo* synthesized pro-inflammatory compounds in response to the high affinity IgE receptor (FcεRI) crosslinking. IgE/Antigen-dependent degranulation and cytokine synthesis in MCs have been recognized as relevant pharmacological targets for the control of deleterious inflammatory reactions. Despite the relevance of allergic diseases worldwide, efficient pharmacological control of mast cell degranulation has been elusive. In this work, the xanthone jacareubin was isolated from the heartwood of the tropical tree *Callophyllum brasilense*, and its tridimensional structure was determined for the first time by X-ray diffraction. Also, its effects on the main activation parameters of bone marrow-derived mast cells (BMMCs) were evaluated. Jacareubin inhibited IgE/Ag-induced degranulation in a dose-response manner with an $IC_{50}$ = 46 nM. It also blocked extracellular calcium influx triggered by IgE/Ag complexes and by the SERCA ATPase inhibitor thapsigargin (Thap). Inhibition of calcium entry correlated with a blockage on the reactive oxygen species (ROS) accumulation. Antioxidant capacity of jacareubin was higher than the showed by α-tocopherol and caffeic acid, but similar to trolox. Jacareubin shown inhibitory actions on xanthine oxidase, but not on NADPH oxidase (NOX) activities. *In vivo*, jacareubin inhibited passive anaphylactic reactions and TPA-induced edema in mice. Our data demonstrate that jacareubin is a potent natural compound able to inhibit anaphylactic degranualtion in mast cells by blunting FcεRI-induced calcium flux needed for secretion of granule content, and suggest that xanthones could be efficient anti-oxidant, antiallergic, and antiinflammatory molecules.

## 1. Introduction

Allergies constitute an important public health problem in the world, around 40% of people have some type of allergy manifested as allergic rhinitis (10–30% adults), food allergy (8% children), animal allergy (15% cats and 10% dogs [1,2]), although that an effective treatment for those conditions has been elusive [3]. Current treatments are directed to palliate the symptoms caused by the inflammatory state that occurs in the development of the allergic episode [4], but little progress has been made in preventing the inflammatory condition derived of the production of pro-inflammatory mediators. Evidence indicates that allergies are positively associated with the development of multiple chronic-degenerative diseases, such as atopy [5], chronic-obstructive pulmonary disease (COPD) [6], chronic asthma and some types of cancer [7,8].

Mast cells (MCs) are the main cell type responsible for the acute inflammatory reaction that occurs during an episode of type I hypersensitivity [9]. Allergens (antigens) present in the environment are recognized by IgE antibodies that are bound to the high affinity IgE receptor (FcεRI) present in the membrane of the MCs [10,11]. This

* Corresponding authors at: Instituto de Química, Universidad Nacional Autónoma de México, Circuito Exterior S/N, Ciudad Universitaria, Del. Coyoacán, CP 04510 Ciudad de México, Mexico (R. Reyes-Chilpa). Departamento de Farmacobiología, Centro de Investigación y de Estudios Avanzados del IPN, Sede Sur, Calzada de los Tenorios No. 235, Colonia Granjas Coapa, Del. Tlalpan, CP 14330 Ciudad de México, Mexico (C. González Espinosa).
*E-mail addresses:* chilpa@unam.mx (R. Reyes-Chilpa), cgonzal@cinvestav.mx (C. González-Espinosa).

https://doi.org/10.1016/j.bcp.2018.05.002
Received 17 March 2018; Accepted 3 May 2018
Available online 24 May 2018
0006-2952/ 

leads to the activation of a complex signaling cascade that induce the rapid exocytosis of pre-formed granule compounds (anaphylactic degranulation), synthesis of lipid-derived mediators and long-term production of cytokines with pro-inflammatory activity. After FcεRI crosslinking, the protein tyrosine kinases Lyn and Fyn become activated and mediate the phosphorylation of the β chain of the FcεRI receptor. This creates docking sites for the protein kinase Syk, which associates to the phosphorylated beta chain and is activated by autophosphorylation and Lyn-dependent phosphorylation [12]. Activated Syk results in the phosphorylation of the adapter proteins GAB2 and LAT that disseminate the activation signal by binding different downstream effectors. Phosphorylated GAB2 mediates the activation of the phosphatidylinositol 3 kinase (PI3K), which promotes the membrane accumulation of $PIP_3$ and the initiation of cytoskeletal re-arrangements for granule secretion, whereas phosphorylation of LAT leads to the activation of phospholipase C (PLCγ) that catalyzes the production of diacylglicerol (DAG) and phosphatidylinositol-3-phosphate ($IP_3$) for the release of calcium from intracellular stores. Emptiness of intracellular calcium stores lead to the aggregation of the calcium sensor STIM1 in the endoplasmic reticulum and its association of Orai and TPRC calcium channels in plasma membrane to replenishment of intracellular calcium stores in what is called the store operated calcium entry (SOCE) [13–16]. FcεRI crosslinking also causes a rapid increase on the concentration of reactive oxygen species (ROS) produced by NADPH oxidase [17–19] by a mechanism not well defined yet.

The complexity of the FcεRI signaling system and the lack of detailed knowledge regarding the mechanisms that induce selective mediator production in mast cells, have complicated the development of effective therapeutics for allergic diseases and for inflammatory reactions that depend on mast cells. However, natural polyphenol compounds have been emerged as an important group of chemical agents with the capacity of mast cell inhibition [20–24]. Among the polyphenols isolated from plants with anti-allergic activity recently studied are: A) Flavonoids, including Luteolin and its analogues [25–28], quercetin [25,29], epigallocatechin-3-O-gallate [30]; B) Coumarins such as scoparone, thunberginols A and B [31,32]; C) Sesquiterpene derivatives such deacetyleupaserrin [33]; D) Xanthones, that are present in mangosteen and mango fruits show potent antiflammatory activity in murine mat cells, being nujiangexanthone A, followed by α-, γ-, and β-mangostins and finally mangiferin. Most of these compounds inhibit Syk protein [34–38].

Jacareubin and other xanthones are found in the heartwood of the American tropical tree *Calophyllum brasiliense* (Clusiaceae) where it has been isolated in good yields. Jacareubin has fungistatic and bacteriostatic activity [39,40], and good cytotoxicity activity against KB and HeLa cell lines *in vitro* [41] moderate inhibitory activity of gastric $H^+$, $K^+$-ATPase [42]. In this work we tested the potential antiallergic effect of the jacareubin in a widely-used cellular model of mast cell function (bone marrow-derived mast cells, BMMCs) and also analyzed its effects on *in vivo* models of inflammation. In both systems, jacareubin showed a potent inhibitory activity on MC degranulation and inflammation.

## 2. Materials and methods

### 2.1. Reagents

Anti-dinitrophenyl monoclonal immunoglobulin type E (IgE), 2′7′-dichlorofluorescein diacetate (DCF-DA), dinitrophenyl-human seric albumin (DNP-HSA), evans blue dye, hydrogen peroxide ($H_2O_2$), quercetin, 12-O-tetradecanoylphorbol-13-acetate (TPA), hexadecyltrimethyl-ammonium bromide (HTAB), N,N-dimethylformamide (DMF), Igepal, phosphate-buffered saline (PBS), α-tocopherol, caffeic acid, 3,3′,5,5′,tetramethyl-benzidine (TMB), dihydroethidium (DHE), Trizma base, HCl, triton X-100, EDTA, NaF, EGTA, phenylmethanesulfonyl fluoride, deoxyribonucleic acid, single stranded from salmon testes, nicotinamide adenine dinucleotide (NADPH), HEPES, diphenyleneiodonium chloride (DPI), nitrotetrazolium blue (NBT), $Na_2CO_3$, quercetin, and indomethacin were purchased to Sigma-Aldrich (St. Louis, MO, USA), antioxidant trolox by Calbiochem (San Diego, CA, USA), FURA-2AM by Thermo Fisher Scientific (Waltham, MA, USA), ketamine and xilazine by PISA agropecuaria (Hgo, México), all organic solvents were purchased with J. T. Baker (Center Valley, PA, USA) and jacareubin was purified that described below.

### 2.2. Collection of plant material and purification of jacareubin

*Calophyllum brasiliense* Cambess (Clusiaceae) tree was collected by J.I. Calzada from the Selva Lancandona, Chiapas, Mexico (Bárcenas, 1995 [43]). Identification was done by the collector, a voucher (JIC-3116), and wood sample (00011-XALw) are deposited in the Herbarium and Xylarium “Dr. Faustino Miranda”, both from the Instituto de Ecología, A.C., at Xalapa, Veracruz, México.

### 2.3. Purification and solubilization of Jacareubin

A wood board of *C. brasiliense* kept at room temperature was processed with an edger to obtain drillings. The heartwood shavings (711.5 g) were extracted with methanol at room temperature and the solvent was removed by destillation with a rotary evaporator in vacuum. The dried extract 74 g was subjected to column chromatography silica gel 60, 1 Kg (Merck; Darmstadt, Germany) eluting with hexane – ethyl acetate (7:3). Analysis of fractions was performed by thin layer chromatography using silica gel 60, layer plates G/UV254, 0.20 mm (Macherey-Nagel; Düren, Germany), plates were observed under ultraviolet light 254, 366 nm, and after spraying them with a solution of 1% ceric sulfate in 1 N sulfuric acid.

Fractions 138–227 afforded a mixture of three xanthones (9.85 g), a 6 g sample was subjected to column chromatography (1 m high and 5 cm diameter) using 120 g of silica gel 70/230 (Macherey-Nagel; Düren, Germany) to purify the jacareubin with an initial mobile phase of hexane and increasing polarity with ethyl acetate. Fractions eluted with solvent mixture 87:13 afforded jacareubin after recrystallization with acetone.

Jacareubin was obtained as yellow cubic and rectangular crystalline prisms of 1–5 mm long, melting point 260–270 °C with Fisher Johns Apparatus (Scorpion Scientific; Illinois, USA), reported 256–257 °C with decomposition. Nuclear Magnetic Resonance Spectra were recorded with a Bruker AVANCE III HD 700 MHz (Cambridge Isotope Laboratories, MA, USA). $^1$H NMR (700 MHz, $(CD_3)_2CO$). δ 13.55 (1H, s, 1″-OH), 8.94 (2H, s, 5″ and 6″-OH), 7,62 (1H, d, 8-H), 6.99 (1H, d, 1′-H), 6.68 (1H, d, 7-H), 6.33 (1H, s, 4-H), 5.73 (1H, d, 2′-H), 1.47 (6H, s, 4′-$CH_3$, 5′-$CH_3$) and $^{13}$C NMR (175 MHz, $(CD_3)_2CO$) δ 181.30 (C-9), 161.08 (C-1), 158.67 (C-3), 157.85 (C-4a), 152.25 (C-6), 146.87 (C-5a), 133.23 (C-5), 128.65 (C-2′), 117.47 (C-8), 115.79 (C-7), 114.71 (C-8a), 113.83 (C-1′), 105.21 (C-2), 103.55 (C-9a), 95.52 (C-4), 78.96 (C-3′) and 28.48 (C-4′ and C-5′). Mass spectra (DART) *m/z* (%): 327 $M^+ + 1$ (100); 326 (7) $M^+$, recorded in a AccuTOF JMS-T100LC (Tokio, Japan) using ionization mode Direct Analysis in Real Time.

The spectral purity of the tested jacareubin was determined by High Performance Liquid Chromatography (HPLC) coupled to UV–Vis Photo Diode Array Detector, or to Mass Spectrometer Bruker Esquire 6000 (Bruker; Billerica, MA, USA). In both cases a peak with retention time 15.6–16 min was observed. HPLC was performed with an Agilent 1200 Series Binary SL (Agilent; Santa Clara, CA, USA) using a C-18 Silica Gel column 3.5 μm 100 × 2.1 mm Eclipse Plus (Agilent; Santa Clara, CA, USA), mobile phase: $CH_3CN/H_2O$ (7:3) with $CH_3COOH$ 0.1%. Detector: Waters 2996 UV–Vis Photo Diode Array (Waters; Mildford, MA, USA). Detector: Mass Spectrometer Bruker Esquire 6000 (Bruker; Billerica, MA, USA).

### 2.4. Identification of the three-dimensional structure of jacareubin by X-ray diffraction

A yellow prism of jacareubin, was selected and mounted on glass fiber, then placed on a Bruker D8 venture diffractometer (Bruker; Billerica, MA, USA) with Cu-target micro-focus X-ray source (l = 1.54178 Å) The detector was placed at 50 mm from the crystal. Frames were collected with a scan width of 0.3° in the w scan and the exposure time of 10 sec/frame at 150 K. Frames were integrated with the Bruker SAINT software package (Bruker; Billerica, MA, USA) using a narrow-frame integration algorithm. Systematic absences and intensity statistics were used in monoclinic space group. The structure was solved using Patterson methods using SHELXS-2014/7 program [44]. The remaining atoms were located via a few cycles of least squares refinements and difference Fourier maps. Hydrogen atoms were input at calculated positions, and allowed to ride on the atoms to which they are attached. Thermal parameters were refined for hydrogen atoms on the phenyl groups using a Ueq = 1.2 Å and a Ueq = 1.5 Å for methyl groups to precedent atom in all cases. For all complexes, the final cycle of refinement was carried out on all non-zero data using SHELXL-2014/7 [44]. Absorption correction was applied using SADABS program. Supplementary data for jacareubin has been deposited at the Cambridge Crystallographic Data Centre. Copies of this information are available free of charge upon request from The Director, CCDC, 12 Union Road, Cambridge CB2 1EZ, UK (fax: +44 1223 336033, email: deposit@ccdc.ac.uk or internet address http://www.ccd.cam.ac.uk) quoting the deposition number CCDC 1845875.

### 2.5. Animals

C57BL/6J male mice (25–30 g body weight), stock number 000664, were purchased from The Jackson Laboratories (Bar Harbor, ME, USA). Mice were kept in sterile conditions (12-h dark/light cycles) with free access to water and food at the Unit for Production and Experimentation of Laboratory Animals (UPEAL) from Centro de Investigación y Estudios Avanzados del Instituto Politécnico Nacional (Cinvestav) in Mexico City. All animal procedures were approved by the Cinvestav Institutional Ethics Committee (protocol 074-13).

### 2.6. BMMC isolation and culture

BMMCs were produced from C57BL6/J mice, as described [45]. Briefly, bone marrow was extracted from the tibias and femurs of mice and cultured in RPMI 1640 (Sigma-Aldrich, St. Louis, MO, USA) medium supplemented with IL-3 (10 ng/ml; PeproTech, Rocky Hill, NJ, USA) and 10% FBS, 100 UI/ml penicillin, 100 mg/ml streptomycin, 50 mM 2-ME, and 13 nonessential amino acids (Invitrogen, Carlsbad, CA, USA). Cultures were maintained for 4 week, and media were changed every 5–7 days. Subsequently, BMMC differentiation was assessed by detecting the expression of the FcεRI receptor on plasma membrane by flow cytometry and evaluating the release of β-hexosaminidase after IgE/Ag stimulation [46]. Only cultures 98% positive for FcεRI receptor expression and showing a dose response of β-hexosaminidase release after IgE/Ag addition were used in the study. For each experiment, BMMCs were sensitized with 100 ng/mL a monoclonal anti-DNP IgE (clone SPE-7; Sigma-Aldrich, St. Louis, MO, USA) for 24 h at 37 °C. Routinely, after sensitization, cells were collected and resuspended in fresh culture medium or Tyrode's BSA buffer (135 mM NaCl, 5 mM KCl, 1 mM $MgCl_2$, 1.8 mM $CaCl_2$, 5.6 mM glucose, 0.5g/l BSA, and 20 mM HEPES pH 7.4) for citotoxicity and calcium experiments. For ROS production experiments, sensitized cells were washed and resuspended in Tyrodés Buffer without BSA.

### 2.7. Solubilization of jacareubin for experiments with isolated cells

For *in vitro* testing of the effects of jacareubin on mast cells, the compound was dissolved in 0.1% ethanol which was used as vehicle in all experiments.

### 2.8. Citotoxicity assay

We used the colorimetric assay for the quantification of cell death and cell lysis Cytotoxicity Detection Kit (LDH, Roche Cat. No. 11 644 793 001 (Roche; Mannheim, Germany), following the supplier's instructions we used the BMMC Cell-free culture supernatant pretreated for 15 min with six concentrations of jacareubin from 300 pM to 30 μM.

### 2.9. Determination of β-hexosaminidase activity

MC degranulation was tested by measuring the activity of β-hexosaminidase in cell supernatants as described [47]. Briefly, two million of IgE-sensitized cells were centrifuged at 500 × *g* during 5 min and suspended in 1 mL Tyrode's/BSA buffer. Independent groups of cells were treated with vehicle, 0.003, 0.03, 0.3, 3, or 30 μM jacareubin for 15 min and then stimulated with antigen (1, 3, 9, or 27 ng/mL DNP-HSA) during 30 min at 37 °C. After this treatment, cells were placed on ice for 2 min and centrifuged to 12,000 × *g* for 10 min at 4 °C. Sixty microliters of supernatant (Triton-treated cell pellet) were placed in a 96-well plate containing 40 μL of 1 mM p-nitrophenyl-N-acetyl-β-D-glucosaminide (P-NAG) (Sigma-Aldrich, St. Louis, MO, USA), and incubated for one hour at 37 °C before the addition of 120 μL of "stop" solution ($Na_2CO_3$ 0.1 M/$Na_2HCO_3$ 0.1 M). β-hexosaminidase release was quantified by spectrophotometry in a microplate reader (Tecan Sunrise; Männedorf, Switzerland) at 405 nm, as described [48].

### 2.10. Determination of intracellular calcium concentration ($[Ca^{2+}]i$)

Intracellular calcium concentrations $[Ca^{2+}]i$ were measured in IgE-sensitized BMMCs subjected to distinct treatments. To do this, ten million cells were collected and suspended in Tyrode's/BSA buffer in the presence of 5 μM Fura 2-AM for 30 min at 37 °C to allowing the loading of the cells. Fura 2-AM- loaded BMMCs were then suspended in 2 mL Tyrode's/BSA buffer and placed in the cuvette. Fluorescence at 510 nm after excitation at 340 nm was determined in intervals of 1.16 s using a spectrofluorometer (Fluoromax 3 Jobin Yvon, Horiba, Japan). Calcium concentration was calculated using the equation and parameters described by Grynkiewicz [49]. In a standard experiment, basal fluorescence was recorded during 100 s prior to the addition of the antigen DNP-HSA (27 ng/mL) or Thapsigargin (1 μM). In some protocols, we used BMMCs suspended in $Ca^{2+}$-free Tyrode's/BSA buffer and then added 1.8 mM $CaCl_2$ (final concentration) at 200 s to determine extracellular calcium entry.

### 2.11. ROS production and antioxidant activity

Two million of senstitized BMMC were collected and resuspended in 1 mL buffer Tyrode's without BSA in 1.5 mL flat top eppendorf tubes for each condition. Pre-incubation with vehicle, jacareubin or the antioxidant Trolox was performed for 15 min at 37 °C and then DCF-DA 10 μM was added for 15 min, after cells were stimulated with antigen (27 ng/mL of DNP-HSA) for another 15 min. Once finished the reaction, the tubes were centrifuged at 750 × *g* at 4 °C for 5 min, the supernatant was discarded and 300 μL of Igepal 0.1% at 37 °C were added, pipetting vigorously to break the cell pellet. Tubes were then centrifuged at 12,000 × *g* for 5 min at 4 °C and 200 μL of the supernatant were placed in a 96-well plate. Fluorescence was determined by exciting at 488 nm and detecting emission at 565 nm in a BioTek Microplate luminometer, model FLx800 (BioTek; Winooski, VT, USA) for 1 h, taking readings every 15 min (modified method) [29], values shown are the average of the five measurements made.

### 2.12. NADPH oxidase activity

NADPH oxidase activity was assessed by the fluorogenic oxidation of DHE to ethidium (Eth) by superoxide [50]. In brief, $1 \times 10^6$ BMMCs were resuspended by pippeting in 40 μL ice-cold lysis buffer (20 mM tris HCl pH 7.4, 1% triton X-100, 150 mM NaCl, 1 mM EDTA, 50 mM NaF, 1 mM, EGTA and 1 mM phenylmethanesulfonyl fluoride) and subjected to three freeze/thaw cycles using liquid nitrogen and ice, respectively. Lysates were incubated with DHE (0.02 mmol/L), salmon testes DNA (0.5 mg/mL) and NADPH (0.2 mmol/L) in HEPES buffer (25 mmol/L HEPES, and 1 mmol/L EDTA) in presence or absence of 0.3, 3 and 30 μM of Jacareubin. The NADPH oxidase inhibitor, diphenyleneiodonium chloride (DPI; 0.1 mmol/L), was used to confirm that NADPH oxidase was the source of superoxide. Eth-DNA fluorescence was measured at an excitation of 480 nm and emission of 610 nm for 2.5 h at 37 °C using a fluorescence microplate reader (Synergy HT multi-mode reader, Biotek, Winooski, VT, USA).

### 2.13. Xanthine oxidase activity

Oxidation of DHE by superoxide produced by xanthine oxidase (0.1 mU) was tested in a master mix containing xanthine (0.122 mM), EDTA (0.122 mM), DNA (0.5 mg/mL), nitrotetrazolium blue (NBT, 30.6 μM), $Na_2CO_3$ (49 mM) [51]. Eth-DNA fluorescence was measured at an excitation of 480 nm and emission of 610 nm for 2.5 h at 37 °C using a fluorescence microplate reader (Synergy HT multi-mode reader, Biotek, Winooski, VT, USA). When needed, jacareubin resuspended in ethanol was added immediately before the addition of the enzyme. Vehicle (ethanol) *per se* did not modify the activity of the enzyme.

### 2.14. Passive cutaneous anaphylaxis model (PCA)

Each mouse was anesthetized with 17 μL ketamine and 1.1 μL of xilazyine dissolved in 160 μL of saline solution by intraperitoneal (i.p.) injection. For IgE sensitization, 5μL 100 ng of monoclonal anti-DNP IgE were administered in the left ear and 5 μL saline were injected in the right ear (control ear). Twenty four hours after sensitization, animals were challenged with 100 μL 200 μg of DNP-HSA antigen dissolved in 1% Evans Blue dye, administered through the tail vein [28,52]. Vehicle or different doses of jacareubin were administered intraperitoneally to each mouse 2 h before challenge with antigen. Once the mouse was exposed to the antigen, the mice were allowed to rest with free access to food and water for 30 min. Mice were sacrificed using a $CO_2$ chamber, and similar portions of the ears of each mouse were cut, weighed and incubated for 12 h at 65 °C with 300 μL of N, N Dimethylformamide to extract all Evans blue dye from the tissue of the ear. Two hundred microliters of each sample was taken and read in a spectrophotometer VersaMax ROM v.2.14 (Molecular Devices; San Jose, CA, USA) at 620 nm.

### 2.15. TPA-induced edema model in mice ear

The TPA-induced ear edema assay in mice Swiss Webster (Charles River, Wilmington, MA, USA), was performed as previously reported [53] with some modifications. A solution of TPA (2.5 μg) in ethanol (10 μL) was applied topically to both faces (5 μL each ear) of the right ear of the mice. After 10 min, solutions of the tested substances dissolved in ethanol-acetone 1:1 were applied (10 μL in each face of the ear). The left ear received ethanol (10 μL) first, and 20 μL of the ethanol-acetone mixture subsequently. Four hours later mice were sacrificed in a $CO_2$ chamber. A 7 mm diameter plug was removed from each ear. The swelling was assessed as the difference in weight between the left and the right ear. Edema inhibition (EI %) was calculated by the equation: $EI\% = 100 - \left(\frac{B \times 100}{A}\right)$ where A is the edema induced by TPA alone and B is the edema induced by TPA plus sample. Indomethacin dissolved in acetone:ethanol 1:1 was used as the reference compound. All animal procedures were approved by the CICUAL-IQ Institutional Ethics Committee (protocol CICUAL-IQ-004-17).

### 2.16. Mieloperoxidase (MPO) assay

Tissue MPO activity was measured in biopsies taken from ears 4 h after TPA administration using an adapted method of Bradley [54] and Suzuki [55]. Each mouse ear biopsy was placed in an eppendorf tube with 1.0 mL of 80 mM phosphate-buffered saline (PBS) pH 5.4 containing 0.5% hexadecyltrimethylammonium bromide (HTAB). Each sample was homogenized for 30 s at 4 °C with a small sample laboratory Tissue Tearor Homogenizer model 125 (OMNI International; Kennesaw, GA, USA). The homogenate was freeze-thawed at room temperature for 3 times, sonicated during 20 s and centrifuged at 13,400 × *g* for 15 min at 4 °C. The resulting supernatant (10 μL) were poured into 96-well plate and 180 μL of 80 mM PBS (pH 5.4) without HTAB were added. Microtiter plate was heated at 37 °C then, 20 μL of 0.017% hydrogen peroxide were added to each well. For the MPO assay, 20 μL of 18.4 mM 3,3′,5,5′, tetramethylbenzidine in 50% aqueous dimethylformamide were added to start the reaction. Microtiter plates were incubated at 37 °C for 5 min. The reaction was stopped with 20 μL of 2 M $H_2SO_4$. MPO enzyme activity was assessed colorimetrically using a BioTek Microplate Reader (BioTek; Winooski, VT, USA) at absorbance wavelength of 450 nm. MPO activity (measured by quadruplicated in each sample) was expressed as percentage inhibition in respect with the control.

### 2.17. Statistical analysis

All data were represented as percentage mean ± standard deviation of mean (SD) using the GraphPad Prism® software version 6 (GraphPad Software; La Jolla, CA, USA). Statistical analysis was done by analysis of variance ANOVA one way followed by Dunnett test were used to compare several groups with a control additionally by analysis with Student's *t*-test and Kolmogorov-Smirnoff's test. Pearson's correlation coefficient was calculated for the edema and MPO. Values of $p \leq 0.05$ were considered to be significant.

## 3. Results

### 3.1. X-ray diffraction, NMR and HPLC analysis of Jacareubin

$^1H$ and $^{13}C$ NMR data of Jacareubin isolated from *C. brasiliense* heartwood are in line with those previously reported from the related species *Garcinia xantochymus* , and from the fungus *Amauroderma amoiensis* [56,57]. Jacareubin is a tetracyclic polyphenol, it presents a core structure composed by C6–C3–C6 system with an extra ring derived from cyclization of a γ,γ-dimethylallyl substituent attached to C-2 and C-3 of ring A. This is the first time that Jacaraeubin crystal molecular structure is reported based on X-ray diffraction (Fig. 1A). The compound is planar and rigid with three hydroxyl groups, hydroxyl on C-1 is forming an intramolecular H-bond with O-4 of the carbonyl group. The H-atom on O6 is displayed in two positions, refined as 57/43% of site occupational factor, showing intramolecular H-bond with O2 and O5 atoms and intermolecular H-bond with O6. The crystal planar cell show that arrangement jacareubin molecules in a wedge arrangement, B ring of one molecule is overlapped with the B ring of another molecule through H bridge established by the hydroxyls on C5 and C6, another hydrogen bond is formed between the O2 of one molecule and the hydroxyl in C6 of another molecule (Fig. 1B). HPLC-MS showed a major peak (99.39%) corresponding to 16 min, which coincided with the molecular mass of Jacareubin *m/z* $M^+ - 1 = 325$ (Fig. 1C and D) indicating the purity of the used preparation.

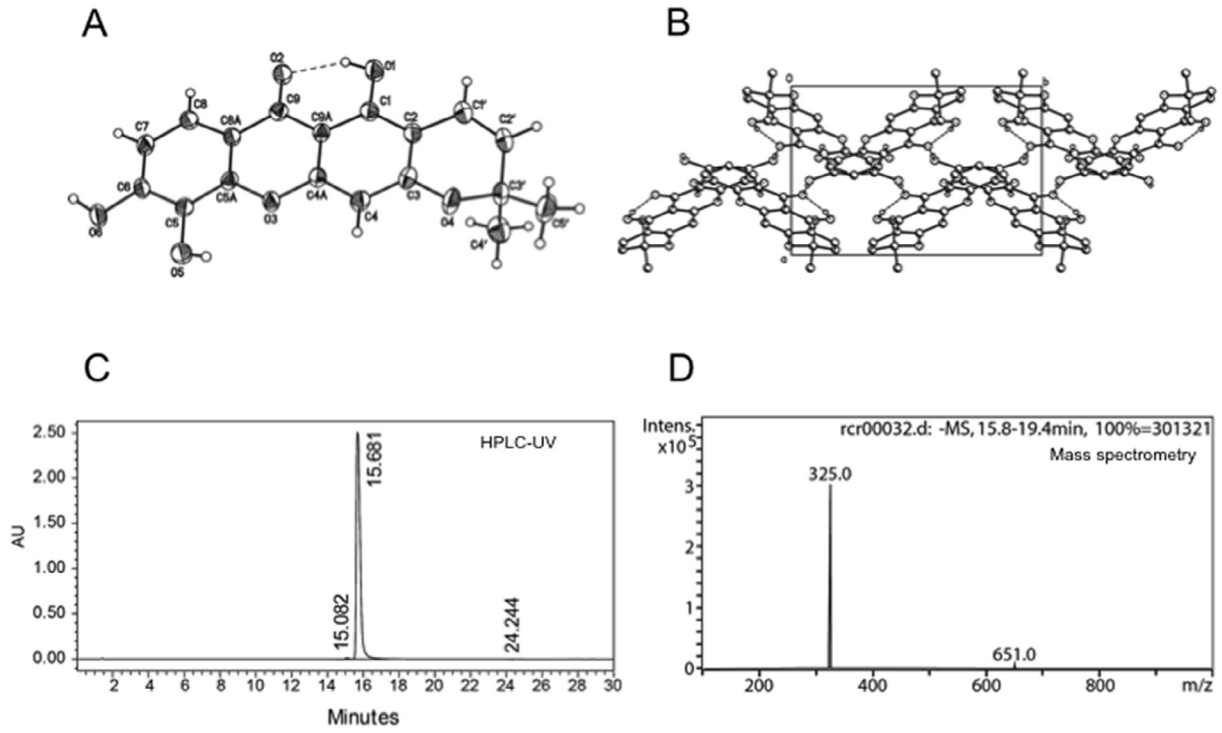


**Fig. 1.** X-ray structure and purity of Jacareubin utilized in this study. A) Tridimensional structure of Jacareubin obtained by X-ray diffraction. B) Crystallographic cell. Panels C) and D) Purity of Jacareubin used in this study determined by HPLC-UV and Mass Spectrometry.

### *3.2. Jacareubin inhibits mast cell degranulation activated by FcεRI triggering.*

Utilizing the release of LDH to evaluate cell death, we found that jacareubin does not show cytotoxic activity on BMMCs at concentrations ranging from 3 nM to 30 μM. As can be observed on Fig. 1A, no significant release of LDH was observed after a 15 min incubation with the compound, compared with an important death detected with hydrogen peroxide treatment. Due to those results, this range of concentrations was therefore used for subsequent experiments.

To evaluate the actions of jacareubin on mast cell activation, BMMCs were sensitized overnight with 100 ng/mL of a monoclonal anti-DNP IgE. After this, cells were incubated in the presence of different concentrations of jacareubin at 37 °C. After 15 min, cells were stimulated with distinct concentrations of a specific antigen (DNP-HSA) and the activity of β-hexosaminidase in the supernatant was determined. As can be observed on Fig. 2B, jacareubin inhibited (IgE/Ag)-induced degranulation in a concentration-dependent fashion ($IC_{50}$ = 0.046 μM). Also, effects of jacareubin were tested on degranulation induced by Thap, an inhibitor of the sarco/endoplasmic reticulum $Ca^{2+}$-ATPase (SERCA), which activates secretion by increasing the intracellular calcium content in MCs [16] independently of FcεRI receptor crosslinking. Jacareubin was able to inhibit Thap-induced degranulation in a concentration-dependent manner (Fig. 2C). Finally, degranulation triggered with the $PKC_{\alpha/\beta}$ activator (TPA) plus the calcium ionophore A23187 was also sensitive to the actions of jacareubin (Fig. 2D).

### *3.3. Jacareubin interferes with FcεRI-induced intracellular calcium rise in BMMCs*

The effects of jacareubin on FcεRI receptor-induced calcium mobilization in BMMCs were evaluated. FURA2-AM-loaded cells were incubated with vehicle or different concentrations of jacareubin 15 min before to be stimulated with 27 ng/mL DNP-HSA and changes on FURA-2-AM fluorescence were registered as described in the Material and Methods section. As observed in Fig. 3 A, B and C, addition of antigen caused a rapid increase in $[Ca^{2+}]i$, which reached maximal values around 300 s after stimulation. Preincubation with jacareubin prevented calcium rise in a dose-dependent manner, reaching full inhibition at 30 μM (Fig. 3C). Quantification of the rate of calcium rise and maximal calcium levels reached with each treatment is shown on Table 1. Addition of jacareubin did not modify the immediate rate of calcium increase when used at 0.3 or 3 μM and this parameter was affected only with 30 μM. However, maximal increase on $[Ca^{2+}]i$ was affected from 0.3 μM (Fig. 3A).

Intracellular calcium rise after FcεRI crosslinking in mast cells is controlled by the emptiness of intracellular stores and by the opening of membrane calcium channels. In order to dissect the point of action of jacareubin, we incubated BMMCs with vehicle or different concentrations of that compound in a calcium free buffer and stimulated them with IgE/Ag. As expected, after addition of calcium to the cuvette (to reach 1.8 mM extracellular $Ca^{2+}$), an important increase of intracellular calcium concentration was observed due to the calcium entry trough the opened membrane channels (Fig. 4A). Pre-incubation with jacareubin blocked FcεRI-induced extracellular calcium entrance in a dose-response fashion. When 0.3 μM of Jacareubin was used, only a slight difference was observed with respect to untreated cells, but the addition of 3 μM blocked the maximal calcium concentration by 50% and 30 μM fully inhibited calcium influx (Fig. 4B and C). Closer analysis of the parameters of calcium entrance showed that Jacareubin decreased the rate and the maximal $[Ca^{2+}]i$ (Table 2).

Intracellular calcium concentration after FcεRI increases due to the activation of two main pathways: the receptor-operated calcium entry (ROCE) and the store-operated calcium entry (SOCE) [58–60]. The first one occurs due to the activation of calcium channels with the participation of proteins and messengers that does not induce the emptiness of intracellular calcium stores [58,59]. On the other hand, SOCE occurs after the activation of the $IP_3$ receptor in the endoplasmic reticulum and is triggered when intracellular stores are mobilized and the cell requires to refills those storage compartments [14,15,61]. SOCE can be pharmacologically activated by Thap, a sesquiterpene lactone that inhibits

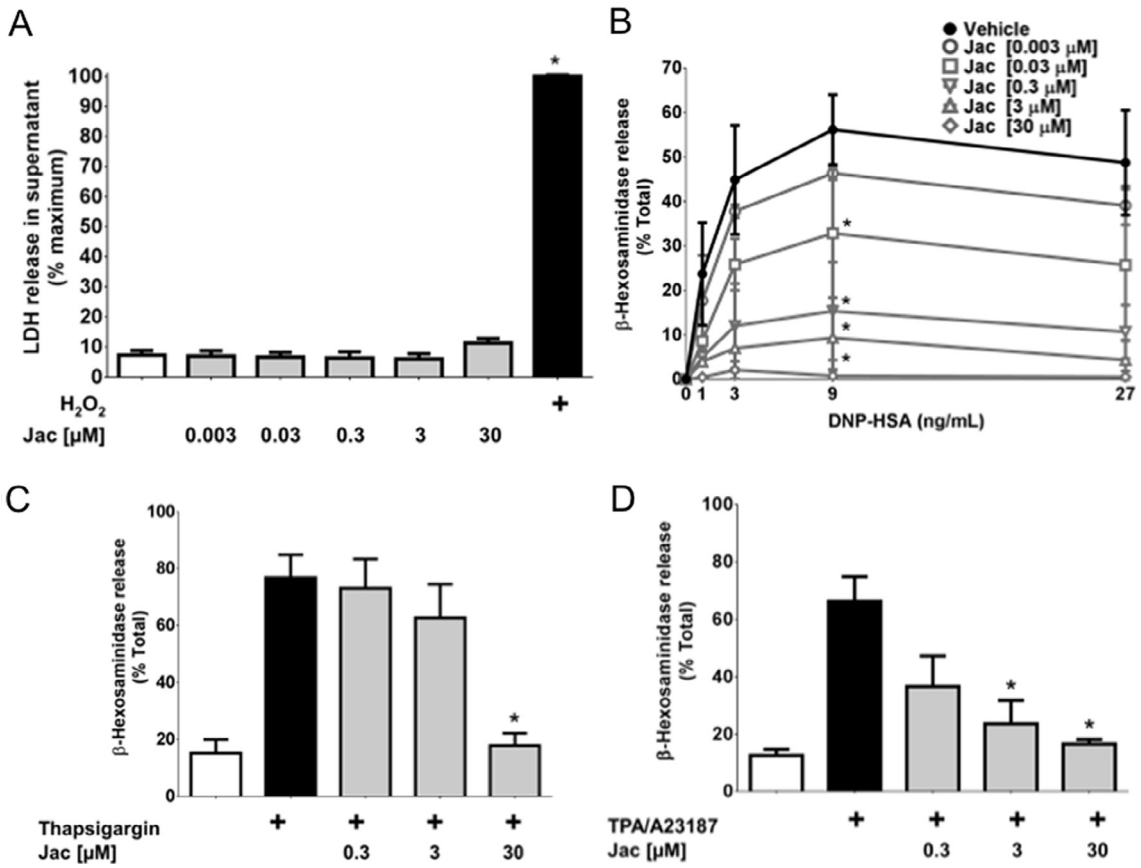


**Fig. 2.** Jacareubin inhibits degranulation stimulated by different agents in mast cells in a dose-dependent fashion. A. Toxicity of jacareubin in BMMCs measured by LDH release on cell supernatants, $H_2O_2$ treatment was included as a positive control. n = 3. B) Concentration-response curve of IgE/Ag-induced degranulation in BMMCs pre-treated with different concentrations of Jacareubin or with vehicle alone, n = 3–6. C) Effect of Jacareubin pre-treatment on Thap-induced degranulation in BMMCs, n = 3. D) Effect of jacareubin pre-treatment on TPA/A23187-induced degranulation, n = 3. One way ANOVA with Dunnett's multiple comparisons test ($^*p < 0.05$).

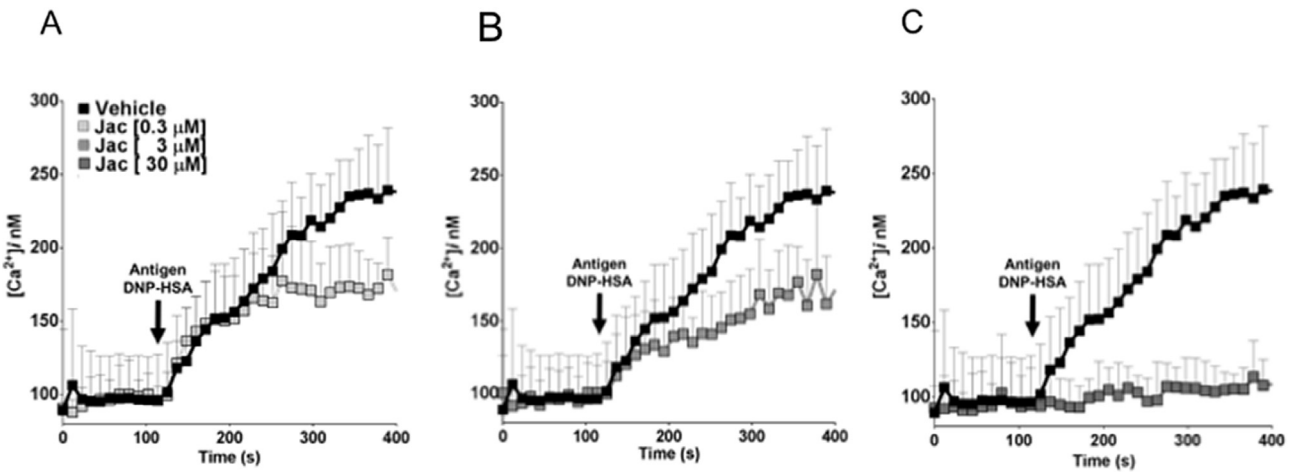


**Fig. 3.** Jacareubin inhibits FcεRI-induced calcium mobilization in mast cells in a concentration-dependent manner. A) – C) Representative traces of intracellular calcium rise induced by the specific antigen DNP-HSA added to BMMCs pre-treated with vehicle or different concentrations of jacareubin, n = 3–6. One way ANOVA with Dunnett's multiple comparisons test ($^*p < 0.05$).

the sarco/endoplasmic reticulum $Ca^{2+}$-ATPase (SERCA). In order to analyze if jacareubin could inhibit SOCE, cells were treated with vehicle or with different concentrations of jacareubin for 15 min in free $Ca^{2+}$ buffer. Basal $[Ca^{2+}]i$ was measured for 100 s before the addition of Thap (Fig. 5). After 100 s, $Ca^{2+}$ was added to the cuvette to reach 1.8 mM and changes on $[Ca^{2+}]i$ were followed for 200 s. As can be observed on Fig. 5, Thap induced, as expected, a discrete rise on $[Ca^{2+}]i$ corresponding to the emptiness of intracellular calcium stores and, after addition of extracellular $Ca^{2+}$, the entry of this ion through the STIM1/Orai-mediated mechanism of calcium replenishment of endoplasmic reticulum. Pre-treatment with jacareubin (0.3 μM) diminished maximal $Ca^{2+}$ increase (Fig. 5A), whereas at higher concentrations (3 and 30 μM) importantly inhibited both the rate of $Ca^{2+}$ rise and the maximal $Ca^{2+}$ (Fig. 5B and C and Table 3).

**Table 1**
Effect of Jacareubin on FcεRI-induced calcium mobilization in BMMCs.

| Treatment | Rate of increase $[Ca^{2+}]i$ | Max $[Ca^{2+}]i$ (nM) |
|---|---|---|
| Vehicle | 0.648 ± 0.222 | 239.3 ± 42.41 |
| Jac [0.3 μM] | 0.584 ± 0.334 | 181.8 ± 25.19 |
| Jac [3 μM] | 0.335 ± 0.065 | 182.1 ± 50.83 |
| Jac [30 μM] | 0.095 ± 0.122* | 113.4 ± 24.14* |

BMMCs were pre-treated with vehicle or distinct jacareubin concentrations and increase on intracellular calcium concentration after FcεRI receptor stimulation was registered. Data from those graphs (Fig. 3) were utilized for this table. One way ANOVA with Dunnett's multiple comparisons test (*p < 0.05).

**Table 2**
Effect of Jacareubin on extracellular calcium flux stimulated by FcεRI receptor in BMMCs.

| Treatment | Rate of increase $[Ca^{2+}]i$ | Max $[Ca^{2+}]i$ (nM) |
|---|---|---|
| Vehicle | 1.407 ± 0.221 | 264.7 ± 14.65 |
| Jac [0.3 μM] | 1.216 ± 0.181 | 266.3 ± 20.77 |
| Jac [3 μM] | 0.368 ± 0.106* | 161.4 ± 29.84* |
| Jac [30 μM] | 0.080 ± 0.047* | 104.5 ± 23.75* |

BMMCs were treated with vehicle or distinct jacareubin concentrations and increase on intracellular calcium concentration was registered after FcεRI stimulation. Data from those graphs (Fig. 4) were utilized for this table. One way ANOVA with Dunnett's multiple comparisons test (*p < 0.05).

### 3.4. Jacareubin interferes with ROS production induced by IgE/Ag in mast cells

Since a common feature between ROCE and SOCE observed in distinct MC preparations is their modulation by the production of reactive oxygen-species (ROS) [59,62,63], we hypothesized that jacareubin could inhibit the production of ROS triggered by FcεRI receptor and this could cause its effect on intracellular calcium rise in MCs. To test this hypothesis, we first determined the antioxidant capacity of jacareubin and compared it with other molecules with reported antioxidant properties, exploring the possible relationship between antioxidant capacity and inhibition of MC activation. Fig. 6A shows that jacareubin reduces DPPH at lower concentrations than α-tocopherol and trolox, whereas, compared to quercetin, showed less antioxidant capacity. The antioxidant capacity of quercetin and trolox was related to their ability to block IgE/Ag-dependent degranulation, since lower concentrations of quercetin were needed to inhibit β-hexosaminidase release (Fig. 6B). However, when compared with jacareubin, the xanthone showed higher capacity of inhibition of IgE/Ag-induced degranulation and calcium influx than trolox and quercetin (Fig. 6B and C). When the mentioned compounds were tested on their ability to block the FcεRI-dependent production of reactive oxygen species, jacareubin inhibited DCF oxidation in a dose-response fashion (Fig. 6D).

In order to explore the mechanism by which jacareubin could inhibit ROS accumulation in BMMCs, cells were stimulated with IgE/Ag in the presence of buffer or different concentrations of the xanthone and the activity of the NADPH oxidase complex (NOX) was determined. As observed in Fig. 7A, jacareubin was not able to block the FcεRI-dependent stimulation of NOX at any of the concentrations tested. The NOX inhibitor DPI was used as a control and the expected effect of this compound was observed. However, in a cell-free assay, activity of xanthine oxidase was inhibited by jacareubin in a dose-response fashion (Fig. 7B).

### 3.5. Jacareubin inhibits mast-cell dependent changes in vascular permeability and inflammatory reactions in vivo

In order to test the effects of Jacareubin on IgE/Ag-induced degranulation of mast cells *in vivo*, we utilized the murine passive anaphylaxis model, where the immediate changes on vascular permeability are entirely dependent on mast cell activation [28,52]. As can be observed on Fig. 8A, jacareubin inhibited FcεRI-dependent inflammation up to 80% at doses between 1 and 33.3 mg/kg i.p, when administered 2 h before DNP-HSA challenge. Utilized doses did not produce any effect on mice, since were below the concentrations where toxicity of this xanthone has been observed *in vivo* [64].

In order to evaluate the anti- inflammatory activity of jacareubin on conditions that have been associated with other immune cells (monocytes and neutrophils), we tested the effect of that compound on the TPA-induced inflammation model in mouse ear, determining the produced edema and the activity of myeloperoxidase. As can be observed on Fig. 8B, jacareubin inhibited TPA-induced edema in a dose-dependent fashion, from 7 to 68% and this blockage was similar to the observed with indomethacin. Regarding the MPO activity, jacareubin inhibited from from 13 to 81% (Fig. 8C).

## 4. Discussion

In this study the structure of the xanthone Jacareubin was determined by X-ray diffraction for the first time, and its effects on mast cell degranulation were evaluated. Jacareubin showed high inhibitory activity on FcεRI-induced degranulation of mast cells by blocking the extracellular calcium influx activated either by IgE/Ag complexes,

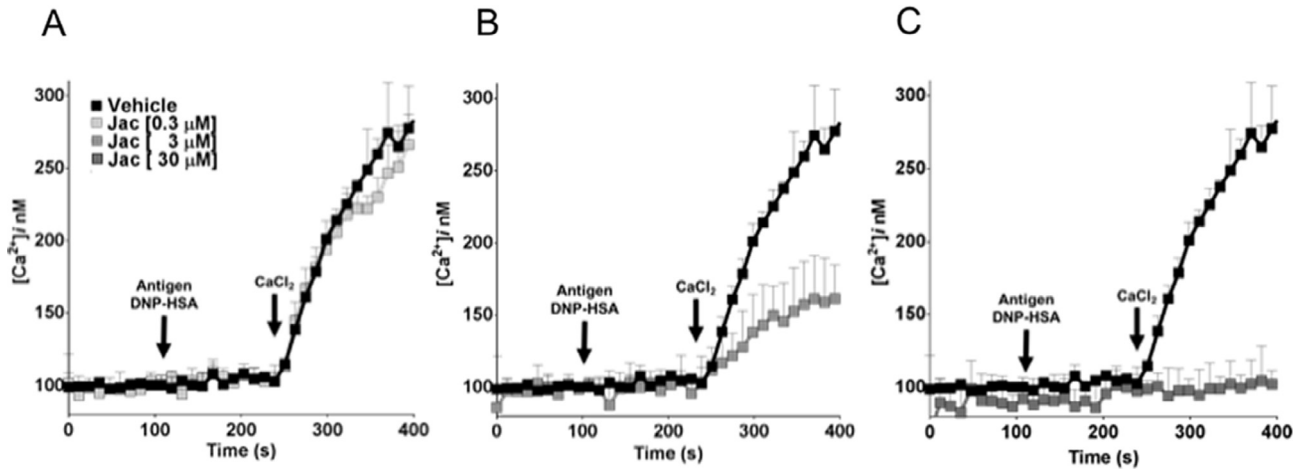


**Fig. 4.** Jacareubin inhibits extracellular calcium influx stimulated by FcεRI receptor in mast cells. A) – C) BMMCs were suspended in calcium-free buffer and the specific antigen DNP-HSA was added. After 100 s, calcium was added to the cuvette to reach 1.8 mM. A) – C). Representative traces of intracellular calcium rise in cells pre-treated with vehicle or different concentrations of jacareubin, n = 3. One way ANOVA with Dunnetťs multiple comparisons test (*p < 0.05).

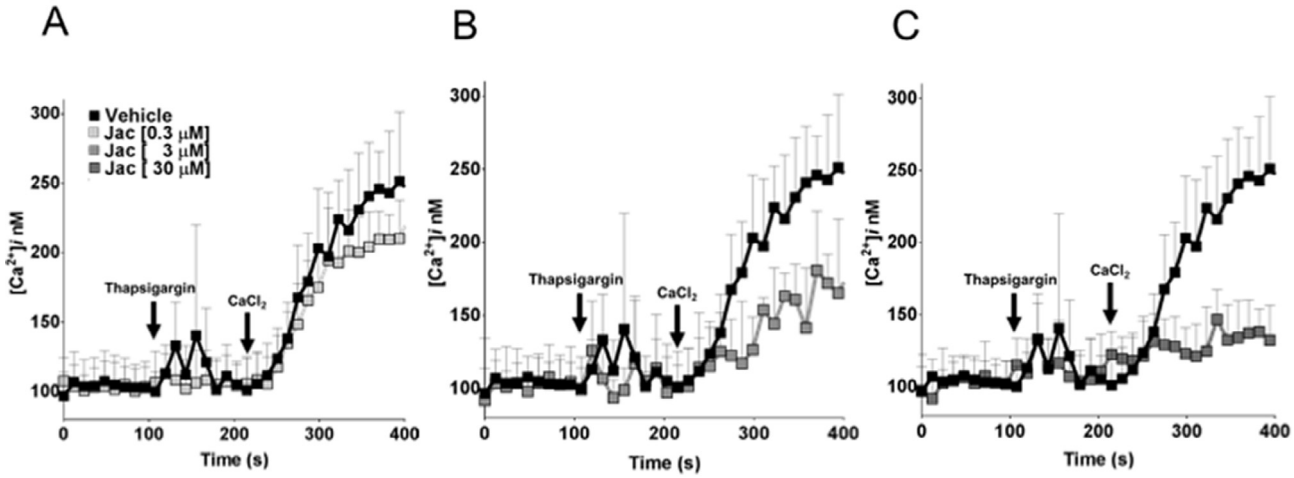


**Fig. 5.** Jacareubin inhibits Thap-induced calcium influx in mast cells in a dose-response fashion. A) – C) Representative traces of intracellular calcium rise induced by Thap (1μM) in BMMCs pre-treated with vehicle or different concentrations of jacareubin in $Ca^{2+}$-free medium, n = 3–5. One way ANOVA with Dunnett's multiple comparisons test ($^{*}p < 0.05$).

**Table 3**
Effect of Jacareubin on extracellular calcium flux stimulated by Thapsigargin in BMMCs.

| Treatment | Rate of increase $[Ca^{2+}]i$ | Max $[Ca^{2+}]i$ (nM) |
|---|---|---|
| Vehicle | 1.212 ± 0.491 | 251.3 ± 49.96 |
| Jac [0.3 μM] | 0.931 ± 0.312 | 210.2 ± 27.60 |
| Jac [3 μM] | 0.423 ± 0.164* | 180.7 ± 40.68* |
| Jac [30 μM] | 0.092 ± 0.088* | 146.6 ± 20.80* |

BMMCs were treated with vehicle or distinct jacareubin concentrations and increase on intracellular calcium concentration was registered after Thapsigargin addition. Data from those graphs (Fig. 5) were utilized for this table. One way ANOVA with Dunnett's multiple comparisons test ($^{*}p < 0.05$).

Thapsigargin or TPA/A23187. Jacareubin also exhibited an important antioxidant activity and this could count to the effect on calcium mobilization, due the dependence of that phenomenon on ROS generation. Whereas jacareubin did not showed significant inhibitory activity on FcεRI-induced NOX activity, it inhibited the activity of xanthine oxidase in a cell-free assay. Finally, this compound exerts anti-inflammatory actions *in vivo*, blocking inflammatory reactions that depend on mast cells but also other immune cells activation.

The planar and rigid structure of jacareubin was clearly evidenciated by X-ray difraction, and may limit the posibility to block nonespecific molecular targets. Xanthones bearing a three ring skeleton have shown anti-inflammatory activity in mast cells, such as nujiangexanthone A, mangostins α, β, and γ, mangiferin and its aglycone norathyriol (Fig. 9) [34–37,65]. Our results show that Jacareubin, is the most potent xanthone, and the only one with an extra ring arising from cyclization of a dimethyl allyl substituent on C-2, conferring hydrophobic properties to the molecule. On the other side, hydroxyl on C-5 and C-6 may allow the interaction of jacaraeubin due to hydrogen bonds with carbonyls of membrane phospolipids, in a similar way to that reported for cholesterol [66]. Interestingly, less potent mangostins and nujiangexanthone bear uncyclized dimethyl allyl substituents, mangiferin is the less potent and the most hydrophylic due to four hydroxyls and a glucose residue. Emodin, an anthraquinone, also with a skeleton similar to xanthones, due to a three ring system but with two carbonyls, is also able to inhibit β-hexosaminidase release stimulated by IgE/Ag in BMMCs [67].

Antioxidant activity of Jacareubin in the DPPH reduction test is similar to that previously reported [56,68]. Antioxidant activity has been proposed as the main mechanism responsible for inhibiting degranulation in mast cells associated for many natural compounds [29,69]. Hydroxyl phenolic groups in xanthones have been thought to importantly contribute to the antioxidant activity of those compounds, but this is not always the case. For instance, γ-mangostin and garcinone A and B, showed a greater antioxidant response than other xanthones with higher number of hydroxyl substituents in the DPPH reduction test [34,56]. Jacareubin showed a better antioxidant activity than α-tocopherol and caffeic acid, despite the fact does not possess a high number of hydroxyl substituents.

Degranulation of mast cells after FcεRI crosslinking has been considered the main target of therapeutic approaches to control inflammation and allergy, since the release of preformed mediators occurs rapidly and the secreted compounds trigger immediate and intense reactions. The search for safety compounds able to inhibit mast cell degranulation has led to the identification of several molecules with different capacities of inhibition and distinct mechanisms of action. We found that jacareubin potently inhibits the secretion of the preformed mediator β-hexosaminidase in BMMCs. Our data show that Jacareubin is one of the most potent of the xanthones so far tested on IgE/Ag-induced degranulation in mast cells. When utilized at 0.046 μM and 30 μM, this compound inhibited 50 and 97% β-hexosaminidase release respectively, while nujiangexanthone A showed maximal inhibitory activity at 50 μM (causing 95% of inhibition of in BMMC) [38], but its $IC_{50}$ was between 1 and 10 μM, and α-mangostin exhibited inhibitory actions $IC_{50}$ between 10 and 20 μM, with maximal inhibition of histamine release on RBL-2H3 cells of 80% at 20 μM [34]. Xanthones are able to inhibit degranulation of mast cells in a wide range of concentrations, for example, mangiferin requires 118 μM for inhibiting 50% of degranulation triggered by the 48/80 compound (a commonly used secretagogue in mast cells) [36]. It is noteworthy, that all concentrations of jacareubin here tested did not induce cytotoxicity in mast cells, this is in line with the observed with other immune cells, such as human blood mononuclear cells (PBMC) [64].

Besides xanthones, other natural products, such as polyphenols, have been found to effectively inhibit the degranulation of mast cells by over 70% and in the same concentration ranges of the inhibitory activity of Jacareubin, those include flavonoids such as luteolin [25,27], tetramethoxyluteolin [28], and quercetin [25], however, given the polarity of the xanthones, they exhibit better solubility than the mentioned flavonoids and this characteristic could favor to reach higher concentrations in tissues [70].

Although evidence showing that some xanthones inhibit calcium mobilization in mast cells has been collected, the specific mechanism for this action has been elusive [34]. Description of the effects of xanthones on the FcεRI receptor signaling system includes, for example, the

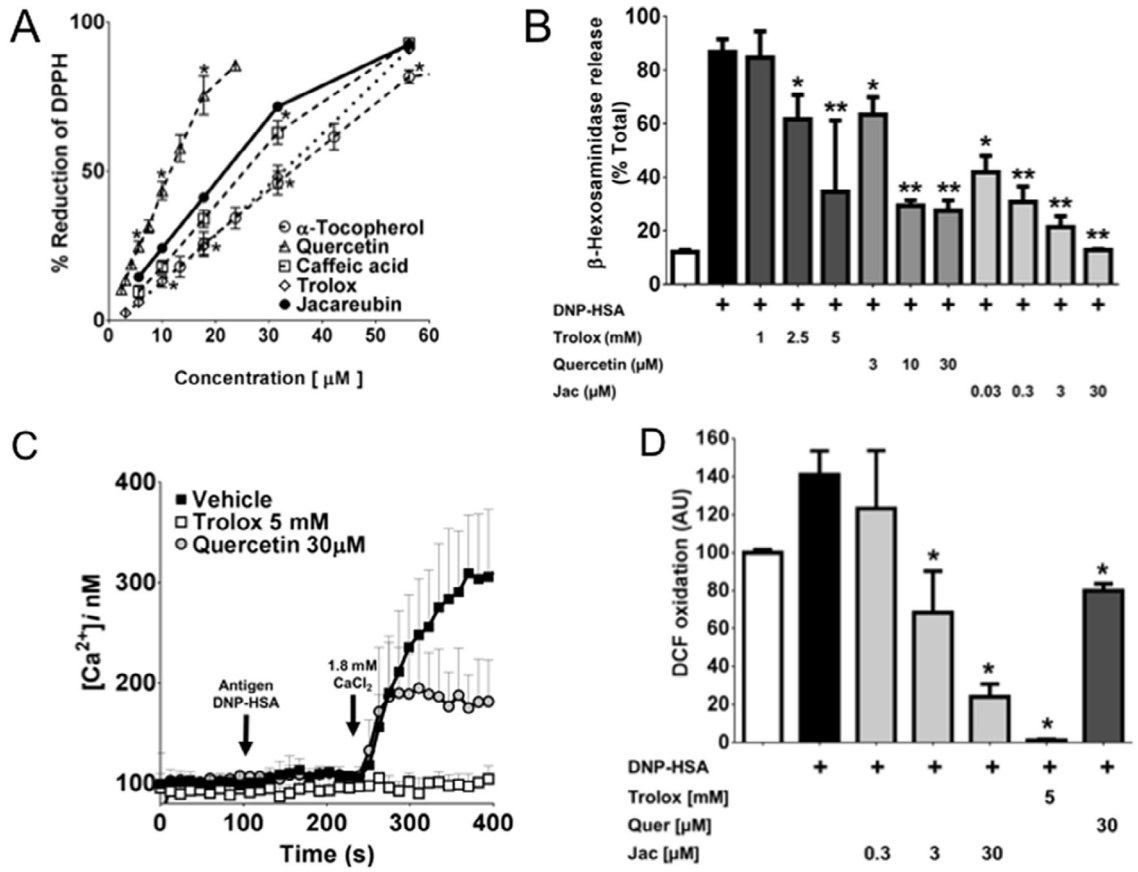


**Fig. 6.** Jacareubin exhibits important antioxidant activity: comparison with trolox and quercetin. A) Antioxidant activity of Jacareubin compared with other antioxidants, determined by DPPH reduction, n = 3. B) Inhibition of FcεRI-induced degranulation by trolox, quercetin and jacareubin (values obtained with jacareubin were taken from Fig. 2B), n = 3. C) Inhibition of IgE/Ag-induced calcium influx by trolox and quercetin, n = 3. D) FcεRI-induced DCF oxidation in BMMCs pre-treated with different concentrations of jacareubin (values obtained from cells pre-treated with trolox and quercetin were included as controls), n = 3. One way ANOVA with Dunnett's multiple comparisons test ($^{*}p < 0.05$).

blockage of the Tyr-phosphorylation of early signaling proteins, such as phospholipase A2, Src family kinases and MAPK [38]. Our results show that Jacareubin is able to efficiently block calcium mobilization in response to FcεRI triggering in BMMCs and seemed to be associated with the blockage of a plasma membrane calcium channels activated by FcεRI and Thap.

In mast cells, FcεRI triggering leads to the activation of PLC which, in turn, produces DAG and $IP_3$ that activates the $IP_3R$ calcium channel causing the emptiness of the intracellular calcium storage pools. This event leads to the entrance of calcium from the extracellular space by

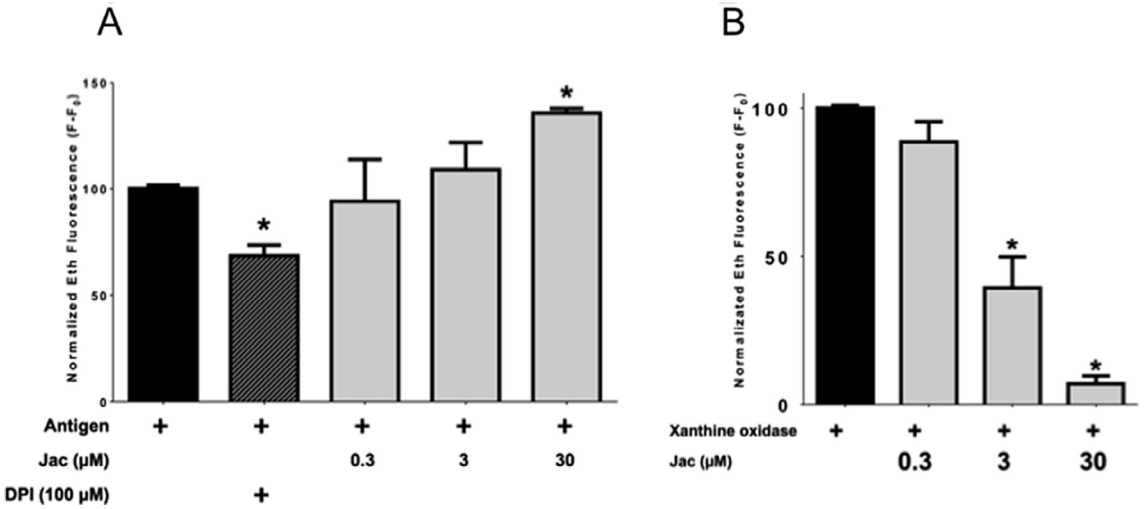


**Fig. 7.** Jacareubin does not inhibit FcεRI-dependent activation of NOX but is able to inhibit Xanthine Oxidase in a cell-free assay. A) IgE/Ag-induced activity of NOX in cells pre-treated with DPI or different concentrations of jacareubin, n = 3. B) Xanthine oxidase activity determined in the presence of distinct concentrations of jacareubin, n = 3. One way ANOVA with Dunnett's multiple comparisons test ($^{*}p < 0.05$).

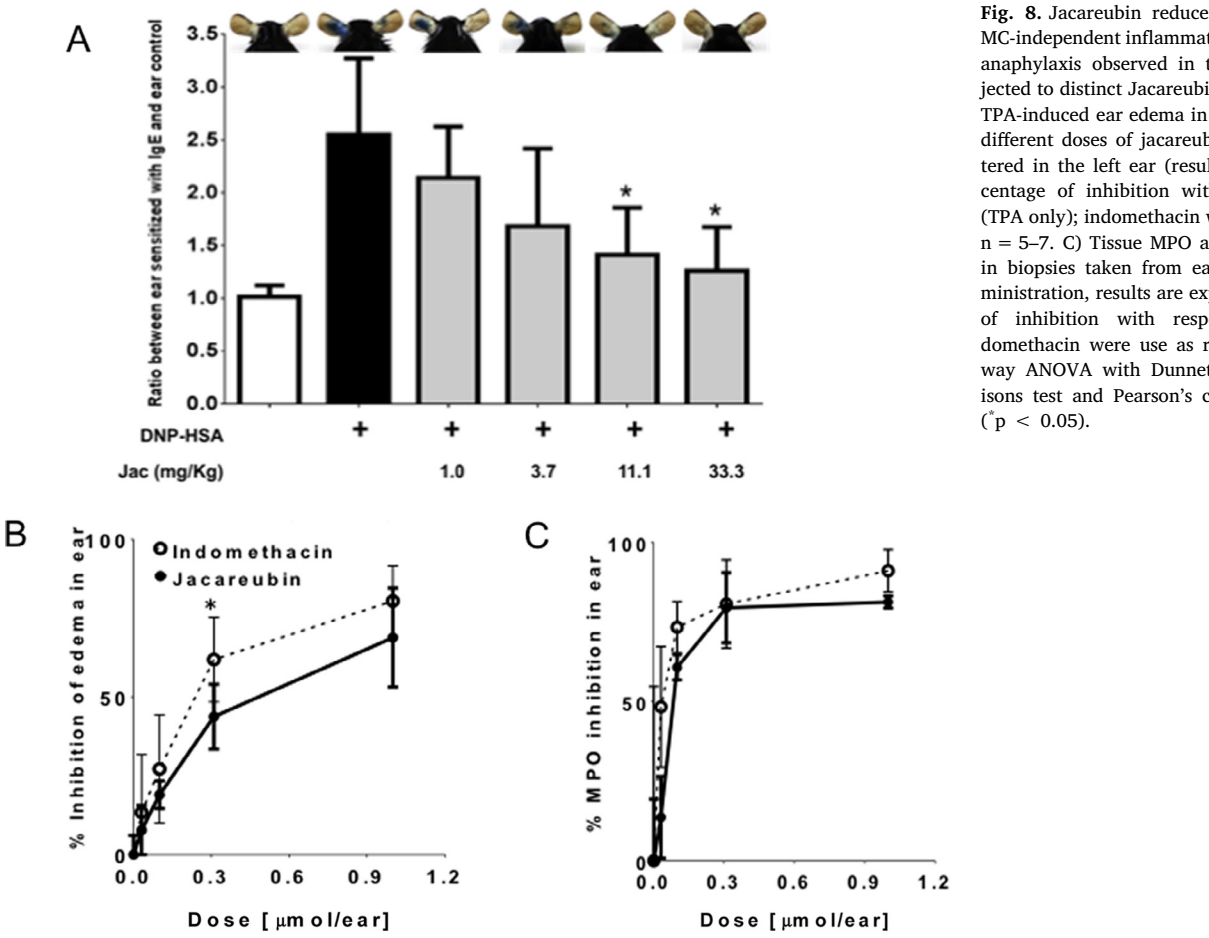


**Fig. 8.** Jacareubin reduces MC-dependent and MC-independent inflammation *in vivo*. A) Passive anaphylaxis observed in the ear of mice subjected to distinct Jacareubin doses, n = 5–10. B) TPA-induced ear edema in mice pretreated with different doses of jacareubin topically administered in the left ear (results are shown as percentage of inhibition with respect to control (TPA only); indomethacin were use as reference. n = 5–7. C) Tissue MPO activity was measured in biopsies taken from ears 4 h after TPA administration, results are expressed as percentage of inhibition with respect to control, indomethacin were use as reference. n = 5. One way ANOVA with Dunnett's multiple comparisons test and Pearson's correlation coefficient ($^{*}p < 0.05$).

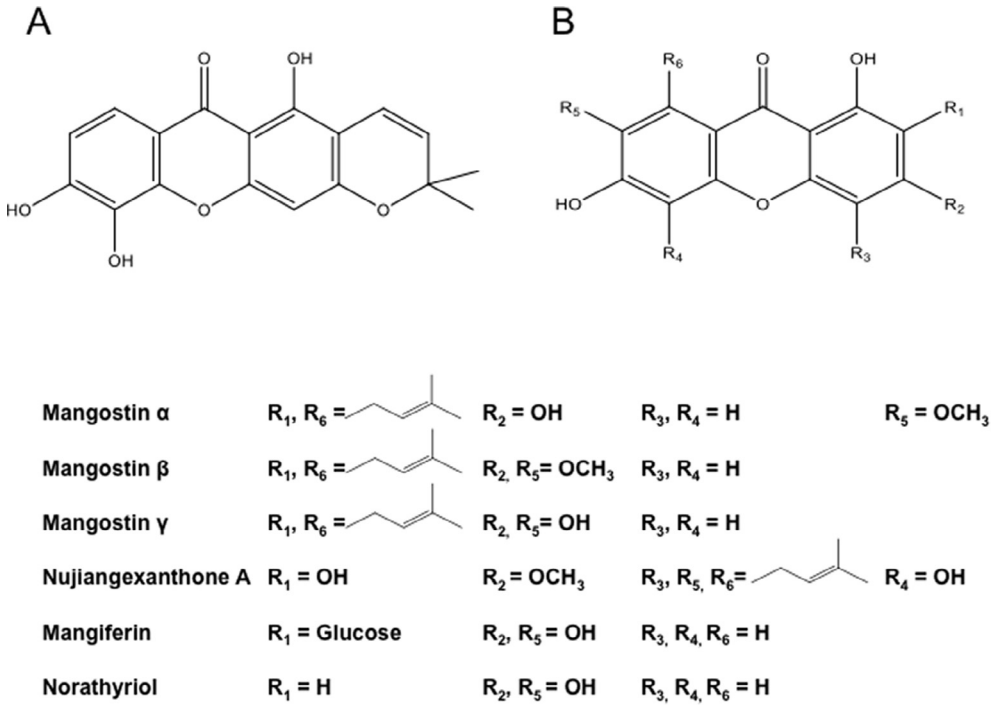


**Fig. 9.** Jacareubin present a unique structural signature for xanthones with anti-inflammatory activity. A) Jacareubin. B) Xanthones with anti-inflammatory activity in mast cells previously described (lower part, substituents on the specific structure of xanthones).

calcium channels that constitute the "store-operated calcium entry" (SOCE), which can be triggered by the inhibitor of the SERCA ATPase Thap. SOCE operates mainly through the ORAI family of ion channels, being Orai1 the most relevant in immune cells [63,71]. After intracellular calcium pools emptiness, the Hand-EF region of the calcium sensor STIM located on the inner side of the endoplasmic reticulum loses the $Ca^{2+}$ that keeps it stabilized, and provokes a conformational change that allows the oligomerization and extension of STIM and forms with ORAI membrane channels the pore to facilitate the re-filling of intracellular $Ca^{2+}$ pools in the endoplasmic reticulum [72,73]

Different studies have suggested that a very close relationship exists between the production of ROS and calcium entry in non-excitable cells [16]. For example, ROS production promotes glutathionylation of cysteines C49 and C56 in the inner region of the endoplasmic reticulum of STIM, which causes the affinity of $Ca^{2+}$ to be reduced by the Hand-EF region of STIM, improving the extension of STIM and its oligomerization with Orai at the plasma membrane [17,72,73]. In mast cells, triggering of FcεRI leads to NADPH oxidase activation and the production of ROS that promote the activation of the LAT-PLCγ signaling axis [74]. Since Jacareubin inhibited the FcεRI-dependent production of ROS, it is possible to hypothesize that this compound could prevent the redox-dependent modifications of STIM needed for SOCE in mast cells.

Jacareubin-dependent blockage of ROS accumulation could also explain the inhibition of degranulation promoted by the combination of TPA plus A23187, since it has been shown that Thap and ionophore A23187 also produce the rapid production of ROS in mast cells [75]. Interestingly, although antioxidant activity of Jacareubin was higher than that showed by trolox and lower than the detected for quercetin, the xanthone was the most potent regarding to the inhibition of IgE/Ag-triggered degranulation. Antioxidant activity did not show a direct correlation with the capacity of the tested compounds to block calcium entry.

The mechanism by which jacareubin blocks IgE/Ag-induced degranulation and calcium mobilization in BMMCs seems does not include the inhibition of NOX. However, xanthine oxidase was inhibited by this xanthone in a cell-free assay. Although the xanthone norathyriol is structurally related to jacareubin and show inhibitory activity on NOX and PLC in neutrophils [65], our data indicate that one possible mechanism of action of jacareubin, besides its capacity of chelating ROS, could be the inhibition of the xanthine oxidase. Antioxidant activity of jacareubin could contribute also to prevent IgE/Ag-triggered PLCγ activation, since it has been demonstrated that ROS production is essential to PLCγ phosphorylation in mast cells [74], see Fig. 10.

Jacareubin could exert inhibitory actions also by additional mechanisms. Evidence has been collected about the inhibition of the protein kinase Syk by other natural compounds such as piceatannol, morin, nujiangexantone A, mangostins α, β and γ, emodin [34,38,67,76,77], then, it is possible to speculate that jacareubin could also inhibit this important kinase involved in FcεRI signaling system.

The inhibitory actions of jacareubin on mast cell-dependent anaphylactic reactions are observed *in vivo*, since this compound suppressed extravastion of Evans blue stimulated by IgE/Ag (an effect mediated by histamine secreted by mast cells) and the edema induced by TPA in mice, a response dependent on prostaglandin production by other immune resident cells [78]. The blockage on the accumulation of ROS could importantly count for this effect, since ROS production is essential for FceRI-induced mast cell degranulation [74] also for the production of prostaglandins in other cells [79]. This effect of jacareubin was similar or more potent to the observed with other natural compounds such as morin (30 mg/kg), teoritin (1 mg/kg) and theanine (1 mg/kg), that inhibited passive cutaneous anaphylaxis by 40, 42 and 44% respectively [77,80–82]. Xanthones similar to jacareubin such as mangostins do not have presented toxic effects in pre-clinical and clinical trials [83,84]. Jacareubin is presented here as a new drug with potential for the development of anti-inflammatory compounds derived from natural products to treat mast cell-related diseases.

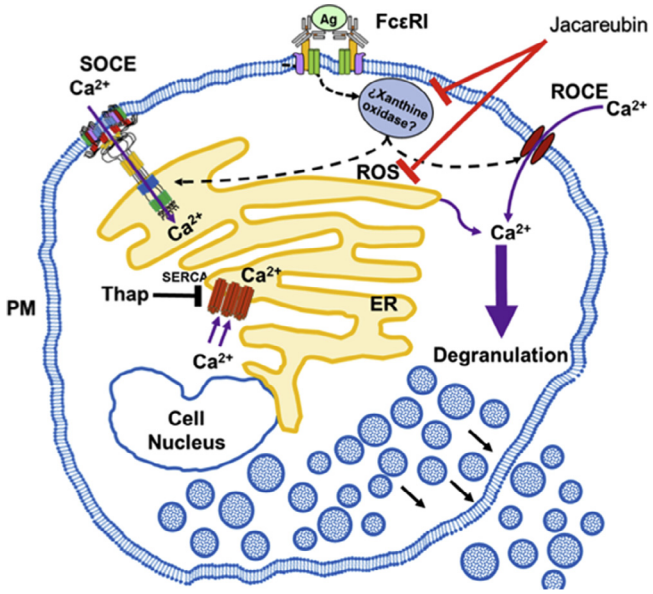


**Fig. 10.** Summary of the points of control of FcεRI signaling system that are modulated by Jacareubin in mast cells. Jacareubin inhibits degranulation and extracellular calcium influx triggered by IgE/Ag and Thap. This inhibition correlates with the blockage of the generation of ROS in this cell type.

## 5. Authorship

JICA performed the isolation, purification and chemical characterizarion of jacareubin. Additionally, performed degranulation assays, ROS production assays and $[Ca^{2+}]i$ measurements, *in vivo* assays of passive cutaneous anaphylaxis in mice and wrote the first draft of the manuscript; SLGG contributed to the isolation and purification of jacareubin and also to the interpretation of the NMR spectra of the xanthone, together with the analysis and discussion of the data; AIS generated all full differentiated and functional BMMCs needed for the study and contribute to the discussion of the results; SHO carried out the structural identification experiments of the jacareubin by X-ray diffraction and contributed with the analysis and discussion of data; ANC performed a DPPH assay, TPA-induced edema model in mouse ear and myeloperoxidase assay; JPCh and ONMC performed NADPH and xanthine oxidase assays. RRCh and CGE performed the study conception and experimental design, they reviewed the main body of the paper and directed the activities of this work.

## Acknowledgements

This work was supported by Conacyt Grants FC-2015-2/1122 and ANR-Conacyt 188565 to CGE, project IN210016 DGAPA-PAPIIT-UNAM to RRCh and scholarship No. 404373 to JICA. Authors want to thank Dr. Jorge Fernández, Ricardo Glaxiola Centeno, Víctor Manuel García Gómez, Benjamín E. Chávez Álvarez, María Antonieta López López and Ramón Gómez Martínez, from the Unit for the Production and Experimental use of Laboratory Animals (UPEAL), at Cinvestav Zacatenco, and Ramón Gómez Martínez from the Animal Facility at Cinvestav Sede Sur; Dr. Beatriz Quiroz Vázquez and Dr. Javier Pérez Flores for NMR and EM determinations; this manuscript constitutes the PhD Thesis of J. I. Castillo-Arellano, who is a student of the Biochemical Sciences PhD Program of the National Autonomous University of Mexico.

## 6. Declarations of interest

None.

## References


[1] R. Pawankar, G.W. Canonica, S.T. Holgate, R.F. Lockey, M.S. Blaiss, World Allergy Organization White Book on Allergy: Update 2013. 2013. doi: 10.1186/1939-4551-7-12.

[2] L.J. Gershwin, Comparative immunology of allergic responses, Annu. Rev. Anim. Biosci. 3 (2015) 327–346, http://dx.doi.org/10.1146/annurev-animal-022114-110930.

[3] Ruby Pawankar, Stephen T. Holgate, L.J. Rosenwasser (Eds.), Allergy Frontiers: Therapy and Prevention Volume 5. Tokyo Berlin Heidelberg New York: Springer, 2010. doi: 10.1007/978-4-431-99362-9.

[4] M. Kristiansen, S. Dhami, G. Netuveli, S. Halken, A. Muraro, G. Roberts, et al., Allergen immunotherapy for the prevention of allergy: a systematic review and meta-analysis, Pediatr. Allergy Immunol. 28 (2017) 18–29, http://dx.doi.org/10.1111/pai.12661.

[5] R.A. El-Feky, Mast cell and atopy, Egypt J. Pediatry Allergy Immunol. 9 (2011) 55–62.

[6] A.B. Roos, M. Mori, H.K. Gura, A. Lorentz, L. Bjermer, H.J. Hoffmann, et al., Increased IL-17RA and IL-17RC in end-stage COPD and the contribution to mast cell secretion of FGF-2 and VEGF, Respir. Res. 18 (2017), http://dx.doi.org/10.1186/s12931-017-0534-9.

[7] G.Y. Jiménez-Andrade, A. Ibarra-Sánchez, D. González, M. Lamas, C. González-Espinosa, Immunoglobulin e induces VEGF production in mast cells and potentiates their pro-tumorigenic actions through a Fyn kinase-dependent mechanism, J. Hematol. Oncol. (2013) 6, http://dx.doi.org/10.1186/1756-8722-6-56.

[8] C.Y. Hwang, Y.J. Chen, M.W. Lin, T.J. Chen, S.Y. Chu, C.C. Chen, et al., Prevalence of atopic dermatitis, allergic rhinitis and asthma in Taiwan: a national study 2000 to 2007, Acta Derm. Venereol. 90 (2010) 589–594, http://dx.doi.org/10.2340/00015555-0963.

[9] D.S. Hurst, P. Venge, Evidence of eosinophil, neutrophil, and mast-cell mediators in the effusion of OME patients with and without atopy, Allergy Eur. J. Allergy Clin. Immunol. 55 (2000) 435–441, http://dx.doi.org/10.1034/j.1398-9995.2000.00289.x.

[10] S.L. Logsdon, H.C. Oettgen, Anti-IgE therapy: clinical utility and mechanistic insights, Curr. Top. Microbiol. Immunol. 388 (2015) 39–61, http://dx.doi.org/10.1007/978-3-319-13725-4_3.

[11] J. Karhausen, S.N. Abraham, How mast cells make decisions, J. Clin. Invest. 126 (2016) 3735–3738, http://dx.doi.org/10.1172/JCI90361.

[12] A. Mócsai, J. Ruland, V.L.J. Tybulewicz, The SYK tyrosine kinase: a crucial player in diverse biological functions, Nat. Rev. Immunol. 10 (2010) 387–402, http://dx.doi.org/10.1038/nri2765.

[13] C. Fasolato, M. Hoth, G. Matthews, R. Penner, Ca2+ and Mn2+ influx through receptor-mediated activation of nonspecific cation channels in mast-cells, Proc. Natl. Acad. Sci. U.S.A. 90 (1993) 3068–3072, http://dx.doi.org/10.1073/pnas.90.7.3068.

[14] A.B. Parekh, A. Fleig, R. Penner, The store-operated calcium current I(CRAC): nonlinear activation by InsP3 and dissociation from calcium release, Cell 89 (1997) 973–980 doi: S0092-8674(00)80282-2 [pii].

[15] A.R. Artalejo, J.C. Ellory, A.B. Parekh, Ca2+-dependent capacitance increases in rat basophilic leukemia cells following activation of store-operated Ca2+ entry and dialysis with high-Ca2+-containing intracellular solution, Pflugers Arch. 436 (1998) 934–939, http://dx.doi.org/10.1007/PL00008088.

[16] T. Yoshimaru, Y. Suzuki, T. Inoue, C. Ra, L-type Ca2+ channels in mast cells: activation by membrane depolarization and distinct roles in regulating mediator release from store-operated Ca2+ channels, Mol. Immunol. 46 (2009) 1267–1277, http://dx.doi.org/10.1016/j.molimm.2008.11.011.

[17] Y. Suzuki, T. Yoshimaru, T. Inoue, O. Niide, C. Ra, Role of oxidants in mast cell activation, Chem. Immunol. Allergy 87 (2005) 32–42, http://dx.doi.org/10.1159/000087569.

[18] T. Inoue, Y. Suzuki, T. Yoshimaru, C. Ra, Nitric oxide positively regulates Ag (I)-induced Ca2+ influx and mast cell activation: role of a nitric oxide synthase-independent pathway, J. Leukoc. Biol. 86 (2009) 1365–1375, http://dx.doi.org/10.1189/jlb.0609387.

[19] T. Itoh, M. Tsukane, M. Koike, C. Nakamura, K. Ohguchi, M. Ito, et al., Inhibitory effects of whisky congeners on IgE-mediated degranulation in rat basophilic leukemia RBL-2H3 cells and passive cutaneous anaphylaxis reaction in mice, J. Agric. Food Chem. 58 (2010) 7149–7157, http://dx.doi.org/10.1021/jf100998c.

[20] G.R.M. Perez, Anti-inflammatory activity of compounds isolated from plants, Sci. World J. 1 (2001) 713–784, http://dx.doi.org/10.1100/tsw.2001.77.

[21] A. Singh, S. Holvoet, A. Mercenier, Dietary polyphenols in the prevention and treatment of allergic diseases, Clin. Exp. Allergy 41 (2011) 1346–1359, http://dx.doi.org/10.1111/j.1365-2222.2011.03773.x.

[22] D.F. Finn, J.J. Walsh, Twenty-first century mast cell stabilizers, Br. J. Pharmacol. 170 (2013) 23–37, http://dx.doi.org/10.1111/bph.12138.

[23] J. Dong Kim, D.K. Kim, H. Soon Kim, A.R. Kim, B. Kim, E. Her, et al., Morus bombycis extract suppresses mast cell activation and IgE-mediated allergic reaction in mice, J. Ethnopharmacol. 146 (2013) 287–293, http://dx.doi.org/10.1016/j.jep.2012.12.046.

[24] J.H. Kim, A.R. Kim, H.S. Kim, H.W. Kim, Y.H. Park, J.S. You, et al., Rhamnus davurica leaf extract inhibits Fyn activation by antigen in mast cells for anti-allergic activity, BMC Complement. Altern. Med. 15 (2015) 80, http://dx.doi.org/10.1186/s12906-015-0607-6.

[25] M. Kimata, M. Shichijo, T. Miura, I. Serizawa, N. Inagaki, H. Nagai, Effects of luteolin, quercetin and baicalein on immunoglobulin E-mediated mediator release from human cultured mast cells, Clin. Exp. Allergy 30 (2000) 501–508, http://dx.doi.org/10.1046/j.1365-2222.2000.00768.x.

[26] I.H. Jeon, H.S. Kim, H.J. Kang, H.S. Lee, S. Jeong, S.J. Kim, et al., Anti-inflammatory and antipruritic effects of luteolin from perilla (P. frutescens L.) leaves, Molecules 19 (2014) 6941–6951, http://dx.doi.org/10.3390/molecules19066941.

[27] S. Sun-Yup, J.R. Park, D.S. Byun, 6-Methoxyluteolin from Chrysanthemum zawadskii var. latilobum suppresses histamine release and calcium influx via down-regulation of FcεRI α chain expression, J. Microbiol. Biotechnol. 22 (2012) 622–627, http://dx.doi.org/10.4014/jmb.1111.11060.

[28] Z. Weng, A.B. Patel, S. Panagiotidou, T.C. Theoharides, The novel flavone tetramethoxyluteolin is a potent inhibitor of human mast cells, J. Allergy Clin. Immunol. 135 (1044–1052) (2015) e5, http://dx.doi.org/10.1016/j.jaci.2014.10.032.

[29] M. Ninomiya, T. Itoh, S. Ishikawa, M. Saiki, K. Narumiya, M. Yasuda, et al., Phenolic constituents isolated from Fragaria ananassa Duch. inhibit antigen-stimulated degranulation through direct inhibition of spleen tyrosine kinase activation, Bioorg. Med. Chem. 18 (2010) 5932–5937, http://dx.doi.org/10.1016/j.bmc.2010.06.083.

[30] Y. Fujimura, D. Umeda, K. Yamada, H. Tachibana, The impact of the 67 kDa laminin receptor on both cell-surface binding and anti-allergic action of tea catechins, Arch. Biochem. Biophys. 476 (2008) 133–138, http://dx.doi.org/10.1016/j.abb.2008.03.002.

[31] Q. Wang, H. Matsuda, K. Matsuhira, S. Nakamura, D. Yuan, M. Yoshikawa, Inhibitory effects of thunberginols A, B, and F on degranulations and releases of TNF-α and IL-4 in RBL-2H3 cells, Biol. Pharm. Bull. 30 (2007) 388–392 10.1248/bpb.30.388.

[32] Y.H. Choi, G.H. Yan, Anti-allergic effects of scoparone on mast cell-mediated allergy model, Phytomedicine 16 (2009) 1089–1094 10.1016/j.phymed.2009.05.003.

[33] T. Itoh, M. Oyama, N. Takimoto, C. Kato, Y. Nozawa, Y. Akao, M. Iinuma, Inhibitory effects of sesquiterpene lactones isolated from Eupatorium chinense L. on IgE-mediated degranulation in rat basophilic leukemia RBL-2H3 cells and passive cutaneous anaphylaxis reaction in mice, Bioorg. Med. Chem. 17 (2009) 3189–3197, http://dx.doi.org/10.1016/j.bmc.2009.02.062.

[34] T. Itoh, K. Ohguchi, M. Iinuma, Y. Nozawa, Y. Akao, Inhibitory effect of xanthones isolated from the pericarp of Garcinia mangostana L. on rat basophilic leukemia RBL-2H3 cell degranulation, Bioorg. Med. Chem. 16 (2008) 4500–4508, http://dx.doi.org/10.1016/j.bmc.2008.02.054.

[35] H.S. Chae, S.R. Oh, H.K. Lee, S.H. Joo, Y.W. Chin, Mangosteen xanthones, α- and γ-mangostins, inhibit allergic mediators in bone marrow-derived mast cell, Food Chem. 134 (2012) 397–400, http://dx.doi.org/10.1016/j.foodchem.2012.02.075.

[36] D. García, M. Escalante, R. Delgado, F.M. Ubeira, J. Leiro, Anthelminthic and antiallergic activities of Mangifera indica L. stem bark components Vimang and Mangiferin, Phyther. Res. 17 (2003) 1203–1208, http://dx.doi.org/10.1002/ptr.1343.

[37] D.G. Rivera, I.H. Balmaseda, A.A. León, B.C. Hernández, L.M. Montiel, G.G. Garrido, et al., Anti-allergic properties of Mangifera indica L. extract (Vimang) and contribution of its glucosylxanthone mangiferin, J. Pharm. Pharmacol. 58 (2006) 385–392, http://dx.doi.org/10.1211/jpp.58.3.0014.

[38] Y. Lu, S. Cai, J. Nie, Y. Li, G. Shi, J. Hao, et al., The natural compound nujiangexanthone A suppresses mast cell activation and allergic asthma, Biochem. Pharmacol. 100 (2015) 61–72, http://dx.doi.org/10.1016/j.bcp.2015.11.004.

[39] R. Reyes-Chilpa, M. Jimenez-Estrada, E. Estrada-Muñiz, Antifungal Xanthones from Calophyllum brasiliensis Heartwood, J. Chem. Ecol. 23 (1997) 1901–1911, http://dx.doi.org/10.1023/B:JOEC.0000006459.88330.61.

[40] K. Yasunaka, F. Abe, A. Nagayama, H. Okabe, L. Lozada-Pérez, E. López-Villafranco, et al., Antibacterial activity of crude extracts from Mexican medicinal plants and purified coumarins and xanthones, J. Ethnopharmacol. 97 (2005) 293–299, http://dx.doi.org/10.1016/j.jep.2004.11.014.

[41] S. Kaennakam, P. Siripong, S. Tip-Pyang, Kaennacowanols A-C, three new xanthones and their cytotoxicity from the roots of Garcinia cowa, Fitoterapia 102 (2015) 171–176, http://dx.doi.org/10.1016/j.fitote.2015.03.008.

[42] R. Reyes-Chilpa, C.H. Baggio, D. Alavez-Solano, E. Estrada-Muñiz, F.C. Kauffman, R.I. Sanchez, et al., Inhibition of gastric H+, K+-ATPase activity by flavonoids, coumarins and xanthones isolated from Mexican medicinal plants, J. Ethnopharmacol. 105 (2006) 167–172, http://dx.doi.org/10.1016/j.jep.2005.10.014.

[43] P.G.M. B. Caracterización tecnológica de veinte especies maderables de la Selva Lacandona, Madera Y Bosques, 1995, 1, 9–38.

[44] G.M. Sheldrick, SHELXT – integrated space-group and crystal-structure determination, Acta Crystallogr. Sect. A Found Crystallogr. 71 (2015) 3–8, http://dx.doi.org/10.1107/S2053273314026370.

[45] I.K. Madera-Salcedo, S.L. Cruz, C. Gonzalez-Espinosa, Morphine prevents lipopolysaccharide-induced TNF secretion in mast cells blocking I B kinase activation and SNAP-23 phosphorylation: correlation with the formation of a -arrestin/TRAF6 complex, J. Immunol. 191 (2013) 3400–3409, http://dx.doi.org/10.4049/jimmunol.1202658.

[46] T.S. Manetz, C. Gonzalez-Espinosa, R. Arudchandran, S. Xirasagar, V. Tybulewicz, J. Rivera, Vav1 regulates phospholipase C activation and calcium responses in mast cells, Mol. Cell. Biol. 21 (2001) 3763–3774, http://dx.doi.org/10.1128/MCB.21.11.3763-3774.2001.

[47] T.S. Manetz, C. Gonzalez-Espinosa, R. Arudchandran, S. Xirasagar, V. Tybulewicz, J. Rivera, Vav1 regulates phospholipase cgamma activation and calcium responses in mast cells, Mol. Cell. Biol. 21 (2001) 3763–3774, http://dx.doi.org/10.1128/

MCB.21.11.3763-3774.2001.
[48] S. Saitoh, R. Arudchandran, T.S. Manetz, W. Zhang, C.L. Sommers, P.E. Love, et al., LAT is essential for FcεRI-mediated mast cell activation, Immunity 12 (2000) 525–535, http://dx.doi.org/10.1016/S1074-7613(00)80204-6.
[49] G. Grynkiewicz, M. Poenie, R.Y. Tsien, A new generation of Ca2+ indicators with greatly improved fluorescence properties, J. Biol. Chem. 260 (1985) 3440–3450 3838314.
[50] M. Satoh, S. Fujimoto, Y. Haruna, S. Arakawa, H. Horike, N. Komai, et al., NAD(P)H oxidase and uncoupled nitric oxide synthase are major sources of glomerular superoxide in rats with experimental diabetic nephropathy, Am. J. Physiol. Ren. Physiol. 288 (2005) F1144–F1152, http://dx.doi.org/10.1152/ajprenal.00221.2004.
[51] L.W. Oberley, D.R. Spitz, [61] Assay of superoxide dismutase activity in tumor tissue, Methods Enzymol. 105 (1984) 457–464, http://dx.doi.org/10.1016/S0076-6879(84)05064-3.
[52] S. Klemm, J. Gutermuth, L. Hültner, T. Sparwasser, H. Behrendt, C. Peschel, et al., The Bcl10-Malt1 complex segregates Fc epsilon RI-mediated nuclear factor kappa B activation and cytokine production from mast cell degranulation, J. Exp. Med. 203 (2006) 337–347, http://dx.doi.org/10.1084/jem.20051982.
[53] R.P. Carlson, O.D. Lynn, J. Chang, A.J. Lewis, Modulation of mouse ear edema by cyclooxygenase and lipoxygenase inhibitors and other pharmacologic agents, Agents Actions 17 (1985) 197–204, http://dx.doi.org/10.1007/BF01966592.
[54] P.P. Bradley, D.A. Priebat, R.D. Christensen, G. Rothstein, Measurement of cutaneous inflammation: estimation of neutrophil content with an enzyme marker, J. Invest. Dermatol. 78 (1982) 206–209, http://dx.doi.org/10.1111/1523-1747.ep12506462.
[55] K. Suzuki, H. Ota, S. Sasagawa, T. Sakatani, T. Fujikura, Assay method for myeloperoxidase in human polymorphonuclear leukocytes, Anal. Biochem. 132 (1983) 345–352, http://dx.doi.org/10.1016/0003-2697(83)90019-2.
[56] F. Zhong, Y. Chen, P. Wang, H. Feng, G. Yang, Xanthones from the bark of Garcinia xanthochymus and their 1,1-diphenyl-2-picrylhydrazyl radical-scavenging activity, Chin. J. Chem. 27 (2009) 74–80, http://dx.doi.org/10.1002/cjoc.200990029.
[57] S.S. Zhang, Q.Y. Ma, X.S. Zou, H.F. Dai, S.Z. Huang, Y. Luo, et al., Chemical constituents from the fungus Amauroderma amoiensis and their in vitro acetylcholinesterase inhibitory activities, Planta Med. 79 (2013) 87–91, http://dx.doi.org/10.1055/s-0032-1327951.
[58] T. Yoshimaru, Y. Suzuki, T. Inoue, C. Ra, L-type Ca2+ channels in mast cells: activation by membrane depolarization and distinct roles in regulating mediator release from store-operated Ca2+ channels, Mol. Immunol. 46 (2009) 1267–1277, http://dx.doi.org/10.1016/j.molimm.2008.11.011.
[59] Y. Suzuki, T. Inoue, C. Ra, L-type Ca2+ channels: a new player in the regulation of Ca2+ signaling, cell activation and cell survival in immune cells, Mol. Immunol. 47 (2010) 640–648, http://dx.doi.org/10.1016/j.molimm.2009.10.013.
[60] I. Ashmole, P. Bradding, Ion channels regulating mast cell biology, Clin. Exp. Allergy 43 (2013) 491–502, http://dx.doi.org/10.1111/cea.12043.
[61] Y. Suzuki, T. Yoshimaru, T. Inoue, C. Ra, Discrete generations of intracellular hydrogen peroxide and superoxide in antigen-stimulated mast cells: reciprocal regulation of store-operated Ca2+ channel activity, Mol. Immunol. 46 (2009) 2200–2209, http://dx.doi.org/10.1016/j.molimm.2009.04.013.
[62] Y. Suzuki, T. Yoshimaru, T. Inoue, C. Ra, Discrete generations of intracellular hydrogen peroxide and superoxide in antigen-stimulated mast cells: reciprocal regulation of store-operated Ca2+ channel activity, Mol. Immunol. 46 (2009) 2200–2209, http://dx.doi.org/10.1016/j.molimm.2009.04.013.
[63] S. Saul, C.S. Gibhardt, B. Schmidt, A. Lis, B. Pasieka, D. Conrad, et al., A calcium-redox feedback loop controls human monocyte immune responses: the role of ORAI Ca2+ channels, Sci. Signal. (2016) 9, http://dx.doi.org/10.1126/scisignal.aaf1639.
[64] W.R. García-Niño, E. Estrada-Muñiz, M. Valverde, R. Reyes-Chilpa, L. Vega, Cytogenetic effects of Jacareubin from Calophyllum brasiliense on human peripheral blood mononucleated cells in vitro and on mouse polychromatic erythrocytes in vivo, Toxicol. Appl. Pharmacol. 335 (2017) 6–15, http://dx.doi.org/10.1016/j.taap.2017.09.018.
[65] M.F. Hsu, S.L. Raung, L.T. Tsao, C.N. Lin, J.P. Wang, Examination of the inhibitory effect of norathyriol in formylmethionyl-leucyl-phenylalanine-induced respiratory burst in rat neutrophils, Free Radic. Biol. Med. 23 (1997) 1035–1045, http://dx.doi.org/10.1016/S0891-5849(97)00132-9.
[66] E. Ikonen, Cellular cholesterol trafficking and compartmentalization, Nat. Rev. Mol. Cell Biol. 9 (2008) 125–138, http://dx.doi.org/10.1038/nrm2336.
[67] D.-Y. Kim, T.-B. Kang, D.-W. Shim, X. Sun, J.-W. Han, Y.-E. Ji, et al., Emodin attenuates A23187-induced mast cell degranulation and tumor necrosis factor-α secretion through protein kinase C and IκB kinase 2 signaling, Eur. J. Pharmacol. 723 (2014) 501–506, http://dx.doi.org/10.1016/j.ejphar.2013.09.066.
[68] X. Zhang, W.U. Jiao, Zhuang Han, Wen-li Mei, D. Hao-Fu, Antioxidant and cytotoxic phenolic compounds of areca nut (Areca catechu), Chem. Res. Chin. Univ. 26 (2010) 161–164.
[69] R. Zalawadia, C. Gandhi, V. Patel, R. Balaraman, The protective effect of Tinospora cordifolia on various mast cell mediated allergic reactions, Pharm. Biol. 47 (2009) 1096–1106 10.3109/13880200903008690.
[70] Z. Weng, B. Zhang, S. Asadi, N. Sismanopoulos, A. Butcher, X. Fu, et al., Quercetin is more effective than cromolyn in blocking human mast cell cytokine release and inhibits contact dermatitis and photosensitivity in humans, PLoS One (2012) 7, http://dx.doi.org/10.1371/journal.pone.0033805.
[71] H.E. Wajdner, J. Farrington, C. Barnard, P.T. Peachell, C.G. Schnackenberg, J.P. Marino, et al., Orai and TRPC channel characterization in FcεRI-mediated calcium signaling and mediator secretion in human mast cells, Physiol. Rep. 5 (2017), http://dx.doi.org/10.14814/phy2.13166.
[72] B.J. Hawkins, K.M. Irrinki, K. Mallilankaraman, Y.C. Lien, Y. Wang, C.D. Bhanumathy, et al., S-glutathionylation activates STIM1 and alters mitochondrial homeostasis, J. Cell Biol. 190 (2010) 391–405, http://dx.doi.org/10.1083/jcb.201004152.
[73] P. Nunes, N. Demaurex, Redox regulation of store-operated Ca2+ entry, Antioxid. Redox Signal. 21 (2014) 915–932, http://dx.doi.org/10.1089/ars.2013.5615.
[74] Y. Suzuki, T. Yoshimaru, T. Matsui, T. Inoue, O. Niide, S. Nunomura, et al., Fc epsilon RI signaling of mast cells activates intracellular production of hydrogen peroxide: role in the regulation of calcium signals, J. Immunol. 171 (2003) 6119–6127.
[75] R. Goldman, S. Moshonov, U. Zor, Generation of reactive oxygen species in a human keratinocyte cell line: role of calcium, Arch. Biochem. Biophys. 350 (1998) 10–18, http://dx.doi.org/10.1006/abbi.1997.0478.
[76] P. Ruzza, B. Biondi, A. Calderan, Therapeutic prospect of Syk inhibitors, Expert Opin. Ther. Pat. 19 (2009) 1361–1376, http://dx.doi.org/10.1517/13543770903207039.
[77] J.W. Kim, J.H. Lee, B.Y. Hwang, S.H. Mun, N.Y. Ko, D.K. Kim, et al., Morin inhibits Fyn kinase in mast cells and IgE-mediated type I hypersensitivity response in vivo, Biochem. Pharmacol. 77 (2009) 1506–1512, http://dx.doi.org/10.1016/j.bcp.2009.01.019.
[78] D. Cosentino-Gomes, N. Rocco-Machado, J.R. Meyer-Fernandes, Cell signaling through protein kinase C oxidation and activation, Int. J. Mol. Sci. 13 (2012) 10697–10721, http://dx.doi.org/10.3390/ijms130910697.
[79] J. Korbecki, I. Baranowska-Bosiacka, I. Gutowska, D. Chlubek, The effect of reactive oxygen species on the synthesis of prostanoids from arachidonic acid, J. Physiol. Pharmacol. 64 (2013) 409–421.
[80] S.J. Han, E.-A. Bae, H.T. Trinh, J.-H. Yang, U.-J. Youn, K.-H. Bae, et al., Magnolol and honokiol: inhibitors against mouse passive cutaneous anaphylaxis reaction and scratching behaviors, Biol. Pharm. Bull. 30 (2007) 2201–2203, http://dx.doi.org/10.1248/bpb.30.2201.
[81] R.G. Glushkov, S.D. Yuzhakov, M.V. Alekseev, O.S. Fominova, V.A. Shorr, G.F. Zhdanov, et al., A new group of 1-and 7-[ω-(benzhydryl-1-alkyl]-3methylxanthine derivatives with antihistamine activity, Pharm. Chem. J. 45 (2011) 1–11, http://dx.doi.org/10.1007/s11094-011-0549-3.
[82] N.H. Kim, H.J. Jeong, H.M. Kim, Theanine is a candidate amino acid for pharmacological stabilization of mast cells, Amino Acids 42 (2012) 1609–1618, http://dx.doi.org/10.1007/s00726-011-0847-9.
[83] C. Chitchumroonchokchai, K.M. Riedl, S. Suksumrarn, S.K. Clinton, A.D. Kinghorn, M.L. Failla, Xanthones in mangosteen juice are absorbed and partially conjugated by healthy adults, J. Nutr. 142 (2012) 675–680, http://dx.doi.org/10.3945/jn.111.156992.
[84] F. Gutierrez-Orozco, M.L. Failla, Biological activities and bioavailability of mangosteen xanthones: a critical review of the current evidence, Nutrients 5 (2013) 3163–3183, http://dx.doi.org/10.3390/nu5083163.

molecules

MDPI

Article

# Chemoinformatic Analysis of Selected Cacalolides from *Psacalium decompositum* (A. Gray) H. Rob. & Brettell and *Psacalium peltatum* (Kunth) Cass. and Their Effects on FcεRI-Dependent Degranulation in Mast Cells

**Jorge Iván Castillo-Arellano [1,2,†], Juan Carlos Gómez-Verjan [3,†], Nadia A. Rojano-Vilchis [2], Myrna Mendoza-Cruz [4], Manuel Jiménez-Estrada [2], Héctor E. López-Valdés [5], Hilda Martínez-Coria [5], Roger Gutiérrez-Juárez [6], Claudia González-Espinosa [1,*], Ricardo Reyes-Chilpa [2,*] and Isabel Arrieta-Cruz [3,*]**

1 Pharmacobiology Department, Center for Research and Advanced Studies of the National Polytechnic Institute, Mexico City 14330, Mexico; jorge.ivan@ciencias.unam.mx
2 Department of Natural Products, Institute of Chemistry, National Autonomous University of Mexico, Mexico City 04510, Mexico; nadiarojano@yahoo.com.mx (N.A.R.-V.); manuelj@unam.mx (M.J.-E.)
3 Department of Basic Research, National Institute of Geriatrics, Ministry of Health, Mexico City 10200, Mexico; carlosverjan132@gmail.com
4 Botanical Garden, Institute of Biology, National Autonomous University of Mexico, Mexico City 04510, Mexico; myrna@ib.unam.mx
5 Division of Research, Faculty of Medicine, National Autonomous University of Mexico, Mexico City 04510, Mexico; helopezv@gmail.com (H.E.L.-V.); hildamcoria@gmail.com (H.M.-C.)
6 Department of Biomedical Sciences, Faculty of High Studies Zaragoza, National Autonomous University of Mexico, Mexico City 09230, Mexico; roger.gutierrez@zaragoza.unam.mx
* Correspondence: cgonzal@cinvestav.mx (C.G.-E.); chilpa@unam.mx (R.R.-C.); arrieta777@mail.com (I.A.-C.); Tel.: +52-55-54832875 (C.G.-E.); +52-55-56224512 (R.R.-C.); +52-55-56551921 (I.A.-C.)
† These authors contributed equally to this work.

Academic Editor: Alessandra Guerrini
Received: 6 November 2018; Accepted: 15 December 2018; Published: 19 December 2018


**Abstract:** Cacalolides are a kind of sesquiterpenoids natural compounds synthesized by *Psacalium decompositum* (A. Gray) H. Rob. & Brettell or *Psacalium peltatum* (Kunth) Cass. Antioxidant and hypoglycemic effects have been found for cacalolides such as cacalol, cacalone or maturine, however, their effects on inflammatory processes are still largely unclear. The main aim of this study was to investigate the biological activities of secondary metabolites from *P. decompositum* and *P. peltatum* through two approaches: (1) chemoinformatic and toxicoinformatic analysis based on ethnopharmacologic background; and (2) the evaluation of their potential anti-inflammatory/anti-allergic effects in bone marrow-derived mast cells by IgE/antigen complexes. The bioinformatics properties of the compounds: cacalol; cacalone; cacalol acetate and maturin acetate were evaluated through Osiris DataWarrior software and Molinspiration and PROTOX server. In vitro studies were performed to test the ability of these four compounds to inhibit antigen-dependent degranulation and intracellular calcium mobilization, as well as the production of reactive oxygen species in bone marrow-derived mast cells. Our findings showed that cacalol displayed better bioinformatics properties, also exhibited a potent inhibitory activity on IgE/antigen-dependent degranulation and significantly reduced the intracellular calcium mobilization on mast cells. These data suggested that cacalol could reduce the negative effects of the mast cell-dependent inflammatory process.

**Keywords:** *Psacalium decompositum*; *Psacalium peltatum*; cacalol; calcium channels; maturin; reactive oxygen species; inflammation

## 1. Introduction

Mast cells are key effectors of type I hypersensitivity reactions (allergies) and other inflammatory reactions, since they secrete numerous pre-formed and *de novo* synthesized pro-inflammatory mediators that promote endothelial activation, smooth muscle contraction and chemotaxis of other immune cells to the site where mast cells are activated [1]. Allergic inflammation differs from other innate inflammatory reactions in that the first are intense, rapid, and can lead to complex life-threatening conditions such as asthma and anaphylaxis [2]. The main mechanism of mast cells activation in allergy is the crosslinking of the high affinity immunoglobulin E (IgE) receptor (FcεRI) with IgE/antigen (IgE/Ag) complexes. FcεRI signal transduction requires the production of reactive oxygen species (ROS) and calcium mobilization, together with the activation of selected kinases to trigger degranulation and the consequent release of histamine, β-hexosaminidase, serotonin and tumor necrosis factor (TNF), in addition to the *de novo* production of prostaglandins, leukotrienes and numerous cytokines [3]. IgE/Ag-dependent degranulation and cytokine synthesis of mast cells have been recognized as relevant pharmacological targets for the control of allergic reactions [4]. However, despite the importance of allergic diseases worldwide, appropriate pharmacological control of mast cells degranulation has not been achieved yet [5]. The FcεRI-dependent degranulation in mast cells is an appropriate model to study the effects of new natural products on inflammation. In fact, some natural compounds have been tested in models of mast cells-dependent inflammation; for example, we have recently described that the xanthone jacareubin, a natural product from the tropical tree *Calophyllum brasiliense* displays potent anti-allergic and anti-inflammatory activities in degranulation of mouse mast cells [6].

On the other hand, *Psacalium decompositum* (A. Gray) H. Rob. & Brettell, belonging from Asteraceae family is a wild herb from the pine forests of Northwest Mexico, commonly known as "matarique" and used locally as a remedy in folk medicine. The Raramuri people and peasants of the State of Chihuahua, use a decoction of the roots and rhizome of this species for the treatment of rheumatic disorders, pain, hepatic and renal colic, neuralgia, ulcers and colds. The roots and rhizome contain a number of sesquiterpenoids cacalolides such as cacalol, cacalone, epicacalone, maturine, 3-hydroxycacalolide, epi-3-hydroxycacalolide [7–9]. Additionally, *P. decompositum* is currently used by the urban populations of Mexico as an antidiabetic remedy; in fact, several studies have examined the hypoglycemic properties of cacalol and other cacalolides [8]. Interestingly, the decoction of the roots from *P. decompositum* has shown clear hypoglycemic effects in healthy mice and in transtiently hyperglycemic rabbits [7]. Besides, polysaccharide fractions obtained from the freeze-dried water extract from *P. decompositum* significantly reduced fasting blood glucose in mild alloxan-diabetic mice suggesting that the aqueous fraction, containing fructan-type oligosaccharides, is responsible for the hypoglycemic effects observed [8,10]. Recently, treatment with a fructooligosaccharides fraction from *P. decompositum* was shown to significantly reduce cholesterol, triglycerides, IL-6, IFN-γ, MCP-1, IL-1β and VEGF levels, as well as a decrease in body weight in an animal model of obesity. These observations suggest novel anti-inflammatory and hypolipidemic properties of the fructooligosaccharides fraction [11]. Meanwhile, the hexane extract and two compounds, cacalol and cacalone isolated from *P. decompositum*, have been shown to inhibit inflammation in the carrageenan-induced edema of the rat paw; these compounds also exhibited a dose-dependent anti-inflammatory activity in the TPA-induced mouse ear edema. In these models cacalone had the most prominent activity [12].

In medicinal plant markets of Mexico City, *Psacalium peltatum* (Kunth) Cass., is a common substitute for *P. decompositum*, because the former grows in the nearby pine forests. *P. peltatum* is also kown as "matarique" and the roots and rhizome also contain cacalolides, such as maturin, maturin acetate, and maturinin, but not cacalol or cacalone. Few studies have shown the potential effects of maturine acetate in the inflammatory process; maturine acetate reduces the production of pro-inflammatory cytokines (TNF-α and IL-1β) by lypopolysaccharide (LPS)-activated peritoneal macrophages. Maturine acetate also stimulates the proliferation of murine macrophages and

splenocytes, induces lysosomal enzyme activity, pinocytosis and NK cell activity, as well as increases the release of IL-2, IL-15 and IFN-γ in immunosuppressed mice, showing relevant immunostimulatory activities [13,14].

Despite all the available literature, there is currently no information about the physicochemical, pharmacokinetic, medicinal chemistry and toxicoinformatic properties of some cacalolides. Thus, we aimed to examine the biological activities of secondary metabolites from *P. decompositum* and *P. peltatum* through two not mutually exclusive approaches: (1) bioinformatic analysis: chemoinformatic and toxicoinformatic; and (2) pharmacological investigations based on ethnomedical use.

Chemoinformatic and toxicoinformatic have demonstrated to be reasonable alternatives for the early estimation of absorption, distribution, metabolism, excretion and toxicity (ADMET) properties and represent substantial time and cost reductions during the drug discovery phase [15]. This is the reason why in recent years several groups have used this type of computational methodologies to improve and accelerate drug design.

With the aim of providing detailed information about of the compounds, in this work we performed a chemoinformatic and toxicoinformatic analysis of four cacalolides: cacalol, cacalol acetate, cacalone and maturin acetate isolated from *P. decompositum* and *P. peltatum*. Besides, we described a potential anti-inflammatory/anti-allergic activity of these compounds on mast cells not previously reported. Furthermore, we postulate a possible molecular mechanism for the inhibition of inflammation by these compounds.

## 2. Results

### *2.1. Chemoinformatic and Toxicoinformatic Analysis of Cacalolides from P. decompositum and P. peltatum*

The bioinformatic properties of the cacalolides: cacalol, cacalone, cacalol acetate and maturin acetate (Figure 1) were examined. Among all cacalolides only cacalol displayed high water solubility conferring it some advantages such as a good drug gastrointestinal absorption and adequate blood-brain barrier penetration. According to Lipinski, Ghose and Lead-likenes classification, cacalol had the best score regarding bioavailability, biosynthesis and pharmacokinetics. Interestingly, all studied cacalolides exhibited a very low toxicity and in no case mutagenic or tumorigenic effects were detected (Table 1).

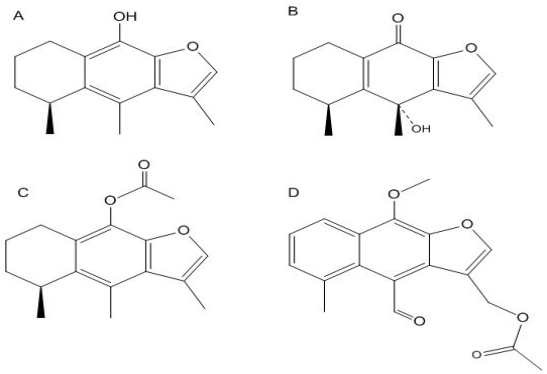


**Figure 1.** Chemical structures of cacalolides from two species of matarique (*P. decompositum* and *P. peltatum*): (**A**) cacalol; (**B**) cacalone; (**C**) cacalol acetate; (**D**) maturin acetate.

**Table 1.** Estimated physicochemical, pharmacokinetic, medicinal chemistry and toxicoinformatic properties of cacalolides *.

| | | Cacalol | Cacalone | Cacalol Acetate | Maturin Acetate |
|---|---|---|---|---|---|
| **Physicochemical Properties** | Log P | 3.65 | 2.56 | 3.42 | 3.20 |
| | Log S | −5.56 | −4.04 | −4.34 | −5.09 |
| | TPSA | 33.37 A | 50.44 A | 39.44 A | 65.74 A |
| | MW | 230.30 g/mol | 246.30 g/mol | 272.34 g/mol | 312.34 g/mol |
| | RB | 0 | 0 | 2 | 5 |
| | BD | 1 | 1 | 0 | 0 |
| | BA | 2 | 3 | 3 | 5 |
| | Molar refractivity | 70.64 | 68.83 | 78.26 | 86.20 |
| **Pharmacokinetic Properties** | GI absorption | High | High | High | High |
| | BBB permeable | Yes | Yes | Yes | Yes |
| | P-gp substrate | Yes | Yes | No | No |
| | CYP1A2 inhibitor | Yes | No | No | Yes |
| | CYP2C19 inhibitor | Yes | Yes | Yes | Yes |
| | CYP2C9 inhibitor | No | No | No | Yes |
| | CYP2D6 Inhibitor | No | No | No | No |
| | CYP3A4 inhibitor | No | No | No | Yes |
| | Log Kp (Skin permeation) | −4.62 cm/s | −6.14 cm/s | −5.79 cm/s | −5.99 cm/s |
| **Medicinal Chemistry Properties** | Lipinski | Yes | Yes | Yes | Yes |
| | Ghose | Yes | Yes | Yes | Yes |
| | Bioavailability Score | 0.55 | 0.55 | 0.55 | 0.55 |
| | Lead-likeness | No, 2 Violations | No, 1 violation | Yes | Yes |
| | Synthetic accessibility | 2.75 | 4.32 | 4.72 | 3.77 |
| **Toxicoinformatic Properties** | Toxicity Class | 5 | 4 | 5 | 5 |
| | Mutagenic | None | None | None | None |
| | Tumorigenic | None | None | None | None |
| | Irritant | None | None | High | None |
| | Reproductive effects | None | None | None | None |
| | Possible Toxic Target | None | None | None | Amine oxidase prostaglandin G/H synthase 1 |
| | Toxic Fragments | None | None | None | None |

* Theoretical values. Abbreviations: GI—Gastrointestinal absorption; BBB—Blood brain barrier; P—gp-Glycoprotein P; GPCR—Receptor of protein G; MW—Molecular weight; RB—Rotatable bonds; BD—Number of H donors; BA—Number of H-bond acceptors; TPSA—Total polar surface area.

Because cacalol showed interesting physicochemical, pharmacokinetic and toxicoinformatic properties among all analyzed cacalolides, we next attempted to indentify its most important biological targets through the use of an in silico approach. We found that some molecules involved in the regulation of the immune system could potentially interact with cacalol including: Fc epsilon receptor, MAPK signaling, PI3K-AKT pathway and nerve growth factor (Table 2).

**Table 2.** Enrichment analysis (GO and Pathway) of the main 50 targets that interact with cacalol using network pharmacology approaches *.

| Compound | Pathway or GO Term | Count | *p*-Value | Data Base |
|---|---|---|---|---|
| Cacalol | Innate immune system (hsa-168249) | 24 | $2.43 \times 10^{-20}$ | Reactome |
| | VEGFA-VEGFR2 pathway (hsa-4420097) | 12 | $4.42 \times 10^{-12}$ | Reactome |
| | Fc epsilon receptor signaling (hsa-2454202) | 12 | $4.42 \times 10^{-12}$ | Reactome |
| | PI3K-Akt pathway (hsa04151) | 12 | $4.91 \times 10^{-12}$ | KEGG [1] |
| | MAPK signaling pathway (hsa04010) | 11 | $7.89 \times 10^{-12}$ | KEGG [1] |
| | Protein kinase activity (GO:0004672) | 26 | $1.58 \times 10^{-31}$ | GO-MF [2] |

* Theoretical values. [1] Kyoto Encyclopedia of genes and genomes. [2] Gene Ontology-Molecular Function.

## 2.2. Experimental Validation of Anti-Inflammatory/Anti-Allergic Activity

To validate the anti-inflammatory/anti-allergic properties of cacalol that were predicted by bioinformatic analysis, we performed in vitro pharmacological assays using a very well established IgE/Antigen-dependent degranulation cellular model in bone marrow-derived mast cells (BMMCs).

### 2.2.1. Cacalolides Inhibit Mast Cell Degranulation Activated by FcεRI Triggering In Vitro

In order to validate the potential inhibitory activity of tested cacalolides, their effect on FcεRI-dependent activation of BMMCs was evaluated, taking advantage of this cellular model that has been widely utilized to determine the potential anti-inflammatory activity of a number of natural and synthetic compounds [4,5].

Among the four compounds evaluated, cacalol showed the highest inhibitory activity on IgE/Antigen-dependent degranulation. Cacalol, at 30 μM, produced an 88% inhibition of degranulation, followed by maturine acetate and cacalol acetate which, at 100 μM concentrarion, caused an inhibition of almost 100% and 85%, respectively. Finally, cacalone produced a blockage close to 100% at a concentration of 300 μM (Figure 2).

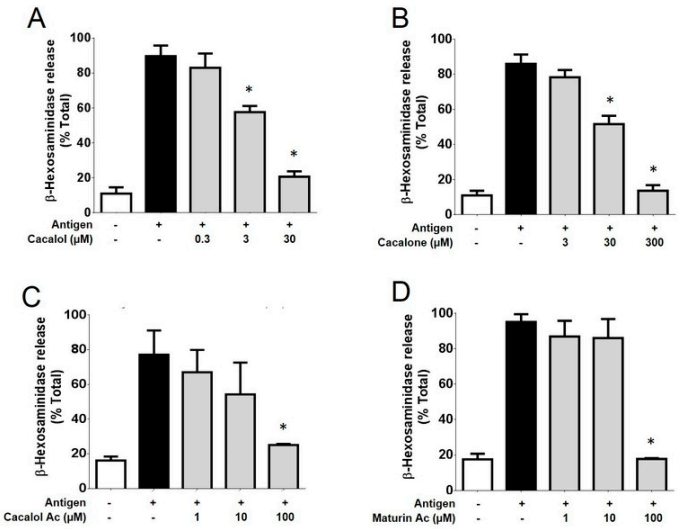


**Figure 2.** Cacalolides inhibit degranulation stimulated by antigen in bone marrow-derived mast cells. Effect of cacalol (**A**) cacalone (**B**) cacalol acetate (**C**) and maturine acetate (**D**) pre-treatment on DNP-HSA-induced degranulation, $n = 3$. * $p \leq 0.05$.

### 2.2.2. Cacalol Interfered with FcεRI-Induced Intracellular Calcium Mobilization

Cacalol caused a 40% inhibition of the intracellular calcium $[Ca^{2+}]i$ mobilization required for IgE/antigen-induced degranulation at concentrations between 0.3 and 3 μM, while at 30 μM it almost completely inhibited $[Ca^{2+}]i$ mobilization in bone marrow-derived mast cells (Figure 3).

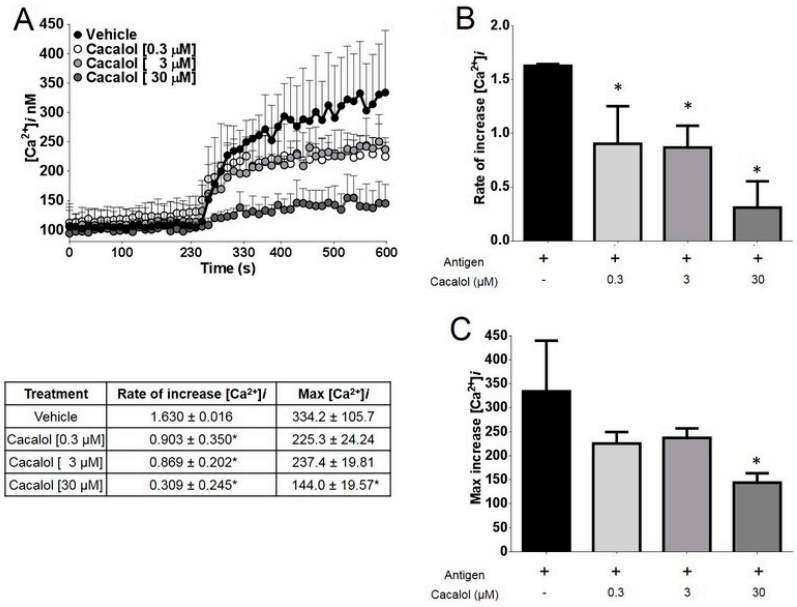


| Treatment | Rate of increase $[Ca^{2+}]i$ | Max $[Ca^{2+}]i$ |
|---|---|---|
| Vehicle | 1.630 ± 0.016 | 334.2 ± 105.7 |
| Cacalol [0.3 μM] | 0.903 ± 0.350* | 225.3 ± 24.24 |
| Cacalol [ 3 μM] | 0.869 ± 0.202* | 237.4 ± 19.81 |
| Cacalol [30 μM] | 0.309 ± 0.245* | 144.0 ± 19.57* |

**Figure 3.** Cacalol inhibits intracellular calcium influx stimulated by FcεRI receptor in bone marrow-derived mast cells. (**A**) Representative trace of intracellular calcium rise in cells pre-treated with either vehicle or different concentrations of cacalol; (**B**) Rate of increase of $[Ca^{2+}]i$; (**C**) Maximum concentration of $[Ca^{2+}]i$. $n = 3$. * $p \leq 0.05$.

### 2.2.3. Cacalol Interferes with ROS Production Induced by IgE/Ag Complexes

Cacalol at concentrations between 30 and 300 μM almost completely inhibited the production of ROS in bone marrow-derived mast cells challenged with IgE/Ag complexes, compared to the reference antioxidant Trolox (5 mM) (Figure 4).

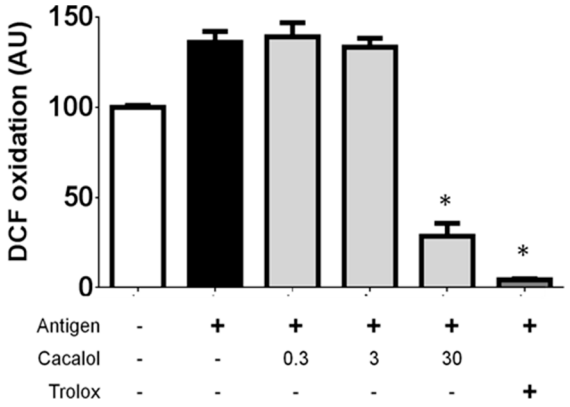


**Figure 4.** Cacalol inhibits FcεRI-triggered degranulation in BMMCs as the antioxidant Trolox does. * $p \leq 0.05$.

## 3. Discussion

Natural products have proven to be a rich source in the search and development of new drugs, either used directly or as inspiring molecules in drug development. Many of them are already in use for treatment of several diseases all over the world [16].

In the present study, we have used computational tools to perform a preliminary examination of the main pharmacokinetic, medicinal chemistry and toxicoinformatic properties of selected cacalolides in order to further assess their therapeutic potential. The use of computer-aided drug discovery tools has been shown to save time and resources, and to facilitate the drug discovery process [17]. First at all, none of the four compounds examined in this study yielded any toxicity parameter derived from the chemoinformatic analysis. There are no toxicological studies reported previously for these cacalolides, except for a recent in vitro study demonstrating that cacalol from *Cacalia delphiniifolia* (an Asian herbal plant) failed to induce apoptosis in human mammary epithelial cells. In contrast, this cacalolide induced apoptosis in breast cancer cells and displayed cytotoxic effects in this cellular model [18].

Our analysis also revealed that the compounds directly interacted with signaling pathways associated with the immune system including the FcεRI receptor pathway, the VEGF receptor (VEGFR2), and intracellular targets such as the activation of the PI3K-Akt kinases of the MAPKs kinases and the activation of other non-specific protein kinases.

In vitro results on FcεRI dependend-degranulation of mast cells indicate that cacalol had a higher activity than other similar sesquiterpene compounds tested. This is probably due to its unstable chemical structure, which may allow for quick decomposition into other more stable compounds by assimilating electrons derived from ROS [19] produced by FcεRI activation. The activation of membrane calcium channels linked to the Stored Operated Calcium Entry (SOCE) in mast cells may need the activation of Fc-receptors in multiple cell types of the immune system [20,21]. Interestingly, cacalol acetate, a more stable derivative generated by synthetic chemical acetylation of cacalol, is showed less inhibitory activity in the mast cells degranulation assay. In the same way, maturin acetate, a naturally occurring compound of "matarique" (*P. peltatum*), also stable under our experimental conditions, displayed an activity similar to that of cacalol acetate. This low activity was probably due to the fact that the acetyl group in both compounds conferred more stability to these molecules, which prevents them from accepting unpaired electrons from ROS [14,22]. Finally, although cacalone has been described as a more potent anti-oxidant and anti-inflammatory compound than even cacalol in the in vivo model of skin inflammation induced by TPA [12], this compound displayed poor anti-inflammatory activity in mast cells. These contrasting results are probably explained by the fact that the two models evaluated the inflammation produced by different immune cells and that cacalone was a 1:1 mixture with its putatively inactive epicacalone isomer [23]. Nevertheless, cacalol is not the only sesquiterpene possessing good inhibitory activity in the mast cell degranulation assay triggered by the FcεRI receptor. Other sesquiterpenes reported in the literature such as parthenolide, also inhibits the degranulation of mast cells by reducing the activation of NFκB and Fyn-dependent microtubule formation [24]. Additional sesquiterpenes possessing inhibitory activity similar to cacalol include deacetyleupaserrin, (3*S*,6*R*,7*R*,8*R*)-3-hydroxy-8-acetoxy-sarracenyloxygermacra-1(10),4,11(13)-trien-6,12-olide, (3*S*,6*R*,7*R*,8*R*)-3-hydroxy-8-(2′-methyl-butyroyloxy)-14-oxomelampa-1(10), 4-dien-6,12-olide and eupaformosanin, are mechanistically associated to the inhibition of p38 and Akt phosphorylation as well as to the partial inhibition of intracellular calcium mobilization ($[Ca^{2+}]i$) [25].

## 4. Materials and Methods

### 4.1. Reagents

All organic solvents were purchased from J.T. Baker (Radnor, PA, USA). 2′7′-dichlorofluorescein diacetate (DCF-DA), dinitrophenyl-human seric albumin (DNP-HSA), igepal, and indomethacin were obtained from Sigma-Aldrich (St. Louis, MO, USA). The antioxidant Trolox was from Calbiochem

(San Diego, CA, USA), FURA-2AM from Thermo Fisher Scientific (Waltham, MA, USA). Finally, cacalol, cacalone and maturin acetate was purified as described below.

### *4.2. Isolation and Purification of Cacalolides*

Cacalol and cacalone were isolated and purified from *P. decompositum* roots as previously described [26]. Cacalol acetate: acetylation of cacalol to obtain cacalol acetate was carried out as previously reported [27]. Maturin acetate was purified as described [13]. The compounds' identities were corroborated by their $^{1}$H-NMR or $^{13}$C-NMR spectral data (see the Supplementary) obtained on a Bruker Avance III 300 MHz (Cambridge Isotope, Tewksbury, MA, USA), or High Performance Liquid Chromatography (HPLC) performed an Agilent 1200 Series Binary SL (Agilent; Santa Clara, CA, USA) using a Eclipse Plus C18, 2.1 × 100 mm, 3.5µm (Agilent; Santa Clara, CA, USA), Detector: Waters 2996 UV-Vis Photo Diode Array (Waters, Mildford, MA, USA) or Gas Chromatography coupled to Mass Spectrometry (GC-MS) was performed with a JEOL GCmate (Peabody, MA, USA) were compared with those reported in the literature, establishing that four compounds were in fact cacalol, cacalol acetate, cacalone and maturin acetate.

### *4.3. Chemical Characterization*

*Cacalol*: $^{1}$H-NMR (300 MHz, $CHCl_3$, δ ppm) 7.24–7.22 (m, 1H), 4.78 (s, 1H), 3.24–3.01 (m, 1H), 2.98 (dd, *J* = 17.3, 4.9 Hz, 1H), 2.60 (m, 1H), 2.53 (s, 3H), 2.38 (d, 3H), 1.95–1.72 (m, 4H), 1.20–1.19 (d, *J* = 7.0 Hz, 3H); GC-MS shown peak with purity 93% at 23.9 min, this peak corresponded according to MS with the molecular weight of cacalol EI + MS *m*/*z* 230 ($M^+$, 58), 215 (100) coinciding with what was previously reported [28].

*Cacalol acetate*: $^{1}$H-NMR (300 MHz, $CHCl_3$, δ ppm) 7.24–7.23 (d, 1H), 3.29–3.22 (m, 1H), 2.87–2.78 (m, 1H), 2.57 (s, 3H), 2.39 (s, 3H), 2.38–2.37 (d, 3H), 1.94–1.76 (m, 4H), 1.21–1.18 (d, 3H); and $^{13}$C-NMR (75 MHz, ($CHCl_3$, δ ppm) 168.65, 145.18, 141.42, 135.43, 131.42, 127.09, 126.86, 124.93, 116.74, 29.97, 28.92, 23.43, 21.38, 20.49, 16.59, 14.26, 11.27.

*Cacalone-epicacalone* mixture (CEM): $^{1}$H-NMR (300 MHz, $CHCl_3$) 7.25 (d, 1H), 3.10–3.06 (m, 1H), 2.87–2.84 (m, OH), 2.49–2.44 (m, 1H), 2.19–2.18 (d, 3H), 1.73–167 (m, 5H), 1.58 (s, 3H), 1.29–1.27 (d, 3H); GC-MS shown two peak with purity 78.8% at 26.3 and 27 min, these peaks corresponded according to MS to the molecular weight of cacalone and epi-cacalone isomer. EI + MS *m*/*z* 246 ($M^+$, 45 and 60), 231 (70 and 90), 204 (20 and 40), 191 (100) coinciding with what was previously reported [23,29]. The residual peaks may represent cacalol and radulifolin B based on their MS spectra.

*Maturin acetate*: $^{1}$H-NMR (300 MHz, $CHCl_3$, δ ppm) 11.01 (s, 1H), 8.32–8.29 (dd, 1H), 7.84 (s, 1H), 7.43–7.41 (d, 2H), 5.34 (s, 2H), 4.45 (s, 3H), 2.80 (s, 3H), 2.09 (s, 3H). HPLC shown one peak with purity 99% at 29.2 min, according to MS this peak corresponded to the molecular weight of maturin acetate. EI + MS *m*/*z* 312 ($M^+$, 100), 254 (90) coinciding with what was previously reported [13].

### *4.4. Chemoinformatic Analysis*

To calculate the bioinformatics properties of the compounds we used Osiris DataWarrior (DataWarrior V4.7.2, Idorsia Pharmaceuticals Ltd., Allschwil, Switzerland), it is a freeware software that calculates lipophilicity, expressed as compound log P (clogP), solubility in water, expressed as logS, molecular weight, drug-likeness indices and drug score; moreover, toxicological properties of the compounds may also be shown. Osiris was used to assess the possible toxicity risks as well as the aforementioned biophysical properties of cacalol, cacalol acetate, cacalone, and maturin acetate. The description of a computational medicinal chemistry can be found in a previous report [30].

### *4.5. Properties Calculated Using Molinspiration and PROTOX*

CLogP (octanol/water partition coefficient) is calculated by the methodology developed by Molinspiration as the sum of fragment-based contributions and correction factors. Molecular polar surface area (PSA), topological polar surface area (TPSA) were calculated based in the sum of

fragmented contributions. Molecular PSA has been shown to be a very good descriptor characterizing drug absorption, including intestinal absorption, bioavailability, CaCo-2 permeability, blood-brain barrier penetration, while rodent oral toxicity can be estimated by using the PROTOX web server. Based on toxic classes defined according to the globally harmonized system of classification for the labeling of chemicals six classes exist: Class I is fatal if swallowed ($LD_{50}$ < 5 mg/kg), Class II is fatal if swallowed ($LD_{50}$ < 50 mg/Kg), Class III toxic if swallowed ($LD_{50}$ < 300 mg/Kg), Class IV harmful if swallowed ($LD_{50}$ < 2000 mg/Kg), Class V may be harmful if swallowed ($LD_{50}$ < 5000 mg/Kg), Class VI non-toxic ($LD_{50}$ > 5000 mg/Kg). The PROTOX web server was used to perform an in silico prediction of rodent oral toxicity according to The European Parliament and Council of the European Union Regulation (REACH) [31].

### *4.6. Properties Calculated Using Swiss ADME*

Swiss Bioinformatic Institute possesses a web server that calculates several ADME properties that could help to delve in the pharmaceutical properties of cacalol, cacalol acetate, cacalone, and maturin acetate in order to determine its potential to reach clinics. The complete description of the computational medicinal chemistry algorithm was published [32]. We use consensus Log P from 5 different predictions (iLOGP, XLOGP3, WLOGP, MLOGP, Silicos-IT); Log S (Silicos-IT) which is fragmental method calculated; Ghose improvement for the Lipinski rule of Five [33], and synthetic accessibility from 1 very easy to 10 very difficult, implemented in the software.

### *4.7. Network Pharmacology*

Since cacalol was the most interesting compound we wanted to identify the most important biological targets and pathways that could interact with such compound through the use of a network pharmacology approach. Predictive models were used including DRAR-CPI [34] and SEA [15]. Enrichment Analysis for Targets: Analysis of network interaction related to the first 50 targets that interact with each compound was performed using Comparative Toxicogenomics Database (CTD) [35]. The main molecular function as well as the main KEGG and Reactome pathways along with related diseases was determined. The most significantly enriched terms ($p < 0.05$, $p$-values was corrected using the Benjamini-Hochberg procedure) were listed in Table 2.

### *4.8. Animals*

C57BL/6J male mice, 25–30 g of body weight, stock number 000664, were purchased from The Jackson Laboratory (Bar Harbor, ME, USA). Mice were kept in sterile conditions, under a 12 h dark/light cycle, with free access to water and food at the Unit for the Production of Experimental Animals Laboratory (UPEAL) from Center for Research and Advanced Studies of the National Polytechnic Institute (Cinvestav) at Mexico City. All animal procedures were approved by the Cinvestav Institutional Ethics Committee (protocol number: 074-13).

### *4.9. Bone Marrow-Derived Mast Cells Isolation and Culture*

Bone marrow-derived mast cells (BMMCs) were isolated from C57BL6/J mice, as described [36]. Briefly, bone marrow was extracted from the tibias and femurs of mice and cultured in RPMI 1640 (Sigma-Aldrich, St. Louis, MO, USA) medium supplemented with IL-3 (10 ng/mL; PeproTech, Rocky Hill, NJ, USA) and 10% FBS, 100 UI/mL penicillin, 100 mg/mL streptomycin, 50 mM 2-ME, and 13 nonessential amino acids (Invitrogen, Carlsbad, CA, USA). Cultures were maintained for 4 weeks, and media were changed every 5–7 days. Subsequently, BMMCs differentiation was assessed by detecting the expression of the FcεRI receptor in the plasma membrane (by flow cytometry) and by evaluating the release of β-hexosaminidase after IgE/Ag stimulation [37]. Only cultures that were 98% positive for FcεRI receptor expression and showing a dose response of β-hexosaminidase release after IgE/Ag addition were used in the study. For each experiment, BMMCs were sensitized with 100 ng/mL a monoclonal anti-DNP IgE (clone SPE-7; (Sigma-Aldrich, St. Louis, MO, USA) for 24 h at 37 °C, because

this condition was shown to increase BMMCs' responsiveness to antigen. Routinely, after sensitization, cells were collected and resuspended in fresh culture medium or Tyrode's BSA buffer (135 mM NaCl, 5 mM KCl, 1 mM $MgCl_2$, 1.8 mM $CaCl_2$, 5.6 mM glucose, 0.5 g/L BSA, and 20 mM HEPES pH 7.4 for calcium experiments. For the ROS production experiments, sensitized cells were washed and resuspended in Tyrode's Buffer without BSA.

### *4.10. Solubilization of Cacalol, Cacalol Acetate, Cacalone and Maturin Acetate for Experiments*

For in vitro testing of the effects of cacalol, cacalol acetate, cacalone and maturine acetate on mast cells, the compound was dissolved in 0.1% DMSO which was also used as vehicle in all experiments.

### *4.11. β-Hexosaminidase Degranulation Assay*

Two million IgE-sensitized cells were centrifuged at 500× *g* during 5 min and suspended in 1 mL Tyrode's/BSA buffer of the following composition: 20 mM HEPES pH 7.4, 135 mM NaCl, 5 mM KCl, 1.8 mM $CaCl_2$, 1 mM $MgCl_2$, 5.6 mM glucose and 0.05% bovine serum albumin. Separate groups of cells were treated with vehicle, 3, 30 or 300 µM of cacalolides for 15 min and then stimulated with antigen (27 ng/mL DNP-HSA) during 30 min at 37 °C. After this treatment, cells were placed on ice for 2 min and centrifuged at 12,000× *g* for 10 min at 4 °C. Sixty µL of supernatant or (20 µL of Triton-treated cell pellet) were placed in an ELISA plate containing 40 µL of 1mM *p*-nitrophenyl-*N*-acetyl-β-D-glucosaminide (*p*-NAG), and incubated for one hour at 37 °C before the addition of 120 µL of "stop" solution ($Na_2CO_3$ 0.1M/$Na_2HCO_3$ 0.1M). β-hexosaminidase release was quantified by spectrophotometry in an ELISA plate reader (Tecan Sunrise, Männedorf, Switzerland) at 405 nm, as described [38].

### *4.12. Calcium Mobilization Intracellular Determination ([$Ca^{2+}$]i)*

Intracellular calcium concentrations [$Ca^{2+}$]*i* were measured in IgE-sensitized BMMCs. Briefly, cells were collected and suspended in Tyrode's/BSA buffer with 5 µM Fura 2-AM for 30 min at 37 °C to load the cells. Ten million of fura 2-AM-loaded BMMCs were suspended in 2 mL Tyrode's/BSA buffer and placed in the cuvette. We monitored the fluorescence in intervals of 1.16 s until we reached 400 s on a spectrofluorometer (Fluoromax 3 Jobin Yvon, Horiba, Fukuoka, Japan) with a wavelength of 340 nm and 380 nm for excitation and 510 nm for emission respectively. Calcium concentration was calculated using the equation $[Ca^{2+}]i = Kd\ [(F - F_{min})/(F_{max} - F)]$, where Kd is the dissociation constant of calcium-Fura2AM (wavelength), $F_{max}$ is fluorescence maximum concentration obtained by lysis of all cells with Triton [concentration] and $F_{min}$ is the minimum fluorescence obtained by the addition of EDTA [concentration]. F was the current fluorescence of the sample. Basal fluorescence was recorded during 100 s prior to challenge with DNP-HSA antigen (27 ng/mL). [$Ca^{2+}$]*i* was calculated with the parameters and equation described by Grynkiewicz [39]. In some experiments, we used BMMCs suspended in $Ca^{2+}$-free Tyrode's/BSA buffer and then added 1.8 mM $CaCl_2$ (final concentration) at 200 s.

### *4.13. ROS Production and Antioxidant Activity*

The cells were sensitized with IgE for 24 h prior to challenge. 2 × $10^6$ BMMC/mL were used in 1.5 mL flat top Eppendorff tubes for each treatment. They were preincubated 15 min prior to stimulating the cells with cacalolides. Trolox was used as a positive control of the antioxidant activity [40,41]. Antigen challenge (27 ng/mL of DNP-HSA) was performed for 15 min. DCF-DA [10 µM] was added for 15 min before terminating each of the stimuli, then the tubes were centrifuged at 4 °C for 5 min, the supernatant was removed and 300 µL of igepal 0.1% at 37 °C, was added by vigorous pipetting to break the cell button. The tubes were then centrifuged for 5 min at 4 °C and 200 µL were placed in a 96-well plate and read at a wavelength of 488 nm and 565 nm for excitation and emission in a model FLx800 luminometer (Biotek, Winooski, VT, USA) for 1 h, taking readings every 15 min [42].

### *4.14. Statistical Analysis*

All data were represented as percentage mean +/− standard error of the mean using the GraphPad Prism® software version 6 (GraphPad Software; La Jolla, CA, USA). Statistical analysis was performed through one way analysis of variance (ANOVA) followed by Dunnett test to compare several groups with a control. Additionally analysis with Student's t-test and Kolmogorov-Smirnoff's test were performed. Values of $p \leq 0.05$ were considered statistically significant.

## 5. Conclusions

In this work we confirmed that bioinformatics tools are useful to corroborate the validity of ethnobotanical information and also to improve decision making in the identification of compounds derived from natural products with pharmacological and pharmaceutical potential. Cacalol, a molecule possessing very specific medicinal pharmacological properties and superior to those of other similar sesquiterpenes still requires more research to ensure that it remains stable under the usual environmental conditions.

**Supplementary Materials:** Nuclear Magnetic Resonance (NMR) and Gas Chromatography–Mass Spectrometry (GC-MS) of cacalol, cacalol acetate, cacalone and maturine acetate.

**Author Contributions:** Conceptualization, J.I.C.-A., C.G.-E., R.G.-J., R.R.-C. and I.A.-C.; Data curation, J.C.G.-V., R.R.-C. and I.A.-C.; Formal analysis, J.I.C.-A., J.C.G.-V., N.A.R.-V., M.M.-C., M.J.-E., H.E.L.-V., H.M.-C., R.R.-C. and I.A.-C.; Funding acquisition, C.G.-E., R.R.-C. and I.A.-C.; Investigation, R.G.-J., R.R.-C. and I.A.-C.; Methodology, J.I.C.-A., J.C.G.-V., N.A.R.-V., M.M.-C., M.J.-E., H.E.L.-V., H.M.-C., C.G.-E. and R.G.-J.; Resources, M.M.-C., M.J.-E., H.E.L.-V., H.M.-C., C.G.-E., R.G.-J., R.R.-C. and I.A.-C.; Software, J.C.G.-V.; Supervision, C.G.-E., R.R.-C. and I.A.-C.; Writing–original draft, J.I.C.-A. and J.C.G.-V.; Writing–review & editing, H.E.L.-V., H.M.-C., C.G.-E., R.G.-J., R.R.-C. and I.A.-C.

**Funding:** This research was funded in part by National Council of Science and Technology from Mexico, grant number: [FOSISS-262444] to I.A.-C.; grant number: [Conacyt-ANR-188565] and [Conacyt-FC1122] to C.G.-E.; and by Secretariat of Science, Technology and Innovation of Mexico City, grant number: [INGER-DI-CRECITES-002-2018] to I.A.-C.

**Acknowledgments:** The authors thank to Alfredo Ibarra Sánchez from Cinvestav for his expert technical assistance in the preparation of mast cells.

**Conflicts of Interest:** The authors declare no conflict of interest.

## References

1. Mukai, K.; Tsai, M.; Saito, H.; Galli, S.J. Mast cells as sources of cytokines, chemokines and growth factors. *Immunol. Rev.* **2018**, *282*, 121–150. [CrossRef] [PubMed]
2. Beghdadi, W.; Madjene, L.C.; Benhamou, M.; Charles, N.; Gautier, G.; Launay, P.; Blank, U. Mast cells as cellular sensors in inflammation and immunity. *Front. Immunol.* **2011**, *2*, 1–15. [CrossRef] [PubMed]
3. Blank, U.; Madera-Salcedo, I.K.; Danelli, L.; Claver, J.; Tiwari, N.; Sánchez-Miranda, E.; Vázquez-Victorio, G.; Ramírez-Valadez, K.A.; Macias-Silva, M.; González-Espinosa, C. Vesicular trafficking and signaling for cytokine and chemokine secretion in mast cells. *Front. Immunol.* **2014**, *5*, 1–18. [CrossRef] [PubMed]
4. Singh, J.; Shah, R.; Singh, D. Targeting mast cells: Uncovering prolific therapeutic role in myriad diseases. *Int. Immunopharmacol.* **2016**, *40*, 362–384. [CrossRef]
5. Zhang, T.; Finn, D.F.; Barlow, J.W.; Walsh, J.J. Mast cell stabilisers. *Eur. J. Pharmacol.* **2016**, *778*, 158–168. [CrossRef] [PubMed]
6. Castillo-Arellano, J.I.; Guzmán-Gutiérrez, S.L.; Ibarra-Sánchez, A.; Hernández-Ortega, S.; Nieto-Camacho, A.; Medina-Campos, O.N.; Pedraza-Chaverri, J.; Reyes-Chilpa, R.; González-Espinosa, C. Jacareubin inhibits FcεRI-induced extracellular calcium entry and production of reactive oxygen species required for anaphylactic degranulation of mast cells. *Biochem. Pharmacol.* **2018**, *154*, 344–356. [CrossRef]
7. Alarcón-Aguilar, F.J.; Roman-Ramos, R.; Jimenez-Estrada, M.; Reyes-Chilpa, R.; Gonzalez-Paredes, B.; Flores-Saenz, J.L. Effects of three Mexican medicinal plants (Asteraceae) on blood glucose levels in healthy mice and rabbits. *J. Ethnopharmacol.* **1997**, *55*, 171–177. [CrossRef]

8. Alarcón-Aguilar, F.J.; Jimenez-Estrada, M.; Reyes-Chilpa, R.; Gonzalez-Paredes, B.; Contreras, C.C.; Roman-Ramos, R. Hypoglycemic activity of root water decoction, sesquiterpenoids, and one polysaccharide fraction from *Psacalium decompositum* in mice. *J. Ethnopharmacol.* **2000**, *69*, 207–215. [CrossRef]
9. Romo de Vivar, A.; Pérez-Castorena, A.L.; Arciniegas, A.; Villaseñor, J.L. Secondary metabolites from Mexican species of the tribe *Senecioneae* (Asteraceae). *J. Mex. Chem. Soc.* **2007**, *51*, 160–172.
10. Jimenez-Estrada, M.; Merino-Aguilar, H.; Lopez-Fernandez, A.; Rojano-Vilchis, N.A.; Roman-Ramos, R.; Alarcon-Aguilar, F.J. Chemical characterization and evaluation of the hypoglycemic effect of fructooligosaccharides from *Psacalium decompositum*. *J. Complement. Integr. Med.* **2011**, *8*, 1413–1423. [CrossRef]
11. Merino-Aguilar, H.; Arrieta-Baez, D.; Jiménez-Estrada, M.; Magos-Guerrero, G.; Hernández-Bautista, R.J.; del Susunaga-Notario, A.C.; Almanza-Pérez, J.C.; Blancas-Flores, G.; Román-Ramos, R.; Alarcón-Aguilar, F.J. Effect of fructooligosaccharides fraction from *Psacalium decompositum* on inflammation and dyslipidemia in rats with fructose-induced obesity. *Nutrients* **2014**, *6*, 591–604. [CrossRef] [PubMed]
12. Jimenez-Estrada, M.; Chilpa, R.R.; Apan, T.R.; Lledias, F.; Hansberg, W.; Arrieta, D.; Aguilar, F.A. Anti-inflammatory activity of cacalol and cacalone sesquiterpenes isolated from *Psacalium decompositum*. *J. Ethnopharmacol.* **2006**, *105*, 34–38. [CrossRef] [PubMed]
13. Rojano-Vilchis, N.A.; Jimenez-Estrada, M.; Nieto-Camacho, A.; Torres-Avilez, A.; Bye, R.A.; Chavez-Avila, V.M.; Canales-Martinez, M.; Martinez-Elizalde, K.S.; Rodriguez-Monroy, M.A. Isolation and anti-inflammatory effects of maturin acetate from the roots of *Psacalium peltatum* (Asteraceae). *J. Med. Plants Res.* **2013**, *7*, 1600–1607. [CrossRef]
14. Del Carmen Juárez-Vázquez, M.; Alonso-Castro, A.J.; Rojano-Vilchis, N.; Jiménez-Estrada, M.; García-Carrancá, A. Maturin acetate from Psacalium peltatum (Kunth) Cass. (Asteraceae) induces immunostimulatory effects in vitro and in vivo. *Toxicol. In Vitro* **2013**, *27*, 1001–1006. [CrossRef]
15. Wang, Z.; Liang, L.; Yin, Z.; Lin, J. Improving chemical similarity ensemble approach in target prediction. *J. Cheminform.* **2016**, *8*, 2–10. [CrossRef] [PubMed]
16. Chin, Y.W.; Balunas, M.J.; Chai, H.B.; Kinghorn, A.D. Drug discovery from natural sources. *AAPS J.* **2006**, *8*, E239–E253. [CrossRef] [PubMed]
17. Leelananda, S.P.; Lindert, S. Computational methods in drug discovery. *Beilstein. J. Org. Chem.* **2016**, *12*, 2694–2718. [CrossRef] [PubMed]
18. Liu, W.; Furuta, E.; Shindo, K.; Watabe, M.; Xing, F.; Pandey, P.R.; Mo, Y.Y. Cacalol, a natural sesquiterpene, induces apoptosis in breast cancer cells by modulating Akt-SREBP-FAS signaling pathway. *Breast Cancer. Res. Treat.* **2011**, *128*, 57–68. [CrossRef] [PubMed]
19. Jiménez-Estrada, M.; Reyes-Chilpa, R.; Navarro-Ocaña, A.; Baez, D.A. Reactivity of several reactive oxygen species (ROS) with the sesquiterpene cacalol. *Nat. Prod. Comm.* **2008**, *3*, 479–482.
20. Feske, S. ORAI1 and STIM1 deficiency in human and mice: Roles of store-operated $Ca^{2+}$ entry in the immune system and beyond. *Immunol. Rev.* **2009**, *231*, 189–209. [CrossRef]
21. Saul, S.; Gibhardt, C.S.; Schmidt, B.; Lis, A.; Pasieka, B.; Conrad, D.; Jung, P.; Gaupp, R.; Wonnenberg, B.; Diler, E.; et al. A calcium-redox feedback loop controls human monocyte immune responses: The role of ORAI$Ca^{2+}$ channels. *Sci. Signal.* **2016**, *9*, ra26. [CrossRef] [PubMed]
22. Gómez-Vidales, V.; Granados-Oliveros, G.; Nieto-Camacho, A.; Reyes-Solís, M.; Jiménez-Estrada, M. Cacalol and cacalol acetate as photoproducers of singlet oxygen and as free radical scavengers, evaluated by EPR spectroscopy and TBARS. *RSC Adv.* **2014**, *4*, 1371–1377. [CrossRef]
23. Inman, W.D.; Luo, J.; Jolad, S.D.; King, S.R.; Cooper, R. Antihyperglycemic sesquiterpenes from *Psacalium decompositum*. *J. Nat. Prod.* **1999**, *62*, 1088–1092. [CrossRef] [PubMed]
24. Miyata, N.; Gon, Y.; Nunomura, S.; Endo, D.; Yamashita, K.; Matsumoto, K.; Hashimoto, S.; Ra, C. Inhibitory effects of parthenolide on antigeninduced microtubule formation and degranulation in mast cells. *Int. Immunopharmacol.* **2008**, *8*, 874–880. [CrossRef] [PubMed]
25. Itoh, T.; Oyama, M.; Takimoto, N.; Kato, C.; Nozawa, Y.; Akao, Y.; Iinuma, M. Inhibitory effects of sesquiterpene lactones isolated from Eupatorium chinense L. on IgE-mediated degranulation in rat basophilic leukemia RBL-2H3 cells and passive cutaneous anaphylaxis reaction in mice. *Bioorg. Med. Chem.* **2009**, *17*, 3189–3197. [CrossRef] [PubMed]

26. Campos, M.G.; Oropeza, M.; Torres-Sosa, C.; Jimenez-Estrada, M.; Reyes-Chilpa, R. Sesquiterpenoids from antidiabetic *Psacalium decompositum* block ATP sensitive potassium channels. *J. Ethnopharmacol.* **2009**, *123*, 489–493. [CrossRef] [PubMed]
27. Anaya, A.L.; Hernández-Bautista, B.E.; Torres-Barragán, A.; León-Cantero, J.; Jiménez-Estrada, M. Phytotoxicity of cacalol and some derivatives obtained from the roots of *Psacalium decompositum* (A. Gray) H. Rob. & Brettell (Asteraceae), matarique or maturin. *J. Chem. Ecol.* **1996**, *22*, 393–403. [CrossRef] [PubMed]
28. Kedrowski, B.L.; Hoppe, R.W. A concise synthesis of (+/−)-cacalol. *J. Org. Chem.* **2008**, *73*, 5177–5179. [CrossRef] [PubMed]
29. Yuste, F.; Diaz, E.; Walls, F.; Jankowski, K. The structure of cacalone. *J. Org. Chem.* **1976**, *41*, 4103–4106. [CrossRef]
30. Sander, T.; Freyss, J.; von Korff, M.; Rufener, C. DataWarrior: An open-source program for chemistry aware data visualization and analysis. *J. Chem. Inf. Model.* **2015**, *55*, 460–473. [CrossRef] [PubMed]
31. Drwal, M.N.; Banerjee, P.; Dunkel, M.; Wettig, M.R.; Preissner, R. ProTox: A web server for the in silico prediction of rodent oral toxicity. *Nucl. Acids Res.* **2014**, *42*, W53–W58. [CrossRef] [PubMed]
32. Daina, A.; Zoete, V. A Boiled-egg to predict gastrointestinal absorption and brain penetration of small molecules. *Chem. Med. Chem.* **2016**, *11*, 1117–1121. [CrossRef] [PubMed]
33. Ghose, A.K.; Viswanadhan, V.N.; Wendoloski, J.J. A knowledge-based approach in designing combinatorial or medicinal chemistry libraries for drug discovery. 1. A qualitative and quantitative characterization of known drug databases. *J. Comb. Chem.* **1999**, *1*, 55–68. [CrossRef] [PubMed]
34. Luo, H.; Chen, J.; Shi, L.; Mikailov, M.; Zhu, H.; Wang, K.; He, L.; Yang, L. DRAR-CPI: A server for identifying drug repositioning potential and adverse drug reactions via the chemical protein interactome. *Nucl. Acids Res.* **2011**, *39*, W492–W498. [CrossRef]
35. Mattingly, C.J.; Colby, G.T.; Forrest, J.N.; Boyer, J.L. The Comparative toxicogenomics database (CTD). *Environ. Health Perspect.* **2003**, *111*, 793–795. [CrossRef]
36. Madera-Salcedo, I.K.; Cruz, S.L.; Gonzalez-Espinosa, C. Morphine prevents lipopolysaccharide-induced TNF secretion in mast cells blocking IB kinase activation and SNAP-23 phosphorylation: Correlation with the formation of a β-Arrestin/TRAF6 complex. *J. Immunol.* **2013**, *191*, 3400–3409. [CrossRef]
37. Manetz, T.S.; Gonzalez-Espinosa, C.; Arudchandran, R.; Xirasagar, S.; Tybulewicz, V.; Rivera, J. Vav1 regulates phospholipase cgamma activation and calcium responses in mast cells. *Mol. Cell. Biol.* **2001**, *21*, 3763–3774. [CrossRef] [PubMed]
38. Saitoh, S.; Arudchandran, R.; Manetz, T.S.; Zhang, W.; Sommers, C.L.; Love, P.E.; Rivera, J.; Samelson, L.E. LAT is essential for Fc(epsilon)RI-mediated mast cell activation. *Immunity* **2000**, *12*, 525–535. [CrossRef]
39. Grynkiewicz, G.; Poenie, M.; Tsien, R.Y. A new generation of $Ca^{2+}$ indicators with greatly improved fluorescence properties. *J. Biol. Chem.* **1985**, *260*, 3440–3450.
40. Davies, M.J.; Forni, L.G.; Willson, R.L. Vitamin E analogue Trolox CEsr and pulse-radiolysis studies of free-radical reactions. *Biochem. J.* **1988**, *255*, 513–522.
41. Bentayeb, K.; Rubio, C.; Nerín, C. Study of the antioxidant mechanisms of Trolox and eugenol with 2,2′-azobis (2-amidinepropane) dihydrochloride using ultra-high performance liquid chromatography coupled with tandem mass spectrometry. *Analyst* **2012**, *137*, 459–470. [CrossRef] [PubMed]
42. Itoh, T.; Tsukane, M.; Koike, M.; Nakamura, C.; Ohguchi, K.; Ito, M.; Akao, Y.; Koshimizu, S.; Nozawa, Y.; Wakimoto, T.; et al. Inhibitory effects of whisky congeners on IgEmediated degranulation in rat basophilic leukemiaRBL2H3 cells and passive cutaneous anaphylaxis reaction in mice. *J. Agric. Food. Chem.* **2010**, *58*, 7149–7157. [CrossRef] [PubMed]


**Sample Availability:** Samples of the compounds are available from the authors.

molecules

MDPI

Article

# Mexican Propolis: A Source of Antioxidants and Anti-Inflammatory Compounds, and Isolation of a Novel Chalcone and ε-Caprolactone Derivative

**Silvia Laura Guzmán-Gutiérrez [1], Antonio Nieto-Camacho [2], Jorge Ivan Castillo-Arellano [3], Elizabeth Huerta-Salazar [2], Griselda Hernández-Pasteur [2], Mayra Silva-Miranda [1], Omar Argüello-Nájera [4], Omar Sepúlveda-Robles [5], Clara Inés Espitia [6,*] and Ricardo Reyes-Chilpa [2,*]**

1 Departamento de Inmunología, Catedrática CONACyT-Instituto de Investigaciones Biomédicas, Universidad Nacional Autónoma de México, Ciudad Universitaria, Coyoacán 04510, Ciudad de México, Mexico; laura.guzman@iibiomedicas.unam.mx (S.L.G.-G.); mayra_1203@yahoo.com.mx (M.S.-M.)

2 Departamento de Productos Naturales, Instituto de Química, Universidad Nacional Autónoma de México, Ciudad Universitaria, Coyoacán 04510, Ciudad de México, Mexico; camanico2015@yahoo.com (A.N.-C.); lizquim2@unam.mx (E.H.-S.); yolotzin_gris@hotmail.com (G.H.-P.)

3 Departamento de Farmacobiología, CINVESTAV-SUR, Instituto Politécnico Nacional, Calzada de los Tenorios 235, Col. Granjas Coapa C.P. 14330, Ciudad de México, Mexico; jorge.ivan.df@gmail.com

4 El Colegio de la Frontera Sur, Ecosur-San Cristóbal, Carretera Panamericana y Periférico Sur s/n Barrio María Auxiliadora, San Cristóbal de Las Casas C.P. 29290, Chiapas, Mexico; arguello@ecosur.mx

5 Catedrático CONACyT—Unidad de Investigación Médica en Epidemiología Clínica, Hospital de Pediatría, Centro Médico Nacional Siglo XXI, Instituto Mexicano del Seguro Social (IMSS), Av. Cuauhtémoc No. 330, Colonia Doctores, Delegación Cuauhtémoc C.P. 06720, Ciudad de México, Mexico; sero__82@hotmail.com

6 Departamento de Inmunología, Instituto de Investigaciones Biomédicas, Universidad Nacional Autónoma de México, Ciudad Universitaria, Coyoacán 04510, Ciudad de México, Mexico

* Correspondence: espitia@biomedicas.unam.mx (C.I.E.); chilpa@unam.mx (R.R.-C.); Tel.: +55-56223860 (C.I.E.); +55-56224512 (R.R.-C.)

Received: 19 December 2017; Accepted: 16 January 2018; Published: 6 February 2018

**Abstract:** The propolis produced by bees are used in alternative medicine for treating inflammation, and infections, presumably due to its antioxidant properties. In this context, five propolis from México were investigated to determine their inhibitory lipid peroxidation properties. The ethyl acetate extract from a red propolis from Chiapas State (4-EAEP) was the most potent ($IC_{50}$ = 1.42 ± 0.07 μg/mL) in the TBARS assay, and selected for further studies. This extract afforded two new compounds, epoxypinocembrin chalcone (**6**), and an ε-caprolactone derivative (**10**), as well as pinostrobin (**1**), izalpinin (**2**), cinnamic acid (**3**), pinocembrin (**4**), kaempherol (**5**), 3,3-dimethylallyl caffeate in mixture with isopent-3-enyl caffeate (**7a** + **7b**), 3,4-dimethoxycinnamic acid (**8**), rhamnetin (**9**) and caffeic acid (**11**). The HPLC profile, anti-mycobacterial, and antioxidant properties of this extract was also determined. Most of the isolated compounds were also tested by inhibition of reactive oxygen species (ROS) in challenged mouse bone marrow-derived mast cells (BMMCs), and DPPH. Their anti-inflammatory activity was evaluated by TPA, and MPO (myeloperoxidase) activity by ear edema test in mice. The most potent compounds were **7a** + **7b** in the TBARS assay ($IC_{50}$ = 0.49 ± 0.06 μM), and **2** which restored the ROS baseline (3.5 μM). Our results indicate that 4-EAEP has anti-oxidant, and anti-inflammatory properties due to its active compounds, suggesting it has anti-allergy and anti-asthma potential.

**Keywords:** Mexican propolis; red propolis; epoxypinocembrin chalcone; ε-lactone; antioxidant activity; anti-inflammatory activity

## 1. Introduction

Propolis is a resinous product made by bees from plant exudates or resins that bees mix with wax and their salivary secretions. The bees use the propolis as a building material to reduce the entry at their hives, to repair cracks, and strengthen the walls, mainly at the edges. They also use it to varnish the interior of their hive, in order to avoid proliferation of pathogenic microorganisms and, to embalm the corpses of intruder animals that are not possible to remove due to their large sizes, avoiding in this way their putrefaction [1].

Scientific studies are shown that propolis possess pharmacological activities such as anti-oxidant, anti-inflammatory, anti-viral, anti-fungal, immunomodulator, anti-cancer, local anesthetic, hepatoprotector, radioprotector, chemopreventive, and even as a neuroprotector [1–3]. The antimicrobial activity of propolis has been known since ancient times; therefore, it has been integrated into the medicinal products heritage. However, the pharmacological effects of propolis are strongly marked by their composition and depends on the place where these were collected, the type of vegetation, season and species of bee [4–6]. Thus, the propolis are very variable and complex, differing in their chemical composition and properties; for instance, it is possible to find propolis of different colors, flavors, and textures.

The great diversity of propolis demands that during their study, to take in account its geographical origin and even season of collection [7–10]. European propolis contains flavonoid aglycones, phenolic acids and their esters [11]. In Brazilian propolis there was found prenylated derivatives of *p*-coumaric acid and acetophenone [12], diterpenes, lignans and flavonoids [13]. The main components of Cuban propolis are polyisoprenylated benzophenones [14]. From Chilean propolis 17 compounds were isolated that belong to the phenylpropane, benzaldehyde, dehydrobenzofuran, or benzopyran classes [15]. Among the isolated compounds from propolis, pinostrobin (**1**) is the most studied. It has been demonstrated that this flavanone has anti-inflammatory and neuroprotective effects and the ability to reduce ROS, modulate mitochondrial function, and regulate apoptosis, also can protect the brain against damage from ischemic stroke [16]. The flavonoids chrysin and kaempferol (**5**) have been identified as responsible for the anti-allergic effect of Chinese propolis. Other common components of propolis, such as caffeic acid and caffeic acid phenethyl ester, induce apoptosis in human tumor cells in vitro [17].

In Mesoamerica the culture of *Melipona beecheii* (bee without sting) and consumption of honey was a common practice in pre-Columbian times. After the conquest of México in 1521, the beekeeping with the European bee (*Apis mellifera*) was also developed in several regions. Nowadays, México is one of the main honey bee producers in the world; the States of Yucatán, Campeche, Jalisco and Chiapas are the major contributors. In the case of Mexican propolis, different type of compounds have been isolated, such as, phenylallylflavanones [18,19], 1,3-diarylpropane, 1,3-diarylpropene derivatives, flavanones, isoflavans, and pterocarpans [20].

In this work, we assessed the inhibition of lipid peroxidation by TBARS assay of five propolis samples of *Apis mellifera* from the States of Chiapas, and Yucatán, México. The sample 4 from Chiapas State was a red propolis, and its ethyl acetate extract (4-EAEP) was the most potent in the TBARS assay and therefore selected for further chemical and pharmacological studies. From this extract two new and ten known compounds were isolated. We also assessed the anti-inflammatory, anti-oxidant and anti-mycobacterial activities of this extract and its majoritarian compounds.

## 2. Results

### 2.1. Screening of Antioxidant Activity

Five Mexican propolis were obtained from the States of Chiapas, and Yucatán, and examined for their antioxidant activity in the TBARS assay (Table 1). Only the samples 2, 3, and 4 (4-EAEP) showed activity at 10 μg/mL, and their $IC_{50}$ were calculated. The most potent extract 4-EAEP with $IC_{50} = 1.42 \pm 0.07$ μg/mL was selected for further chemical and pharmacological studies.

**Table 1.** Propolis from México and screening activity of their extracts in TBARS assay.

| Propolis Sample/Location (Altitude), State | Extract | %Inhibition (10 μg/mL) | $IC_{50}$ (μg/mL) |
|---|---|---|---|
| **1** Tapachula (177 m), Chiapas | Hexane | 1.32 | |
| | Ethyl acetate | 5.28 | |
| | Methanol | 9.23 | |
| **2** La Trinitaria (1558 m), Chiapas | Hexane | 52.58 | 46.17 ± 0.83 |
| | Ethyl acetate | 94.68 | 8.11 ± 0.16 |
| | Methanol | 96.11 | 11.17 ± 0.61 |
| **3** Pantelhó (1056 m), Chiapas | Hexane | 21.37 | |
| | Ethyl acetate | 35.28 | 25 ± 1.39 |
| | Methanol | 64.00 | 11.59 ± 88 |
| **4** San Cristóbal de las Casas (2200 m), Chiapas | Ethyl acetate (**4-EAEP**) | 99.28 | 1.42 ± 0.07 |
| **5** Rancho San Pedro Chenchelá (227 m), Yucatán | Hexane | 12.06 | |
| | Ethyl acetate | 23.33 | |
| | Methanol | 20.47 | |

## 2.2. Chemical Analysis of the Most Potent Extract

The 4-EAEP was subjected to CC (40 g) and afforded 12 compounds (Figure 1). Two new compounds, epoxypinocembrin chalcone (**6**), and a ε-caprolactone derivative (**10**) have not been previously reported, and their identification is presented next.

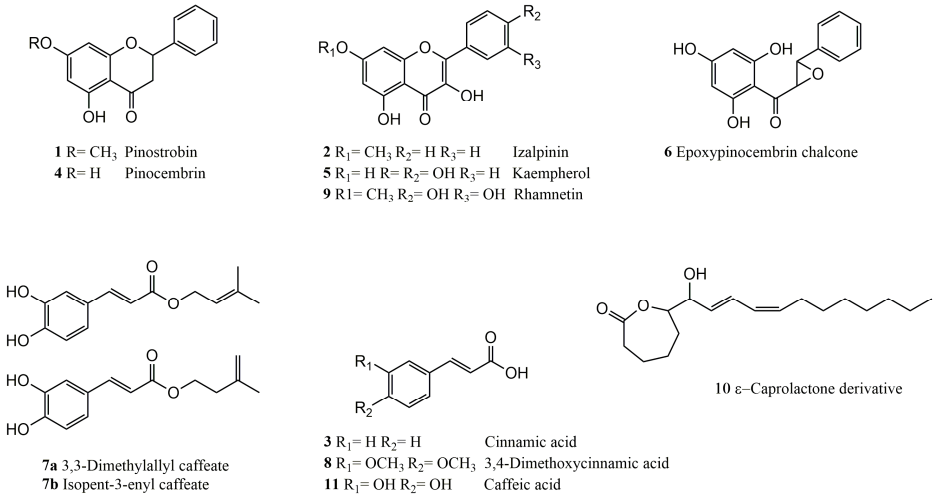


**Figure 1.** Chemical structures of compounds isolated from propolis extract.

### 2.2.1. Structure Elucidation of Epoxypinocembrin Chalcone (**6**)

The $^{1}$H-NMR revealed five aromatic protons as two signals at δ 7.53 (2H, dd *J* = 2 Hz, 2.1 Hz) and δ 7.41 (3H, m), indicating a flavonoid monosubstituted aromatic ring. In addition, two doublets at δ 5.94 (1H, d, *J* = 2.1 Hz) and δ 5.90 (1H, d, *J* = 2.1 Hz) were assigned to two *meta*-coupled protons of the aromatic A ring, therefore this must be tetrasubstituted. A pair of doublets at δ 5.07 (1H, d, *J* = 11.55 Hz) and δ 4.54 (1H, d, *J* = 11.58 Hz) indicated two methines on a carbon attached to oxygen, and the coupling constant indicated these pair of hydrogens must be in the *cis* position.

The combined analysis of its $^{13}$C and HSQC spectrums revealed the presence of 15 carbons assigned to nine methines (seven aromatic and two bonded to oxygen) and six quaternary carbons (one carbonyl and five aromatic). With this information we initially proposed a one tetrasubstituted benzene ring attached to a monosubstituted benzene ring through a dihydroxypropanone chain. However, the high resolution mass spectral data by ESI-MS (positive mode) indicated a $[M + H]^+$ ion at *m*/*z* 273.07 suggesting the molecular formula $C_{15}H_{13}O_5$, therefore our proposal had an extra hydroxyl

group. In addition, IE-MS showed the base peak with $m/z$ 153, that corresponds to the molecular ion trihydroxybenzonium minus 119 (Figure 2), in agreement with a phenyloxiranyl group [21,22]. This suggested that the compound had an epoxychalcone structure (Figure 2). The $J^2$, and $J^3$ connections C-H were determined from the HMBC spectrum, the carbonyl carbon C-9 showed correlations with H-7 and H-8; at the same time C-1 show cross peaks with H-7 and H-8; and C-7 with H-2 and C-6, indicated a phenyloxyranyl group attached to a substituted phenyl ketone. NOEs enhancements can be observed via the 2D NOE technique (NOESY). NOE between H-7/H-8/H-2/H-6. The final proposal is depicted (Figure 2) and the complete assignments of $^1$H- and $^{13}$C-NMR are shown in Table 2.

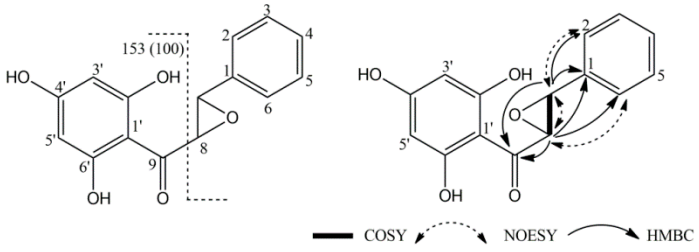


**Figure 2.** Structure of epoxypinocembrin chalcone **6** and selected EI-MS fragments, and NMR correlations.

**Table 2.** $^1$H- and $^{13}$C-NMR chemical shifts of epoxypinocembrin chalcone (**6**).

| Position | $\delta_H$ (*J* in Hz) | $\delta_C$ | Position | $\delta_H$ (*J* in Hz) | $\delta_C$ |
|---|---|---|---|---|---|
| **1** | | 138.55 | **1′** | | 101.81 |
| **2** | 7.53 dd (7,2.1) | 128.92 | **2′** | | 165.34 [a] |
| **3** | 7.41 m | 129.4 | **3′** | 5.94 d (2.1) [b] | 97.45 [b] |
| **4** | 7.39 m | 129.9 | **4′** | | 168.84 |
| **5** | 7.41 m | 129.4 | **5′** | 5.90 d (2.1) [b] | 96.35 [b] |
| **6** | 7.53 dd (7,2.1) | 128.92 | **6′** | | 164.38 [a] |
| **7** | 5.07 d (11.5) | 85.04 | | | |
| **8** | 4.54 d (11.5) | 73.71 | | | |
| **9** | | 198.18 | | | |

[a], [b] Assignments may be reversed.

### 2.2.2. Structure Elucidation of the ε-Caprolactone Derivative **10**

The DART mass spectrum indicated the molecular formula $C_{18}H_{30}O_3$, and four degrees of unsaturation. The EI mass spectrum showed the fragments pattern of allylic chain present in the molecule. The $^{13}$C-NMR (175 Hz) revealed 18 signals and in agreement with HSQC and HMBC experiments there were assigned to one carbonyl, one methyl, 10 methylene, and six methine groups. The carbonyl group (δ 179.9, C-1) was one of the four unsaturations of the molecule, while the IR spectrum suggested the presence of a lactone ring (1707 cm$^{-1}$). In addition in the $^{13}$C spectrum four olefin methines signals were noticed at δ 133.53, 128.37, 129.43 and 133.08 (C-8, C-9, C-10 and C-11, respectively); the HSQC spectrum showed the corresponding $^1$H spectrum signals at δ 5.73, 6.56, 6.00 and 5.41 (H-8, H-9, H-10 and H-11, respectively). The coupling constants and the HMBC experiment revealed the diene system (H-11/C-9 and H-8/C10). The values of the coupling constant between H-8 (δ 5.75, $J$ = 15.7 Hz) and H-9 (δ 6.56, $J$ = 15, 11.1) indicated the presence of *trans*-olefinic protons, while that between H-10 (δ 6.0, $J$ = 11.1, 11.1) and H-11 (δ 5.41, $J$ = 11, 7.7) showed a *cis*-double bond. The TOCSY spectrum reveled that H-8 was coupled to an allylic methine proton at δ 3.96 (H-7) indicating the presence of an allylic alcohol (IR, 3266.55 cm$^{-1}$), which in turn is also coupled to another methine in δ 3.48 (H-6) attached to an oxygen, and consecutively with two additional methylenes: $H_2$-5 (δ 1.34) and $H_2$-4 (δ 1.53), while on the other side of the molecule, H-11 has coupling with a methylene at δ 2.19 ($H_2$-12) and a methylene at δ 14.4 ($H_3$-18) [23,24].

The IR spectrum showed an absorption band at 1707 $cm^{-1}$ which was assigned to the carbonyl of a seven member lactone on basis of the following evidences. In the HMBC spectrum correlations between the carbonyl carbon C-1 with the protons of two methylene groups $H_2$-2 (δ 2.22) and $H_2$-3 (δ 1.6) were observed the at the same time $H_2$-3 had a correlation with C-5 (δ 30.5). The signals observed in the TOCSY experiment also supported this idea, in so much as H-2 had correlation with H-3 (δ 1.59), H-4 (δ 1.53) and H-5 (δ 1.34). On the other hand, the NOE correlations between H-10/H-8/H-11 and H-7/H-9/H-6 were observed. Thus, the structure of **10** was determined as shows in the Figure 3. The complete assignments of $^1$H- and $^{13}$C-NMR spectra are given in Table 3.

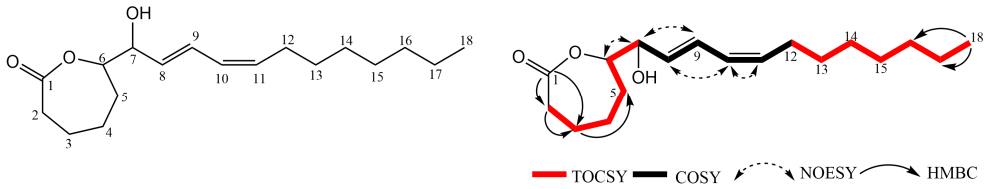


**Figure 3.** Structure and selected NMR correlations of ε-caprolactone derivative.

**Table 3.** $^1$H- and $^{13}$C- NMR chemical shifts of ε-caprolactone derivative.

| Position | $\delta_H$ (*J* in Hz) | $\delta_C$ | Position | $\delta_H$ (*J* in Hz) | $\delta_C$ |
|---|---|---|---|---|---|
| **1** | | 179.9 | **10** | 6.00 dd (11.1, 11.1) | 129.43 |
| **2** | 2.21 t (7.6) | 36.70 | **11** | 5.41 dt (11, 7.7) | 133.08 |
| **3** | 1.59 q (7.1) | 26.75 | **12** | 2.19 td (8.05,7.6) | 28.63 |
| **4** | 1.53 m | 33.75 | **13** | 1.39 q (7.14) | 30.55 |
| **5** | 1.34 m | 30.5 | **14** | 1.28–1.36 m | 30.48 |
| **6** | 3.48 m | 75.69 | **15** | 1.28–1.36 m | 26.83 |
| **7** | 3.96 dd (7,6) | 76.9 | **16** | 1.28–1.36 m | 32.51 |
| **8** | 5.73 dd (15, 7) | 133.53 | **17** | 1.28–1.36 m | 23.61 |
| **9** | 6.56 ddt (15, 11.1, 1.1) | 128.37 | **18** | 0.9 t (7) | 14.4 |

### 2.2.3. HPLC Profile of 4-EAEP

The HPLC chromatogram of 4-EAEP (Figure 4) allowed us to observe the complete composition of propolis extract, and each of the isolated compounds, indicating the method is helpful for monitoring their presence in other samples. The chromatogram confirmed that the most abundant compounds are the flavonone pinocembrin (**4**) followed by the flavonol pinostrobin (**1**), the mixture of prenylated phenylproponoids (**7a** + **7b**) and the flavonol izalpinin (**2**), while the new compounds **6** and **10** were the scarcest.

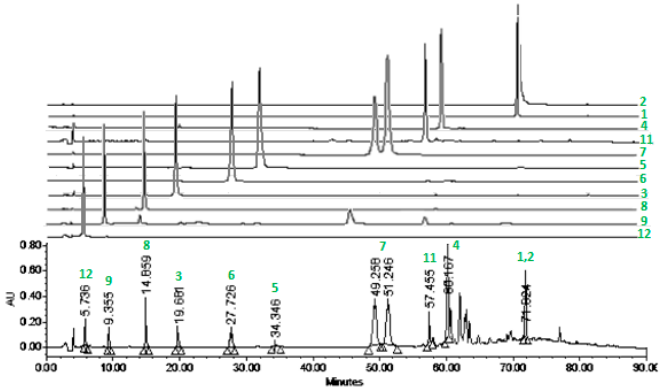


**Figure 4.** Chromatogram of propolis extract (5 mg/mL, 20 μL injection) at 236 nm. (**1**) ($\lambda_{max}$ 289 nm), (**2**) ($\lambda_{max}$ 266.6 nm), (**3**) ($\lambda_{max}$ 277.2 nm), (**4**) ($\lambda_{max}$ 290.2 nm), (**5**) ($\lambda_{max}$ 266.6 nm), (**6**) ($\lambda_{max}$ 291.4 nm), (**7**) ($\lambda_{max}$ 327 nm), (**8**) ($\lambda_{max}$ 322.2 nm), (**9**) ($\lambda_{max}$ 323.4 nm), (**10**) ($\lambda_{max}$ 236 nm), (**11**) ($\lambda_{max}$ 324.6 nm).

## 2.3. Biological Activity

### 2.3.1. TBARS

In the TBARS assay 4-EAEP showed antioxidant activity in concentration-dependent manner with an $IC_{50}$ = 1.42 ± 0.07 μg/mL, and was the most potent effect exhibited by this extract. The most active compounds were **7a** + **7b** $IC_{50}$ = 0.49 ± 0.06 μM, followed by **5** $IC_{50}$ = 4.87 ± 0.11 μM, **6** $IC_{50}$ = 59.96 ± 6.4 μM, **2** $IC_{50}$ = 112.78 ± 27.37 μM. In the Figure 5 the comparison of $IC_{50}$ (μg/mL) of the different tested compounds with the propolis extract is shown. The positive control was BHT ($IC_{50}$ = 1.22 ± 0.44 μM). The compounds **1**, **4** and **8** were not active.

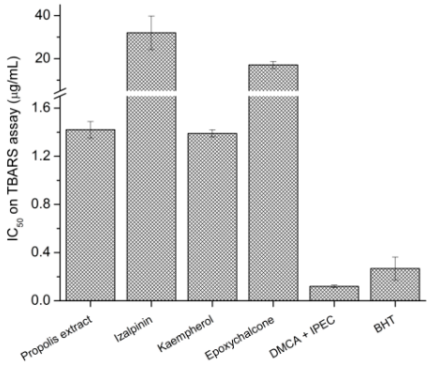


**Figure 5.** Comparison of $IC_{50}$ levels of tested compounds isolated of propolis extract in TBARS assay. Data represent the mean ± SEM ($n$ = 3).

### 2.3.2. Determination of ROS in the Antigen-Induced Mast Cell Degranulation

The 4-EAEP at 20 μg/mL was able to restore ROS baseline associated to activation FcεRI by antigen, corroborating the presence of one or more compounds with antioxidant activity. The ROS inhibition of some purified compounds was tested (Figure 6). The compound **2** was the most potent, since 3.5 μM restore completely the ROS baseline, then followed by **4** (30 μM), **7a** + **7b** (100 μM), and finally the **8** (300 μM), the **1** was not active.

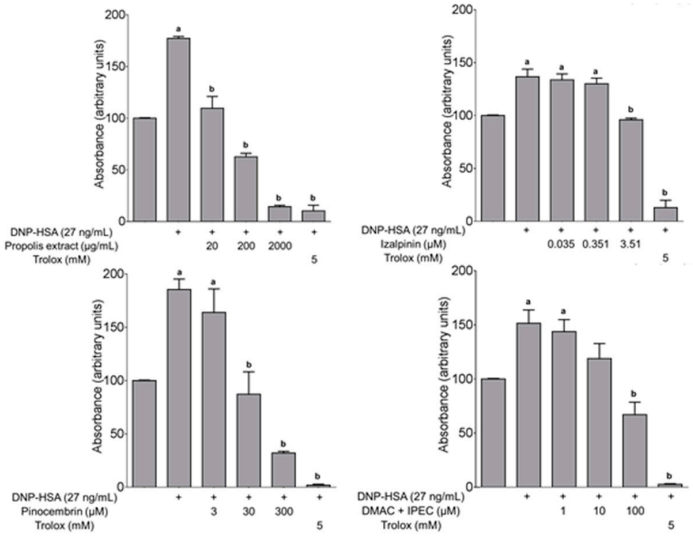


**Figure 6.** The inhibition of ROS production in stimulated mast cells. DMAC + IPEC mixture of 3,3-dimethylallyl caffeate and isopent-3-enyl caffeate (**7a** + **7b**). Data represent the mean ± SEM ($n$ = 3). ANOVA followed by Tukey's test, * $p < 0.05$. (**a**) Significant difference compared to the control group and (**b**) to the stimulated group. (+) Groups with DNP-HAS antigen.

### 2.3.3. DPPH Scavenging Capacity

In the case of DPPH assay, the 4-EAEP had an $IC_{50}$ = 16.55 ± 0.87 µg/mL. The compounds **7a** + **7b**, showed free radical scavenging activity, with an $IC_{50}$ = 13.63 ± 0.2 µM, and **5** with an $IC_{50}$ = 26.02 ± 0.08 µM. The positive controls were BTH ($IC_{50}$ = 16.51 ± 1.27 µg/mL) and α-tocopherol (41.15 ± 0.14 µM). The **1**, **2**, **3**, **4**, **6** and **8** not had activity.

### 2.3.4. Anti-Inflammatory Effect and Inhibition of Myeloperoxidase

The 4-EA EP showed in the TPA model an $IC_{50}$ = 1.21 mg/ear, while for the positive control, indomethacin showed an $IC_{50}$ = 0.84 mg/ear, indicating that the 4-EAEP had activity. Only the isolated pinocembrin (**4)** had activity, with an $IC_{50}$ = 2.53 µmol/ear (0.64 mg/ear), while celecoxib had 0.91 µmol/ear. The histological sections from mice ears were shown in Figure 7, where we can see the 4-EAEP diminution of cells migration observed in the inflammation process. The 4-EAEP at 1 mg/ear produced a diminish of levels of myeloperoxidase at level of 95.46 ± 0.002%, as comparison, indomethacin at 0.358 mg/ear achieved inhibition of 91.08 ± 0.006%. Pinocembrin at 0.81 mg/ear produced 91.09 ± 3.66% of inhibition [25,26]. **1**, **2**, **3**, **5**, **6**, **7**, **8** and **9** were not active.

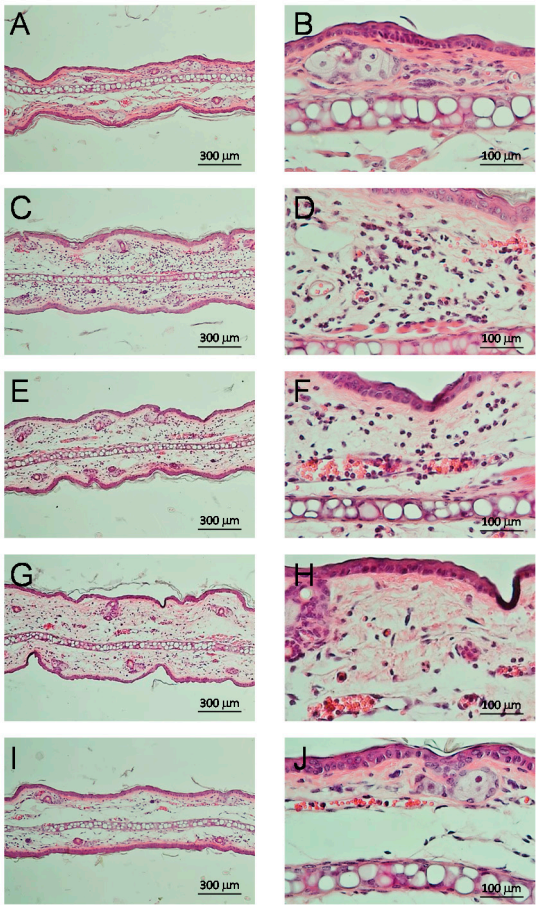


**Figure 7.** Representative histological sections from mice ears stained with hematoxylin-eosin (10×, left column and 40×, right column), after 4 hours of TPA application and 4-EAEP at different doses. (**A**,**B**) Basal; (**C**,**D**) TPA; 4-EAEP (**E**,**F**) 0.56 mg/ear; (**G**,**H**) 1 mg/ear and (**I**,**J**) 1.71 mg/ear.

### 2.3.5. Anti-Mycobacterial Activity

The anti-mycobacterial activity of 4-EAEP was evaluated and had a MIC = 250 µg/mL and the toxicity in the VERO cells was $IC_{50}$ = 179 µg/mL. The isolated cinnamic acid (**3**) also presented a moderated activity with a MIC = 250 µg/mL.

## 3. Discussion

### *3.1. Screening*

The extracts of five propolis samples from the Southeast States of México, Chiapas and Yucatán were analyzed for their antioxidant activity in the TBARS assay. Only the samples 2, 3, and 4, collected at the higher altitudes showed relevant activity. The most potent ($IC_{50}$ = 1.42 ± 0.07 μg/mL) was 4-EAEP (Table 1) from a red propolis collected at San Cristobal de las Casas (2200 m), while those collected nearby to sea level were almost inactive. San Cristobal de las Casas predominant natural vegetation is pine-oak forests, and wetlands, agriculture is devoted to maize, but horticulture, floriculture, and cultivation of temperate fruit trees is also practiced. Pesticides are used in the case of floriculture [27].

### *3.2. Chemical Analysis and HPLC Profile of 4-EAEP*

The extract 4-EAEP afforded 12 compounds, six flavonoids, five phenylpropanoids, and one fatty acid lactone (Figure 1). Two of the compounds are new: epoxypinocembrin chalcone (**6**), and an ε-caprolactone derivative **10**. The compound **6** could arise from the known pinocembrin chalcone, which has been previously isolated from propolis of Poland [28], Canada [29], among others. Regarding to compound **10**, it could arise from cyclization of polyunsaturated octadecanoic acid, it is well known that fatty acids are constituents of propolis of different regions [30].

The majoritarian compounds of 4-EAEP were the flavonones pinocembin (**4**), pinostrobin (**1**), the mixture of prenylated phenylproponoids (**7a** + **7b**), and the flavonol izalpinin (**2**) (Figure 4). The overall chemical composition of this extract resembled those from European propolis [11]. Previously it has been studied a Mexican red propolis from Champotón located at the nearby State of Campeche [20] isolating in addition to flavanones, isoflavans and pterocarpans characteristic of Papilionoideae plant species. Champotón is located at sea level, tropical vegetation may be the main reason for the differences in composition with our red propolis. Our results support the idea that geographic origin, altitude, natural vegetation, and predominant cultivated and ruderal plant species, determine the chemical composition of propolis and their pharmacological properties.

### *3.3. Biological Activity*

The 4-EAEP, and their compounds isolated in good yield, were tested for antioxidant activity, in the tree different tests (TBARS, DPPH and ROS), as well as for anti-inflammatory (TPA) and anti-mycobacterial properties. In general, the best results were obtained for antioxidant activity, specially inhibiting lipid peroxidation as evaluated by TBARS production, and inhibition ROS production in mouse mast cells, followed by scavenging activity of free radical DPPH. The extract and several compounds also showed anti-inflammatory activity. The 4-EAEP showed low anti-mycobacterial activity, and toxicity in the VERO was also low.

The most potent effect exhibited by 4-EAEP was inhibition of lipid peroxidation in a concentration-dependent manner. This assay measures through MDA the total lipid hydroperoxides content, formed in a later stage of lipid oxidation. The high activity of 4-EAEP in this model should be due to the activity of the majority of the isolated compounds. The mixture of isomers **7a** + **7b** was 2.4 times more potent that positive control BHT, followed by **5**, **6** and **2**. The lipid peroxidation can lead to cell membranes to lose their integrity, and therefore their functions Moreover, the aldehydes formed by lipid oxidation can react with proteins and nucleic acids, which determines cytotoxic, genotoxic and mutagenic effects, as well as a pathogenic role in several diseases [31].

The 4-EAEP was able to restore ROS baseline associated to activation FcεRI by antigen, corroborating the presence of one or more compounds with antioxidant activity. The compound **2** was the most potent, followed by **4**, **7a** + **7b**, and finally **8**. These results show the capacity of the isolated compounds to restore the equilibrium of ROS production at cell level; on the other hand, this is the first time that these compounds are tested in this model. In the case of mixture **7a** + **7b**, although these

compounds have been indicated as topic allergens, this experiment shows that at a certain concentration they can help to reduce the oxidative stress in stimulate mast cells and the molecular mechanism is independent and different to that previously described [32,33]. The increase in ROS production by the molecular protein complex of NADPH oxidase in mast cells, after cross-linking of FcεRI with IgE/Ag, is associated with the importance of ROS for the activation of receptor-operated calcium entry (ROCE), which favors the entry of calcium through activated membranal calcium channel into the cell, resulting in the mobilization and release of the pro-inflammatory content of the preformed granules in mast cells [34]. This model simulates what happens in an acute inflammatory process observed in chronic degenerative diseases, such as allergies and asthma, where mast cells play an important role. Kaempferol (**5**), a component of 4-EAEP has been identified as an anti-allergic component on mast cells of the ethanol extract of a Chinese propolis [35]. Additionally, it has been investigated the effects of an aqueous extract of propolis (13%), administered as an adjuvant to therapy to patients with mild to moderate asthma [36]. At the end of the treatment, patients receiving propolis showed a marked reduction in the incidence and severity of nocturnal attacks and improvement of ventilator functions that was associated with decreases of prostaglandins, leukotrienes, pro-inflammatory cytokines (TNF-α, IL-6, IL-8) and increased IL-10.

In the case of DPPH assay, the EAEP had a similar activity to positive control BTH. Only the mixture of **7a** + **7b** showed free radical scavenging activity, and was three times more potent that α-tocopherol. Regarding to anti-inflammatory activity, pinocembrin (**4**) was active, but the extract showed a mild effect, probably because it is mixed with other substances. This is the first report of the anti-inflammatory effect of pinocembrin in TPA model in mice and its respective $IC_{50}$. The histological sections from mice ears treated with 4-EAEP showed diminution of cell migration in the inflammation process. Related to this result, the enzyme myeloperoxidase is produced by neutrophils, and increases its activity when an inflammatory process is triggered by TPA administration. Pinocembrin (**4**) and 4-EAEP also produced a decrease of levels of myeloperoxidase. Pinocembrin (**4**) has been reported with neuroprotective, anti-oxidative, and anti-inflammatory effects both in vitro and in vivo [25,26]. Several biological activities [37,38], have been attributed to pinocembin (**4**), and pinostrobin (**1**), and support the pharmacological properties of 4-EAEP.

## 4. Materials and Methods

### *4.1. Propolis*

The propolis samples 1, 2, 3, and 5 were from local *Apis mellifera* bee breeders, while sample 4 proceeds from a wild colony, probably Africanized. All the samples were collected by one of the coauthors, Omar Argüello-Nájera, using the scraping technique, then ground in a coffee mill, and extracted with solvents with increasing polarity consecutively at room temperature. Each sample was extracted first with hexane, and then the residue with ethyl acetate and methanol. The exception was propolis 4, quite insoluble in hexane, but was completely dissolved in ethyl acetate, therefore this extract (4-EAEP) was the only one prepared. The solvents were eliminated in a rotatory evaporator, and the extracts stored in dark bottles at 4 °C. All the extracts were screened for their capacity to inhibit lipid peroxidation in the TBARS assay, the most potent was 4-EAEP, and therefore was selected to study its chemical composition, its anti-oxidant, anti-inflammatory and anti-mycobacterial activity.

### *4.2. General Experimental Procedures*

IR spectra were recorded on Tensor 27 spectrophotometer (Bruker, Billerica, MA, USA). NMR spectra were obtained on an Avance III 400 MHz or 700 MHz spectrometer (Bruker Billerica, MA, USA). EIMS were obtained on a MStation JMS-700 mass spectrometer (Jeol Ltd., Tokyo, Japan) and The AccuTOF JMS-T100LC (Jeol Ltd., Tokyo, Japan). CC (Sev-Prendo, Puebla, México) was carried out with silica gel 60 (Macherey-Nagel, Düren, Germany). SC was carried out with sephadex$^{TM}$ LH-20 (GE Healthcare

Bio-Sciences AB, Uppsala, Sweden). To monitor CC and SFpre-coated TLC-sheets ALUGRAM®Xtra SIL G/UV254 with silica gel 60, layer 0.20 mm (Macherey-Nagel, Düren, Germany).

### *4.3. Isolation Procedure of Compounds*

The 4-EAEP (40 g) was fractionated by CC (hexane-ethyl acetate gradient), fractions with similar TLC patterns were combined. Compound **1** (118 mg) was obtained from fractions 39–40 eluted with a 95:5 mixture [39]. Compound **2** (18 mg) was obtained from fractions 89–99 eluted with a 90:10 mixture [40]. Compounds **3** (41 mg) and **4** (59 mg) were obtained from fractions 100–102 eluted with an 80:20 mixture [39]. Compound **8** (52 mg) was obtained from 237–240 eluted with a 60:40 mixture [41]. Compound **9** (10 mg) from fractions 265–272 eluted with a 60:40 mixture [42]. The pooled fractions 169–186 from the first column were next subjected to CC (hexane-ethyl acetate gradient). Compound **5** (11 mg) was obtained from subfractions 46–60 [43], **6** (16 mg) from subfractions 100–104 and **7** (25 mg) from subfractions 149–159 [44]. All compounds eluted with a 92:8 mixture. The pooled fractions 305–339 from the first column was next subjected to SC (eluted with 100% methanol). Compound **10** (8 mg) was obtained from subfractions 7–6. Compound **11** (9 mg) was obtained from subfraction 12 [45]. The identification of the isolated compounds (Figure 1) was achieved by comparison of their physical and spectroscopic data with those of the literature.

Two new compounds, epoxypinocembrin chalcone (**6**), and a substituted ε-caprolactone **10** have not been previously reported, and their identification is thoroughly presented in the Results section.

*Pinostrobin* (**1**) White crystals, m.p. 87–90 °C. $^{1}$H-NMR (300 MHz, $CDCl_3$). δ 12.02 (1H, s, 5-OH), 7.44 (5H, m, H-2′, H-3′, H-4′, H-5′ and H-6′), 6.08 (1H, d, *J* = 2.4, H-6), 6.07 (1H, d, *J* = 2.1, H-8), 5.42 (1H, dd, *J* = 3, 12.9, H-2), 3.81 (3H, s, $OCH_3$-7), 3.09 (1H, dd, *J* = 12.9, 17.1, H-3a), 2.82 (1H, dd, *J* = 3, 17.1, H-3b). $^{13}$C-NMR ($CDCl_3$): δ 195.89 (C-4), 168.14 (C-7), 164.31 (C-5), 162.94 (C-9), 138.53 (C-1′), 129.02 (C-3′, C-4′ and C-5′), 126.28 (C-2′ and C-6′), 103.31 (C-10), 95.30 (C-8), 94.42 (C-6), 79.38 (C-2), 55.83 ($OCH_3$ C-7), 43.54 (C-3). ESI-MS (positive mode): *m*/*z* 271.09 $[M + H]^+$. EI-MS: *m*/*z* (relative abundance) 270 $[M^+]$ (100), 269 $[M - H]^+$ (50), 193 (55), 166 (42), 138 (17), 95 (14) [39,46].

*Izalpinin* (**2**) Yellow needles, m.p. 208–210 °C.$^{1}$H-NMR ($CDCl_3$). δ 11.65(1H, s, 5-OH), 8.2 (2H, m, H-2′, H-6′), 7.52 (3H, m, H-3′, H-4′, H-5′), 6.51 (1H, d, *J* = 2.2, H-8), 6.39 (1H, d, *J* = 2.2, H-6), 3.81 (3H, s, $OCH_3$-7). $^{13}$C-NMR ($CD_3OD$): δ 175.74 (C-4), 166.15 (C-7), 161.05(C-5), 157.21 (C-9), 145.38 (C-2), 136.75 (C-3), 130.89 (C-1′), 130.42 (C-4′), 128.77 (C-3′, C-5′), 127.77 (C-2′, C-6′), 104.19 (C-10), 98.19 (C-6), 92.43 (C-8), 56.03 ($OCH_3$ C-7) [40]. ESI-MS (positive mode): *m*/*z* 285.07 $[M + H]^+$. EI-MS: *m*/*z* (relative abundance) 285 $[M + H]^+$ (18), 284 $[M^+]$ (100), 283 $[M - H]^+$ (25), 241 (8), 105 (15), 77 (8) [18,40].

*Cinnamic acid* (**3**) White powder m.p. 133–135 °C $^{1}$H-NMR ($CDCl_3$). δ 7.81 (1H, d, *J* = 15.9, H-3), 7.56 (2H, m, H-2′ and H-6′), 7.56 (3H, m, H-3′, H-4′ and H-5′), 6.46 (1H, d, *J* = 15.9, H-2). 177.62, 147.26, 134.2, 130.90, 129.11, 128.52, 117.46. EI-MS: *m*/*z* (relative abundance) 149 $[M + H]^+$ (10), 148 $[M^+]$ (100), 147 $[M - H]^+$ (95), 131 (28), 103 (42), 102 (25), 77 (33), 51 (17) [47].

*Pinocembrin* (**4**) Beige powder, m.p. 198–201 °C. $^{1}$H-NMR (300 MHz, $CDCl_3$ + drop of DMSO-D6). δ 12.02 (1H, s, 5-OH), 7.42 (5H, m, H-2′, H-3′, H-4′, H-5′ and H-6′), 5.96 (1H, d, *J* = 2.1, H-6), 5.93 (1H, d, *J* = 2.1, H-8), 5.44 (1H, dd, *J* = 3, 12.6, H-2), 3.06 (1H, dd, *J* = 12.9, 17.1, H-3a), 2.77 (1H, dd, *J* = 3.3, 17.1, H-3b). $^{13}$C-NMR ($CDCl_3$): δ 194.68 (C-4), 166.53 (C-7), 163.51 (C-5), 162.32 (C-9), 138.13 (C-1′), 128.17 (C-3′, and C-5′), 128.12 (C-4′), 125.72 (C-2′ and C-6′), 101.67 (C-10), 96.01 (C-6), 94.94 (C-8), 78.25 (C-2), 42.53 (C-3). ESI-MS (positive mode): *m*/*z* 257.08 $[M + H]^+$. EI-MS: *m*/*z* (relative abundance) 256 $[M^+]$ (100), 255 $[M - H]^+$ (63), 179 (80), 152 (65), 124 (34), 69 (15) [39,48].

*Kaempherol* (**5**) Yellow powder. $^{1}$H-NMR ($CD_3OD$) δ 8.07 (2H, dd, *J* = 2.05, 8.85, H-2′ y H-6′), 6.9 (2H, dd, *J* = 2.05, 8.9, H-3′ and H-5′), 6.38 (1H, d, *J* = 2.05, H-8), 6.17 (1H, d, *J* = 2.1, H-6). $^{13}$C-NMR ($CD_3OD$): δ 177 (C-4), 166.11 (C-7), 162.47 (C-5), 160.56 (C-4′), 158.31 (C-9), 148 (C-2), 137.09 (C-3), 130.66 (C-2′ and C-6′), 123.75 (C-1′), 116.32 (C-3′, C-5′), 104.41 (C-10), 99.47 (C-6), 94.6 (C-8) [43].

*Epoxypinocembrin chalcone* (**6**). White crystals, m.p. 99–102 °C. $^{1}$H- and $^{13}$C-NMR Table 1. ESI-MS (positive mode): $m/z$ 273.07 $[M + H]^+$. EI-MS: $m/z$ (relative abundance) 273 $[M + H]^+$ (8), 272 $[M^+]$ (40), 153 (100), 120 (20), 91 (28), 28 (16), 18 (16).

*3,3-Dimethylallyl caffeate* (**7a**). Crystalline light beige powder. $^{1}$H-NMR ($CDCl_3$). δ 7.52 (1H, d, $J$ = 16, Hα), 7.03 (1H, d, $J$ = 1.6, H-2), 6.93 (1H, dd, $J$ = 1.6, 8, H-6), 6.77 (1H, d, $J$ = 8, H-5), 6.23 (1H, d, $J$ = 16, Hβ), 5.4 (1H, tdq, $J$ = 1.6, 2.8, 7.2, H-2′), 4.67 (2H, d, $J$ = 7.2, H-1′), 1.77 (3H, s, H-5′), 1.75 (3H, s, H-4′). Compound **7a** was obtained as a mixture with *isopent-3-enyl caffeate* (**7b**). $^{1}$H-NMR ($CDCl_3$). δ 7.52 (1H, d, $J$ = 16, Hα), 7.03 (1H, d, $J$ = 1.6, H-2), 6.93 (1H, dd, $J$ = 1.6, 8, H-6), 6.77 (1H, d, $J$ = 8, H-5), 6.23 (1H, d, $J$ = 16, Hβ), 4.82 (1H, s, H-5), 4.77 (1H, s, H-5), 4.28 2H, t, $J$ = 6.8, H-1′), 2.41 (2H, t, $J$ = 6.8, H-2′), 1.78 (3H, s, H-4′) [44].

*3,4-Dimethoxycinnamic acid* (**8**). Crystalline white powder, m.p. 183–185 °C $^{1}$H-NMR ($CDCl_3$) δ 7.73 (1H, d, $J$ = 15.8, H-7), 7.14 (1H, dd, $J$ = 2.1, 8.1, H-6), 7.07 (1H, d, $J$ = 2, H-2), 6.88 (1H, d, $J$ = 8.3, H-5), 6.32 (1H, d, $J$ = 15.9, H-8), 3.92 (6H, s, $OCH_3$). $^{13}$C-NMR ($CD_3OD$): δ 172.5 (C-9), 151.2 (C-4), 149.4 (C-3), 147.1 (C-7), 127.2 (C-1), 123.2 (C-6), 115.0 (C-8), 111.2 (C-5), 110.22 (C-2), 109.99 (C-5), 56.1 ($OCH_3$), 56.0 ($OCH_3$). ESI-MS (positive mode): $m/z$ 209.08 $[M + H]^+$. EI-MS: $m/z$ (relative abundance) 208 $[M^+]$ (100), 309 $[M - H]^+$ (13), 193 (15), 147 (6), 133 (7), 119 (7), 91(9), 77 (10), 51 (7) [41].

*Rhamnetin* (**9**). Yellow powder. m.p. 282–287 °C. $^{1}$H-NMR ($CD_3OD$): δ 7.76 (1H, d, $J$ = 2.15, H-2′), 7.66 (1H, dd, $J$ = 2.17, 8.47, H-6′), 6.89 (1H, d, $J$ = 8.5, H-5′), 6.59 (1H, d, $J$ = 2.2, H-8), 6.32 (1H, d, $J$ = 2.2, H-6), 3.89 (3H, s, $OCH_3$). ESI-MS (positive mode): $m/z$ 317 $[M + H]^+$. EI-MS: $m/z$ (relative abundance) 316 $[M^+]$ (100), 317 $[M - H]^+$ (21), 315 (13), 273 (12), 194 (16), 137 (12) [42].

*ε-Caprolactone derivative* (**10**). Beige amorphous powder, m.p. 87–90 °C. $^{1}$H and $^{13}$C-NMR Table 2. ESI-MS (positive mode): $m/z$ 295.22 $[M + H]^+$.

*Caffeic acid* (**11**). Slightly brown powder. m.p. $^{1}$H-NMR ($CD_3OD$): δ 7.53 (1H, d, $J$ = 15.87, H-7), 7.03 (1H, d, $J$ = 2.1, H-2), 6.93 (1H, dd, $J$ = 2.1, 8.1, H-6), 6.77 (1H, d, $J$ = 8.1, H-5), 6.22 (1H, d, $J$ = 15.87, H-8) $^{13}$C-NMR ($CD_3OD$): δ 171.06 (C-9), 149.42 (C-4), 146.94 (C-7), 146.79 (C-3), 127.83 (C-1), 122.81 (C-6), 116.49 (C-5), 115.64 (C-8), 115.09 (C-2). ESI-MS (positive mode): $m/z$ 181.05 $[M + H]^+$. EI-MS: $m/z$ (relative abundance) 181 $[M + H]^+$ (12), 180 $[M^+]$ (100), 163 (39), 134 (41), 89 (21), 43 (18) [45].

### *4.4. HPLC Analysis of Propolis*

The analysis was run on a Breeze HPLC-PDA system (Waters Corporation, Milford, MA, USA), equipped with degasser, 1525 binary pump and 2998 PDA. Separation was achieved on a Luna PFP(2) column (100 Å 250 mm × 4.6 mm, 5 µm particle size (Phenomenex, Torrance, CA, USA), at room temperature, using a gradient system composed by the binary phases (A) water and (B) acetonitrile, both with 0.1% of acetic acid. The elution gradient was: 0–3 min 25% B, 3–10 min 30% B, 10–40 min 40% B, 40–60 min 60% B and 60–92 min 90% B. The flow employed was 1 mL/min [49]. The injected volume was 20 µL. The concentration of the solutions depended of its λ maximum for each compound.

### *4.5. Animals*

The animals were provided by the Bioterio of IFC, UNAM, and their handling followed the Mexican Official Norm NOM-062-ZOO-1999 and international rules. The experimental procedures were approved by Ethic Committee (CICUAL-IQ-004-17). Groups of six CD1 male mice (25–30 g) were used for TPA assay and groups of three male Wistar rats (200–250 g) were used for TBARS. The animals were maintained under a 12 h light/dark cycle (22 °C ± 1 °C) with free access to food and water.

### *4.6. Inhibition of Lipid Peroxidation Measured by TBARS Assay*

The tested compounds were **1**, **2**, **4**, **6**, **7a** + **7b** and **8**. Lipid peroxidation was measured by TBARS assays using rat brain homogenates. Three rats were sacrificed with $CO_2$. Each whole brain was dissected and homogenized in PBS to produce a 1/10 ($w/v$) homogenate [50]. The homogenate was

centrifuged for 10 min at 800 rcf, the supernatant protein content was adjusted with PBS at 2.66 mg of protein/mL. 375 µL of supernatant plus 50 µL of EDTA (20 µM) and 25 µL of each sample solved in DMSO were incubated at 37 °C for 30 min. Lipid peroxidation was started adding 50 µL of freshly prepared 100 µM $FeSO_4$ solution, and incubated at 37 °C for 1 h. Concentration of TBARS was calculated by interpolation in a standard curve of TMP as a precursor of MDA [51]. Results were expressed as nmoles of TBARS per mg of protein. The inhibition ratio ($I_R$(%)) was calculated using following formula $I_R = (Abs_{control} - Abs_{sample}) \times 100/Abs_{control}$. BHT and α-tocopherol were used as positive standards.

### *4.7. Determination of Reactive Oxygen Species (ROS) in the Antigen-Induced Mast Cell Degranulation*

The concentrations tested were selected based on preliminary assays with logarithmic scale. The tested compounds were **1**, **2**, **4**, **7a** + **7b** and **8**. The 4-EAEP was tested at 20, 200 and 2000 µg/mL; for **1** was 0.074–7.4 µM, for **2** was 0.035–3.5 µM; for **4** was 3–300 µM, for **7** was 1–100 µM and for **8** was 3–300 µM. Trolox was used as positive control (5 mM). The experiments were carried out with sensitized $2 \times 10^6$ BMMC/mL [52] in a 1 mL by treatment, 15 min after add the compounds, the cells was stimulated, with the antigen DNP-HSA (27 ng/mL) and at the same time the indicator DCF-DA (10 µM) was added, 15 min after stop reaction at 4 °C. Then the tubes were centrifuged at 1500 rpm at 4 °C by 5 min, the supernatant was eliminated and 300 µL of Igepal (0.1%) was added at 37 °C, the mixture was pipetted to smash the cell bottom. Next, the tubes were centrifuged at 10,000 rpm by 5 min at 4 °C and 200 µL of supernatant were transferred at 96 well plate and red in Luminometer FLx88 (Biotek, Winooski, VT, USA), at 488 nm of $\lambda_{excitation}$ and 565 nm of $\lambda_{emission}$. The plate was red each 15 min during 1 h [34].

### *4.8. DPPH Scavenging Capacity*

The activity of compounds **1**, **2**, **3**, **4**, **5**, **6**, **7a** + **7b** and **8** were assessed. Fifty µL of test compounds in ethanol at different concentrations was added to an ethanolic solution of DPPH (133.33 µM, 0.150 mL). Reaction mixtures were incubated at 37 °C for 30 min in the dark. After incubation the absorbance was measured at 515 nm in a microplate reader Synergy HT (BioTek Instruments, Winooski, VT, USA). The scavenging capacity (%) is calculated as $[(Abs_{control} - Abs_{sample})/(Abs_{control}) \times 100]$; α-tocopherol was used as standard [50].

### *4.9. Evaluation of Anti-Inflammatory Effect by TPA Assay*

The effect of compounds **1**, **2**, **3**, **4**, **5**, **6**, **7**, **8** and **9** were tested, in the primary screening was determined that only the compound **4** had activity. Groups of five CD1 male mice were used, one group for vehicle, other group for reference drug (indometacin, Sigma, St. Louis, MO, USA) and four groups for each dose tested of pinocembrin (**4**). The animals were anesthetized with Pisabental (sodium pentobarbital, PISA, Ciudad de México, México). The right ear received topically TPA 2.5 µg in ethanol (10 µL), the left ear only ethanol. 10 min after in the right ear the test substances (1 µmol/ear), indomethacin (0.31 µmol/ear) or vehicle were applied. 4 h later, the mice were killed with $CO_2$. From each ear was removed a 7 mm diameter plugs. The swelling was assessed as the difference in weight between right and left ear plugs [53]. The anti-inflammatory activity was expressed as inhibition of edema (IE): IE (%) = 100 − [B × 100/A], where A = edema induced by TPA alone, and B = edema induced by TPA plus sample.

### *4.10. Myeloperoxidase (MPO) Assay*

Tissue MPO activity was measured in biopsies taken from ears 4 h after TPA administration, only for vehicle, indometacin and compound **4** groups. Each biopsy was homogenized for 30 s at 4 °C. The homogenate was sonicated 20 s, and centrifuged at 12,000 rpm for 15 min at 4 °C. 10 µL of the supernatant were mixture with 180 µL of 80 mM PBS (pH 5.4) without HTAB at 37 °C. Then, 20 µL of 0.017% $H_2O_2$ and 20 µL of 18.4 mM 3,3′,5,5′-tetramethylbenzidine were added to start the reaction.

Microtiter plates were incubated at 37 °C for 5 min. The reaction was stopped with the addition of 20 µL of $H_2SO_4$ (2M) and the Abs was measured a microplate reader using a BioTek Microplate Reader Synergy HT (BioTek Instruments, Winooski, VT, USA) at 405 nm. MPO activity was expressed as optical density/biopsy [54].

### *4.11. Histological Cuts*

Histological cuts were obtained as described elsewhere [55]. Briefly, ear specimens were fixed in solution of 10% formalin. Ears were dehydrated, embedded in paraffin, and sectioned. Five-µm sections were stained with hematoxylin-eosin. Infiltration of cells was evaluated in selected areas (10× and 20× objective).

### *4.12. Evaluation of Anti-Mycobacterial Activity by REMA (Resazurin Microtiter Assay)*

*Mycobacterium tuberculosis* H37Rv ATCC 27294 were cultivated in 7H9-glycerol-10% ADC-0.01% tyloxapol médium at 37 °C until reach 0.4 OPD. Stock solution of 4-EAEP was prepared in DMSO (10 mg/mL) and rifampin were used as reference drug (16–0.001 mg/mL). Plates were incubated for 6 days, and then 30 µL of 0.01% resazurin sodium salt (Sigma-Aldrich, St. Louis, MO, USA) were added to each well and re incubated for 2 days more. Colors were interpreted visually as blue (no growth), pink (growth) and MIC as the last well in which blue color were observed [47].

### *4.13. Evaluation of Cytotoxicity in Vero Cells*

Vero cell line from ATCC® CCL-81™ were cultured in RPMI 1640 medium (10% of FBS and non-essential aminoacids). 10,000 Vero cells per well were incubated for 24 h in 100 µL of RPMI medium. After that, these cells were washed and new fresh medium with compounds at different concentrations was added and incubated for 48 h (37 °C and 5% $CO_2$ atmosphere), after, 10 mL of MTT (5 mg/mL) were add to each well and re incubated for 4 h. The medium was removed and 100 µL of DMSO were used to solubilize the formazan. Abs were determinate at 570 nm and cytotoxicity were calculated as % = $(1 - (Abs_{sample}/Abs_{control})) \times 100$ [56].

### *4.14. Statistical Analysis*

All data were represented as mean ± standard error (SEM). Data were analyzed by one-way ANOVA followed by Tukey's test. $IC_{50}$, was estimated by means of a linear regression.

## 5. Conclusions

We reporting two new compounds, epoxypinocembrin chalcone, and an ε-caprolactone derivative, as well as nine known compounds isolated from a red propolis from Chiapas, México. The propolis extract showed high capacity to prevent lipid peroxidation, being the active principles 3,3-dimethylallyl caffeate and isopent-3-enyl caffeate. Moreover, the extract showed an anti-oxidant activity at low concentrations in two models, mainly associated with izalpinin and pinocembrin, since these reduced the high ROS levels of mast cells, induced by the cross-linking of the antigen with the IgE antibody and its high affinity receptor FcεRI, that are involved in acute allergic inflammatory reactions. Also, the propolis extract and pinocembrin showed anti-inflammatory activity in the model of TPA dependent on the activation of neutrophils and macrophages. For this reason, this study supports that the use of standardized propolis extracts could be useful for the treatment of chronic degenerative inflammatory processes such as allergy and asthma.

**Acknowledgments:** This work was supported by Project IN210016 PAPIIT-UNAM and by Project Nuevas Alternativas de Tratamiento para Enfermedades Infecciosas, of IIB, UNAM. A part of the NMR analysis was made in the LURMN of Instituto de Química. The authors also would like to thank Beatriz Quiroz, Ma. del Rocío Patiño, Luis Velasco, Javier Pérez, María del C. García, Erika Segura, Claudia Rivera Cerecedo, Héctor Malagón Rivero and Daniela Rodríguez Montaño for technical assistance. To Pharmacobiology Department of Cinvestav and M.Sc. Alfredo Ibarra Sánchez by generated all cells needed for the study and take the electron micrographs of mast cells.

**Author Contributions:** Silvia Laura Guzmán-Gutiérrez wrote the paper and performed the chemical analysis and spectroscopic elucidation of the compounds' structure; Antonio Nieto-Camacho did TPA, TBARS, DPPH and MPO experiments; Jorge Iván Castillo-Arellano accomplished mast cells experiments and contributed with the writing of the article; Elizabeth Huerta-Salazar performed the spectroscopic analysis; Griselda Hernández-Pasteur worked in the isolation of the compounds; Mayra Silva-Miranda implemented the anti-mycobacterial activity; Omar Argüello-Nájera was the collector of propolis and contributed with the writing of the article; Omar Sepúlveda-Robles supported the HPLC analysis and the writing of the article; Clara Inés Espitia and Ricardo Reyes-Chilpa conceived and designed the experiments and reviewed writing of the article at all stages. The latter also contributed to spectroscopic elucidation of the compounds' structure.

**Conflicts of Interest:** The authors declare no conflicts of interest.

## References


1. Bankova, V.S.; de Castro, S.L.; Marcucci, M.C. Propolis: Recent advances in chemistry and plant origin. *Apidologie* **2000**, *31*, 3–15. [CrossRef]
2. Kubina, R.; Kabala-Dzik, A.; Dziedzic, A.; Bielec, B.; Wojtyczka, R.D.; Buldak, R.J.; Wyszynska, M.; Stawiarska-Pieta, B.; Szaflarska-Stojko, E. The Ethanol Extract of Polish Propolis Exhibits Anti-Proliferative and/or Pro-Apoptotic Effect on HCT 116 Colon Cancer and Me45 Malignant Melanoma Cells In Vitro Conditions. *Adv. Clin. Exp. Med.* **2015**, *24*, 203–212. [CrossRef] [PubMed]
3. Orsolic, N.; Saranovic, A.B.; Basic, I. Direct and indirect mechanism(s) of antitumour activity of propolis and its polyphenolic compounds. *Planta Med.* **2006**, *72*, 20–27. [CrossRef] [PubMed]
4. Bankova, V.; Boudourova-Krasteva, G.; Sforcin, J.M.; Frete, X.; Kujumgiev, A.; Maimoni-Rodella, R.; Popov, S. Phytochemical evidence for the plant origin of Brazilian propolis from Sao Paulo state. *Z. Naturforsch. C* **1999**, *54*, 401–405. [CrossRef] [PubMed]
5. Bueno-Silva, B.; Marsola, A.; Ikegaki, M.; Alencar, S.M.; Rosalen, P.L. The effect of seasons on Brazilian red propolis and its botanical source: Chemical composition and antibacterial activity. *Nat. Prod. Res.* **2017**, *31*, 1318–1324. [CrossRef] [PubMed]
6. Toreti, V.C.; Sato, H.H.; Pastore, G.M.; Park, Y.K. Recent progress of propolis for its biological and chemical compositions and its botanical origin. *Evid. Based Complement. Altern. Med.* **2013**, *2013*, 697390. [CrossRef] [PubMed]
7. Alday, E.; Valencia, D.; Carreno, A.L.; Picerno, P.; Piccinelli, A.L.; Rastrelli, L.; Robles-Zepeda, R.; Hernandez, J.; Velazquez, C. Apoptotic induction by pinobanksin and some of its ester derivatives from Sonoran propolis in a B-cell lymphoma cell line. *Chem. Biol. Interact.* **2015**, *242*, 35–44. [CrossRef] [PubMed]
8. Alday-Provencio, S.; Diaz, G.; Rascon, L.; Quintero, J.; Alday, E.; Robles-Zepeda, R.; Garibay-Escobar, A.; Astiazaran, H.; Hernandez, J.; Velazquez, C. Sonoran propolis and some of its chemical constituents inhibit in vitro growth of Giardia lamblia trophozoites. *Planta Med.* **2015**, *81*, 742–747. [CrossRef] [PubMed]
9. Hernandez, J.; Goycoolea, F.M.; Quintero, J.; Acosta, A.; Castaneda, M.; Dominguez, Z.; Robles, R.; Vazquez-Moreno, L.; Velazquez, E.F.; Astiazaran, H.; et al. Sonoran propolis: Chemical composition and antiproliferative activity on cancer cell lines. *Planta Med.* **2007**, *73*, 1469–1474. [CrossRef] [PubMed]
10. Vargas-Sanchez, R.D.; Torrescano-Urrutia, G.R.; Acedo-Felix, E.; Carvajal-Millan, E.; Gonzalez-Cordova, A.F.; Vallejo-Galland, B.; Torres-Llanez, M.J.; Sanchez-Escalante, A. Antioxidant and antimicrobial activity of commercial propolis extract in beef patties. *J. Food Sci.* **2014**, *79*, C1499–C1504. [CrossRef] [PubMed]
11. Bankova, V.; Popova, M.; Bogdanov, S.; Sabatini, A.G. Chemical composition of European propolis: Expected and unexpected results. *Z. Naturforsch. C* **2002**, *57*, 530–533. [CrossRef] [PubMed]
12. Marcucci, M.C.; Ferreres, F.; Garcia-Viguera, C.; Bankova, V.S.; De Castro, S.L.; Dantas, A.P.; Valente, P.H.; Paulino, N. Phenolic compounds from Brazilian propolis with pharmacological activities. *J. Ethnopharmacol.* **2001**, *74*, 105–112. [CrossRef]
13. Bankova, V. Recent trends and important developments in propolis research. *Evid. Based Complement. Alternat. Med.* **2005**, *2*, 29–32. [CrossRef] [PubMed]
14. Cuesta-Rubio, O.; Frontana-Uribe, B.A.; Ramirez-Apan, T.; Cardenas, J. Polyisoprenylated benzophenones in cuban propolis; biological activity of nemorosone. *Z. Naturforsch. C* **2002**, *57*, 372–378. [CrossRef] [PubMed]
15. Valcic, S.; Montenegro, G.; Timmermann, B.N. Lignans from Chilean propolis. *J. Nat. Prod.* **1998**, *61*, 771–775. [CrossRef] [PubMed]

16. Wang, Y.J. Phase II Study of Pinocembrin Injection to Treat Ischemic Stroke—Randomized, Double-blind, Placebo-Controlled, Multicenter Study. Available online: https://clinicaltrials.gov/ct2/show/NCT02059785?term=pinocembrin&rank=1 (accessed on 28 November 2017 ).
17. Kabala-Dzik, A.; Rzepecka-Stojko, A.; Kubina, R.; Jastrzebska-Stojko, Z.; Stojko, R.; Wojtyczka, R.D.; Stojko, J. Comparison of Two Components of Propolis: Caffeic Acid (CA) and Caffeic Acid Phenethyl Ester (CAPE) Induce Apoptosis and Cell Cycle Arrest of Breast Cancer Cells MDA-MB-231. *Molecules* **2017**, *22*, 1554. [CrossRef] [PubMed]
18. Li, F.; Awale, S.; Tezuka, Y.; Esumi, H.; Kadota, S. Study on the constituents of Mexican propolis and their cytotoxic activity against PANC-1 human pancreatic cancer cells. *J. Nat. Prod.* **2010**, *73*, 623–627. [CrossRef] [PubMed]
19. Li, F.; He, Y.M.; Awale, S.; Kadota, S.; Tezuka, Y. Two new cytotoxic phenylallylflavanones from Mexican propolis. *Chem. Pharm. Bull.* **2011**, *59*, 1194–1196. [CrossRef] [PubMed]
20. Lotti, C.; Campo Fernandez, M.; Piccinelli, A.L.; Cuesta-Rubio, O.; Márquez Hernández, I.; Rastrelli, L. Chemical Constituents of Red Mexican Propolis. *J. Agric. Food Chem.* **2010**, *58*, 2209–2213. [CrossRef] [PubMed]
21. Colegate, S.M.; Din, L.B.; Ghisalberti, E.L.; Latiff, A. Tepanone, a retrochalcone from Ellipeia cuneifolia. *Phytochemistry* **1992**, *31*, 2123–2126. [CrossRef]
22. Huang, W.-Z.; Zhang, C.-F.; Zhang, M.; Wang, Z.-T. A New Biphenylpropanoid from Alpinia Katsumadai. *J. Chin. Chem. Soc.* **2007**, *54*, 1553–1556. [CrossRef]
23. Mazur, P.; Meyers, H.V.; Nakanishi, K.; El-Zayat, A.A.E.; Champe, S.P. Structural elucidation of sporogenic fatty acid metabolites from aspergillus nidulans. *Tetrahedron Lett.* **1990**, *31*, 3837–3840. [CrossRef]
24. Řezanka, T.; Dembitsky, V.M. γ-Lactones from the soft corals Sarcophyton trocheliophorum and Lithophyton arboreum. *Tetrahedron* **2001**, *57*, 8743–8749. [CrossRef]
25. Liu, R.; Gao, M.; Yang, Z.H.; Du, G.H. Pinocembrin protects rat brain against oxidation and apoptosis induced by ischemia-reperfusion both in vivo and in vitro. *Brain Res.* **2008**, *1216*, 104–115. [CrossRef] [PubMed]
26. Sala, A.; Recio, M.C.; Schinella, G.R.; Manez, S.; Giner, R.M.; Cerda-Nicolas, M.; Rosi, J.L. Assessment of the anti-inflammatory activity and free radical scavenger activity of tiliroside. *Eur. J. Pharmacol.* **2003**, *461*, 53–61. [CrossRef]
27. Calderón-Cisneros, A.; Soto-Pinto, L. Transformaciones agrícolas en el contexto periurbano de la ciudad de San Cristóbal de Las Casas, Chiapas. *LiminaR* **2014**, *12*, 125–143.
28. Popova, M.; Giannopoulou, E.; Skalicka-Wozniak, K.; Graikou, K.; Widelski, J.; Bankova, V.; Kalofonos, H.; Sivolapenko, G.; Gawel-Beben, K.; Antosiewicz, B.; et al. Characterization and Biological Evaluation of Propolis from Poland. *Molecules* **2017**, *22*, 1159. [CrossRef] [PubMed]
29. García-Viguera, C.; Ferreres, F.; Tomás-Barberán, F.A. Study of Canadian Propolis by GC-MS and HPLC. *Z. Naturforsh.* **1993**, *48c*, 731–735.
30. Uzel, A.; Sorkun, K.; Oncag, O.; Cogulu, D.; Gencay, O.; Salih, B. Chemical compositions and antimicrobial activities of four different Anatolian propolis samples. *Microbiol. Res.* **2005**, *160*, 189–195. [CrossRef] [PubMed]
31. Sánchez-Valle, V.; Méndez-Sánchez, N. Estrés oxidativo, antioxidantes y enfermedad. *Rev. Investig. Med. Sur.* **2013**, *20*, 161–168.
32. Hausen, B.M.; Wollenweber, E. Propolis allergy. (III). Sensitization studies with minor constituents. *Contact Dermat.* **1988**, *19*, 296–303. [CrossRef]
33. Hausen, B.M.; Wollenweber, E.; Senff, H.; Post, B. Propolis allergy. (II). The sensitizing properties of 1,1-dimethylallyl caffeic acid ester. *Contact Dermat.* **1987**, *17*, 171–177. [CrossRef]
34. Itoh, T.; Tsukane, M.; Koike, M.; Nakamura, C.; Ohguchi, K.; Ito, M.; Akao, Y.; Koshimizu, S.; Nozawa, Y.; Wakimoto, T.; et al. Inhibitory effects of whisky congeners on IgE-mediated degranulation in rat basophilic leukemia RBL-2H3 cells and passive cutaneous anaphylaxis reaction in mice. *J. Agric. Food Chem.* **2010**, *58*, 7149–7157. [CrossRef] [PubMed]
35. Nakamura, R.; Nakamura, R.; Watanabe, K.; Oka, K.; Ohta, S.; Mishima, S.; Teshima, R. Effects of propolis from different areas on mast cell degranulation and identification of the effective components in propolis. *Int. Immunopharmacol.* **2010**, *10*, 1107–1112. [CrossRef] [PubMed]
36. Khayyal, M.T.; El-Ghazaly, M.A.; El-Khatib, A.S.; Hatem, A.M.; de Vries, P.J.; el-Shafei, S.; Khattab, M.M. A clinical pharmacological study of the potential beneficial effects of a propolis food product as an adjuvant in asthmatic patients. *Fundam. Clin. Pharmacol.* **2003**, *17*, 93–102. [CrossRef] [PubMed]

37. Lan, X.; Wang, W.; Li, Q.; Wang, J. The Natural Flavonoid Pinocembrin: Molecular Targets and Potential Therapeutic Applications. *Mol. Neurobiol.* **2016**, *53*, 1794–1801. [CrossRef] [PubMed]
38. Patel, N.K.; Jaiswal, G.; Bhutani, K.K. A review on biological sources, chemistry and pharmacological activities of pinostrobin. *Nat. Prod. Res.* **2016**, *30*, 2017–2027. [CrossRef] [PubMed]
39. Bertelli, D.; Papotti, G.; Bortolotti, L.; Marcazzan, G.L.; Plessi, M. (1) H-NMR simultaneous identification of health-relevant compounds in propolis extracts. *Phytochem. Anal.* **2012**, *23*, 260–266. [CrossRef] [PubMed]
40. Muñoz, O.; Pena, R.C.; Ureta, E.; Montenegro, G.; Caldwell, C.; Timmermann, B.N. Phenolic compounds of propolis from Central Chilean matorral. *Z. Naturforsch. C* **2001**, *56*, 273–277. [CrossRef] [PubMed]
41. Kelley, C.J.; Harruff, R.C.; Carmack, M. Polyphenolic acids of Lithospermum ruderale. II. Carbon-13 nuclear magnetic resonance of lithospermic and rosmarinic acids. *J. Org. Chem.* **1976**, *41*, 449–455. [CrossRef]
42. Mattarei, A.; Biasutto, L.; Rastrelli, F.; Garbisa, S.; Marotta, E.; Zoratti, M.; Paradisi, C. Regioselective *O*-derivatization of quercetin via ester intermediates. An improved synthesis of rhamnetin and development of a new mitochondriotropic derivative. *Molecules* **2010**, *15*, 4722–4736. [CrossRef] [PubMed]
43. Abdullah, N.H.; Salim, F.; Ahmad, R. Chemical Constituents of Malaysian U. cordata var. ferruginea and Their in Vitro alpha-Glucosidase Inhibitory Activities. *Molecules* **2016**, *21*, 525. [CrossRef] [PubMed]
44. Kartal, M.; Yildiz, S.; Kaya, S.; Kurucu, S.; Topcu, G. Antimicrobial activity of propolis samples from two different regions of Anatolia. *J. Ethnopharmacol.* **2003**, *86*, 69–73. [CrossRef]
45. Jeong, C.-H.; Jeong, H.R.; Choi, G.N.; Kim, D.-O.; Lee, U.; Heo, H.J. Neuroprotective and anti-oxidant effects of caffeic acid isolated from Erigeron annuus leaf. *Chin. Med.* **2011**, *6*, 25. [CrossRef] [PubMed]
46. Ching, A.Y.L.; Wang, T.S.; Sukari, M.A.; Lian, G.E.C.; Rahmani, M.; Khalid, K. Characterization of flavonoid derivatives from *Boesenbergia rotunda* (L.). *Malays. J. Anal. Sci.* **2007**, *11*, 154–159.
47. Palomino, J.C.; Martin, A.; Camacho, M.; Guerra, H.; Swings, J.; Portaels, F. Resazurin microtiter assay plate: Simple and inexpensive method for detection of drug resistance in Mycobacterium tuberculosis. *Antimicrob. Agents Chemother.* **2002**, *46*, 2720–2722. [CrossRef] [PubMed]
48. Ma, X.M.; Liu, Y.; Shi, Y.P. Phenolic derivatives with free-radical-scavenging activities from Ixeridium gracile (DC.) Shih. *Chem. Biodivers.* **2007**, *4*, 2172–2181. [CrossRef] [PubMed]
49. de Aguiar, S.C.; Zeoula, L.M.; Franco, S.L.; Peres, L.P.; Arcuri, P.B.; Forano, E. Antimicrobial activity of Brazilian propolis extracts against rumen bacteria in vitro. *World J. Microbiol. Biotechnol.* **2013**, *29*, 1951–1959. [CrossRef] [PubMed]
50. Dominguez, M.; Nieto, A.; Marin, J.C.; Keck, A.S.; Jeffery, E.; Cespedes, C.L. Antioxidant activities of extracts from Barkleyanthus salicifolius (Asteraceae) and Penstemon gentianoides (Scrophulariaceae). *J. Agric. Food Chem.* **2005**, *53*, 5889–5895. [CrossRef] [PubMed]
51. Esterbauer, H.; Cheeseman, K.H. Determination of aldehydic lipid peroxidation products: Malonaldehyde and 4-hydroxynonenal. *Methods Enzymol.* **1990**, *186*, 407–421. [PubMed]
52. Martin-Avila, A.; Medina-Tamayo, J.; Ibarra-Sanchez, A.; Vazquez-Victorio, G.; Castillo-Arellano, J.I.; Hernandez-Mondragon, A.C.; Rivera, J.; Madera-Salcedo, I.K.; Blank, U.; Macias-Silva, M.; et al. Protein Tyrosine Kinase Fyn Regulates TLR4-Elicited Responses on Mast Cells Controlling the Function of a PP2A-PKCalpha/beta Signaling Node Leading to TNF Secretion. *J. Immunol.* **2016**, *196*, 5075–5088. [CrossRef] [PubMed]
53. Rao, Y.K.; Fang, S.H.; Tzeng, Y.M. Anti-inflammatory activities of flavonoids isolated from Caesalpinia pulcherrima. *J. Ethnopharmacol.* **2005**, *100*, 249–253. [CrossRef] [PubMed]
54. Marin-Loaiza, J.C.; Nieto-Camacho, A.; Cespedes, C.L. Antioxidant and anti-inflammatory activities of Pittocaulon species from Mexico. *Pharm. Biol.* **2013**, *51*, 260–266. [CrossRef] [PubMed]
55. Mescher, A.L. *Junqueira's Basic Histology: Text and Atlas*, 13th ed.; McGraw-Hill Education: New York, NY, USA, 2013; p. 520.
56. Mosmann, T. Rapid colorimetric assay for cellular growth and survival: Application to proliferation and cytotoxicity assays. *J. Immunol. Methods* **1983**, *65*, 55–63. [CrossRef]


**Sample Availability:** Not available.

International Immunopharmacology 64 (2018) 298–307

Contents lists available at ScienceDirect

International Immunopharmacology

journal homepage: www.elsevier.com/locate/intimp

# Anandamide inhibits FcεRI-dependent degranulation and cytokine synthesis in mast cells through $CB_2$ and GPR55 receptor activation. Possible involvement of $CB_2$-GPR55 heteromers

Silvia L. Cruz[a,*], Elizabeth Sánchez-Miranda[a,b,1], Jorge Ivan Castillo-Arellano[a,1], Rodolfo Daniel Cervantes-Villagrana[a], Alfredo Ibarra-Sánchez[a], Claudia González-Espinosa[a,*]

[a] Departamento de Farmacobiología, Centro de Investigación y de Estudios Avanzados del Instituto Politécnico Nacional (Cinvestav), Sede Sur, Mexico
[b] Departamento de Sistemas Biológicos, Universidad Autónoma Metropolitana Xochimilco, Mexico City, Mexico

ARTICLE INFO

*Keywords:*
Endocannabinoids
Anandamide (AEA)
Anaphylactic degranulation
FcεRI
Mast cell
GPR55 receptors
Calcium rise
GPCR heterodimers

ABSTRACT

Activation of high affinity receptor for IgE (FcεRI) by IgE/antigen complexes in mast cells (MCs) leads to the release of preformed pro-inflammatory mediators stored in granules by a $Ca^{2+}$-dependent process known as anaphylactic degranulation. Degranulation inhibition has been proposed as a strategy to control allergies and chronic inflammation conditions. Cannabinoids are important inhibitors of inflammatory reactions but their effects on IgE/Ag-mediated MCs responses are not well described. In this study, we analyzed the effect of the endocannabinoid anandamide (AEA), the selective $CB_2$ receptor agonist HU308, and the GPR55 receptor agonist lysophosphatidylinositol (LPI) on FcεRI-induced activation in murine bone marrow-derived mast cells (BMMCs). Our results show that AEA, HU380 and LPI inhibited FcεRI-induced degranulation in a concentration-dependent manner. This effect was mediated by $CB_2$ and GPR55 receptor activation through a mechanism insensitive to pertussis toxin. Degranulation inhibition was prevented by $CB_2$ and GPR55 antagonism, but not by $CB_1$ receptor blockage. AEA also inhibited calcium-dependent cytokine mRNA synthesis induced by FcεRI crosslinking, without affecting early phosphorylation events. In addition, AEA, HU308 and LPI inhibited intracellular $Ca^{2+}$ rise in response to IgE/Ag. $CB_2$ and GPR55 receptor antagonism could not prevent the inhibition produced by AEA and HU308, but partially blocked the one caused by LPI. These results indicate that AEA inhibits IgE/Ag-induced degranulation through a mechanism that includes the participation of $CB_2$ and GPR55 receptors acting in close crosstalk, and show that $CB_2$-GPR55 heteromers are important negative regulators of FcεRI-induced responses in MCs.

## 1. Introduction

Endocannabinoids are polyunsaturated fatty acids synthesized on demand upon distinct physiological stimuli. Arachidonoyl ethanolamine (AEA or anandamide) and 2-arachidonoylglycerol (2-AG) are the best-characterized members of this group [1,2]. Endocannabinoids bind with different affinities to classical $CB_1$ and $CB_2$ receptors coupled to $G_{i/o}$ proteins causing adenylyl cyclase activity inhibition, increased potassium channels conductance and decreased conductance of calcium channels. In addition, $CB_1$ and $CB_2$ receptors regulate phosphorylation and activation of mitogen activated protein kinases (MAPKs) [3]. Endocannabinoids modulate distinct innate and adaptive immune functions [4], including prostaglandin production during inflammation [5], T and B cell proliferation [6–8], neutrophil degranulation and chemotaxis [9], and cytokine production in activated leukocytes [10]. Although many endocannabinoid effects in immune cells are mediated by $CB_1$ and $CB_2$ receptors [11,12], some others are not [13]. In particular, AEA blocks T-type and L-type $Ca^{2+}$ channels [14,15], acts as a partial

*Abbreviations:* AEA, anandamide; BMMCs, bone marrow-derived mast cells; FcεRI, high affinity IgE receptor; 2-AG, 2-arachidonoylglycerol; DNP-HSA, dinitrophenol coupled to human serum albumin (antigen); IgE, immunoglobulin E; TNF, Tumor Necrosis Factor; IL, interleukin; CB, cannabinoid receptor; PKC, protein kinase C; LPI, lysophosphatidylinositol; PI3K, phosphoinositide 3-kinase; $TRPV_1$, transient receptor potential cation channel, subfamily V member 1; NFAT, nuclear factor of activated T-cells

* Corresponding authors at: Departamento de Farmacobiología, Centro de Investigación y de Estudios Avanzados (Cinvestav), Sede Sur, Calzada de los Tenorios 235, Col. Granjas Coapa, CP 14330 Mexico City, Mexico.
*E-mail addresses:* slcruzm@cinvestav.mx (S.L. Cruz), cgonzal@cinvestav.mx (C. González-Espinosa).
[1] ESM and JICA equally contributed to this work.

https://doi.org/10.1016/j.intimp.2018.09.006
Received 24 December 2017; Received in revised form 4 September 2018; Accepted 6 September 2018

$TRPV_1$ agonist [16], and activates PPAR [17] and GPR55 receptors [18].

Mast cells (MCs) have an important role in the physiopathology of inflammation [19,20]. They are well known initiators of allergic reactions due to the presence of the high affinity IgE receptor (FcεRI) on their cellular membrane, and secrete a number of pro-inflammatory and immunoregulatory mediators after activation [21,22]. Intensive research, directed to identify compounds able to inhibit IgE/Ag-induced MCs activation, has been conducted worldwide to better cope with the important burden of allergic diseases [23–25]. IgE/Ag-mediated cross-linking of FcεRI activates a complex signaling cascade that involves the Src family kinases Lyn and Fyn [26,27]. In turn, phosphorylation of specific substrates and the formation of multiple protein aggregates lead to the release of preformed mediators stored in granules in a PKC- and calcium-dependent process known as anaphylactic degranulation [28,29]. In addition to granule content exocytosis, the rise in intracellular $Ca^{2+}$ concentration $[Ca^{2+}]_i$ contributes to the activation of specific transcription factors (such as NFAT, AP-1 and NFκB), inducing cytokine mRNA synthesis and cytokine secretion [30–32]. Like other cells in the immune system, MCs respond to endocannabinoids and express cannabinoid receptors [33]. It is assumed that the anti-inflammatory effects of cannabinoids used for the treatment of MCs-associated diseases, such as pain and inflammation [34], arthritis [35], colitis [36], ocular disease [37] and atopic dermatitis [38], are related to MC activity inhibition. Although it is known that endocannabinoids regulate MC maturation [39] and inhibit mediator secretion [40,41], a detailed description of the effects of cannabinoids on MCs, and the identification of the molecular targets of those compounds is far from complete.

The objectives of this work were to study the effects of AEA on IgE/Ag-induced degranulation of bone marrow-derived mast cells (BMMCs) and to determine the role of cannabinoid receptors and $Ca^{2+}$ mobilization on these effects. This research shows that AEA inhibits BMMCs degranulation by mechanisms involving both $CB_2$ and GPR55 receptor activation.

## 2. Materials and methods

### 2.1. Drugs

The following compounds were used in this study and bought from Sigma-Aldrich (St. Louis, MO, USA): Anandamide, AM251 ($CB_1$ receptor antagonist and GPR55 agonist), AM630 ($CB_2$ receptor antagonist), HU308 ($CB_2$ agonist), LPI (GPR55 agonist), ML193 (GPR55 antagonist), AMG9810 ($TRPV_1$ receptor antagonist), A23187 (calcium ionophore), Fura-2AM, the thrombin receptor activator peptide 6 (TRAP-6), dinitrophenol coupled to human serum albumin (DNP-HSA, Ag), monoclonal anti-DNP IgE (SPE-7 clone), bovine serum albumin (BSA), phorbol-myristate-acetate (PMA), ethylene glycol-bis (β-aminoethyl-ether)-*N*,*N*,*N*′,*N*′-tetracetic acid (EGTA), triton X-100, and $CaCl_2$ were obtained from Merck and IL-3 and stem cell factor (SCF) from Peprotech. Anandamide, AM251 and AM630 were initially dissolved in absolute ethanol and then diluted with deionized water until maximal ethanol concentration in cell samples was 0.05%. AMG9810, A23187, Fura-2AM, ML193, and PMA were dissolved in dimethyl sulfoxide (DMSO) and diluted until maximal DMSO concentration in cell samples was 0.05%. Stock of HU308 was prepared in ethanol and diluted in Tyrode's buffer. Stock of LPI was dissolved in a mixture of chloroform: methanol: water 70:27:3 and diluted in Tyrode's buffer to final concentration. DNP-HSA, EGTA, Triton X-100, anti-DNP antibody and TRAP-6 were dissolved in deionized water.

### 2.2. Antibodies

Antibodies (Abs) against p-Tyr (Cat. No. 9411) and p-Src (Tyr 416, Cat No. 2101) were bought from Cell Signaling. Abs against PLCγ1 (Cat No. sc7290), Syk (Cat No. sc1077) and Lyn (Cat No. sc15) were purchased from Santa Cruz Biotechnology. Primary antibodies from Cell Signaling were used at 1:5000 dilution and those from Santa Cruz Biotechnology, at 1:1000. Secondary antibodies were obtained from Millipore and used at 1:15000.

### 2.3. Mice, cell culture and IgE sensitization

BMMCs were differentiated from bone marrow obtained from tibias of C57BL/6J mice (stock No. 000664, Jackson Laboratory, Maine, USA). For data shown on Fig. 5B and C, BMMCs from 129S1/SvlmJ WT (stock No. 002448) and $Fyn^{-/-}$ (stock No. 002271) from Jackson Laboratory were used, as previously described [31]. The protocol for BMMCs generation was approved by the Cinvestav Institutional Committee for the Care and Use of Laboratory Animals (CICUAL, protocol 074-13), following the rules of the Mexican Official Norm for the use and care of laboratory animals (NOM-062-ZOO-1999). Bone marrow was cultured in RPMI 1640 media supplemented with 50 μM β-mercaptoethanol, 25 mM HEPES pH 7.4, 1 mM pyruvate, 20 ng/mL IL-3, 10 ng/mL SCF, antibiotic/antimycotic, non-essential aminoacids and 10% FBS during four to six weeks. BMMCs development was followed by flow cytometry using an anti IgE monoclonal antibody (BD Biosciences) and only cultures showing > 98% FcεRI-positive cells were used for the experiments. For all the experiments BMMCs were sensitized with 300 ng/mL of an IgE anti-dinitrophenol (DNP) monoclonal antibody (Clone SPE-7, SIGMA) overnight at 37 °C. For cytokine mRNA detection, cells were sensitized for 24 h with 100 ng/mL of the same monoclonal IgE. In all cases, unbound antibody was removed by collecting the cells through centrifugation and re-suspension in the corresponding buffer depending on the assay.

### 2.4. Degranulation assay

One million IgE-sensitized cells were centrifuged at 500 × *g* during 5 min and suspended in 1 mL Tyrode's/BSA buffer of the following composition: 20 mM HEPES pH 7.4, 135 mM NaCl, 5 mM KCl, 1.8 mM $CaCl_2$, 1 mM $MgCl_2$, 5.6 mM glucose and 0.05% bovine serum albumin (BSA). Independent groups of cells were treated with vehicle, 2.5, 10, 25 or 50 μM AEA for 15 min and then stimulated with antigen (1, 3, 9, or 27 ng/mL DNP-HSA) during 30 min at 37 °C. After this treatment, cells were placed on ice for 2 min and centrifuged to 12,000 × *g* for 10 min at 4 °C. Sixty microliters of supernatant or 20 μL of Triton-treated cell pellet were placed in an ELISA plate containing 40 μL of 1 mM *p*-nitrophenyl-*N*-acetyl-β-D-glucosaminide (PNAG), and incubated for 1 h at 37 °C before the addition of 120 μL of "stop" solution ($Na_2CO_3$ 0.1 M/$Na_2HCO_3$ 0.1 M). β-Hexosaminidase release was quantified by spectrophotometry in an ELISA plate reader (Tecan Sunrise) at 405 nm, as described [42].

### 2.5. Viability test

To determine the viability of the cells, the Muse™ Count Viability Kit from Millipore was used. Briefly, 1.5 million IgE-sensitized BMMCs were treated with AEA at different concentrations during 15 min and the reagent MCH100102 (included in the kit) was added in a 1:20 dilution. The Viability Intuitive Software included in the analyzer generated the corresponding dot plot providing the percentage of live cells in each sample.

### 2.6. Determination of intracellular calcium concentration ($[Ca^{2+}]_i$)

Intracellular calcium concentrations ($[Ca^{2+}]_i$) were measured in IgE-sensitized BMMCs. To do this, cells were collected and suspended in Tyrode's/BSA buffer with 5 μM Fura 2-AM for 30 min at 37 °C to load it. Then, eight million of Fura 2-AM-loaded BMMCs were suspended in 2 mL Tyrode's/BSA buffer and placed in the cuvette of a

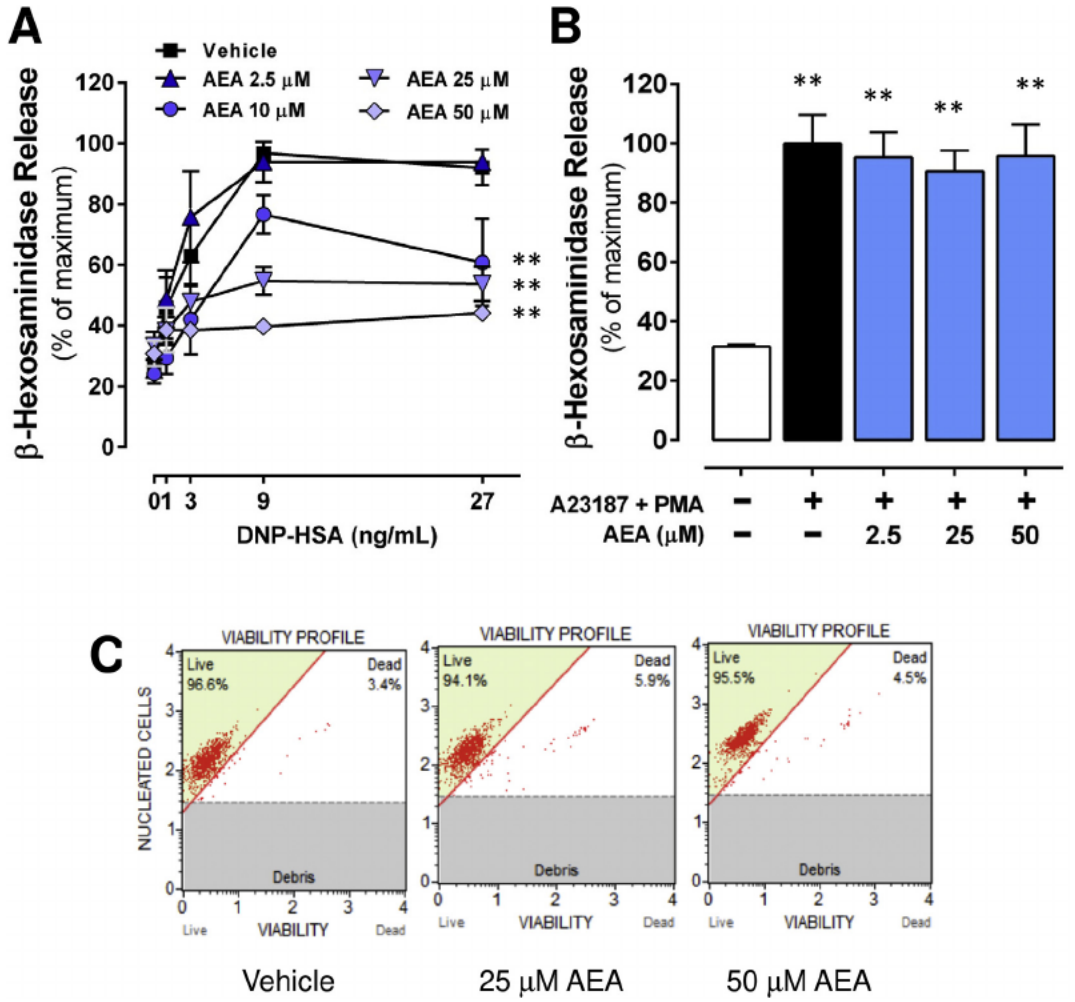


**Fig. 1.** Anandamide (AEA) inhibits IgE/Ag-induced but not calcium ionophore/PMA-induced β-hexosaminidase release in BMMCs. A. Independent groups of IgE-sensitized BMMCs were pre-treated with vehicle or AEA for 15 min and then stimulated with different concentrations of antigen (DNP-HSA) for 30 min at 37 °C. After this time, β-hexosaminidase activity was measured in the supernatant of stimulated cells. Each point represents the mean ± S.E.M. of 3 to 5 independent experiments. $^{**}p < 0.01$; one-way ANOVA followed by Dunnett's test *vs.* DNP/HSA (27 ng/mL). B. Cells were pre-treated as in A but were stimulated with a combination of the calcium ionophore A23187 (200 nM) and the PKC activator PMA (100 nM). β-Hexosaminidase release was measured 30 min after stimulation. Data shown are the mean ± S.E.M. of 3 to 5 independent experiments. $^{**}p < 0.01$, one-way ANOVA followed by Dunnett's test. C. Sample dot blots of cell viability after treatment with the vehicle, 25 μM and 50 μM AEA.

spectrofluorometer (Fluoromax 3 Jobin Yvon). Basal fluorescence was recorded during 100 s prior to any pharmacological treatment. $[Ca^{2+}]_i$ was calculated with the parameters and equation described in a previous work [31].

### 2.7. Semi-quantitative RT-PCR

Two million IgE-sensitized BMMCs were treated with inhibitors or IgE/Ag for different times and then lysed with TRIzol reagent (Sigma-Aldrich). RNA was isolated following the instructions included with the reagent and suspended in 7 μL of RNA secure solution (Ambion). Two micrograms of RNA were used for cDNA synthesis utilizing a cDNA synthesis kit from Thermo Scientific. Ten microliters from each cDNA synthesis reaction were used for the amplification of selected cytokines. The following primers were utilized: TNF, 5′-TTCTGTCTACTGAACTTCGGGGTGATCGGTCC-3′ (sense) and 5′-GTATGAGATAGCAAATCGGCTGACGGTGTGGG-3′ (antisense) [43]; IL-2, 5′-TTCAAGCTCCACTTCAAGCTCTACAGCGGAAG-3′ (sense) and 5′-GACAGAAGGCTATCCATCTCCTCAGAAAGTCC-3′ (antisense) [44]; IL-4, 5′-CCAGCTAGTTGTCATCCTGCTCTTCTTTCTCG-3′ (sense) and 5′-CAGTGATGTGGACTTGGACTCATTCATGGTGC-3′ (antisense) [44]; IL-6, 5′-ATGAAGTTCCTCTCTGCAAGAGACT-3′ (sense) and 5′-CACTAGGTTGCCGAGTAGATCTC-3′ (antisense) [45]; IL-3, 5′-GATACCCACCGTTTAACCAGAACGTTG-3′ (sense) and 5′-TCCACGGTTAGGAGAGACGGAG-3′ (antisense) [46]; IL-10, 5′-ATGCAGGACTTTAAG GGTTACTTGGGTT-3′ (sense) and 5′-ATTTCGGAGAGAGGTACAAACGAGGTTT-3′ (antisense) [47]; and GAPDH 5′-TGAAGGTCGGTGTGAACGGATTTGGC-3′ (sense) and 5′-CATGTAGGCCATGAGGTCCACCAC-3′ (antisense) [45]. Alignment temperatures were used as described in the correspondent references, and optimal cycle number for amplification in IgE/Ag-stimulated BMMCs was determined as reported previously [48]. The products were separated on 2% agarose gels with ethidium bromide dye and quantified utilizing a ChemiDoc (BioRad) equipment with the ImageLab 5.0 version program. For endocannabinoid receptor mRNA detection, pellets from two million sensitized cells were solubilized in 0.5 mL of TRI-Reagent (Sigma-Aldrich) at room temperature and total RNA was extracted following instructions suggested by the provider. First strand cDNA synthesis was generated with the Fermentas Life Sciences first-strand synthesis system. Primers for amplification: $CB_1$, forward, 5′-CGTGGGCAGCCTGTTCCTCA-3′; reverse, 5′-CATGCGGGCTTGGTCTGG3′ [49], $CB_2$, forward, 5′-CCGGAAAAGAGGATGGCAATGAAT-3′; reverse, 5′-CTGCTGAGCGCCCTGGAGAAC-3′, [49]; and GPR55, forward 5′-GGACTCATTGGTACTCCTAAGCTGT-3′; reverse, 5′-GCAGATCCCAAAGGTCTTCCT-3′ [50]. These primers were obtained from Sigma Aldrich. PCR conditions:

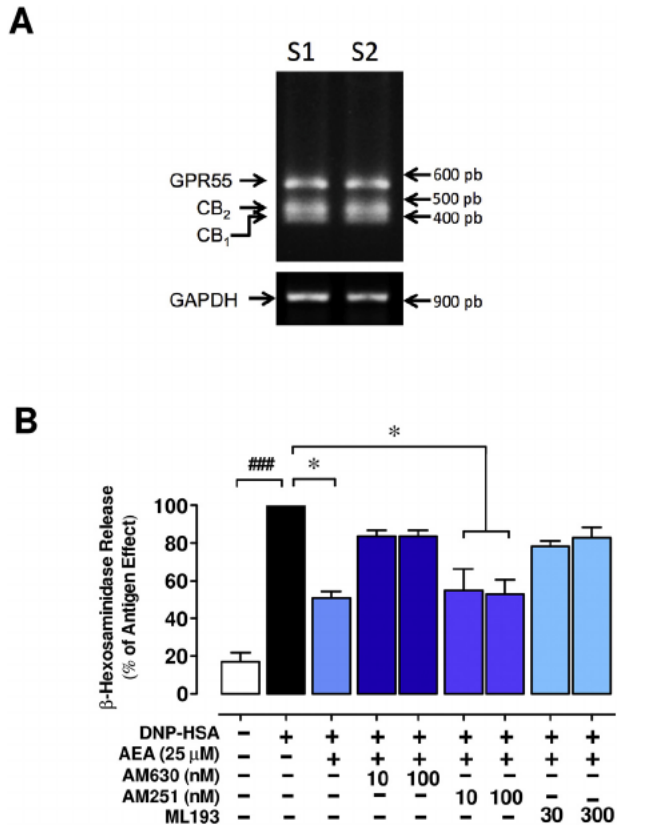


**Fig. 2.** AEA inhibits FcεRI-dependent degranulation by a mechanism that is independent of $CB_1$ receptors and $G_i$ proteins, but dependent on the activation of $CB_2$ and GPR55 receptors. A. Semi-quantitative RT-PCRs to detect $CB_1$, $CB_2$ and GPR55 receptors in BMMCs. Gel images show results obtained with two samples (S1 and S2) of cells from two independent BMMC cultures. B. Two million BMMCs were pre-incubated with different concentrations of AM251, AM630 or ML193 ($CB_1$, $CB_2$ and GPR55 receptor antagonists, respectively) for 15 min, then treated with vehicle or 25 μM AEA for 15 min and finally stimulated with DNP-HSA (27 ng/mL) for 30 min. After those treatments, β-hexosaminidase release was measured in the supernatant of stimulated cells. Data shown are the mean ± S.E.M. of 3 to 5 independent experiments. $^{###}p < 0.001$ *vs.* non-stimulated cells, Student's *t*-test; $^{*}p < 0.05$ *vs.* antigen-treated cells, one-way ANOVA followed by Dunnett's test.

95 °C for 10 min; 95 °C for 45 s, 60 °C for 1 min, 72 °C for 45 s and a final step of 72 °C for 7 min. Thirty amplification cycles were performed for the detection of cannabinoid receptors and 25 cycles was used for GAPDH. PCR products were separated on 2% TBE-agarose gels and dyed with ethidium bromide. Pictures of the gels were taken using the MiniBis Pro from BioImaging Systems.

### 2.8. Immunoprecipitation and western blot

Thirty million IgE-sensitized BMMCs stimulated in specific conditions were suspended in a lysis buffer containing 1% NP-40 (Igepal), 20 μg/mL leupeptin, 10 μg/mL pepstatin, 10 μg/mL aprotinin, 1 mM sodium pyrophosphate, 1 mM orthovanadate and 60 mM β-octylglucoside dissolved in PBS pH 7.4. Lysates were centrifuged at 14,000 ×*g* for 10 min at 4 °C and supernatants were kept frozen at −80 °C until use. Then, supernatants were quickly thawed and incubated overnight with 50 μL of protein A-Sepharose beads loaded with 10 μg of the corresponding primary antibodies (Abs) at 4 °C. Beads were then carefully recovered by centrifugation and washed three times with 500 μL of lysis buffer without β-octylglucoside. Beads were resuspended in 50 μL of Laemmli buffer, boiled during 5 min and centrifuged at low velocity for 5 min. Forty microliters of each sample were separated by denaturing 10 to 15% acrylamide gels and then transferred onto polyvinylidene fluoride (PVDF) membranes (Perkin Elmer, Akron, OH, USA). Membranes were blocked with 6% nonfat milk for 1 h in TBST buffer and washed once with TBST before the addition of primary Abs overnight. After several washes with TBST, blots were incubated with the appropriate dilutions of secondary Abs. Western blots were developed using the Immobilon Western Chemiluminescent HRP substrate from Millipore.

### 2.9. Statistical analysis

Results in graphs of β-hexosaminidase release are expressed as the mean ± S.E.M. of three to five independent experiments using distinct primary cell cultures. Representative traces taken from three independent experiments from distinct cell cultures are used to illustrate $Ca^{2+}$ mobilization data. Comparisons between two groups were performed using Student's *t*-test and comparisons among several experimental groups were conducted with a one-way or two-way analysis of variance (ANOVA) followed by Dunnett's post-hoc test. Statistical analyses were conducted using raw values, but some graphs are presented with normalized data for comparison purposes. SigmaPlot 11.0 was utilized for statistical analysis and GraphPad Prism 5 for graphics.

## 3. Results

### 3.1. AEA inhibits FcεRI-mediated degranulation of BMMCs in a concentration-dependent manner without altering degranulation machinery or cell viability

First, we assessed the effect of anandamide on BMMCs degranulation. Fig. 1A shows β-hexosaminidase release induced by different concentrations of the antigen (DNP-HSA) in BMMCs pre-treated with vehicle or AEA. As shown, maximal degranulation was obtained after 9 ng/mL of antigen in vehicle-treated cells. AEA pretreatment significantly inhibited antigen-induced degranulation in a concentration-dependent manner. This inhibition was almost complete at 50 μM AEA and occurred for a wide range of DNP concentrations. Fig. 1B depicts the release of β-hexosaminidase produced by the combined administration of the calcium ionophore A23187 and PKC activator PMA in cells treated with distinct amounts of AEA. The endocannabinoid had no effect on FcεRI-independent degranulation even at high concentrations, which suggests that AEA does not inhibit the events that occur after PKC activation and calcium mobilization triggering in BMMCs nor does it alter the general secretory machinery for anaphylactic degranulation. A viability test showed that AEA treatment did not compromise cell survival at any concentration tested (Fig. 1C).

### 3.2. Neither $TRPV_1$ nor TRPC3-6 receptors play a role in the anandamide-dependent inhibition of IgE/Ag-induced degranulation

It has been established that $TRPV_1$ channels are activated and desensitized by AEA at relatively high concentrations [16]. In order to determine if these channels were involved in the inhibitory effects of AEA observed in our experiments, we studied IgE/Ag-triggered degranulation in BMMCs pre-incubated with several concentrations of the $TRPV_1$ receptor antagonist AMG9810 alone, and in the presence of AEA. AMG9810 by itself did not affect the degranulation produced by DNP-HSA at any concentration (data not shown), and concentrations of 10–1000 nM AMG9810 did not prevent the inhibitory effect of AEA (Supplementary Fig. 1). On the other hand, it is known that activation of TRPC family channels after FcεRI triggering contributes to degranulation in mast cells [51,52]. To test the possible involvement of TRPC3-6 receptors on the inhibitory effects of AEA, we took advantage of the fact that those channels are not activated in BMMCs generated from Fyn kinase-deficient mice [51]. Therefore, we tested the effect of AEA in BMMCs derived from $Fyn^{-/-}$ mice stimulated with IgE/Ag.

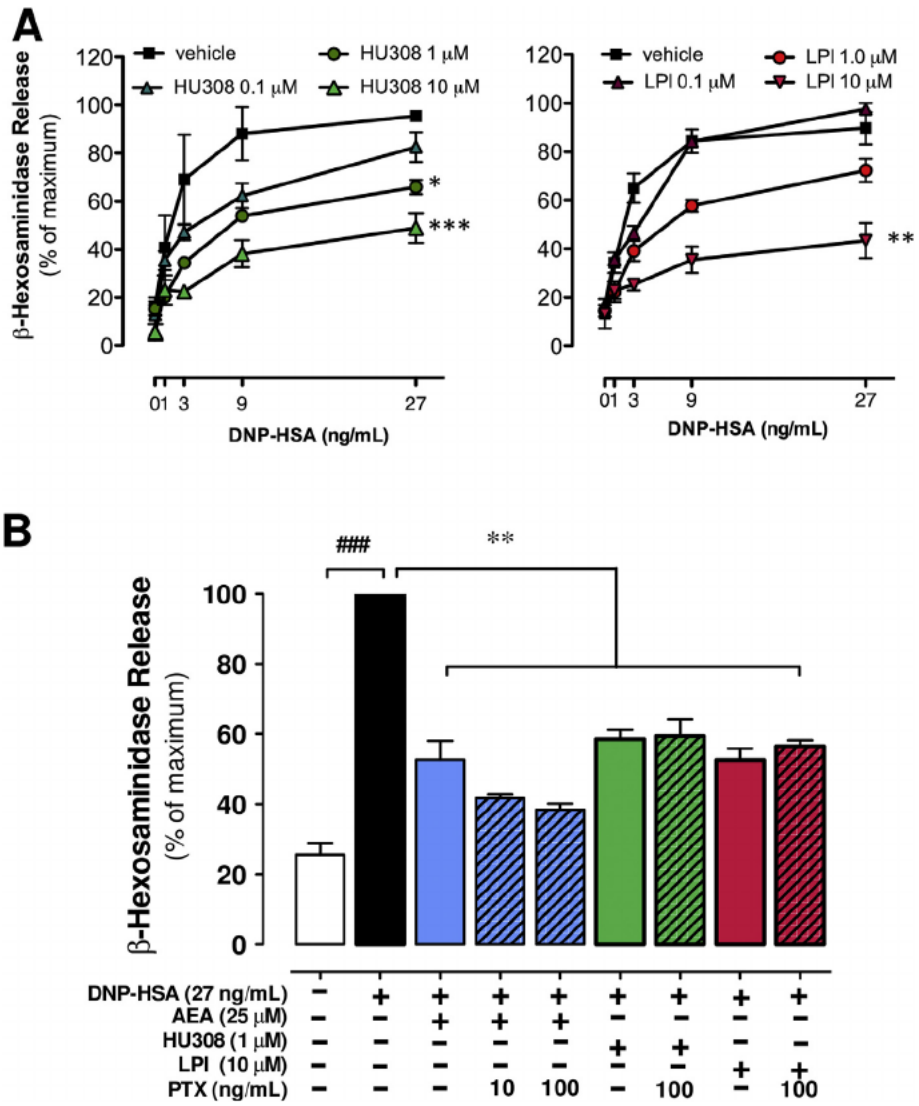


**Fig. 3.** AEA and LPI concentration-dependently inhibit FcεRI-dependent degranulation by a mechanism that is insensitive to pertussis toxin. A. Independent groups of IgE-sensitized BMMCs were pre-treated with vehicle, HU308 or LPI for 15 min and then stimulated with different concentrations of antigen (DNP-HSA) for 30 min at 37 °C. After this time, β-hexosaminidase activity was measured in the supernatant of stimulated cells. Data shown are the mean ± S.E.M. of 3 to 5 independent experiments. $^{**}p < 0.01$, one-way ANOVA followed by Dunnett's test. B. BMMCs were pre-incubated with pertussis toxin (10 or 100 ng/mL) for 2 h and then treated with vehicle, AEA, HU308 or LPI for 15 min before stimulation with DNP-HSA (27 ng/mL) for 30 min. β-Hexosaminidase was measured in the supernatant of stimulated cells. Data shown are the mean ± S.E.M. of 3 to 5 independent experiments. $^{###}p < 0.001$ *vs.* non-stimulated cells; Student's *t*-test; $^{**}p < 0.05$ *vs.* antigen-treated cells, one-way ANOVA followed by Dunnett's test.

Because FcεRI-induced degranulation is lower in Fyn$^{-/-}$ cells [51,52], normalized values of degranulation are presented in Supplementary Fig. 1B to show that AEA inhibited degranulation in the same proportion in WT and Fyn-deficient cells.

### 3.3. AEA inhibits FcεRI-induced degranulation with the participation of $CB_2$ and GPR55 receptors

In order to determine if classical cannabinoid receptors were involved in the effects of AEA, we first confirmed, by RT-PCR, that $CB_1$, $CB_2$ and GPR55 receptors were expressed in BMMCs (Fig. 2A). Next, we used distinct antagonists to block the inhibitory actions of AEA. Fig. 2B shows the effects of 25 μM AEA in cells with different pre-treatments. AEA inhibitory effect was prevented by both the specific $CB_2$ receptor antagonist AM630 and the GPR55 antagonist ML193, but not by AM251 (a $CB_1$ receptor antagonist and GPR55 agonist). None of the antagonists tested altered IgE/Ag-induced degranulation *per se* (data not shown).

### 3.4. $CB_2$ and GPR55 agonists inhibit FcεRI-induced degranulation in mast cells via PTX-insensitive G proteins

Because AM630 and ML193 blocked AEA inhibitory actions, we tested the effect of selective agonists for $CB_2$ and GPR55 receptors on FcεRI-induced degranulation. Fig. 3A shows that the $CB_2$ specific agonist HU308 and the GPR55 selective agonist LPI inhibited MC degranulation in a concentration-dependent manner, as AEA did. The doses needed for maximal degranulation blockage with HU308 and LPI were lower (10 μM) than those needed for AEA to produce similar effects (25 μM). We then evaluated if the inhibition caused by 1 μM HU308 could be prevented by pre-treatment with 100 nM AM630 or 300 nM ML193 and found that antagonists prevented the effects of those compounds (percentage of β-hexosaminidase release inhibition: HU308 = 58.3 ± 2.2 *vs.* AM630 pre-treated = 81.1 ± 2.9 and ML193 pre-treated = 86.6 ± 3.4; $p < 0.001$). A similar situation was observed with LPI, but to a lesser extent (percentage of β-hexosaminidase release inhibition: LPI = 55.4 ± 2.5 *vs.* AM630 pre-treated = 74.5 ± 1.2 and ML193 pre-treated = 82.9 ± 1.9; $p \leq 00.1$). These data support the idea that both $CB_2$ and GPR55 receptors are involved in the HU308 and LPI inhibitory effects on degranulation.

Next, we tested if classical pertussis toxin (PTX)-sensitive $G_i$ proteins mediated the inhibitory effects on degranulation produced by AEA, HU308 and LPI. BMMCs were pre-treated with different amounts of PTX and then stimulated with IgE/Ag, measuring the activity of secreted β-hexosaminidase 30 min after stimulation. As shown in Fig. 3B, PTX pre-treatment did not prevent the inhibitory effect of AEA, HU308 or ML193. A control test for the activity of the PTX used in these experiments was performed. As expected, PTX inhibited β-hexosaminidase release triggered by the $G_i$-coupled PAR-1 receptor agonist

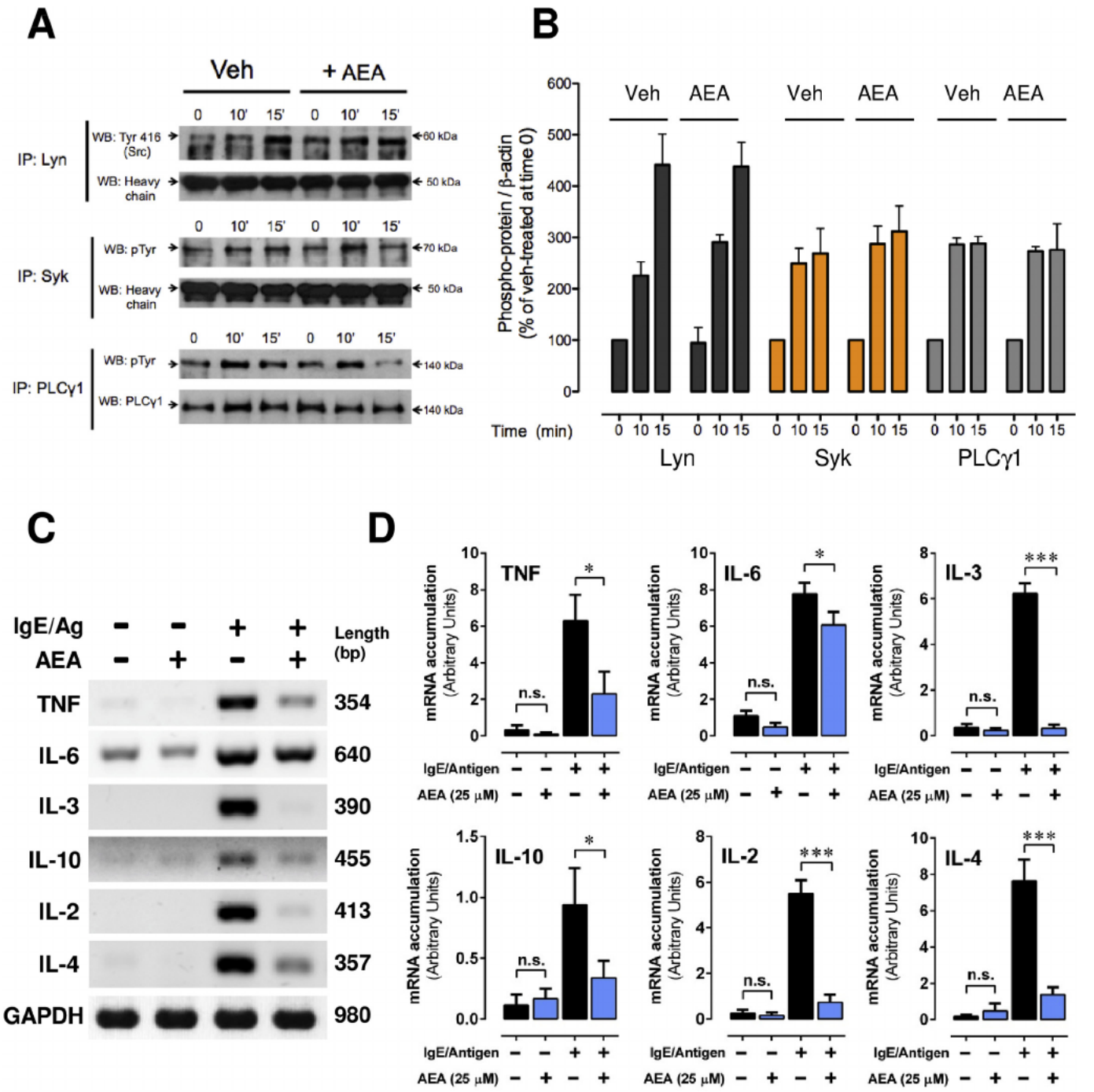


**Fig. 4.** AEA does not inhibit initial phosphorylation events, but blocks $Ca^{2+}$-dependent cytokine mRNA synthesis stimulated by FcεRI receptor in BMMCs. A. Western blot of Lyn, Syk and PLCγ1 obtained by immunoprecipitation after stimulation of FcεRI receptors in cells pre-treated with vehicle or AEA (25 μM) for 0, 10 or 15 min. B. Densitometric quantification of the bands shown in Panel A. C. Semi-quantitative RT-PCR to detect the production of TNF, IL-6, IL-3, IL-10, IL-2, and IL-4 mRNA in cells pre-treated with vehicle (Veh) or AEA (25 μM) for 15 min and then stimulated with DNP-HSA antigen (27 ng/mL) for 1 h. Western blot and agarose gel images are representative of three independent experiments performed with distinct cell cultures D. Quantification of cytokine mRNA production shown in Panel C. Bars represent the mean ± S.E.M. $*p < 0.05$, $***p < 0.001$ *vs.* antigen-stimulated cells, Student's *t*-test.

(TRAP-6) in a concentration-dependent fashion (Supplementary Fig. 2).

### *3.5. Anandamide does not block early phosphorylation events triggered by FcεRI receptor, but inhibits IgE/Ag-induced cytokine synthesis*

FcεRI receptor activation promotes rapid kinase activation and calcium mobilization needed for degranulation in mast cells [26]. After those initial events, FcεRI triggering leads to *de novo* cytokine mRNA synthesis. We explored if AEA could prevent early phosphorylation events triggered by FcεRI crosslinking. As observed in Fig. 4A, pre-treatment with AEA did not alter tyrosine phosphorylation of Lyn and Syk kinases or PLCγ1.

Also, we analyzed changes in the expression of different relevant cytokines in cells treated with AEA to obtain information about the elements of the FcεRI signal transduction system that could be affected. As previously reported in this cell preparation [48], basal expression of TNF, IL-6, IL-3, IL-10, IL-2 and IL-4 was very low or not detectable in the absence of stimulation (Fig. 4B). AEA at 25 μM had no effect by

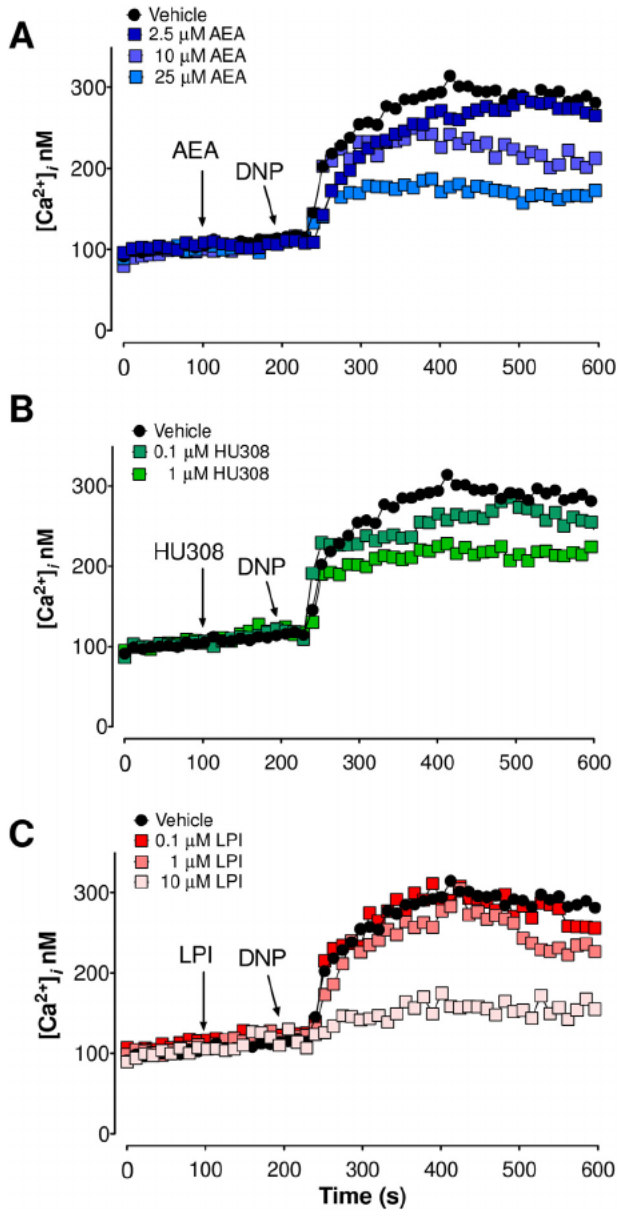


**Fig. 5.** AEA, HU308 and LPI inhibit maximal intracellular calcium increase induced by FcεRI receptor triggering. BMMCs were loaded with Fura-2AM as described in the Materials and methods section. After basal fluorescence registration, vehicle, AEA (Panel A), HU308 (Panel B) or LPI (Panel C) was added to the cuvette. After 100 s, cells were stimulated with 27 ng/mL antigen (DNP-HSA). Fluorescence was registered to reach a final time of 500 s. Data shown are the mean ± S.E.M. of two to three independent experiments performed with distinct cell cultures.

itself, but significantly prevented cytokine mRNA synthesis stimulated by IgE/Ag at optimal time. Quantification of these data is shown in Fig. 4C. Inhibition was particularly evident in calcium-dependent cytokine expression [30], *i.e.*, IL-2, IL-3, IL-4 and TNF. These results suggest that AEA inhibits calcium-dependent cytokine gene expression triggered by FcεRI stimulation.

### *3.6. AEA, HU308 and LPI inhibit antigen-induced calcium mobilization in BMMCs with the participation of GPR55 cannabinoid receptors*

To analyze the effects of AEA on calcium mobilization, we measured changes in intracellular calcium concentration ($[Ca^{2+}]_i$) elicited by IgE/Ag in BMMCs pre-treated with different concentrations of AEA, HU308 and LPI. None of the three agonists had an effect on basal calcium levels, but they did reduce the increase in $[Ca^{2+}]_i$ induced by DNP-HSA in a concentration-dependent manner (Fig. 5). We then tested the effects of the $CB_2$ antagonist AM630 and the GPR55 antagonist ML193 on calcium mobilization inhibition produced by AEA, HU308 and LPI. Neither $CB_2$ receptor blockage nor GPR55 antagonism prevents AEA or HU308 effects. However, AM630 and ML193 partially prevent LPI effects (Fig. 6).

## 4. Discussion

Main results obtained in this work are presented in Table 1 and can be summarized as follows: 1) AEA inhibits FcεRI receptor-induced degranulation with the participation of $CB_2$ and GPR55 receptors by a PTX-insensitive mechanism; 2) AEA does not block early FcεRI-induced phosphorylation events, but prevents calcium-dependent cytokine production; 3) BMMCs express $CB_1$, $CB_2$ and GPR55 receptor mRNAs. When $CB_2$ and GPR55 receptors are stimulated separately, they mimic the inhibitory actions of AEA on degranulation; 4) specific antagonism of $CB_2$ and GPR55 shows that both receptors play an important role in the inhibitory effects of AEA, HU308 and LPI on degranulation. As to FcεRI-induced $[Ca^{2+}]_i$ rise: 5) AEA, HU308 and LPI inhibit this parameter; 6) neither $CB_2$ receptor blockage nor GPR55 antagonism prevent AEA inhibitory effects; 7) ML193, but not AM630, blocks the inhibitory actions of HU308; and 8) both AM630 and ML193 partially prevent LPI-induced inhibition of $[Ca^{2+}]_i$ rise.

Cannabinoids have been proven to be important regulators of the immune system [4]. Together with the control of immune cell proliferation and differentiation, they exert important effects on chronic and acute inflammatory reactions [12]. Although the effects of those compounds have been widely documented and their use is considered a promising therapeutic strategy for inflammation-related diseases [53], the molecular mechanisms by which they exert their actions are not fully understood.

In the present study, AEA inhibited IgE/Ag-dependent degranulation in a concentration-dependent fashion without altering the viability of the cells or the general secretory machinery of MCs. AEA is an important endocannabinoid produced in response to nerve and immune cell stimulation [54]. It is a partial agonist of $CB_1$ ($K_i$ = 61–543 nM) and $CB_2$ receptors ($K_i$ = 279–1940 nM) [55], as well as a GPR55 receptor agonist at low nanomolar concentrations [56]. $CB_1$ and $CB_2$ cannabinoid receptors are GPCRs coupled to PTX-sensitive $G_{i/o}$ proteins [56,57], while the GPR55 receptor couples to the PTX insensitive $G_{12/13}$ proteins. The inhibition on degranulation caused by AEA observed in the present study was the same when PTX was added to the cells; therefore, neither $CB_1$ nor $CB_2$ receptors mediate this effect. Our data are in line with those reported previously, where inhibitory actions of endocannabinoids were observed using distinct models of MCs activation. For example, palmitoylethanolamide (PEA) blocks the PMA-induced secretion of nerve growth factor [58] and 2-AG inhibits antigen-dependent histamine release in sensitized guinea pig MCs [59]. However, the sensitivity to PTX was not addressed in those studies.

The insensitivity to PTX found in our study could be interpreted as the result of direct GPR55 activation by AEA. However, our findings suggest that $CB_2$ receptors are also involved. This is based on the fact that both HU308 (a highly selective $CB_2$ receptor agonist) [60] and LPI (GPR55 endogenous agonist) prevented MC degranulation. In support to this idea, GPR55 is expressed in our BMMCs and is functional because selective blockage of this receptor with ML193 inhibits AEA actions. To the best of our knowledge, this is the first time that an inhibitory action of GPR55 on the FcεRI signaling system is reported. Our results are in line with those reported by Cantarella and coworkers, who observed that GPR55 activation prevents the release of nerve growth factor stimulated by PMA in the human cell line HMC-1 [58]. Our data also add to the notion that LPI is an important lipid mediator capable of modulating the intensity of inflammatory reactions through GPR55

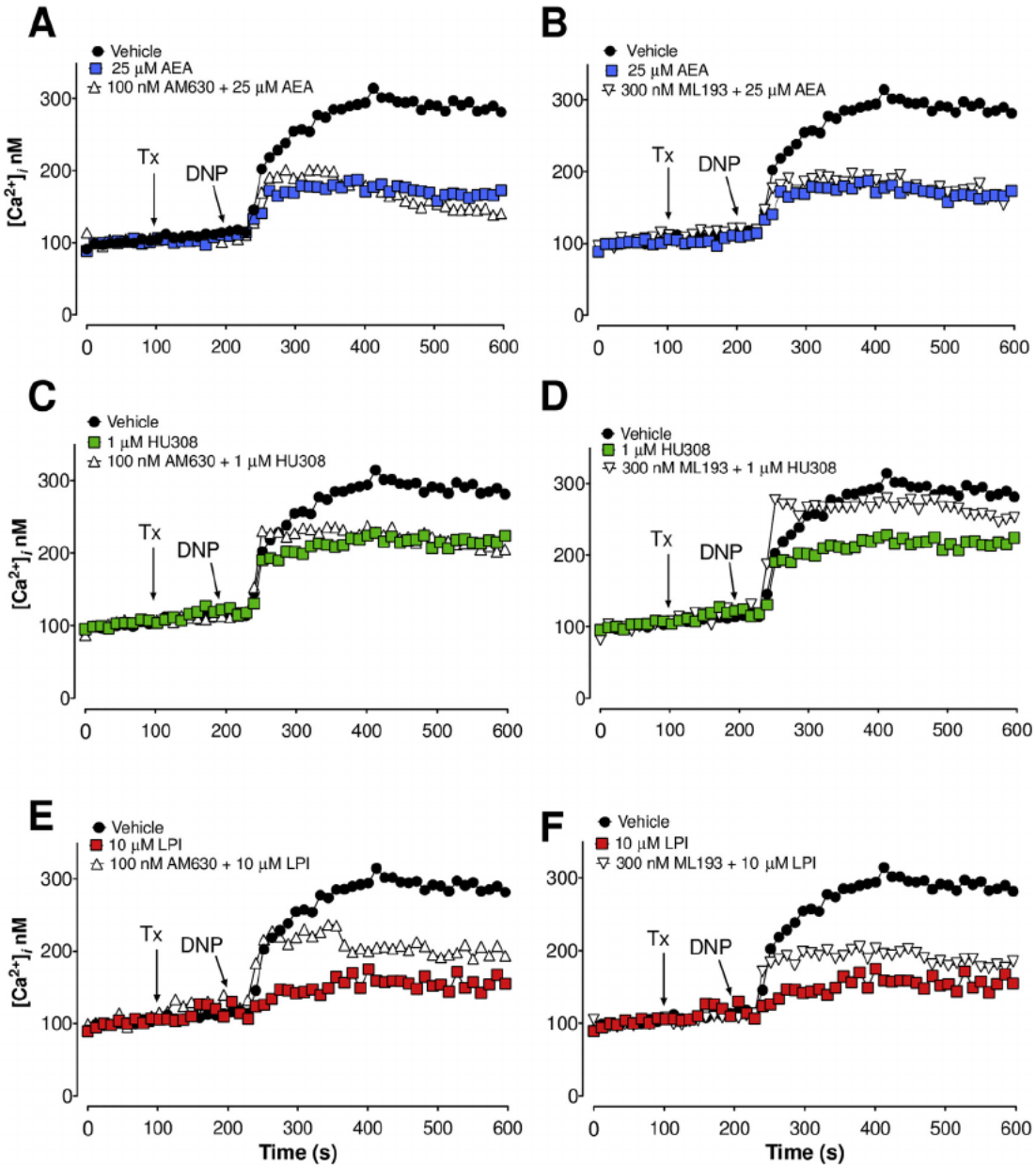


**Fig. 6.** Blockage of $CB_2$ has no effect on AEA and HU308 inhibitory actions on FcεRI-receptor mediated calcium rise, but partially reverses LPI-mediated effects. GPR55 receptor antagonism prevents HU308 and LPI inhibitory actions, but not those produced by AEA. BMMCs were loaded with Fura-2AM and AM630 or ML193 as described in the Materials and methods section. After basal fluorescence registration, vehicle, AEA (A, B), HU308 (C, D) or LPI (E, F) was added to the cuvette (Tx). After 100 s, cells were stimulated with 27 ng/mL antigen (DNP-HSA). Fluorescence was registered to reach a final time of 500 s. Data shown are the mean ± S.E.M. of two to three independent experiments performed with distinct cell cultures.

activation [61]. In this regard, it has been shown that LPI levels increase in different inflammatory conditions [62,63]. Also, GPR55 stimulation has been proposed as a therapeutic strategy for pathologies related to intestinal contractility, colonic motility and vasoconstriction [61] where MCs contribute to tissue damage. We hope that our finding of the inhibitory role of GPR55 on MCs would open new avenues in the search for molecules able to limit diseases related to MCs.

It has been shown that GPR55 receptors coupled to $G_{12/13}$ proteins down-regulate reactive oxygen species (ROS) production and degranulation in human neutrophils [9]. MCs degranulation stimulated by IgE/Ag also requires the generation of ROS [64]; therefore, the possibility to explore the inhibitory actions of AEA on ROS production in MCs is an attractive idea. On the other hand, there is evidence that activation of another $G_{12/13}$-coupled receptor (LPA5) by lysophosphatidic acid inhibits B cell antigen receptor (BCR) by diminishing calcium mobilization. Our data support the hypothesis that GPR55 and other receptors coupled *via* PTX insensitive proteins (particularly $G_{12/13}$) can modulate selected effector functions in immune cells.

Interestingly, we observed that not only GPR55 but also $CB_2$ receptor antagonism blocked the inhibitory actions of AEA, HU308 and LPI on FcεRI-induced degranulation. These results strongly suggest that a $CB_2$-GPR55 heteromer mediates this inhibition. Our findings are in line with the observation that a $CB_2$ receptor antagonist prevents the inhibitory effects of 2-AG on histamine release in MCs [59] and also blocks the effects of the $CB_2$ receptor agonist S-777469 on skin MCs [65]. However, the participation of GPR55 was not addressed in those studies.

As to the mechanism behind the inhibitory actions of AEA, we found that it does not block early FcεRI-induced phosphorylation events, but prevents calcium-dependent cytokine production. FcεRI signal

**Table 1**
Summary of the effects of AEA, HU308 and LPI, and their antagonists on degranulation and intracellular calcium increase produced by IgE/Ag stimulation on BMMCs.

| | Pre-Tx | Degranulation | $Ca^{2+}$ rise |
|---|---|---|---|
| IgE/Ag | Saline | ↑↑↑↑ | ↑↑↑↑ |
| AEA ($CB_1$,$CB_2$ and GPR55 receptor agonist) | Saline | ↓↓↓ | ↓↓↓ |
| | AM251 ($CB_1$ antagonist, GPR55 agonist) | ↓↓↓ | N/A |
| | AM630 ($CB_2$ antagonist) | Reverses inhibition | ↓↓↓ |
| | ML193 (GPR55 antagonist) | Reverses inhibition | ↓↓↓ |
| HU308 ($CB_2$ receptor agonist) | Saline | ↓↓↓ | ↓↓↓ |
| | AM630 | Reverses inhibition | ↓↓↓ |
| | ML193 | Reverses inhibition | Reverses inhibition |
| LPI (GPR55 receptor agonist) | Saline | ↓↓↓ | ↓↓↓ |
| | AM630 | Reverses inhibition | Partially reverses |
| | ML193 | Reverses inhibition | Partially reverses |

transduction system is composed by multiple branches connecting the IgE/Ag-dependent crosslinking of the receptor with degranulation, lipid mediator release and cytokine production [26,66,67]. One of the most important initial events is the tyrosine phosphorylation of protein kinase Lyn that continues with the activation of protein kinase Syk. Then, tyrosine phosphorylation of distinct adapters allows the recruitment of effector enzymes, such as phospholipase C (PLC)γ, which controls protein kinase C activation and calcium release from intracellular stores. Our data show that AEA does not affect those early events on FcεRI signaling, but importantly blocks cytokine mRNA production. It is well known that a number of transcription factors, implicated in the accumulation of IL-2, IL-4, TNF and other cytokines, are regulated by calcium mobilization in MCs. Present results indicate that the point(s) of the inhibitory actions of anandamide is (are) located downstream the early kinase activation and before the activation of transcription factors. These results are in line with data generated in T cells, where Δ-9-tetrahydrocannabinol suppressed the DNA-binding activity of NFAT and NFκB transcription factors on the *CD40L* gene promoter and inhibited T-cell receptor (TCR)-induced calcium rise without significant impairment of ZAP70, PLCγ1/2, Akt and GSK3β phosphorylation [68]. Our data add to the description of inhibitory actions of endocannabinoids on the activation of transcription factors involved in cytokine synthesis in immune cells. They also suggest that common negative regulatory pathways operate in innate and adaptive immune cells.

The formation of active dimers between distinct GPCRs has been identified as a biochemical mechanism that modifies the intensity and quality of signals generated by a given ligand [69]. It is known that $CB_2$ and GPR55 receptors are co-expressed in several cell types, such as neutrophils and cancer cells [70,71]. These receptors activate different pathways *via* ligand- and concentration-specific crosstalk [72]. The formation of $CB_2$ and GPR55 receptor heterodimers is capable of down-regulating MC activation *via* non-classical mechanisms in response to cannabinoids, opening the possibility of using $CB_2$ receptor agonists to trigger GPR55-mediated inhibitory effects to limit MC-dependent inflammatory reactions, where the levels of LPI could not reach the threshold to trigger GPR55 activation.

Supplementary data to this article can be found online at https://doi.org/10.1016/j.intimp.2018.09.006.

## Authorship

SLC and CGE performed the study conception and experimental design, wrote the paper and directed the activities of this work. ESM and JICA performed most of the degranulation assays, $[Ca^{2+}]_i$ measurements regarding to the effects of anandamide, HU308 and LPI on BMMCs, some RT-PCRs and contributed to the writing of the article; RDCV performed initial degranulation and $[Ca^{2+}]_i$ measurements, together with analysis of Fyn KO cells and the effect of AM9810. AIS generated all BMMCs needed for the study, performed the RT-PCR for cytokine mRNA analysis and immunoprecipitation experiments, and contributed to the discussion of the results.

## Acknowledgments

This paper was supported by the National Council of Science and Technology (Conacyt), Mexico and the Agence Nationale de la Recherche (ANR), France. (Grant ANR-Conacyt 188565) to CGE; Conacyt-Frontiers of Science Grant Number 1122 to CGE; and Conacyt-Basic Science Grant Number 239192 to SLC.

## Conflict of interest disclosure

Authors declare no conflict of interests.

## References

[1] M. Maccarrone, et al., Endocannabinoid signaling at the periphery: 50 years after THC, Trends Pharmacol. Sci. 36 (5) (2015) 277–296.
[2] V. Chevaleyre, K.A. Takahashi, P.E. Castillo, Endocannabinoid-mediated synaptic plasticity in the CNS, Annu. Rev. Neurosci. 29 (2006) 37–76.
[3] A.C. Howlett, et al., International Union of Pharmacology. XXVII. Classification of cannabinoid receptors, Pharmacol. Rev. 54 (2) (2002) 161–202.
[4] R. Tanasescu, C.S. Constantinescu, Cannabinoids and the immune system: an overview, Immunobiology 215 (8) (2010) 588–597.
[5] B.M. Fonseca, et al., Endogenous cannabinoids revisited: a biochemistry perspective, Prostaglandins Other Lipid Mediat. 102-103 (2013) 13–30.
[6] H. Schwarz, F.J. Blanco, M. Lotz, Anadamide, an endogenous cannabinoid receptor agonist inhibits lymphocyte proliferation and induces apoptosis, J. Neuroimmunol. 55 (1) (1994) 107–115.
[7] T.K. Eisenstein, J.J. Meissler, Effects of cannabinoids on T-cell function and resistance to infection, J. NeuroImmune Pharmacol. 10 (2) (2015) 204–216.
[8] M. Lee, K.H. Yang, N.E. Kaminski, Effects of putative cannabinoid receptor ligands, anandamide and 2-arachidonyl-glycerol, on immune function in B6C3F1 mouse splenocytes, J. Pharmacol. Exp. Ther. 275 (2) (1995) 529–536.
[9] N.A. Balenga, et al., GPR55 regulates cannabinoid 2 receptor-mediated responses in human neutrophils, Cell Res. 21 (10) (2011) 1452–1469.
[10] J.L. Croxford, T. Yamamura, Cannabinoids and the immune system: potential for the treatment of inflammatory diseases? J. Neuroimmunol. 166 (1–2) (2005) 3–18.
[11] B.L. Kaplan, The role of CB1 in immune modulation by cannabinoids, Pharmacol. Ther. 137 (3) (2013) 365–374.
[12] C. Turcotte, et al., The CB2 receptor and its role as a regulator of inflammation, Cell. Mol. Life Sci. 73 (23) (2016) 4449–4470.
[13] M. Oz, Receptor-independent actions of cannabinoids on cell membranes: focus on endocannabinoids, Pharmacol. Ther. 111 (1) (2006) 114–144.
[14] A. Jarrahian, C.J. Hillard, Arachidonylethanolamide (anandamide) binds with low affinity to dihydropyridine binding sites in brain membranes, Prostaglandins Leukot. Essent. Fat. Acids 57 (6) (1997) 551–554.
[15] M. Oz, Y. Tchugunova, M. Dinc, Differential effects of endogenous and synthetic cannabinoids on voltage-dependent calcium fluxes in rabbit T-tubule membranes: comparison with fatty acids, Eur. J. Pharmacol. 502 (1–2) (2004) 47–58.
[16] A. Toth, P.M. Blumberg, J. Boczan, Anandamide and the vanilloid receptor (TRPV1), Vitam. Horm. 81 (2009) 389–419.
[17] S.E. O'Sullivan, D.A. Kendall, Cannabinoid activation of peroxisome proliferator-activated receptors: potential for modulation of inflammatory disease, Immunobiology 215 (8) (2010) 611–616.
[18] H. Sharir, M.E. Abood, Pharmacological characterization of GPR55, a putative cannabinoid receptor, Pharmacol. Ther. 126 (3) (2010) 301–313.
[19] C. Cardamone, et al., Mast cells as effector cells of innate immunity and regulators of adaptive immunity, Immunol. Lett. 178 (2016) 10–14.
[20] C.F. Johnzon, E. Ronnberg, G. Pejler, The role of mast cells in bacterial infection, Am. J. Pathol. 186 (1) (2016) 4–14.
[21] K. Mukai, et al., Mast cells as sources of cytokines, chemokines, and growth factors, Immunol. Rev. 282 (1) (2018) 121–150.
[22] S.J. Galli, M. Tsai, IgE and mast cells in allergic disease, Nat. Med. 18 (5) (2012) 693–704.
[23] J.I. Silverberg, Public health burden and epidemiology of atopic dermatitis,

Dermatol. Clin. 35 (3) (2017) 283–289.
[24] P.A. Loftus, S.K. Wise, Epidemiology and economic burden of asthma, Int. Forum Allergy Rhinol. 5 (Suppl. 1) (2015) S7–10.
[25] I.T. Harvima, et al., Molecular targets on mast cells and basophils for novel therapies, J. Allergy Clin. Immunol. 134 (3) (2014) 530–544.
[26] R. Suzuki, J. Scheffel, J. Rivera, New insights on the signaling and function of the high-affinity receptor for IgE, Curr. Top. Microbiol. Immunol. 388 (2015) 63–90.
[27] A.M. Gilfillan, J. Rivera, The tyrosine kinase network regulating mast cell activation, Immunol. Rev. 228 (1) (2009) 149–169.
[28] U. Blank, J. Rivera, The ins and outs of IgE-dependent mast-cell exocytosis, Trends Immunol. 25 (5) (2004) 266–273.
[29] U. Blank, The mechanisms of exocytosis in mast cells, Adv. Exp. Med. Biol. 716 (2011) 107–122.
[30] S.M. Hatfield, N.W. Roehm, Cyclosporine and FK506 inhibition of murine mast cell cytokine production, J. Pharmacol. Exp. Ther. 260 (2) (1992) 680–688.
[31] Y. Baba, et al., Essential function for the calcium sensor STIM1 in mast cell activation and anaphylactic responses, Nat. Immunol. 9 (1) (2008) 81–88.
[32] J.V. Falvo, A.V. Tsytsykova, A.E. Goldfeld, Transcriptional control of the TNF gene, Curr. Dir. Autoimmun. 11 (2010) 27–60.
[33] A.H. Lau, S.S. Chow, Effects of cannabinoid receptor agonists on immunologically induced histamine release from rat peritoneal mast cells, Eur. J. Pharmacol. 464 (2–3) (2003) 229–235.
[34] K. Starowicz, D.P. Finn, Cannabinoids and pain: sites and mechanisms of action, Adv. Pharmacol. 80 (2017) 437–475.
[35] N. Barrie, et al., Endocannabinoids in arthritis: current views and perspective, Int. J. Rheum. Dis. 20 (7) (2017) 789–797.
[36] K.L. Leinwand, et al., Manipulation of the endocannabinoid system in colitis: a comprehensive review, Inflamm. Bowel Dis. 23 (2) (2017) 192–199.
[37] E.A. Cairns, et al., Seeing over the horizon - targeting the endocannabinoid system for the treatment of ocular disease, J. Basic Clin. Physiol. Pharmacol. 27 (3) (2016) 253–265.
[38] A. Wollenberg, A. Seba, A.S. Antal, Immunological and molecular targets of atopic dermatitis treatment, Br. J. Dermatol. 170 (Suppl. 1) (2014) 7–11.
[39] K. Sugawara, et al., Endocannabinoids limit excessive mast cell maturation and activation in human skin, J. Allergy Clin. Immunol. 129 (3) (2012) 726–738 (e8).
[40] M.T. Samson, et al., Differential roles of CB1 and CB2 cannabinoid receptors in mast cells, J. Immunol. 170 (10) (2003) 4953–4962.
[41] G. Nam, et al., Selective cannabinoid receptor-1 agonists regulate mast cell activation in an oxazolone-induced atopic dermatitis model, Ann. Dermatol. 28 (1) (2016) 22–29.
[42] T.S. Manetz, et al., Vav1 regulates phospholipase cgamma activation and calcium responses in mast cells, Mol. Cell. Biol. 21 (11) (2001) 3763–3774.
[43] S. Dasgupta, et al., Antineuroinflammatory effect of NF-kappaB essential modifier-binding domain peptides in the adoptive transfer model of experimental allergic encephalomyelitis, J. Immunol. 173 (2) (2004) 1344–1354.
[44] M.R. Hassuneh, P.S. Nagarkatti, M. Nagarkatti, Evidence for the participation of interleukin-2 (IL-2) and IL-4 in the regulation of autonomous growth and tumorigenesis of transformed cells of lymphoid origin, Blood 89 (2) (1997) 610–620.
[45] O.A. Adebanjo, et al., Mode of action of interleukin-6 on mature osteoclasts. Novel interactions with extracellular Ca2+ sensing in the regulation of osteoclastic bone resorption, J. Cell Biol. 142 (5) (1998) 1347–1356.
[46] T. Biedermann, et al., Reversal of established delayed type hypersensitivity reactions following therapy with IL-4 or antigen-specific Th2 cells, Eur. J. Immunol. 31 (5) (2001) 1582–1591.
[47] T. Iwasaki, et al., Regulation of cytokine expression by an autoreactive B cell clone derived from MRL/MP-lpr/lpr mice, Clin. Exp. Immunol. 114 (1) (1998) 1–8.
[48] C. Gonzalez-Espinosa, et al., Preferential signaling and induction of allergy-promoting lymphokines upon weak stimulation of the high affinity IgE receptor on mast cells, J. Exp. Med. 197 (11) (2003) 1453–1465.
[49] S. Jiang, et al., Expression and function of cannabinoid receptors CB1 and CB2 and their cognate cannabinoid ligands in murine embryonic stem cells, PLoS One 2 (7) (2007) e641.
[50] K. Li, et al., A role for O-1602 and G protein-coupled receptor GPR55 in the control of colonic motility in mice, Neuropharmacology 71 (2013) 255–263.
[51] E. Sanchez-Miranda, A. Ibarra-Sanchez, C. Gonzalez-Espinosa, Fyn kinase controls FcepsilonRI receptor-operated calcium entry necessary for full degranulation in mast cells, Biochem. Biophys. Res. Commun. 391 (4) (2010) 1714–1720.
[52] R. Suzuki, et al., Loss of TRPC1-mediated Ca2+ influx contributes to impaired degranulation in Fyn-deficient mouse bone marrow-derived mast cells, J. Leukoc. Biol. 88 (5) (2010) 863–875.
[53] P. Nagarkatti, et al., Cannabinoids as novel anti-inflammatory drugs, Future Med. Chem. 1 (7) (2009) 1333–1349.
[54] F.G. Correa, et al., The endocannabinoid anandamide from immunomodulation to neuroprotection. Implications for multiple sclerosis, Vitam. Horm. 81 (2009) 207–230.
[55] R.G. Pertwee, et al., International Union of Basic and Clinical Pharmacology. LXXIX. Cannabinoid receptors and their ligands: beyond CB(1) and CB(2), Pharmacol. Rev. 62 (4) (2010) 588–631.
[56] E. Ryberg, et al., The orphan receptor GPR55 is a novel cannabinoid receptor, Br. J. Pharmacol. 152 (7) (2007) 1092–1101.
[57] C.M. Henstridge, et al., The GPR55 ligand L-alpha-lysophosphatidylinositol promotes RhoA-dependent Ca2+ signaling and NFAT activation, FASEB J. 23 (1) (2009) 183–193.
[58] G. Cantarella, et al., Endocannabinoids inhibit release of nerve growth factor by inflammation-activated mast cells, Biochem. Pharmacol. 82 (4) (2011) 380–388.
[59] A. Vannacci, et al., The endocannabinoid 2-arachidonylglycerol decreases the immunological activation of Guinea pig mast cells: involvement of nitric oxide and eicosanoids, J. Pharmacol. Exp. Ther. 311 (1) (2004) 256–264.
[60] L. Hanus, et al., HU-308: a specific agonist for CB(2), a peripheral cannabinoid receptor, Proc. Natl. Acad. Sci. U. S. A. 96 (25) (1999) 14228–14233.
[61] M. Alhouayek, J. Masquelier, G.G. Muccioli, Lysophosphatidylinositols, from cell membrane constituents to GPR55 ligands, Trends Pharmacol. Sci. 39 (6) (2018) 586–604.
[62] M. Kurano, et al., Possible involvement of minor lysophospholipids in the increase in plasma lysophosphatidic acid in acute coronary syndrome, Arterioscler. Thromb. Vasc. Biol. 35 (2) (2015) 463–470.
[63] J.M. Moreno-Navarrete, et al., The L-alpha-lysophosphatidylinositol/GPR55 system and its potential role in human obesity, Diabetes 61 (2) (2012) 281–291.
[64] Y. Suzuki, et al., Role of oxidants in mast cell activation, Chem. Immunol. Allergy 87 (2005) 32–42.
[65] T. Haruna, et al., The inhibitory effect of S-777469, a cannabinoid type 2 receptor agonist, on skin inflammation in mice, Pharmacology 99 (5–6) (2017) 259–267.
[66] S. Kraft, J.P. Kinet, New developments in FcepsilonRI regulation, function and inhibition, Nat. Rev. Immunol. 7 (5) (2007) 365–378.
[67] P. Draber, et al., Signal transduction and chemotaxis in mast cells, Eur. J. Pharmacol. 778 (2016) 11–23.
[68] T. Ngaotepprutaram, B.L. Kaplan, N.E. Kaminski, Impaired NFAT and NFkappaB activation are involved in suppression of CD40 ligand expression by Delta(9)-tetrahydrocannabinol in human CD4(+) T cells, Toxicol. Appl. Pharmacol. 273 (1) (2013) 209–218.
[69] I. Gomes, et al., G protein-coupled receptor heteromers, Annu. Rev. Pharmacol. Toxicol. 56 (2016) 403–425.
[70] N.A. Balenga, et al., Heteromerization of GPR55 and cannabinoid CB2 receptors modulates signalling, Br. J. Pharmacol. 171 (23) (2014) 5387–5406.
[71] E. Moreno, et al., Targeting CB2-GPR55 receptor heteromers modulates cancer cell signaling, J. Biol. Chem. 289 (32) (2014) 21960–21972.
[72] H. Yang, J. Zhou, C. Lehmann, GPR55 - a putative "type 3" cannabinoid receptor in inflammation, J. Basic Clin. Physiol. Pharmacol. 27 (3) (2016) 297–302.